The specificity of B-cell response in multiple sclerosis

Maggiore, Cosimo

THE SPECIFICITY OF B-CELL RESPONSE IN MULTIPLE SCLEROSIS

Cosimo Maggiore

Submitted for the degree of Doctor of Philosophy

2013

Department of Infection, Inflammation and Repair, within the Bone and Joint Research Unit, William Harvey Research Institute and Centre for Neuroscience and Trauma, Blizard Institute

Barts and The London School of Medicine and Dentistry

Queen Mary University of London

Statement of Originality

The work described in this thesis was carried out in the Department of Infection, Inflammation and Repair, within the Bone and Joint Research Unit, William Harvey Research Institute and in the Centre for Neuroscience and Trauma, Blizard Institute, Barts and the London School of Medicine and Dentistry, Queen Mary University of London.

Unless stated otherwise, the author performed the experiments described.

I hereby state that this thesis entitled 'The specificity of B-cell response in multiple sclerosis' has not been submitted for a degree or any other qualification at any other university.

Cosimo Maggiore, 2013

Acknowledgements

I would like to thank my supervisors: Dr. Ahuva Nissim and Prof. Gavin Giovannoni.

My grateful thanks go to Dr. Ahuva Nissim for the day-to-day supervision and for the opportunity to work in her team. Thank you also for her patience and encouragement during the years.

I would like to express my gratitude to Prof. Gavin Giovannoni for giving me the opportunity to undertake this project and for the constant support. Thank you also for the continuous advices and availability.

I would like to extend my thanks to everyone in Bone and Joint Research Unit, William Harvey Research Institute and Neuroimmunology Unit, Neuroscience and Trauma Centre, Blizard Institute, QMUL.

My thanks go to Dr. Djordje Gveric, Prof. Richard Reynolds and the UK MS Tissue bank staff for the brain tissues supplied and used in this study.

I would like to thank Prof. Jo Martin for the supervision with the pathological work and the help with the ethics.

I would like to thank all my family for their support. A particular thank you to my parents, Carmine and Teresa, with love.

Abstract

Introduction:

One of the pathological features of multiple sclerosis (MS) is the presence of a long lived chronic inflammation in the central nervous system (CNS) with presence of oligoclonal IgG and IgM bands (OCBs) in the cerebrospinal fluid (CSF) derived from clonally expanded B cells. In my PhD I have tested the hypothesis that the intrathecal B cells response is antigen driven and screened putative candidate antigenic epitopes.

Materials and methods:

Brain tissues were supplied from The UK Multiple Sclerosis Tissue Bank. Total RNA was extracted from the brain tissues from 14 patients with MS after homogenization of the snap frozen blocks and cDNA obtained. VH and VL fragments were amplified from IgM and IgG and cloned in an in house vector to build a phage display single chain fragment variable (scFv) antibody library. The library was used to analyse the VH and VL usage, somatic mutation and clonal expansion in the MS brain and to select for scFv specific to putative autoantigens candidates.

Results and discussion:

Two libraries of VH only and VH plus VL gene segments from MS brain's B cells were built. The sequences analysis has revealed a biased usage of VH and VL and evidence of clonal expansion thus supporting an antigen driven response. The auto-antigen candidates chosen for screening the libraries were the myelin basic protein (MBP)-proteolipid protein (PLP) fusion protein MP4 and specific binders were selected as highlighted with monoclonal phage ELISA.

Conclusion:

A MS disease specific phage display antibody library was built to facilitate the analysis of the disease specific V gene usage in the MS brain. Selection using this library has provided a proof of concept that this library is functional. The

library will be used in the future to identify human antibody fragments against candidate autoantigens either for diagnostic or therapeutic applications.

Table of Contents

Statement of Originality....2

Acknowledgements....3

Abstract....4

Table of Contents....6

List of Figures....9

List of Tables....12

List of Abbreviations....14

Chapter 1: Introduction....16

1.1 Multiple Sclerosis....16

1.1.1 Epidemiology....16

1.1.2 Susceptibility....18

1.1.2.1 Genetics....18

1.1.2.2 Environmental risk factors....19

1.1.3 Immunopathogenesis....22

1.1.3.1 Innate Immunity....24

1.1.3.2 Adaptive Immunity....25

1.1.3.3 B cells and MS....27

1.1.4 Diagnosis, Clinical course and Prognosis....31

1.1.4.1 Neuroimaging....34

1.1.4.2 Evoked potentials....35

1.1.4.3 Laboratory....35

1.1.5 Therapy 42

1.1.5.1 Clinical trials (anti CD20) 44

1.2 “Auto-antigens” in MS 47

1.3 Phage display 54

1.3.1 Antibody molecule 54

1.3.2 Antibody phage display 56

1.4 Hypothesis and Objectives 63

Chapter 2: Materials and Methods 64

2.1 Patients 64

2.2 Immunohistochemistry 64

2.3 Laser capture microdissection 65

2.4 Tissue homogenization, RNA extraction and cDNA synthesis 66

2.5 RT-PCR 67

2.6 Immune libraries construction 71

2.6.1 Inserts preparation 71

2.6.2 Cloning of V genes into vector 74

2.6.2.1 Preparation of Vector 76

2.6.2.2 Ligation 77

2.6.2.3 Preparation of competent *E. coli* TG1 77

2.6.2.4 Transformation 77

2.6.2.5 Library size 78

2.6.2.6 Sequencing 78

2.7 Libraries selection 78
2.7.1 Rescue of MS and Tomlinson I libraries 79
2.7.1.1 Production of KM13 helper phage from stock 79
2.7.1.2 Production of large quantities of phages 79
2.7.2 Target Protein Analysis 81
2.7.2.1 SDS-Polyacrylamide Gel Electrophoresis (SDS-PAGE) 81
2.7.2.2 Coomassie Blue Detection of Proteins 81
2.7.2.3 Protein concentration 82
2.7.3 Selection of antigen specific binders from phage libraries 83
2.7.4 Screening by ELISA 84
2.7.4.1 ELISA with polyclonal and monoclonal phages 84
2.7.4.2 ELISA with soluble scFv antibody fragments 85
Chapter 3: Lymphoid network in MS brain tissues 86
3.1 Histopathology of supplied tissues 89
3.2 Gene Expression 97
Chapter 4: Immune phage-displayed libraries from B cells of MS patients' brains 122
Chapter 5: MP4 specific scFv raised from the MS library 159
Chapter 6: Discussion 179
References 187

List of Figures

Figure 1.1 Prevalence and distribution of MS in different continents: 17

Figure 1.2 GWAS Manhattan plot in MS 18

Figure 1.3 MS clinical course patterns 33

Figure 1.4 CSF IgG index 36

Figure 1.5 Igs IEF Patterns 38

Figure 1.6 Schematic diagram of V-region.....54

Figure 1.7 3D structure of an IgG.....55

Figure 1.8 Schematic diagram of an antibody molecule and fragments.....55

Figure 1.9 Schematic representation of a filamentous phage 56

Figure 1.10 Phagemid vector map of pIT2.....58

Figure 1.11 Mimicking the B cell development by phage technology.....59

Figure 1.12 Steps followed to build my antibody phage display library.....61

Figure 1.13 Antibody phage display selection.....62

Figure 2.1 Schematic map of VH primers on mRNA 72

Figure 3.1.1 Follicle-like aggregate scheme.....87

Figure 3.1.2 Examples of immune infiltrates and aggregates 94

Figure 3.1.3 Sequence of events in laser capture microdissection 95

Figure 3.1.4 1% Agarose gel PCR products from microdissected lymphoid aggregate.....96

Figure 3.2.1 Cellular interactions in dark and light zone 98

Fig.3.2.2 Nanodrop quantification and evaluation of RNA extraction 102

Figure 3.2.3 RNA quality checked by 1% denaturing agarose gel 103

Figure 3.2.4 Examples of electropherogram by 2100 bioanalyser 105

Figure 3.2.5 Correlation post-mortem parameters and RIN 108

Figure 3.2.6 Reference genes primers design for SYBR Green chemistry 115

Figure 3.2.7 GAPDH and HMBS primers check against BLAST database 116

Figure 3.2.8 Optimization matrices results 117

Figure 3.2.9 Reference genes expression range 118

Figure 3.2.10 Reference genes dissociation curves and 2% agarose gel bands 119

Figure 4.1 Strategy of library construction.....127

Figure 4.2 1% Agarose of VH PCR products 130

Figure 4.3 1% Agarose gel of Vk PCR products 131

Figure 4.4 1% Agarose gel of Vk3 PCR products 131

Figure 4.5 1% Agarose gel of Vλ PCR products 132

Figure 4.6 VH usage observed vs expected 135

Figure 4.7 VH usage MS vs Healthy Controls transcriptome 136

Figure 4.8 D segments usage 138

Figure 4.9 D Usage 138

Figure 4.10 JH Usage 139

Figure 4.11 Vk Usage 141

Figure 4.12 Vk segments usage 141

Figure 4.13 Jk Usage 142

Figure 4.14 V Lambda Usage 144

Figure 4.15 Distribution lengths VH CDR3 146
Figure 4.16 Comparison lengths VH CDR3 healthy vs MS 146
Figure 4.17 VH family distribution of R/S ratio 147
Figure 4.18 Net Charge VH CDR3 148
Figure 4.19 Mutations 149
Figure 4.20 Gene signature in the VH4 clones 150
Figure 4.21 Hot and Cold spots of VH4 gene signature 151
Figure 4.22 CDRs and FRs AA substitutions 152
Figure 5.1 Fusion protein MP4 schematic drawing 161
Figure 5.2 Helper phage titer 162
Figure 5.3 SDS-PAGE analysis of the proteins used for selections and ELISAs 163
Figure 5.4 Tomlinson I library output after each round of selection 164
Figure 5.5 Polyclonal phage ELISAs 167
Figure 5.6 Tomlinson I library monoclonal phage ELISAs 169
Figure 5.7 MS antibody libraries output after each round of selection 171
Figure 5.8 MP4 Polyclonal phage ELISA 173

List of Tables

Table 1.1 MRI criteria MAGNIMS.....35

Table 2.1 Details of MS patients and non neurological controls.....64

Table 2.2 Sequences and details of reference genes primers 67

Table 2.3 Sequences and details of target genes primers 68

Table 2.4 MIQE checklist.....70

Table 2.5 List of Primers for amplifications of human VH genes.....73

Table 2.6 List of Primers for amplifications of human Vk genes.....73

Table 2.7 List of Primers for amplifications of human Vλ genes.....74

Table 2.8 Bacterial growth media formulations 76

Table 2.9 Protein analysis buffer formulations 82

Table 3.1.1 Primary antibody specificity targeting the lymphoid infiltrates 90

Table 3.1.2 Primary antibody specificity targeting areas of demyelination.....90

Table 3.1.3 Primary antibody specificity for EBV screening 90

Table 3.2.1 Samples characteristics 99

Table 3.2.2 Post-mortem parameters and respective RINs 106

Table 3.2.3 Endogenous reference genes analysed for data normalization....109

Table 3.2.4 Optimization matrices for primers concentration 117

Table 3.2.5 Candidate reference genes analysed with different methods.....120

Table 4.1 VH amino acid sequences 134

Table 4.2 Vk amino acid sequences 140

Table 5.1 Sequences of the 3rd round clones.....170

Table 5.2 Enrichment on MP4 of the phage antibodies pool derived from VH only library.....172

Table 5.3 Sequences from the 3rd round of selection of VH only and 4th round of VH+VL libraries.....176

List of Abbreviations

- ◊ Ab — Antibody
- ◊ Ag — Antigen
- ◊ Amp — Ampicillin
- ◊ BBB — Blood-Brain Barrier
- ◊ BCB — Blood-CSF Barrier
- ◊ BSA — Bovine Serum Albumin
- ◊ CDMS — Clinically Definite Multiple Sclerosis
- ◊ CIS — Clinically Isolated Syndrome
- ◊ CNS — Central Nervous System
- ◊ DPTA — Diethylene Triamine Pentaacetic Acid
- ◊ EDTA — Ethylene Diamine Tetra Acetate
- ◊ ELISA — Enzyme Linked Immunosorbent Assay
- ◊ FLAIR — Fluid-Attenuation Inversion Recovery
- ◊ HRP — Horse Raddish Immune Peroxidase
- ◊ IPTG — Isopropyl β-D-thiogalactoside
- ◊ Kan — Kanamicin
- ◊ MHC — Major Histocompatability Complex
- ◊ MPBS — Marvel Milk Phosphate Buffered Saline
- ◊ MRZR — Measles, Rubella and Varicella Zoster Reaction
- ◊ MS — Multiple Sclerosis

◊ NaCl	Sodium Chloride
◊ NAWM	Normal Appearing White Matter
◊ OCB	Oligoclonal Bands
◊ O.D. 400	Optical Density 400
◊ O.D. 600	Optical Density 600
◊ PBS	Phosphate Buffered Saline
◊ PCR	Polymerase Chain Reaction
◊ PEG	Polyethylene glycol
◊ RIS	Radiologically Isolated Syndrome
◊ RT	Room Temperature
◊ scFv	Single Chain Variable Fragment
◊ TMB	3,3’,5,5’-tetramethylbenzidine

Chapter 1: Introduction

1.1 Multiple Sclerosis

"....I was obliged to have my letters read to me, and their answers written for me, as my eyes were so attacked that when fixed upon minute objects indistinctness of vision was the consequence: Until I attempted to read, or to cut my pen, I was not aware of my Eyes being in the least attacked. Soon after, I went to Ireland, and without anything having been done to my Eyes, they completely recovered their strength and distinctness of vision ..."

This is possibly the first patient's description of multiple sclerosis (MS) and was taken from the diary of Sir Augustus D'Este, grandson of King George III (1822-1848) (Pearce 2005).

1.1.1 Epidemiology

MS is a putative autoimmune disease of the central nervous system (CNS) and affects over 1 million individuals worldwide. MS is a long lasting neurological disease with a mean survival ranging from 30 to 40 years from the onset of disease symptoms, including patients with a benign course (Compston and Coles 2008; Kingwell et al. 2012). The risk of developing MS is higher in women with an increased trend described in the last decades leading to a sex ratio F:M of around 3.2 (Ramagopalan et al. 2010). In the world the highest prevalence rates have been shown for Scotland and its offshore islands ranging from 145 to 193 per 100.000 (Pugliatti et al. 2002), higher than other Nordic countries with the same latitude, pointing to the hypothesis of the association of high susceptibility and Scottish ancestry (Rothwell and Charlton 1998) and in contrast with rare cases observed in African blacks or Samis populations. The worldwide uneven geographical distribution is correlated to differences in racial susceptibility and it is described a classical relationship prevalence-latitude with areas of decreasing risk with a north to south gradient (Fig.1.1). The disease appears to be much more a person/population-related disease than a place-related one (Compston and Coles 2008; Rosati 2001).

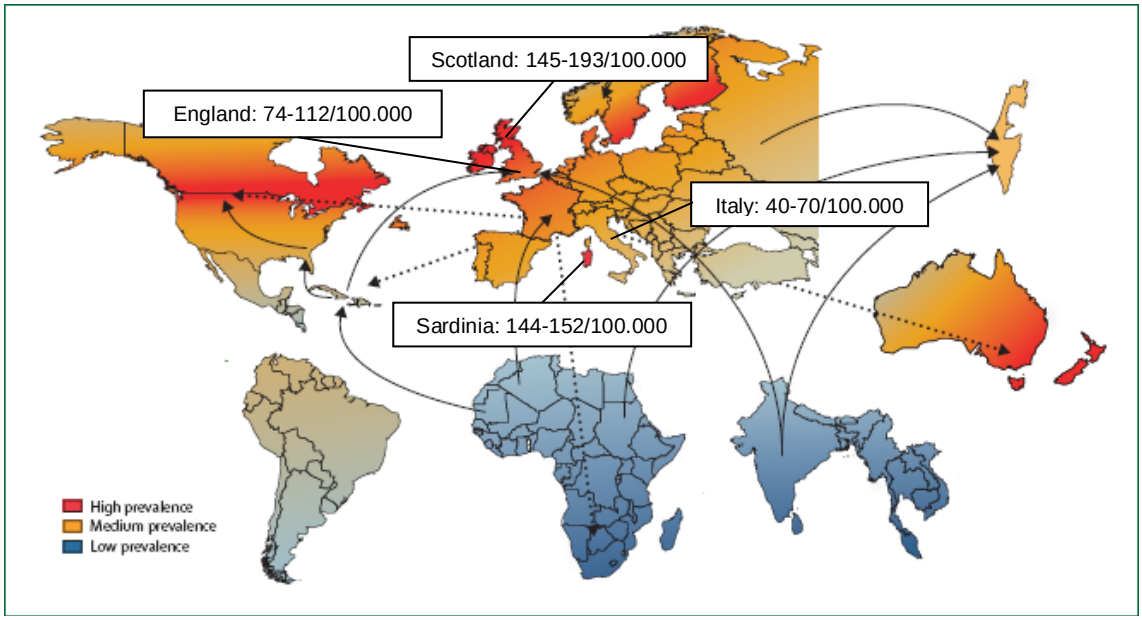

Figure 1.1 Prevalence and distribution of MS in different continents: Atlas showing the MS prevalence in the five continents. Medium prevalence depicted in orange, areas of exceptionally high frequency in red, and areas with low rates in grey-blue. Dotted arrows show major routes of migration from high-risk zone of northern Europe. Solid arrows showing migrants from low-risk to high-risk zones. Prevalence rates showed for some regions in text boxes (figure modified from Compston and Coles 2008; Rosati 2001).

1.1.2 Susceptibility

1.1.2.1 Genetics

Presence of patients in the same family has been observed since the first descriptions of the disease and the results of numerous studies have highlighted an increased risk of developing MS in parallel with the increase in genetic material shared with an affected individual (OMIM 126200). MS genetics does not fit a classical Mendelian inheritance but there is a contribution of genetic factors leading to familial aggregation with a concordance rate for MS diagnosis of about 30% in monozygotic twins and 3-4% in first-degree relatives and with respectively a 300-fold and a 20-40 fold increased MS risk (Ebers et al. 1995). Among all the MS susceptibility loci identified by genome-wide association studies (GWAS) it is possible to divide two different categories based on the functional role of the immunogenetic involvement and the level of association: 1) HLA genes, involved in antigen processing and presentation, with a strong association and 2) non-HLA genes, involved in the immune response, but outside the MHC locus, with a lower association. The hallmark of the association studies in MS susceptibility are summarized by a Manhattan plot, with one skyscraper towering all the others due to the strongest association for SNPs in the HLA-region compared to non-HLA regions (Fig.1.2).

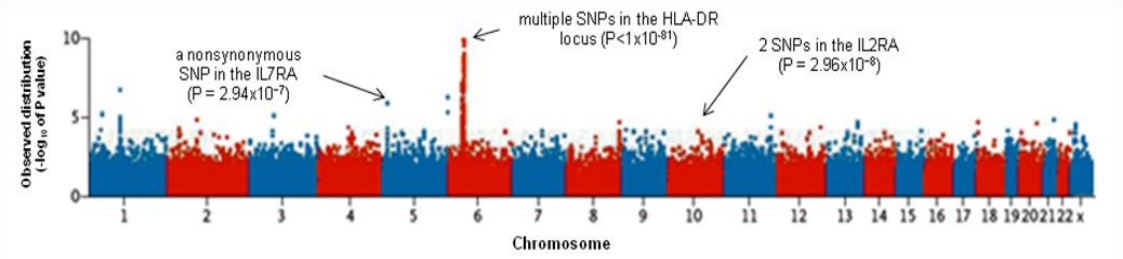

Figure 1.2 GWAS Manhattan plot in MS: The association studies in MS susceptibility have a characteristic profile due to the striking association p-value of multiple SNPs in the HLA-DR locus on chromosome (ch) 6p21 that stands out from the plot. Non-HLA genes such as IL2RA, on ch10p15, and IL7RA, on ch5p13, showed also significantly evidence of association with MS (modified from Hafler et al. 2007).

Particular HLA alleles are strongly associated with MS risk. Studies reviewing the published data and pooled analysis of autoimmune disease-associated variants corroborate the findings showing HLA-DR2 and -DR3 serologically defined haplotypes as being associated with MS susceptibility in European populations (Fernando et al. 2008). The DRB1*15:01 allele has the strongest disease-specific association signal (Rioux et al. 2009) as confirmed by subsequent GWAS studies (Hafler et al. 2007; Patsopoulos et al. 2011; Sawcer et al. 2011). A GWAS by the IMSGC and the Wellcome Trust Case Control Consortium 2 (WTCCC2) has identified 95 distinct non-HLA regions associated with MS and with the most significant Gene Ontology (GO) terms linking these genes to lymphocyte function. The genes detected were, indeed, mainly of immunological relevance and belonged to cytokine pathways, co-stimulatory and signal transduction molecules confirming MS as an immune disorder targeting the brain (Sawcer et al. 2011). Not only the genetic background but also the interactions of the subject at risk with the environment play a role in the development of this complex disease.

1.1.2.2 Environmental risk factors

Although a specific genetic architecture is needed to develop MS, this cannot explain all the risk of this complex disease. Changes in risk occur with migration and geography. Environmental risk factors including infectious and non-infectious factors have to be taken into account (Ascherio and Munger 2007a; Ascherio and Munger 2007b). Among the non-infectious factors the latitude gradient could be explained by the difference in intensity of ultraviolet light in band B (UVB) and consequently its impact on vitamin D (vitD) levels. In fact, a protective effect of vitD on MS susceptibility can be detected from childhood to aduthood and probably *in utero* (Simon et al. 2012). Recently, studies of early life exposure analyzing the dietary habits such as milk intake or vitD intake of mothers, while pregnant, or the so called “month of birth effect” have shown a correlation with increased risk of developing MS in later life (Dobson et al. 2012; Mirzaei et al. 2011). Cigarette smoking has also been shown to contribute significantly to MS susceptibility and to have an effect on disease progression;

smokers have a worse prognosis than non-smokers as defined using either the rate of progression in the expanded disability status scale or MRI measures (Ascherio and Munger 2007b; Zivadinov et al. 2009). The mechanism of how cigarette smoking affects MS susceptibility has been shown to be independent from the action of nicotine, but possibly related to the cigarette smoke itself and its toxic components, mainly cyanide and nitric oxide (Hedstrom et al. 2009). In addition to these environmental risk factors, the causative role of an infectious pathogen in MS has been suggested as early as the first descriptions of the disease by Charcot and one of his students, Pierre Marie in the late 1800s (Tselis 2012). The presence of high concentrations of IgG in the brain and CSF of more than 90% of MS patients and possible epidemics of the disease in isolated populations and low (~30%) MS concordance in identical twins are quoted as evidence to support the role of an infection in MS (Gilden 2005; Gilden et al. 1996). To explain the epidemiology of MS, two hypotheses, having in common the presence of a widespread microbe as cause, have been proposed: the so called “poliomyelitis” and “prevalence” hypotheses. The first postulates that a viral infection can be harmful or protective depending on the age of the infection (Poskanzer et al. 1976); the latter postulates the presence of a pathogen more common in regions of high MS prevalence (Kurtzke 1993). Among the different infectious agents proposed as cause of MS (Giovannoni et al. 2006), EBV, a member of herpes viruses, has been implicated in several major autoimmune diseases, including systemic lupus erythematosus (SLE), rheumatoid arthritis (RA) and MS (Lunemann et al. 2007; Mehraein et al. 2004; Poole et al. 2009). Population based case-control studies and a meta-analysis have shown that the type of immune reaction to EBV and the age of EBV infection are associated with a different MS risk. Subjects who are EBV seronegative have a very “low risk” of developing MS. Individuals with history of symptomatic EBV infection, i.e. infectious mononucleosis (IM), have an increased risk of developing MS (Ascherio and Munger 2007a; Thacker et al. 2006; Zaadstra et al. 2008). Due to the extremely high prevalence of EBV infection in the general population, Canadian, European and American studies on paediatric populations showed significantly larger numerical difference between remote EBV exposure and MS in children (Alotaibi et al. 2004; Banwell

et al. 2007; Pohl et al. 2006). Findings highlighting that MS patients invariably have serologic evidence of remote EBV infection compared to control subjects. Nevertheless, there are some EBV seronegative cases of MS. A study on paediatric MS detected the disease in a low number of seronegative children (2 out of 147 children analysed); if genuinely seronegative, these cases may represent the key to understand the role of EBV infection in MS (Pohl et al. 2006).

Once the genetic and environmental factors interact the disease is triggered and clinical disease ensues. The first clinicopathological studies of MS were made by Jean Martin Charcot 160 years ago. Charcot linked signs and symptoms of the disease with localized damage to nerve fibres of the brain and spinal cord. Since then, knowledge about MS has expanded greatly; we now know that the typical lesion associated with the disease is due to area of demyelination, resulting from acute inflammation with relative axonal involvement – the so called “lesion or plaque”.

1.1.3 Immunopathogenesis

Inflammation, demyelination and neurodegeneration coexist in MS and determine the sequence of events underlying the development of the inflammatory plaque. The sequence of events in the formation of the plaque and its histopathological features can originate with a modification of the blood brain barrier (BBB) integrity. One hypothesis is that the BBB damage could be caused by a systemic infection up-regulating adhesion molecules on endothelium of the brain and altering CNS immune privilege (Frohman et al. 2006). The different presentations of the disease onset, the variable clinical course and the differences seen in the lesions imaged by MRI seem to support a concept of diversity or heterogeneity in multiple sclerosis (Lassmann et al. 1998). Studying acute lesions using 83 cases derived from autopsy and biopsy brain samples, Lucchinetti and colleagues in 2000 proposed a pathogenetic classification based on a distinction between the different pathological aspects of the disease. They proposed a degenerative/infective hypothesis with signs of oligodendrocyte dystrophy and a different autoimmune hypothesis with similarities to autoimmune encephalomyelitis. Lesions have been divided in 4 distinct patterns based on pathological heterogeneity (Lucchinetti et al. 2000; Ludwin 2000). In all four patterns there is demyelination, but a distinct putative initial mechanism mediated by: macrophage toxins in pattern I; presence of autoantibodies and complement deposition in pattern II; endothelial cell damage, microvessel thrombosis with ischemic damage followed by oligodendrocyte apoptosis as in concentric Balo's lesions in pattern III; metabolic damage with primary oligodendrocyte degeneration, resembling an oligodendropathy, in pattern IV (Lassmann et al. 2001). The concept that MS is a pathological heterogeneous disease has been very controversial as the tissue used in these studies were mainly from biopsy specimens which represents a selection bias; cases that are atypical and/or have an unusually aggressive clinical presentation at disease onset are more likely to be biopsied than "classical" MS (Pittock et al. 2005). These findings have been interpreted differently by other groups. For example, one group has described oligodendrocyte apoptosis in very early lesions and has interpreted the

apoptosis being part of lesion formation rather than representing lesion heterogeneity (Barnett and Prineas 2004).

The relapsing remitting course of MS at some point transitions into progressive deterioration with the accumulaton of irreversible disability related to the continuous loss of axons that follows demyelination (Trapp et al. 1998). There appears to be two distinct phases of MS. In the first, or very early phase, that develops over hours to days the newly forming lesion is predominated by oligodendrocyte apoptosis followed by transformation of activated microglia into amoeboid cells with a phagocytic phenotype. These cells then migrate to the cervical lymph nodes and result in the recruitment of a systemic immune response with enlargement of the lesion. The second phase over months to years corresponds to the gradual compartmentalization within the CNS of the immune response that is hypothesized to become isolated from systemic influence (Barnett and Sutton 2006) and it is characterized by areas of complete demyelination with lipid macrophages and presence of large numbers of T cells, B cells and IgG positive plasma cells supporting the theory that plaque formation starts before inflammatory damage (Henderson et al. 2009). Other neuropathological studies analyzing acute and chronic active lesions have not confirmed the oligodendrocyte apoptosis concept and challenge the heterogeneity model of active demyelinating lesions. The results of the study demonstrated rather a homogeneous pattern of demyelination suggesting that heterogeneity could be a characteristic only of the early phase converging during established disease in a homogeneous dominant mechanism mediated by antibody and complement phagocytosis by macrophages (Breij et al. 2008). The presence of lymphoid tissue in the perivascular spaces in old plaques organized in a way that resembles the antibody-producing medulla of lymph nodes, with aggregates of lymphocytes, reticular cells and macrophages, suggests that the lesions present a persistent antigenic stimulus (Prineas 1979). Lymphoid follicle-like structures found in the inflamed cerebral meninges of some multiple sclerosis patients sustain a locally B-cell maturation and formation of a CNS-specific humoral immune response supplying an anatomical explanation for grey matter lesions (Howell et al. 2011; Magliozzi et al. 2007). Furthermore, the presence of B-cells in the Virchow-Robin perivascular spaces

could be interpreted as a transitional step followed by maturation to plasma cells and migration into the plaque areas (Esiri 1980), where the inciting antigen is located as shown by the phenomenon known as capping, observed on macrophages presenting IgG caps bound to Fc receptors and directed against myelin in the plaque rim (Prineas and Graham 1981). In different viral diseases of the CNS, with an inflammatory response, similar findings to MS were observed with Ig containing cells at the site of damage, excess of light chains and IgG as preponderant heavy chain class directing the attention towards an immune response against a viral antigen or supposed viral antigen, not yet defined with certainty, to which the individual has been previously exposed (Esiri 1983). However presence of plasma cells in recent and old plaques, oligoclonal bands in the CSF and clonal expansion of B-cells in the cerebrospinal fluid and brain parenchyma of MS patients support a disease specific Ig production. The data reported show a complex mechanism leading to plaque formation with involvement of different immune cell types and responses.

1.1.3.1 Innate Immunity

Innate immunity is a multi-component system composed of cellular barriers, i.e. the BBB in the CNS, and innate immune peripheral cells of myeloid origin, such as dendritic cells (DC), macrophages, monocytes, NK cells, NKT cells, mast cells, granulocytes, γδ T-cells but also microglia and astrocytes, of non-myeloid origin, in the CNS (Mayo et al. 2012). The cellular component includes dendritic cells, known as professional antigen presenting cells (APCs), which are divided into two subsets, i.e. myeloid (mDCs) and plasmacytoid (pDCs) dendritic cells, based on their cell surface molecules. DCs are found in peripheral blood and in MS lesions. DCs are essential in determining the pro-inflammatory or regulatory fate of the T-cells and consequently the disease course. In RRMS and SPMS patients DCs exhibit altered function with enhanced production of pro-inflammatory cytokines (Karni et al. 2006). Accumulation of pDCs has been also described in the inflamed meninges, of both acute and chronic MS lesions, highlighting their involvement in the immunopathogenesis of MS. INF-β therapy

may work in MS by interfering with DC maturation, increasing the regulatory ability of these cells (Lande et al. 2008). In animal models DCs have shown encephalitogenic properties being the only APC required to initiate adoptive transfer of EAE (Greter et al. 2005). Animal models have also shown that induction of EAE is regulated by toll-like receptors (TLRs); activated microglia express all known TLRs that have been shown to regulate neuroimmune responses (Aravalli et al. 2007; Marta et al. 2009). In addition, histopathological studies of actively demyelinating lesions have shown that microglia are found in areas of neuronal damage; they actively phagocytose neuronal debris and modulate the antineuronal adaptive response (Huizinga et al. 2012). The data reported suggest dual protective and detrimental, roles of the innate immune system in balancing the neuroinflammatory reaction in MS. The innate immune system also represents a potential new target to treat MS.

1.1.3.2 Adaptive Immunity

Genetic, histopathological and animal model studies have shown beyond doubt that the adaptive immune system is involved in the pathogenesis of MS. Numerous therapies targeting the adaptive immune response are used to treat MS. Studies on EAE, disease that can be induced by injecting unaffected animals with autoreactive T-cells, have focused attention on myelin-specific CD4+ T-cells (Baker et al. 1990). Analogous with EAE, autoreactive T-cells have been found in the peripheral blood and CSF of MS patients (Bielekova et al. 2004; Zhang et al. 1994). In the periphery naive T-cells differentiate into either pro-inflammatory encephalitogenic effector Th1, Th17 and Th9 cells that are presumably activated by an unknown trigger, or regulatory Th2 and Tregs cells as a result of the the cytokines milieu produced by APCs (Boppana et al. 2011). Naïve CD4+ T-cells after the initial encounter with the antigen are induced by APC secreting IL-12 to differentiate into Th1 cells with the subsequent production of interferon gamma (INF-γ) and tumor necrosis factor alpha (TNF-α). In comparison, the production of IL-23 by macrophages and dendritic cells combined with inflammatory cytokines TGF-β and IL-1β induces T cells to differentiate into Th17, cells characterized by production of IL-17 and

IL-22. EAE models emphasize the complex interactions between these two IL-12p40-dependent polarities of pathogenic myelin-specific CD4+T-cells that are polarized by either IL-12 or IL-23; both are able to adoptively transfer disease (Kroenke et al. 2008). The IL12/IL23 p40 subunit was targeted in a phase II clinical trial with a neutralizing monoclonal antibody, ustekinumab. Ustekinumab-treated patients showed no reduction in number of new Gd-enhancing lesions. IL-12 or IL-23 are involved early in the development of autoreactive T cells differentiation and ustekinumab may have missed the window in which it could have been effective (Richl et al. 2008; Segal et al. 2008). Histological studies have confirmed that Th17 cells are involved in MS; Th17 cells have been described in perivascular cuffs of acute and chronic active MS lesions (Tzartos et al. 2008). In peripheral lymphoid organs reactivity of myelin-specific T-cells is suppressed by another subset of CD4+ T-cells expressing forkhead box p3 (Foxp3) and high levels of α-chain of the IL2 receptor (CD25). CD4+CD25+Foxp3+ T-cells use a mechanism of suppression that requires cell-cell interactions. These cells are characterized by secretion of IL-10 and TGF-β and are crucial in the maintenance of self-tolerance (Venken et al. 2010). The immunological balance has been hypothesized to be dysregulated in MS by this lineage of T-cells, i.e. Foxp3 regulatory T-cells (Tregs), playing a compromised regulatory role (Comabella and Khoury 2012). Interestingly, CD4+CD25+Tregs obtained from the peripheral blood of RRMS patients are present at the same frequency as in controls but show impaired suppressor function, on proliferation, when co-cultured with CD4+CD25- T-cells. This is supported by the lack of suppression of INF-γ secretion (Viglietta et al. 2004). As described for CD4+ T-cells, adoptive transfer of myelin-specific CD8+ T-cells has encephalitogenic properties and induce EAE in certain mouse strains (Huang et al. 1992). In both perivascular regions and cell infiltrates of actively demyelinating MS lesions, histopathological studies have described CD8+ T-cells as the dominant T-cell subset, outnumbering CD4+ T-cells. Infiltrates in MS lesions have been reported to be dominated by clonally expanded CD8+ T-cells suggesting antigen-driven activation (Babbe et al. 2000) and a pathogenic role with axonal damage resulting in neurodegeneration (Bitsch et al. 2000). Not only are different subsets of T cells involved in the

adaptive response in MS but B cells also appear to play an important role as detailed below.

1.1.3.3 B cells and MS

B-cells can contribute to MS pathogenesis as APC and/or as cells producing antibodies. This dual function explains the difficulties in delineating the exact role of the B cell in the immunopathogenesis of MS (Cross and Waubant 2011; Weber et al. 2011). As highlighted from pathological studies B-cells are present in different areas of the CNS in MS with a gradient of increasing B-cells infiltration from NAWM to recent plaques, with increasing inflammatory activity (Esiri 1977). B-cells presence permeates the CNS of MS patients in perivascular spaces, chronic and active plaques (Prineas 1979; Prineas and Wright 1978) but also as part of meningeal follicle-like structures seen in SPMS as an outcome of the hypothesised compartmentalization of the immune response in chronic inflammation (Aloisi and Pujol-Borrell 2006; Magliozzi et al. 2007; Serafini et al. 2004). B-cells activity has been associated by some authors with the most frequent pattern of actively demyelinating lesions, the so called pattern II lesion that is positive for Igs and with complement deposition and activation (Lucchinetti et al. 2000) and with grey matter lesions, that point to Igs having an active and detrimental effect (Howell et al. 2011; Magliozzi et al. 2007). B-cells are absent from the CSF in normal controls but are found in the majority of CSF samples from people with MS. The B-cells found in the CSF have a memory, and short-lived plasma blast, phenotype that seems to persist throughout the course of the disease and correlates with the intrathecal synthesis of Igs (Cepok et al. 2005a). Intrathecal B cell maturation is driven locally by CXCL13, with a resulting enrichment of plasmablasts and plasma cells (Haas et al. 2011). B-cells that are found in the CSF of MS patients are clonally expanded, presenting somatic hypermutation of Ig genes and expressing a biased VH repertoire indicating an antigen driven response and a germinal centre reaction (Baranzini et al. 1999; Colombo et al. 2000; Haubold et al. 2004; Owens et al. 1998; Owens et al. 2003; Qin et al. 1998; Smith-Jensen et al. 2000). The role of B-cells in the pathogenesis of MS is underscored by the

presence and persistent elevated levels of Igs in the CSF and detection of a CSF restricted oligoclonal electrophoretic profile (Kabat et al. 1942). The specificity and pathological significance of the intrathecal antibody response remains undefined. The analysis of the CSF Ig proteome compared with the transcriptomes of antibody secreting cells (ASC) from CSF and brain lesions has demonstrated an overlap between the two Ig repertoires showing that the antibodies found in the CSF are the shared product of ASC resident in the CNS at different levels (Obermeier et al. 2011; Obermeier et al. 2008). Finding further confirmed by the results of a study showing a shared reactivity between the native CSF IgG and recombinant Abs (rAbs) generated from paired heavy and light V genes of clonally expanded plasma cells found in the CSF of MS patients (Yu et al. 2011). Even so, it has proven challenging to unveil the specific ligands of CSF Igs in absence of a known pathological causative agent. Several studies have selected different mimotopes from phage-displayed random peptide libraries (RPLs) biopanned against CSF and serum IgG of MS patients. Antibodies from CSF and serum of the same patient displayed the same binding specificities but CSF antibodies from different patients displayed different specificities. This finding supported the view of a CNS restricted individual-specific response. Besides, selected phagotopes (epitopes expressed on phage) were reactive against sera from different MS patients and normal individuals underlining that these antibodies could be directed against rather ubiquitous antigens to which many individuals are exposed (Cortese et al. 1998a; Cortese et al. 1998b; Cortese et al. 1996). Further investigated in search for the natural antigens mimicked, one of the mimotopes recognized by antibodies enriched in the CSF of MS patients cross-reacted between a protein of Herpes Simplex Virus type-1 and a protein from MS brain tissue, supporting the concept of mimicry as possible trigger of MS inflammatory process (Cortese et al. 2001). Other studies utilizing various RPLs did identify different amino acid motifs shared by EBV nuclear protein and alpha-beta crystallin (Rand et al. 1998) or with significant linear homology with different EBV components (Fujimori et al. 2011) or with human collagen, 68 KDa neurofilament protein, different viruses from herpesviridae and papillomaviridae families (Dybwad et al. 1997), but also with retroviral agents such as HERV-W and MSRV (Jolivet-

Reynaud et al. 1999). The individual specificity is still debated as another study utilizing RPL not only showed that affinity selected epitopes/mimotopes cross-react between rAbs and native IgG from the same patients but also share specificity with intratechally synthesized IgG from different MS patients but not control patients. Finding pointing to a potentially relevant common shared CNS antigen to the pathogenesis of MS (Yu et al. 2011). In fact as the antibodies are enriched only in the CSF, it is possible that only B cells with a specificity for antigens found in the CNS are able to survive and clonally expand. Furthermore, expression cDNA libraries obtained from human brain and oligodendrocite-precursor cell line screened with CSF and serum of MS patients reacted respectively with EBV proteins expressed in latency phase, EBNA-1 and BRRF2 (Cepok et al. 2005b) or with Alu peptides (Archelos et al. 1998). Nevertheless, the specificity of the OCBs is still debated as well as the involvement of the main myelin antigens in the pathogenetic process. Controversial specificity of the OCBs confirmed by a study showing that none of the rAbs derived from MS CSF B-cells displayed immuno-reactivity to three of the main putative myelin auto-antigens tested (Owens et al. 2009). However recent studies have described reactivity of CSF antibodies, not only against native proteins, but also against denatured proteins, lipids and lipid complexes (Brennan et al. 2011). Nevertheless, the extraction of antibodies from MS lesions has revealed the presence of anti-myelin antibodies at higher concentration and affinity when compared with serum and CSF compartments, indicating the local production or accumulation in the inflammatory tissue of B cells products (O'connor et al. 2005).

Approximately 30% of MS patients have CSF antibodies that react against MBP (Cruz et al. 1987). In children presenting with a first demyelinating episode intrathecal IgG anti-MOG antibody synthesis is seen in a minority of cases with CIS (Brilot et al. 2009). Some authors report the presence of anti-myelin antibodies as useful marker to predict conversion to MS after a first demyelinating episode (Berger et al. 2003), however, this finding was not confirmed by others (Kuhle et al. 2007). The diagnostic utility and significance of myelin autoantibodies is still debated as some other authors described low affinity Igs not only in neuroinflammatory diseases but also in healthy controls

(Lampasona et al. 2004). One of the main aims of my PhD has been to help clarify certain issues in relation to the ongoing debate on the specificity of intrathecal Igs in MS, with the hope of finding a prognostic marker. Interestingly, in a recent study to use an antibody phage display library, Gabibov and colleagues have shown that antibody from blood lymphocytes of 8 RRMS patients cross-react against MBP and EBV latent membrane protein 1 (LMP1) (Gabibov et al. 2011). The importance of the role of B cells as APC has been highlighted by the use of B cell depleting therapies (clinical trials and target Ags discussed further below).

1.1.4 Diagnosis, Clinical course and Prognosis

The clinical onset of the MS may be acute or insidious and the severity can vary from the need for hospitalization to relatively non-specific symptoms. The most common symptoms that patients experience at the onset are in order of frequency sensory disturbances (34%), weakness (22%), visual loss (13%), ataxia (11%), diplopia (8%), vertigo (4.3%), abnormal gait, loss of dexterity or sphincter disturbances. Non-specific symptoms such as malaise, fatigue or headache may precede the onset of MS (Cree 2010; Swingler and Compston 1992). Diagnostic criteria have evolved over the years with the aim of simplifying the diagnosis and to be applied consistently. The most contemporary criteria used are the 2010 revisited McDonald Criteria for Multiple Sclerosis (Polman et al. 2011), that replaced the widely-used Poser criteria (Poser et al. 1983). Although the disease course of MS is characterized by multiple attacks affecting different regions of the CNS over time, the first symptomatic demyelinating event is known as a clinically isolated syndrome (CIS). Natural history studies show that patients presenting with a CIS that have lesions on their initial MRI scan have a 82% risk of having a second attack after 20 years of follow-up and only 21% risk if the brain MRI is normal (Fisniku et al. 2008; Miller et al. 2005a; 2005b). Attacks, exacerbations or “relapses” are linked to plaque formation and the following resolution of the inflammation and remyelination allow the patient to recover. The periods between relapses are called “remissions”, so that the alternating episodes of relapses and remissions give rise to the term relapsing-remitting MS (RRMS). The clinical course of the disease is divided in patterns and in most patients (80-85%) the disease initially follows a RRMS course characterized by relapses followed by varying degrees of recovery. The RR course is defined as by the occurrence of clearly defined relapses with, or without, full or partial recovery. Periods between relapses are characterized by a lack of disease progression. Often, the RRMS evolves into a stage when the disease progresses slowly, i.e. the secondary progressive phase. The SP stage is reached after a median time of 10-20 years (Koch et al. 2010; Tremlett et al. 2006; Weinshenker et al. 1989). The SP course is defined as: initial RR disease course followed by progression with or without occasional relapses, minor remissions, and plateaus. Patients develop progressive

ambulatory disability, with some eventually becoming bed bound. There is a group of patients, who have a progressive course from the onset of the disease without relapses or remissions, this course has been defined primary progressive (PP) (Tullman et al. 2004; Wingerchuk et al. 2001). The PP course is defined as: disease progression from onset with occasional plateaus and temporary minor improvements allowed. The usual clinical pattern seen in MS follows the RR and SP course but a 10-15% of patients present PPMS (Hawker 2010). The most common presenting symptoms described in PPMS are: motor deficit (38.9%), followed by sensory impairment (32.5%), cerebellar symptoms (16%) and brainstem involvement (5.3%). Optic neuropathy is uncommon as an initial feature (Cottrell et al. 1999). In the PPMS population there is no female preponderance as in the RRMS and SPMS, and the mean age of onset is older: 40 years for PPMS versus 30 years for RRMS. The PPMS lesions evaluated by neuroimaging are identical to that of RRMS or SPMS. The number and total volume of plaques within the brain of patients with PPMS tend to be fewer than that observed in RRMS and SPMS, with a distribution of the lesions clustered around the ventricles (Di Perri et al. 2008). Furthermore, actively demyelinating plaques that show uptake of gadolinium-DPTA (Diethylene triamine pentaacetic acid) contrast on brain MRI are observed less often in PPMS (Tremlett et al. 2005). Approximately 5% of patients with MS have progressive symptoms from onset and will also have rare relapses. This disease course is termed progressive-relapsing MS. (Fig.1.3)

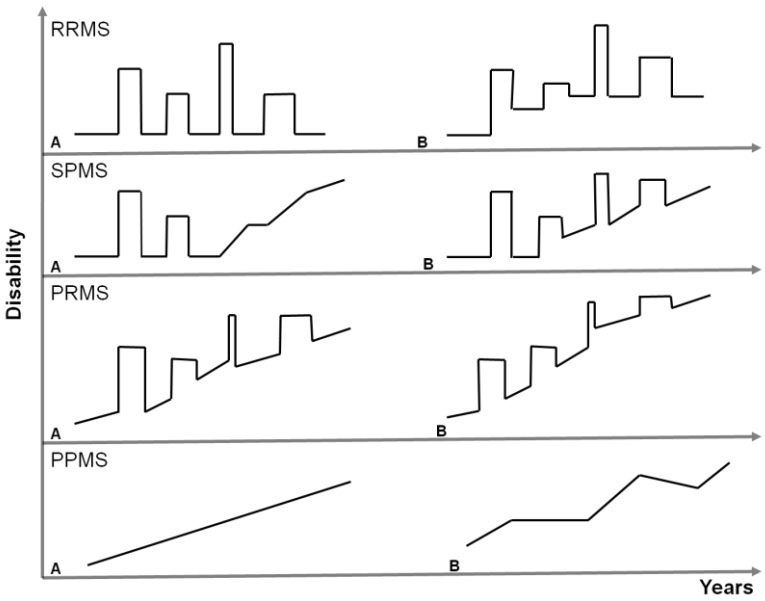

Figure 1.3 MS clinical course patterns: Relapsing remitting MS (RRMS) presenting attacks with full recovery (A) or with sequelae and residual deficit (B); secondary progressive MS (SPMS) with progression of variable rate (A) or with occasional relapses and minor remissions (B); progressive relapsing MS (PRMS) with clear acute relapses with (A) or without (B) full recovery; and primary progressive MS (PPMS) without remissions (A) or with occasional temporary minor improvements (B).

The diagnosis of MS relies on recognition of the clinical pattern of disease with demonstration of lesions that are distributed in time and space and to this purpose several paraclinical tests have been applied to help make the diagnosis of MS and exclude alternative diagnosis.

There are three principal studies that are used to support the diagnosis of MS: neuroimaging, laboratory and electrophysiological tests.

1.1.4.1 Neuroimaging

As highlighted in the diagnostic criteria a central and particularly useful diagnostic role is played by magnetic resonance imaging (MRI). MRI is a sensitive imaging technique in particular for detecting inflammatory demyelinating lesions in the white matter of the brain. The brain MRI is abnormal in 95% to 99% of cases of RRMS. An abnormal MRI is not sufficient to make the diagnosis of MS but it supports the clinical diagnosis in that it can be used to demonstrate both dissemination in time and place and is helpful in excluding other potential diagnoses. MS lesions appear as abnormal signal intensity on T2-weighted sequences: T2, proton density and fluid-attenuation inversion recovery (FLAIR); in fact, almost any alteration in brain tissue composition such as oedema, inflammation, demyelination, gliosis and axonal loss will increase the signal in such sequences highlighting acute and chronic phase lesions (Barkhof and Van Walderveen 1999). Gadolinium enhancement corresponds pathologically to active areas of inflammation and can be used as marker of blood-brain barrier integrity and typically persists for an average of 3 weeks and then subsides (Cotton et al. 2003). Lesion that associated histopathologically with severe tissue destruction and axonal loss, are visualized on T1-weighted images as hypointense lesions called T1 “black holes”. MRI is an important prognostic tool in patients presenting with CIS; MRI useful to determine dissemination in space and time, which is some circumstances can be done with a single MRI scan. Recently new simpler MRI criteria based on the criteria proposed by Swanton et al. have been adopted by the 2010 revisited McDonald diagnostic criteria without compromising specificity and accuracy and increasing sensitivity (Swanton et al. 2006) (Montalban et al. 2010; Swanton et al. 2007).

	DIS	DIT	Ref.
McDonald 2001	≥3 of the following: 9 T2 lesions or 1 Gd-enhancing lesion; ≥3 periventricular lesions; ≥1 juxtacortical lesion; ≥1 posterior fossa lesion 1 spinal cord lesion can replace 1 brain lesion	A Gd-enhancing lesion ≥3 months after CIS onset; A new T2 lesion with reference to a previous scan ≥3 months after CIS onset	McDonald et al 2001
McDonald 2005	≥3 of the following: 9 T2 lesions or 1 Gd-enhancing lesion; ≥3 periventricular lesions; ≥1 juxtacortical lesion; ≥1 posterior fossa lesion or spinal cord lesion A spinal cord lesion can replace a infratentorial lesion Any number of spinal-cord lesions can be included in total lesion count	A Gd-enhancing lesion ≥3 months after CIS onset; A new T2 lesion with reference to a baseline scan obtained ≥30 days after CIS onset	Polman et al. 2005
New Criteria	≥1 lesion in each of ≥2 characteristic locations: periventricular, juxtacortical,posterior fossa, spinal cord All lesions in symptomatic region excluded in brainstem and spinal-cord syndromes	A new T2 lesion on follow-up MRI irrespective of timing of baseline scan	Swanton et al. 2006

Table 1.1 MRI criteria MAGNIMS: Comparison of MRI criteria for dissemination in space (DIS) and time (DIT) (modified from Swanton, Rovira et al. 2007)

1.1.4.2 Evoked potentials

Multimodal evoked potentials are another set of diagnosic tools that can be used to demonstrate clinically silent lesions in specific anatomical pathways. Evoked potentials also provide functional information, for example slowed conduction that is indicative of demyelination (Fuhr and Kappos 2001). Several pathways can be evaluated, i.e. visual, brainstem auditory, somatosensory and motor evoked potentials (Leocani and Comi 2008).

1.1.4.3 Laboratory

The laboratory analysis of the cerebrospinal fluid (CSF) provides additional information regarding the CNS and, in case of neuroimmunological diseases, it provides information on the presence or absence of intrathecal inflammation (Gafson and Giovannoni 2012). Typical CSF parameters that are assessed are the cell count, the CSF/serum albumin ratio to evaluate the blood-brain barrier (BBB), the IgG index a quantitative index of intrathecal Ig production that is

performed on paired CSF and serum samples, CSF glucose and lactate concentrations (Andersson et al. 1994; Deisenhammer et al. 2006).

Of the quantitative CSF tests used to support the diagnosis of MS the IgG index has the highest sensitivity. An elevated IgG index indicates increased production of IgG within the CNS and is found in 70 to 90% of MS cases. The IgG index value results from the ratio of the quotient of IgG concentration in CSF and serum (QIgG) and the quotient of albumin concentration in CSF and serum (QAlb).

IgG index = IgG CSF/IgG serum : albumin CSF/albumin serum

The IgG index simply quantifies the amount of IgG that is synthesised within the CNS correcting for BBB leakage (Link and Tibbling 1977a; 1977b; Tibbling et al. 1977) (Fig.1.4).

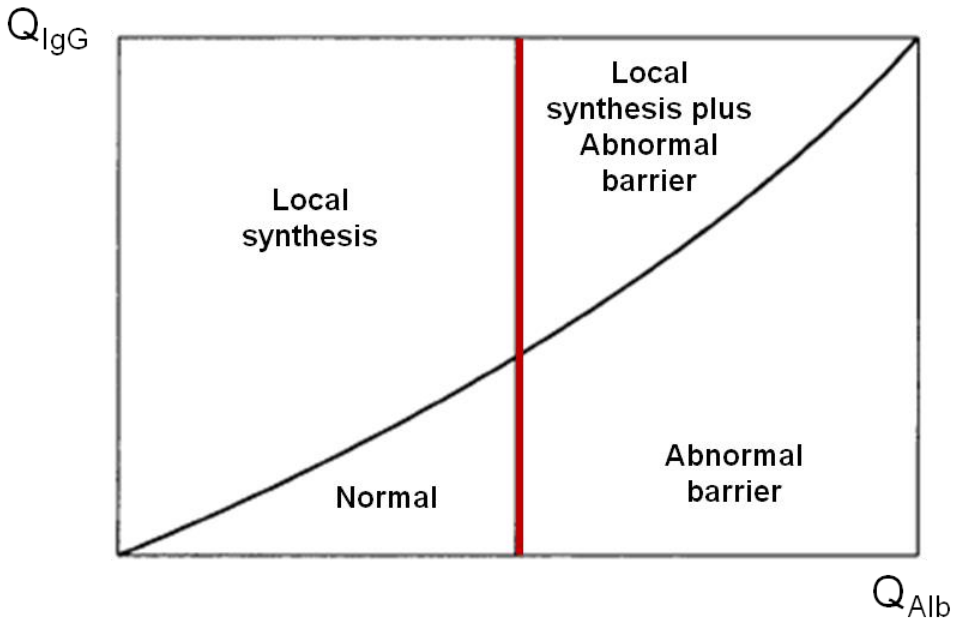

Figure 1.4 CSF IgG index: Values for the quotient of IgG in CSF/IgG in serum (QIgG) are shown on the y axis and values for the quotient of albumin in CSF/albumin in serum (QAlb) are shown on the x axis. The graph evaluates blood brain barrier (BBB) function and IgG local synthesis. The red line separates the normal from abnormal BBB function and the hyperbolic line the local synthesis from not local synthesis (Andersson et al. 1994).

Qualitative test of intrathecal IgG synthesis, however, are more sensitive that quantitative indices. Isoelectric focusing (IEF) is considered the qualitative “gold standard” for detecting OCBs of the IgG class. IEF uses the same amount of IgG in paired CSF and serum specimens that are run in parallel (Davenport and Keren 1988; Kostulas et al. 1987). The strongest consensus is that protein separation by IEF followed by immunoblotting is the most sensitive test for detection of an abnormal Igs production in MS with a sharper and easier interpretation of the results; i.e. an average number of 8 bands are detected in positive samples compared to 2 bands by other tests, i.e. agarose gel electrophoresis (AGE) (Fortini et al. 2003). The presence of OCBs is not MS specific and is found in CNS infections, paraneoplastic disorders of the CNS and other putative autoimmune diseases. The IEF immunoblot findings are classified into patterns based on where the synthesis of Igs takes place, intrathecally or peripherally (Andersson et al. 1994; Freedman et al. 2005). In the CSF of MS patients the increased intrathecal humoral immune response is not limited to Igs of class IgG but in 30-60% of cases Igs of class IgM are found (Villar et al. 2001) and the IEF patterns can be divided in two groups based on the type of Ig detected, IgG or IgM, or on the presence or absence of intrathecal synthesis (Fig.1.5). Even if IgG and IgM have different migration zones, the different patterns reflect the comparison of CSF and serum Igs migration. The intrathecal IgM synthesis (ITMS) in different neurological diseases seems to be a primary response in infectious diseases, as 83% of all the patients with infections analysed within 1 month from symptoms onset were positive and subsequently became negative within 3 months, while in MS patients it appears to be a persistent response with no association found between ITMS and disease duration confirming once again the temporal invariance and the finding of IgG OCBs negative patients that become positive later on (Villar et al. 2001; Villar et al. 2002) (Fig.1.5).

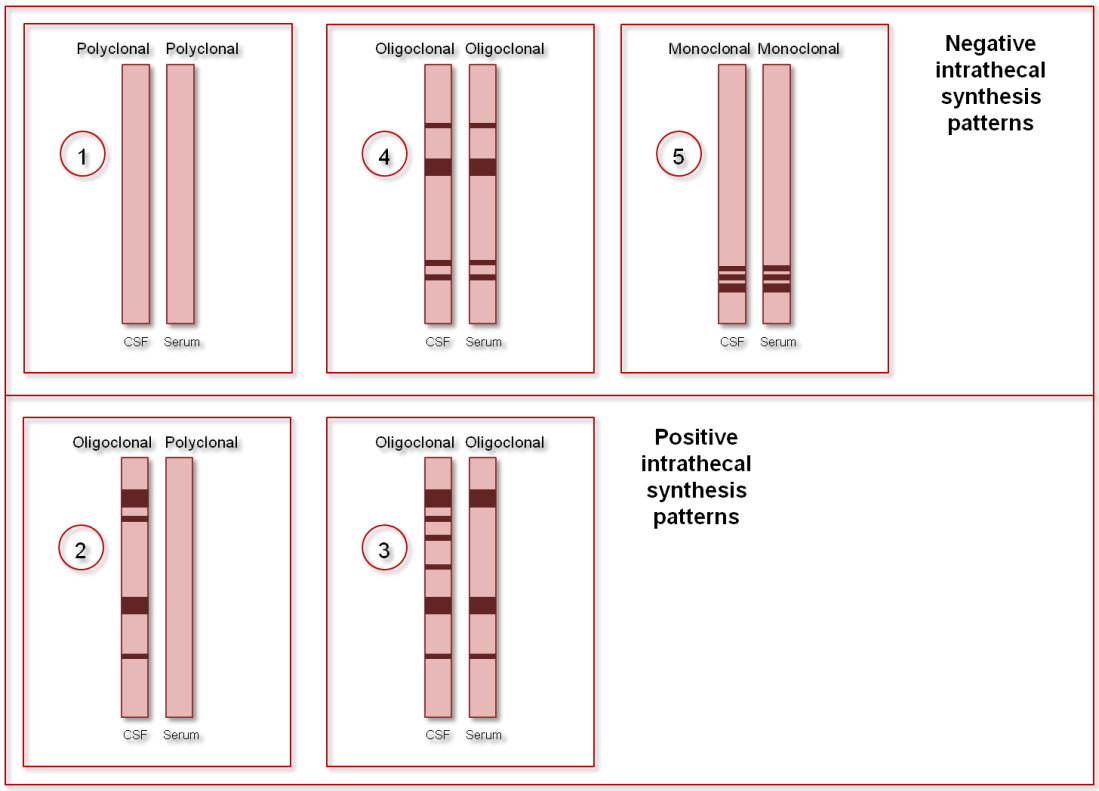

Figure 1.5 Igs IEF Patterns: Type 1: normal pattern; Type 2: intrathecal Igs synthesis as seen in neuroinflammation, neuroinfections and typically MS; Type 3: intrathecal Igs synthesis "plus" in systemic and paraneoplastic diseases; Type 4: systemic inflammation (oligoclonal mirror pattern); Type 5: monoclonal gammopathy (monoclonal mirror pattern or ladder pattern).

The detection of Igs of class IgA in the CSF is controversial as the IEF technique gives artefactual results and there is no consensus on the detection of this class of Igs and consequently this class of Igs is not used for diagnostic purposes (Mehta et al. 1984; Sindic et al. 1984). Nevertheless, 70% of MS patients have intrathecal cells producing IgA (Henriksson et al. 1985) and 7.3% of immunoglobulin-containing cells have been shown to be IgA-positive by an immunohistological study analysing 100 plaques and 100 NAWM areas (Esiri 1977). Clonally expanded IgA-postive plasma cells with somatic hypermutations have been detected in brain lesions of MS patients and IgA antibodies have been localized to the surface of axons. The findings showed evidence of damage in MS plaques with plasma cells likely driven by environmental pathogens that share antigens with axons (Zhang et al. 2005).

In healthy individuals either kappa or lambda light chains are incorporated into complete immunoglobulins in roughly equal proportion. Light chains are synthesized in excess and are found in different biological fluids as polyclonal free light chains (FLC). FLC are considered to have different biological functions, such as enzymatic activity, specific antigen binding activities and immune regulation via binding to different cells, in particular mast cells (Thio et al. 2008; Van Der Heijden et al. 2006). Oligoclonal and monoclonal expansion of FLC occur in some autoimmune diseases, such as MS, and malignancies. In IgG OCBs positive MS patients the normal kappa/lambda ratio is altered with predominance of kappa light chains in 93% of cases of clinically definite MS (CDMS) (Jenkins et al. 2001; Mattson et al. 1982). Intrathecal synthesis of FLC is a marker of an ongoing immune response within the CNS and high levels of FLC can be detected in MS patients and patients with CNS infectious diseases.

The diagnostic importance of OCBs is highlighted by the presence of a single band on the immunoblot. At the initial CSF examination, a single band or isolated monoclonal pattern can lead to three possible developments such as 1) conversion to an oligoclonal pattern, 2) persistence of the intrathecal monoclonal band and 3) disappearance of the band with normal immunoblot on follow up. In the cases that convert to an oligoclonal pattern the clinical diagnosis has mainly been shown to be MS (Davies et al. 2003). In fact the presence of a single band can make the difference with regard to a diagnosis of MS; the presence of a single band should hint for the presence of another disease apart from multiple sclerosis (Ben-Hur et al. 1996). The mentioned cases show the utility of FLC evaluation particularly as the presence of elevated KFLC has been correlated with dissemination in space of MS lesions and has been considered as a substitute for the detection of OCBs in MS diagnostic criteria.

In the clinical practice the absence of OCBs in patients with MS usually raises doubts on the reliability of the diagnosis and leads to review the diagnosis; but patients who fulfill the criteria as having CDMS and also CIS patients do not always show intrathecal synthesis of IgG OCBs. A recent meta-analysis has shown an overall OCB positivity of around 90% in CDMS and of around 70% in CIS patients, if only the studies using IEF with immunofixation were considered (Dobson et al. 2013). The OCBs negative group constitutes 5-50% of all MS patients depending on the populations studied. OCB positivity in the CSF, indeed, has a variable distribution in different MS populations with Northern European countries having the highest rates of positivity, ~95%, and Southern European, South American and Eastern, i.e. Japan (~53%), countries having a lower positivity rate (Lourenco et al. 2013). OCB-positive and OCB-negative MS patients have been analysed by different studies to determine whether constitute different subpopulations regarding clinical, demographic and genetic background. Conflicting data have been highlighted on the OCB-negative MS population with data showing a better, worse or equal disease progression and prognosis. A cross-sectional multicenter study did show a highly significant association among a younger age at onset, an increased EDSS and OCB positivity (Lechner-Scott et al. 2012), confirming a previous UK case-control study showing a better prognosis for disability in OCB-negative patients (Joseph et al. 2009). OCB positivity has been found also to correlate with a higher risk of progressive disease course confirming the same trend found also in a Canadian study (Lourenco et al. 2013). Lack of OCBs has also been correlated with low number of active plaques and low plasma cells infiltration in the brain and meninges based on a clinical-pathological study (Farrell et al. 1985). Findings possibly representing a non-antibody-mediated demyelination pattern (Lucchinetti et al. 2000) and pointing to a possible pathogenic role of autoantibodies (Stendahl-Brodin and Link 1980; Zeman et al. 1996). Other studies have shown the same clinical features between OCB-positive and OCB-negative patients (Imrell et al. 2006) or a better clinical course with less disability and better prognosis in OCB-positive patients (Idiman et al. 2009) in presence of a particular genetic background. Infact OCB-positive and OCB-negative populations seem to differ immunogenetically, with the association of

HLA-DRB1*15:01 allele and risk of MS being more prominent and restricted to OCB positive MS patients, whereas the OCB-negative subgroup of patients being associated to the HLA-DRB1*0404 allele (Idiman et al. 2009; Imrell et al. 2006; Mero et al. 2013).

MRZ reaction

The intrathecal synthesis of IgG is not only useful as a diagnostic tool but may point to the identification of the target antigen(s). In MS the antigenic target of intrathecal OCBs is still unknown and one of the aim of this project is to help clarify their specificity. Nevertheless, numerous studies have identified antibody reactivity against autoantigens (discussed below) as well as against different neurotropic viruses as part of the amnestic immune response. The frequency of intrathecal synthesis of specific IgGs in MS is 75% against measles (M), 60% rubella (R) and 55% varicella-zoster virus (Z). Detection of the combined intrathecal antibody synthesis against measles, rubella and/or zoster virus is named “MRZ reaction” (MRZR) and is found in around 90% of MS patients (Arnadottir et al. 1982; Reiber et al. 1998). MRZR has been recognized as a predictive or prognostic marker for the conversion from CIS to definite MS; approximately 60% of patients with acute monosymptomatic optic neuritis or CIS with intrathecal production of virus-specific oligoclonal antibodies (MRZR) go onto develop definite MS (Frederiksen and Sindic 1998). It has been reported that the MRZ reaction is as specific as OCBs detection for conversion from CIS to MS; the specificity increases when associated with 2 or more T2 hyperintense lesions in MRI (Brettschneider et al. 2009).

1.1.5 Therapy

Almost all current treatments available for MS target the immune system as different immune cell populations interact to cause damage. None of the current therapies has been shown to cure MS; in general these treatments are only partially effective. First-line treatments, known as disease-modifying treatments (DMTs), aim to modify the disease course reducing the number and severity of relapses and hence the acquisition of disability. At resent no treatment has been approved for the treatment of PPMS. The DMTs approved for the treatment of RRMS include several different interferon beta (INFβ) formulations and glatiramer acetate (GA). These agents main mechanisms of action are on different T-cell subsets. These agents have been described as shifting the immune response from a proinflammatory to an anti-inflammatory profile by inhibiting autoreactive Th1 cells and induction of regulatory T cells and Th2 cells. INFβ also acts by reducing lymphocyte trafficking into the CNS and modifying the cytokine milieu (Dhib-Jalbut and Marks 2010). Interferon therapy is limited by the development of binding and neutralizing antibodies in a subset of patients (Farrell et al. 2011; Farrell et al. 2012). The alternative DMT is GA, known as copolymer 1, is a synthetic amino acid polymer composed of a mixture of L-glutamic acid, L-lysine, L-alanine and L-tyrosine. GA may act directly on APCs and modify their cytokine profile and subsequently influence T cell differentiation with expansion of the Treg subset and shift to a regulatory phenotype of CD8+ T cells (Racke et al. 2010).

Other current treatments approved for management of MS are generally considered second-line treatments for highly aggressive cases and are a mAb, natalizumab, and the oral agent, fingolimod. Both agents are immunosuppressants. Natalizumab stops lymphocytes from crossing the endothelium of the CNS. In comparison, fingolimod, traps circulating lymphocytes in peripheral lymphatic tissues. Natalizumab is a humanized mAb that blocks the vascular cell adhesion molecule 1 (VCAM1) / very late antigen-4 (VLA-4) ligand-receptor pair interaction. These molecules are expressed respectively on capillary endothelial cells, monocytes and lymphocytes. Natalizumab inhibits the transmigration of α4-integrin expressing lymphocytes

into the CNS parenchyma (Rudick et al. 2012). The down side of natalizumab therapy is that it also blocks normal CNS immune surveillance and as a result CNS infections, in particular progressive multifocal leukoencephalopathy (PML), are a problem with the drug. The current risk of PML is estimated at 2.13 cases per 1000 patients (95% CI, 1.85-2.44) (Rudick et al. 2012). In 2010 the first oral therapy, fingolimod, was licensed for the treatment of relapsing MS. Fingolimod is a sphingosine 1-phosphate (S1P) receptor modulator that internalises S1P receptor on circulating lymphocytes inhibiting their egress from secondary lymphoid organs and acting as immunomodulator (Sanna et al. 2004). Efficacy has been demonstrated by three phase 3 trials with respect to both relapses and MRI outcomes compared to placebo and INFβ therapy (Cohen et al. 2010; Kappos et al. 2010).

1.1.5.1 Clinical trials (anti CD20)

In MS the presence of OCBs and reports of dramatic improvement from plasma exchange in patients with corticosteroid resistant relapses has resulted in the targeting of B-cells as a therapeutic strategy (Rodriguez et al. 1993). The surface antigen CD20 is expressed specifically on B cell lineage from pre-B cell stage to memory B cell but not on differentiated plasma cells. The B-cell lineage can therefore be targeted via CD20. The chimeric antibody rituximab and the more humanized versions ocrelizumaband fully humanized version, ofatumumab have been tested in clinical trials. Outcomes from these trials have highlighted the importance of Ab-independent B-cell functions and the need of new target molecules specific for distinct B cell subsets (Barun and Bar-Or 2012). Rituximab a chimeric murine/human IgG1 mAb has been tested in 4 clinical trials in RRMS and PPMS. Two open label trials in RRMS have evaluated rituximab safety and tolerability as a monotherapy and efficacy as add-on therapy in patients on standard injectable DMTs. In RRMS the phase I trial confirmed safety and tolerability of two courses of rituximab, 1000mg given intravenously 15 days apart (Bar-Or et al. 2008) and the phase II trial showed a significant reduction in the number of new gadolinium-enhancing (GdE) lesions and number of patients experiencing relapses after 48 weeks (Hauser et al. 2008). The trial met the primary and secondary end points suggesting that rituximab as a potential treatment for RRMS. Approximately 25-30% of the patients treated rituximab developed human anti-chimeric antibodies (HACA) against rituximab but no impact was found on the efficacy measures (Hauser et al. 2008). The add-on study was designed to evaluate the effect of rituximab using a 375mg/m^2 weekly for 4 doses, as in the protocol approved for non-Hodgkin's lymphoma. The patients that finished the study experienced 88% reduction in GdE lesion counts compared to pretreatment MRI scans and tolerated the infusions well (Naismith et al. 2010). The phase II/III trial of rituximab in PPMS patients did not reach the primary efficacy outcome measure in the intent-to-treat group. There was no evidence of significant difference in time to confirmed disease progression (CDP) between the rituximab and placebo treated groups (p=0.1442). However, a significant effect on time to CDP (p=0.0088) was found in the subgroups of patients of younger age (<51

years) and with presence of GdE lesions on baseline MRI irrespective of disease duration. The results of the trial support the efficacy of rituximab on the inflammatory component of the PPMS and underscore once again the need to target neurodegeneration early in the progressive phase (Hawker et al. 2009). Patients with SPMS are currently being recruited into a clinical trial evaluating the efficacy of rituximab administered by combination of intravenous and intrathecal injection on the same day (NCT01212094; updated November 2012). As shown by the previous studies rituximab treatment induces HACA in a variable percentage of patients but their contribution to reducing the efficacy of rituximab is controversial, but are associated with infusion reactions. A new generation of mAbs are being developed to overcome issues of resistance and adverse effects. A new anti-CD20 humanized mAb, ocrelizumab, has being tested in RRMS at two different doses, 600mg and 2000mg, compared to INFβ and placebo in a phase II trial. The results showed efficacy with significant reduction of total number of GdE lesions, of new and enlarging T2 lesions and surprisingly, considering the size of the study, on the annualized relapse rate for both doses used compared to placebo and DMT groups ($p<0.0001$). The death of a 41 years old woman for systemic inflammatory response syndrome (SIRS) has been a cause of concern for the safety profile of ocrelizumab (Chaudhuri 2012; Kappos et al. 2011). In another autoimmune diseases, i.e. rheumatoid arthritis (RA) and SLE, in spite of the efficacy, ocrelizumab development was stopped due to an unfavorable risk/benefit profile (Barun and Bar-Or 2012). Another new generation mAb is the fully humanized anti-CD20 ofatumumab and its safety and efficacy profile is currently being analysed in MS (www.clinicaltrials.gov). The reduction of new GdE lesions and the lower relapse rate of patients undergoing B-cell depleting therapy have shown a central role of this cell population of cells in the pathophysiology of MS. Immunologic studies of patients treated with rituximab have revealed that depletion of circulating B-cells did not impact total and myelin-specific circulating antibodies and similarly at CSF level a depletion of almost 90% of B-cells was associated with concomitant T-cells reduction but no significant differences were reported in IgG concentration, IgG index, IgG synthesis rate or oligoclonal band number when comparing pretreatment samples (Bar-Or et al.

2008; Cross et al. 2006; Naismith et al. 2010; Petereit et al. 2008). The proinflammatory cytokines produced by B cells from MS patients, such as lymphotoxin (LT) and tumor necrosis factor-α (TNF-α), could be the Ab-independent therapeutic target that may explain the results. The B-cell depleting effect of rituximab also reduces the proliferative responses of T cells due to the reduced secretion of LT and TNF-α (Bar-Or et al. 2010). Interestingly treatment of an antibody mediated autoimmune demyelinating disease of the CNS, such as neuromyelitis optica (NMO), with repeated application rituximab as second-line treatment has shown reduced relapses in almost all patients but no reduction of the pathogenic autoantibodies directed against AQP4 water channel, a disease specific marker (Lennon et al. 2004; Pellkofer et al. 2011). In summary the clinical trials utilizing anti-CD20 mAbs to deplete the B cell population have highlighted the important contribution of B-cell regulatory functions in the relapsing phase of the disease but also the persistence of autoantibodies that could be involved in the disease progression and neurodegeneration.

1.2 “Auto-antigens” in MS

A variety of approaches have been used to identify antigens recognized by the Abs found in the serum, CSF and lesions of MS patients. The intrathecal Ig bands recognize many myelin, neuronal and viral proteins. However, this heterogeneous antigenic antibody response, only explains a small part of the antibody specificity in MS. These observations lead me to say that it is not yet clear whether the OCBs in MS, and the antigens they target, are directly related to the pathogenesis of MS or not. Autoantibodies reflect the presence, nature and intensity of an autoimmune response. Several CNS antigens, which include myelin antigens such as myelin basic protein (MBP), proteolipidic protein (PLP), myelin oligodendrocyte glycoprotein (MOG), myelin associated glycoprotein (MAG), nucleotide 3'-phosphodiesterase 2 ', 3'-cyclic (CNPase) but also neuronal, i.e. neurofilaments (Nf), and extracellular matrix, i.e. collagen, antigens have been described as target of autoantibodies, but their role in the pathogenesis of the disease is still debated. In my study I screened my MS antibody libraries against a fusion protein MP4 that allowed me to test two antigens simultaneously, MBP and PLP.

Myelin oligodendrocyte glycoprotein (MOG)

The myelin oligodendrocyte glycoprotein (MOG, 54 kDa) is quantitatively the minor component of myelin contributing to 0.05-0.1% by weight of the myelin proteins. Structurally the main isoform of MOG is composed of an extracellular domain (aa 1-121), two transmembrane domains (aa 122-150; aa 175-199) and two cytoplasmic domains (aa 151-174; aa 200-218); the extracellular portion of MOG has a structure similar to immunoglobulins (“Ig-like structure ") and is glycosylated. The mature MOG protein consists of 218 aa and has a high homology between different species (about 90%) (Ballenthin and Gardinier 1996). An important function of MOG, depends on the exon 3, which, if present, inserts a premature stop codon and thus produces a soluble isoform of the protein. Given the limited amount of MOG in the myelin sheaths and the difficulty in purifying the protein in native form, the function of this soluble isoform is still unknown. Some commentaries on the biochemistry of MOG emphasise MOGs possible involvement as an adhesion molecule, microtubule

stability regulator or complement activator (Johns and Bernard 1999). Most of the T cells recognize self-epitopes along the transmembranous and cytosolic domains of MOG (aa 146-154). The B lymphocyte epitopes are instead located in the extracellular domain of MOG (Haase et al. 2001). Given the important role of anti-MOG Abs in EAE, the presence of these Abs in CSF and serum of patients with MS has been studied extensively. The results are very controversial and showed a frequency of anti-MOG Abs in 0-80% of patients with MS and in 0-60% of healthy controls. Despite the controversy regarding the pathogenic importance of MOG antibodies in MS, these antibodies could be a useful prognostic marker: in a cohort of 103 patients with CIS conversion to clinically definite MS was anticipated by serum positivity for IgG anti-MOG and anti-MBP (Berger et al. 2003). IgG directed against the native protein MOG (linked to the membrane and glycosylated) have been found in patients with CIS and RRMS but marginally or absent in the progressive forms, further emphasizing the possible role of anti-MOG Abs in early disease (Lalive et al. 2006). Recent data have shown that high titers of anti-native MOG antibodies are predominantly present in serum of a cohort of paediatric ADEM patients and children affected by a first demyelinating event (Brilot et al. 2009; Di Pauli et al. 2011). Interestingly NMO cases AQP4 Ab-seronegative is associated with positivity to anti-MOG Abs further confirming the involvement of MOG in the demyelinating process and in the spectrum of NMO disorder in the adult (Kitley et al. 2012).

Myelin basic protein (MBP)

MBP (14-21.5 kDa) is characterized by the presence of numerous positively charged residues and it is located on the cytoplasmic side of the myelin membrane constituting 30% of total myelin proteins (Boggs 2006). The MBP human gene, located on chromosome 18, is organized in 11 exons that encode for the "gene of oligodendrocyte lineage (Golli)-MBP", a form of fetal MBP that is expressed in bone marrow, thymus, spleen and progenitor cell lines of macrophages and B cells in the developing fetus. Only the last 7 of these 11 exons codify for the "classical-MBP" in the differentiated nervous tissue and involved in the autoimmune reaction of MS (Harauz et al. 2009). After events of

alternative splicing and post-translational modification (phosphorylation, methylation, ADP-ribose, citrullination), the classic-MBP represents different isoforms, distinguished by their molecular weight and their distribution in different tissues of CNS (brain, cerebellum, spinal cord) (Pribyl et al. 1993). In animal models in which demyelinating diseases are induced such as EAE, it has been noted that MBP is one of the possible targets against which the inflammatory attack is triggered. Human T lymphocytes recognize a broad set of MBP epitopes, including a dominant epitope at the centre of the molecule (83-99aa) and several others throughout the sequence of polypeptides (68-84aa, 72-84aa, 121-150aa; 111-129aa; 145-170aa; 131-155 aa) (Pette et al. 1990). The immune response given by autoimmune T lymphocytes that recognize MBP varies between patients with MS according to the recognized epitope (Hafler et al. 1997). Regarding the B cell response high levels of anti-MBP Abs are found (isotype IgG) in serum and CSF of patients with RRMS and PPMS, particularly during relapse compared to periods of remission. The autoimmune response against MBP, by either T cells or autoAbs, is their recognition of a common epitope that includes a sequence of 10 amino acids (85-96aa) (Warren et al. 1995). The presence of anti-MBP autoantibodies has not only been described in MS patients but also in healthy individuals with possible qualitative differences between the two sets of antibodies in terms of affinity, epitope specificity and proteolytic activity (Hedegaard et al. 2009). Recombinant Abs derived from blood lymphocytes of 8 RRMS patients have been successfully selected against MBP epitopes (Gabibov et al. 2011). Interestingly, it has been shown that posttranslational modifications of MBP occur in MS patients that accumulate over time. The modified form of MBP, citrullinated MBP (Cao et al. 1999; Mclaurin et al. 1992), induces a stronger immune response than non-citrullinated MBP (Tranquill et al. 2000). In a recent study using antigen arrays including 334 myelin and inflammation-related CNS antigens, epitopes of MBP were recognized by intrathecally produced autoantibodies with a patient specific pattern of reactivity confirming the complexity of the humoral response in each patient (Quintana et al. 2012).

Proteolipidic protein (PLP)

PLP (30 kDa) is an integral membrane protein, highly hydrophobic and it is the major isoform of the PLP gene that encodes also a splicing variant, DM20. PLP crosses the myelin membrane stabilizing it and constitutes 50% of the weight of all the myelin proteins. The functions of this protein seem to be wider than simple myelin membrane adhesion. Recent studies have shown PLP expressed not only in the CNS but also in other peripheral organs including lymphoid tissues (Campagnoni and Skoff 2001). Despite having a basic net charge, PLP post-translational modifications such as the attachment of lateral lipid chains, mainly palmitic acid, increase its hydrophobicity and immunogenicity (Greer and Lees 2002; Pfender et al. 2008). It has been shown that in mouse models of EAE different PLP epitopes result to be encephalitogenic and mice immunized with PLP developed an acute form of disease (Tuohy et al. 1989). A later study showed that thiopalmitoylation of PLP epitopes enhanced immunogenicity and encephalitogenicity (Greer et al. 2001). In MS patients two longitudinal studies have shown correlation between increase in T-cell autoreactivity to PLP epitopes or whole PLP and onset of GdE lesions on MRI scans (Hellings et al. 2002; Pender et al. 2000). Different authors have shown an antibody response to PLP epitopes with B cells secreting anti-PLP antibodies in serum and CSF of MS patients (Sellebjerg et al. 1998; Sun et al. 1991) characterizing a subset of MS patients (Warren and Catz 1994) with brainstem and/or cerebellum lesions, localization determined by antibody levels against a particular PLP epitope and HLA molecules (Greer et al. 2008).

MP4 fusion protein

The autoantigens mentioned above have given controversial results with regard to the involvement of autoAbs in MS pathology. In the EAE model it has also been difficult to demonstrate the role of autoAb-mediated immune pathology due to the difficulties in dissecting out the role of antibodies from the role of other immune cells. The use of B cells KO mice has allowed investigators to demonstrate the encephalitogenic properties of some autoAbs. A recombinant chimeric fusion protein, MP4, containing epitopes from human MBP and an engineered form of PLP (ΔPLP4) has been used in the past as tolerogenic

therapy in the animal model and recently also to demonstrate the pathogenicity of autoAbs (Elliott et al. 1996; Kuerten et al. 2011). Abs induced in WT B6 mice immunised with MP4 develop serum specific Abs compared to mice that are B cell deficient. Transfer of MP4-reactive serum to MP4-immunized B cells deficient mice is then able to induce EAE. The MP4 autoAbs have been shown histologically to stain spinal cord sections and to co-localize in demyelinated plaques (Kuerten et al. 2011). The results confirm the pathogenetic role of autoAbs in autoimmune diseases and in my study I used the same fusion protein to screen my Ab library from MS patients to be able to check if the data could apply to the human condition as detailed in chapter 5.

Neurofilament protein light subunit (Nf-L)

Neurofilaments are neuronal specific proteins and constitute the main part of the scaffold of the axonal cytoskeleton. Nf are heteropolymers and are composed of three subunits, light (Nf-L), medium (Nf-M) and heavy (Nf-H) subunit. The three isoforms present a highly conserved α-helical rod domain flanked by a carboxy-terminal head and an amino-terminal tail of variable lengths. Nf subunits have a calculated molecular weight based on their mass but the molecular mass determined by migration in sodium dodecyl sulphate (SDS) polyacrylamide gels (PAGE) present a range. This molecular weight difference is due to the level of phosphorylation (and glycosylation) that results in various phosphoforms with Nf-L weights corresponding to 61KDa to 68KDa, Nf-M weights 102.5 KDa to 150 KDa, Nf-H weights of 111 KDa to 190 to 210 KDa, respectively based on the calculated or on that as determined by SDS-PAGE migration mass (Petzold 2005). Evaluation of Nf levels found in the CSF has been considered a useful biological marker in various neurodegenerative diseases, such as amyotrophic lateral sclerosis, Alzheimer's disease, MS and other diseases characterized by axonal loss (Giovannoni and Nath 2011; Kuhle et al. 2011). Furthermore, it has been shown that Nf can act as autoantigens with autoantibodies to Nf being found in the serum and CSF of different MS forms. Significantly elevated levels of serum anti-Nf-L IgG antibodies have been found in PPMS patients (Ehling et al. 2004). Intrathecal production of anti-Nf-L antibodies has been found significantly elevated in PPMS and SPMS and

correlated with disease duration and disability (Silber et al. 2002). Intrathecal production of anti-Nf-L antibodies has also been significantly correlated with MRI markers of inflammation and tissue destruction in MS, in particular with cerebral atrophy (Eikelenboom et al. 2003). The use of anti-Nf-L antibodies as surrogate markers of neurodegeneration in MS has been shown by numerous studies but the results are still controversial (Bartos et al. 2007). Further studies are needed to increase our knowledge on their role in the pathogenesis of MS.

Alpha-beta crystallin (αB)

αB is a characteristic example of small Heat Shock Proteins (sHSPs). sHSPs are known for their cellular function to delay the formation of insoluble protein aggregates, “holdase function”, under stressful conditions (Delbecq and Klevit 2013). In normal conditions αB is absent from human lymphoid tissues but it has been shown that in MS, EBV infection stress induces B cells to express αB crystallin leading to its presentation to T cells that can cross-react with CNS myelin (Van Sechel et al. 1999). In MS lesions enhanced level of αB crystallin expression is localized to the cytosol of oligodendrocytes and astrocytes and is seen from the earliest stages of lesional formation and can be used as a marker for very recent myelin uptake by macrophages. αB crystallin laden macrophages act as APC for presentation to T cells initiating or reinvigorating the immune response (Bajramovic et al. 2000). Furthermore, serum antibodies displaying a consistent and prominent reaction to αB crystallin versus other myelin proteins has been ascribed to focal αB accumulation in NAWM in MS brains in preactive lesions and exclusively to oligodendrocytes at this early stage (Van Noort et al. 2010). Further studies on this antigen are needed to better understand its involvement in the adaptive responses in MS.

Extracellular matrix (ECM) antigens

A study has shown perivascular fibrosis in different forms of MS and mainly in progressive MS as feature of chronicity. Increased transcript levels of fibrillar collagens and other ECM components have been observed in active and inactive MS lesions. Mainly found in chronic inactive lesions fibrillar collagen I and III could interact with the immune cells reducing the inflammatory cascade and inhibiting the demyelination enlargement of the lesions (Mohan et al. 2010). The presence in the CNS of new antigens due to the inflammatory cascade could lead to formation of reactive immune cells and autoantibodies production. The availability of *in house* collagen III has given me the opportunity to use this protein as target antigen in my screening.

1.3 Phage display

1.3.1 Antibody molecule

The human immunoglobulins (Ig)s are assembled from multiple gene segments. A typical immunoglobulin is formed from polypeptide chains termed heavy and light chains. Each chain is divided in a variable (V) region and a constant region (C). The heavy-chain V-region is the result of an ordered rearrangement of three gene segments: variable (V), diversity (D) and joining (J) gene segments joined in a single exon at genomic DNA level by a process termed somatic recombination (Alt et al. 1984). The same process determines the formation of the light-chain V-region using two different gene segments: V and J gene segments (Weigert et al. 1980). In my study I will refer to the single heavy or light chain rearranged exon as V gene. The rearranged heavy and light V genes joined with their respective constant gene segments are transcribed and then expressed as an antibody molecule (Fig.1.6).

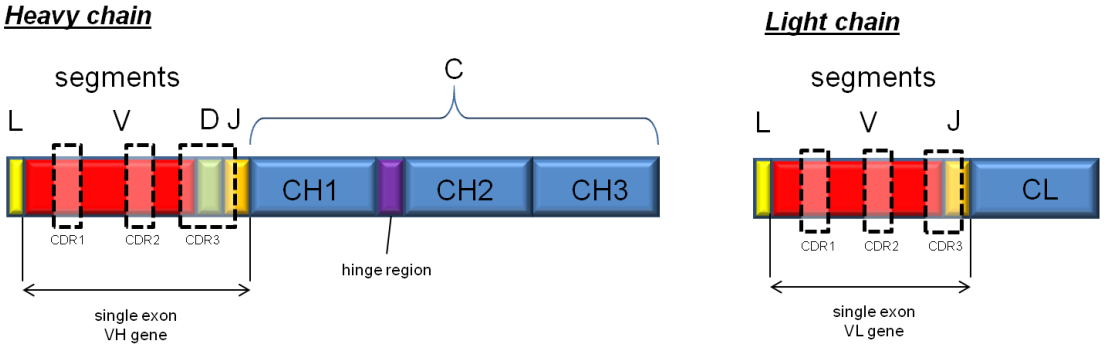

Figure 1.6 Schematic diagram of V-region: The single exon V gene is the result of the junction of VDJ segments in the heavy chain (VH) and VJ segments in the light chain (VL).

The structure of an antibody molecule is Y-shaped and has distinct portions with distinct functions (Fig.1.7 and 1.8). The two arms are the regions that bind to the antigen and are called antigen binding fragment (Fab) regions and the tail forms a region called fragment crystallizable (Fc) region involved in complement and cell receptors binding (Poljak et al. 1973; Silverton et al. 1977).

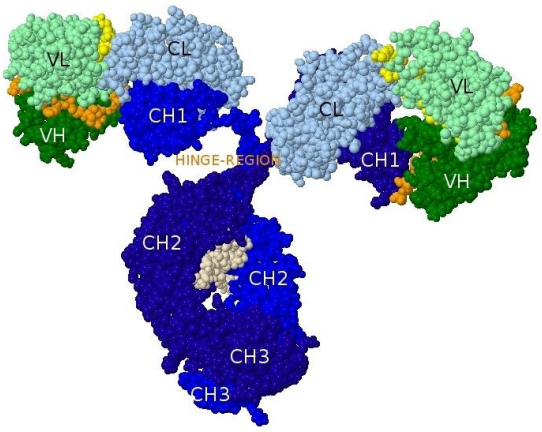

Figure 1.7 3D structure of an IgG: The molecule appears formed of globular subunits. The VH, VL, CH1 and CL subunits present a very similar three-dimensional folding (www.imgt.org).

The light chain can be of two types, kappa (k) and lambda (λ), and the heavy chain of five types. The structure of heavy chain C region determines the name of the five Ig classes: IgM, IgD, IgG, IgA and IgE. Each IgG molecule, 150KDa, is composed of two identical heavy chains, 50KDa, and two identical light chains, 25KDa, connected by disulfide bonds. Heavy and light chains contain three sequences of hypervariability called complementary determining regions (CDR)s and are flanked by less variable ones called framework regions (FR)s. The pairing and folding of heavy and light chains and the juxtaposition of the three CDRs, CDR1, CDR2 and CDR3, form the antigen binding site (Fig.1.8).

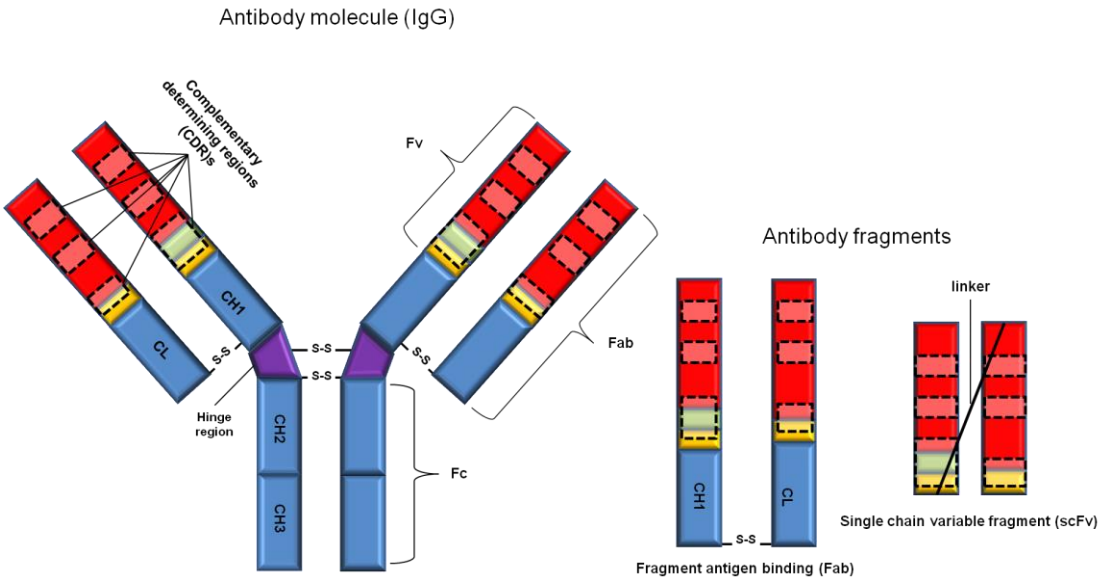

Figure 1.8 Schematic diagram of an antibody molecule and fragments: The variable (V) region of each chain contains three hypervariable regions termed complementary determining regions (CDR)s respectively CDR1, CDR2 and CDR3 that contribute to the formation of the antigen binding site. My library used VH and VL regions joined by a linker sequence to create a single chain variable fragment (scFv) (s-s = interchain disulfide bridges).

1.3.2 Antibody phage display

The phage display technology is the most robust technology to generate and select recombinant Abs *in vitro*. The technology is based on the expression and consequent "display" of peptides or protein fragments on the capsid of bacteriophages, also known simply as "phages". This bacteria-specific viruses are of two major types in nature: lytic and non-lytic, based on their capacity to break the bacterial cell after infection. The main non-lytic phages are the fd and M13 and present a rod like morphology, 1 µm long and 7 nm wide, that gives them the name of filamentous phages (Mao et al. 2009). The M13 phage particle is formed of 5 coat proteins surrounding a single stranded (ss) DNA core. The major coat protein is PVIII (g8p) present in around 2700 copies to cover the length of the particle, the other 4 minor proteins, around 5 copies each, are distributed at the two opposite ends capping the phage with PVI (g6p) and PIII (g3p) at one end and PIX (g9p) and PVII (g7p) at the other one. PIII protein is also necessary for host recognition, binding of the F pilus, and infection. All 5 coat proteins have been used for displaying techniques but usually the g8p and g3p are the most often utilized (Sidhu 2001) (Fig.1.9).

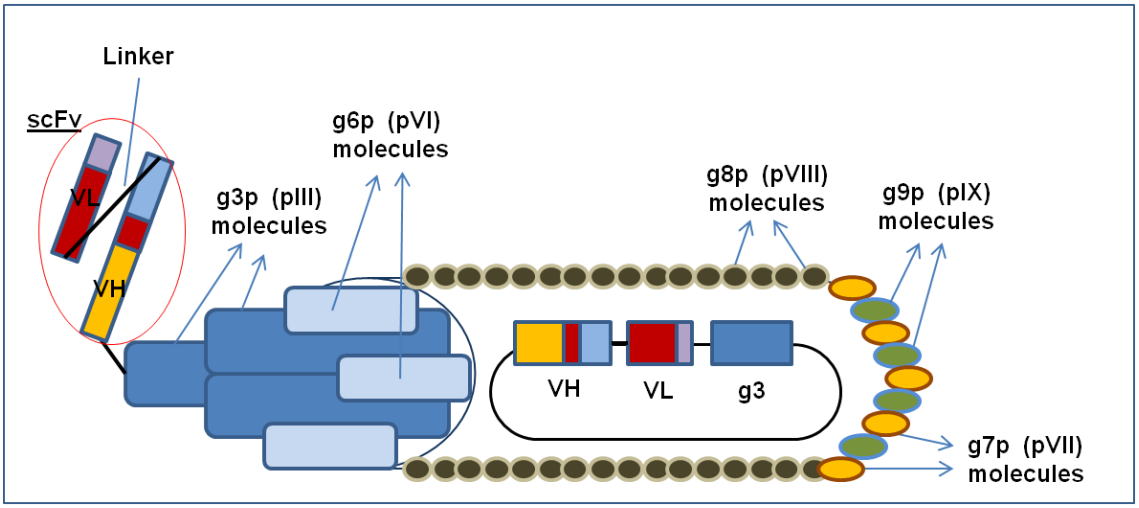

Figure 1.9 Schematic representation of a filamentous phage: The phage illustrated displays a single chain variable fragment molecule (scFv). The scFv is displayed fused to the g3p molecules, a minor coat protein, obtaining a so called monovalent display due to the use of a phagemid vector. In the circular ssDNA VH and VL amplified from MS patients have been cloned and are shown upstream the g3 gene.

In my study the antibody library was built cloning the gene of interest upstream the gIII gene and obtaining a phage exposing on the capsid the codified protein, VH and VL, fused with the phage minor capsid protein g3p (Winter et al. 1994) (Fig.1.9). The vectors used for gene cloning are usually plasmids and phages. In this application usually the V genes encoding the amplified antibodies are cloned in a phagemid, i.e. a hybrid vector containing elements from a phage and a plasmid. A phagemid is developed to contain both replication origins for double stranded and ssDNA and in particular for *E. coli* and M13. Furthermore, it contains a copy of the gene 3 and/or 8, a proper cloning site and an antibiotic resistance gene but lacks the necessary genes to generate a functional particle. The functional phage particle can be obtained only by “rescue” with a helper phage (KM13) supplying the essential genes necessary for amplification and packaging. The phagemid then can grow as plasmid and lead an independent existence in the infected bacteria or be encapsulated in a M13 phage but only by utilizing the missing proteins supplied by the helper phage infecting the same bacterial host (Hoogenboom et al. 1991). The pIT2 phagemid vector derived from pHEN1 (kindly provided by Dr. A. Nissim) was used in this work (Fig.1.10). This vector as phagemid contains only the fusion protein gene necessary for the display and no other phage genes. The V gene sequences for display are then inserted into the coding sequence of the coat protein gene III (gIII) and bound by a linker to obtain a fusion scFv-PIII. Between the displayed sequence and gIII an amber stop codon is present to allow to switch from displayed scFv to expressed soluble antibody fragments by transferring the vector into a non-suppressor strain. Soluble fragments expressed under the presence of a pelB leader signal that directs their transfer into the periplasm. The presence of a functional M13 origin directs ssDNA encapsidation into phage particles and an ampicillin resistance gene allows antibiotic selection of transformants. The antibody cloned can then be purified or detected by presence of different tag sequences interposed between cloned VH-VL genes and g3 (Fig.1.10).

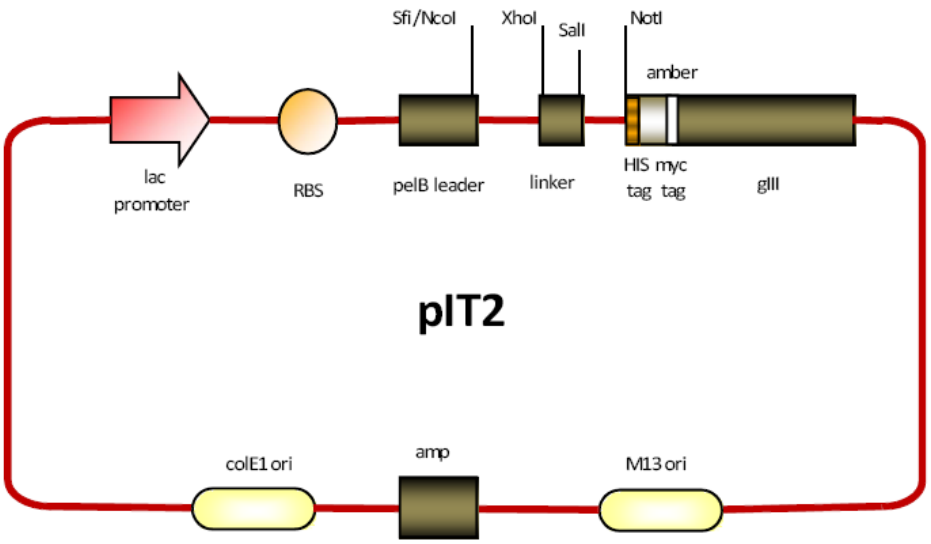

Figure 1.10 Phagemid vector map of pIT2: The earlier vector pHEN1 was modified to improve the cloning of VH and VL regions and to improve the different uses in the phage display library construction obtaining the pIT2 vector. RBS=ribosomal binding site

The usage of a phagemid to clone these sequences increases though the risk of helper phage contamination in my library. A strategy to inactivate any contaminating helper phage, being generated during the co-infection, was developed by employing an helper phage with insertion of a trypsin-cleavable site between the D2 domain of the helper phage PIII, responsible for the binding to the F-pilus, and the D3 domain, responsible for anchoring PIII to the phage (Kristensen and Winter 1998; Riechmann and Holliger 1997). All the PIII domains are essential for phage infectivity and the protease sensitivity of the helper phage allows it to inhibit infection following proteolytic elution. The wild type PIII protein itself contains a trypsin-cleavable site that allows the phage library to be separated from the fusion protein during the elution step but with retention of infectivity. The trypsin-elution process then releases phages bound to the antigen during selection rounds, preserving their infectivity, but at the same time eliminates the helper phage contaminants by inhibiting their possibility to infect the bacterial host during propagation.

The main characteristic of the phage particle is the association between genotype (gene cloned) and respective phenotype (protein displayed), with the advantage to select at the same time the single protein and the corresponding codifying sequence. Besides, the binding specificity can be retained by the antibodies generated.

The mentioned features applied to an antibody library displaying the structure of an antibody reformed entirely or in part allow to replicate the development of the B cell in the immune system. In fact, as shown in the figure below (Fig.1.11) all the steps can be mimicked by the phage technology.

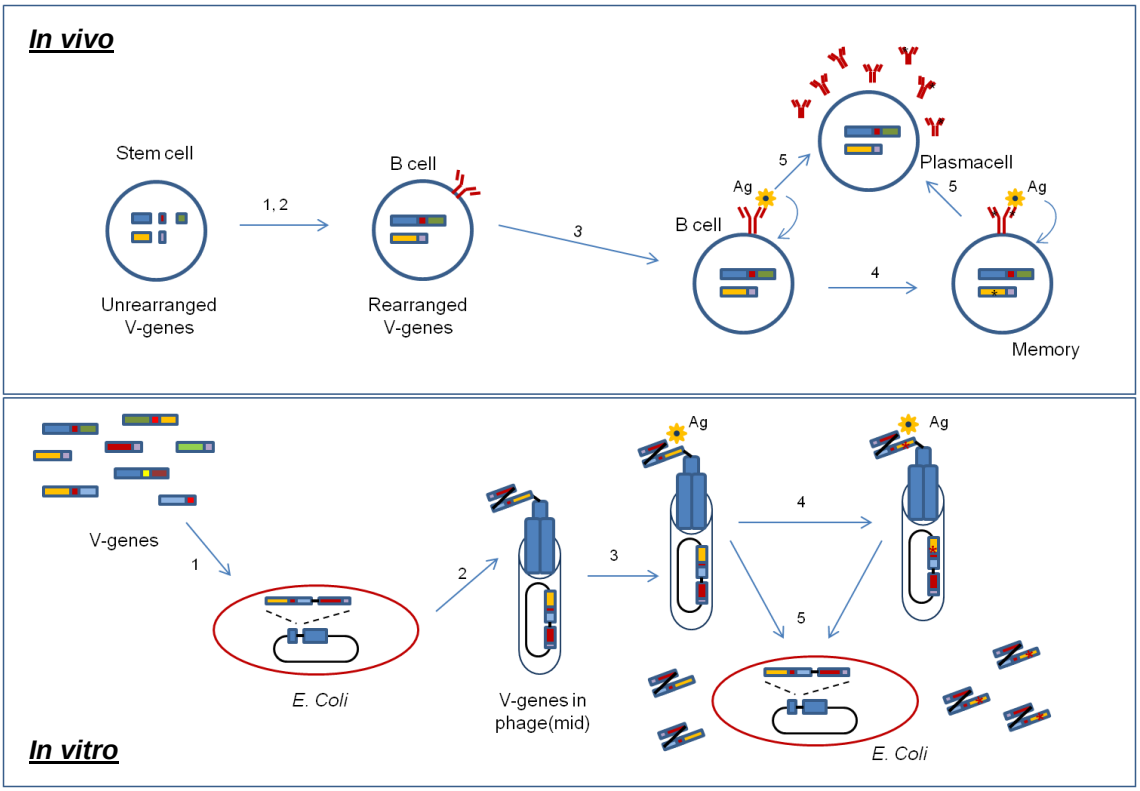

Figure 1.11 Mimicking the B cell development by phage technology: The generation of antibodies by the immune system is compared with the phage display technology. The different steps show the development of B cell from stem cell to plasma cell (1-5). The B cell encountering the antigen (Ag) proliferate (3), differentiate to produce plasma cells secreting Abs (5). The Abs binding affinity is enriched by mutations (4). In the phage technology the rearranged V genes are cloned in a phagemid and expressed on the phage surface (1-2). The Abs are selected on Ag coated plates (3). Phages are enriched by further rounds of selection and their affinity increases (4). The plasma cell is mimicked by infection of bacteria with secretion of free antibody fragments (5) (Winter et al. 1994).

As result, the antibody genes are expressed and the gene products displayed on the surface of the phage as fusion proteins. The resulting collection of phages is called “antibody phage display library”, where each phage particle displays a single antibody.

In general two kinds of libraries can be constructed based on the antibodies repertoire: immune, IgG derived, or naive, IgM derived. Human immune libraries are obtained from V genes derived from immunized individuals or patients and contain V genes heavily biased toward antibodies recognizing the immunogen. The resulting affinity of the antibodies isolated is far higher than that of the antibodies isolated from a naive library of the same size. Naive libraries are intended to be unbiased, and so antibodies can be selected against any antigen. They have been derived from either unimmunized human rearranged V genes or synthetic human V genes. The synthetic libraries are derived from naive repertoires introducing diversity by varying the lengths of the CDRs or targeting specific CDRs positions (De Wildt et al. 2000; Nissim et al. 1994). The synthetic library, Tomlinson I, used in this study as control library was supplied by Dr. Ahuva Nissim. The library used the most common structure in the human antibody repertoire derived from the framework for VH, V3-23/DP47 and JH4b, and Vk, DPK9 and Jk1. The library diversity was obtained by tailored randomization via diversified (DVT) side chains introduced in 18 different amino acid positions in the antigen binding site (De Wildt et al. 2000). The high diversity present in the synthetic library allowed to compare a virtually naive repertoire, able to bind any antigen, with the biased immune repertoire obtained in my MS library.

Once the V genes have been ligated in the vector, the recombinant phagemid is inserted in *E. coli* cells, made competent by electroporation. The ligation and transformation result to be the most crucial passages, and influence directly the diversity and dimension of the obtained library (Fig.1.12). The first naive scFv library obtained from peripheral blood B lymphocites had a size of 10^7 (Marks et al. 1991).

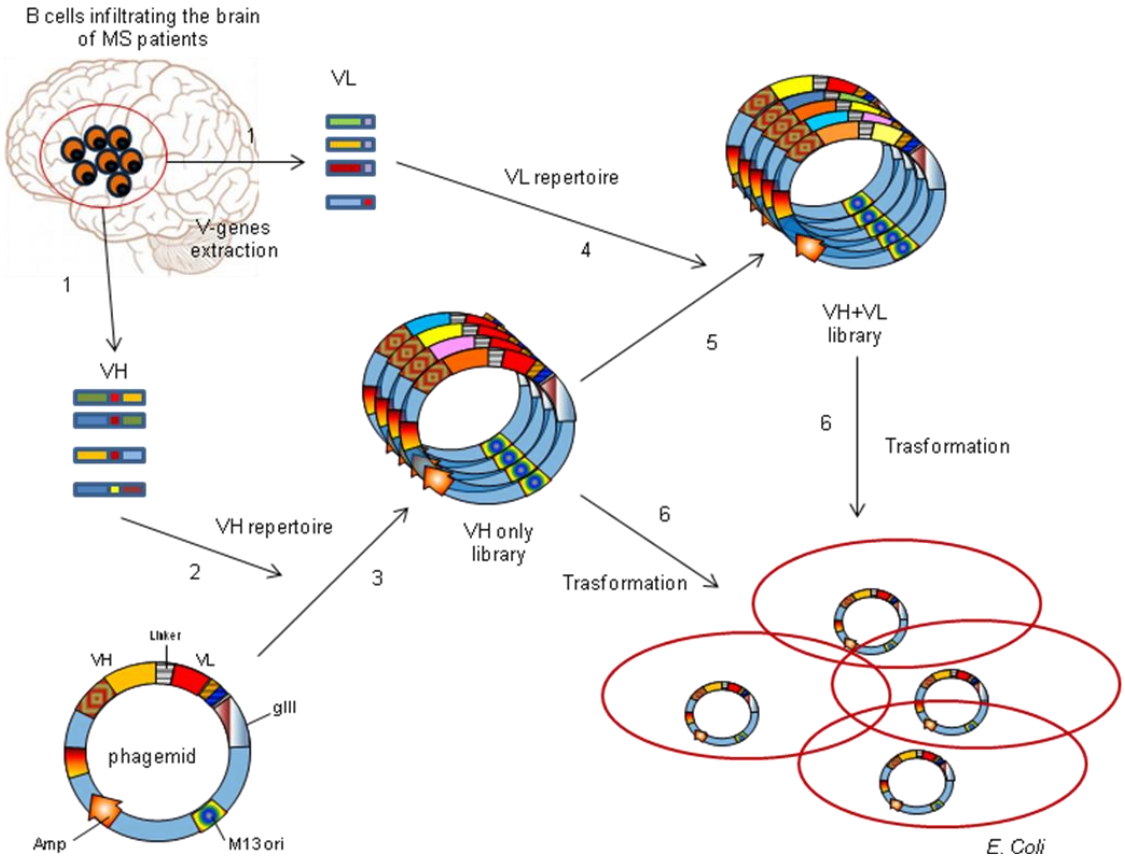

Figure 1.12 Steps followed to build my antibody phage display library: The source of V genes have been the B cells infiltrating the brain of MS patients (1). IgM and IgG repertoires have been amplified by specific primers. VH and VL have been cloned sequentially in a phagemid vector obtaining an intermediate library of VH only (2-5). The final antibody libraries have been inserted in *E. coli* (6).

Once an antibody library is obtained, antigen specific antibodies are isolated by selection on antigens. The diversity of the initial library relies on the diversity of the V genes cloned with highly different specificities represented and low percentage of phages able to bind the antigen of interest. The following process termed biopanning allows one to detect the presence of antibodies with

particular specificities directed towards antigens of interest. Two approaches can be used to identify tissue-specific molecules based on tissue of interest and expression of the molecule targeted: a) *in vitro*, by immobilizing the target molecule onto plastic, biopanning on cell surfaces or by using biotinylated targets and b) *in vivo*, by injection of the library into an animal (George et al. 2003). In my case biopanning on autoantigens involved in MS pathogenicity coated onto solid supports (immunotubes) have been used to select specific antibodies from the library. The phages bind to the antigen based on their specificity and affinity but unspecific binding can occur. Multiple rounds of selection enrich the library with higher affinity binders decreasing the diversity of the library in favour of an increased percentage of specific binders reaching almost 100% in 4-5 rounds. The enrichment allows one to obtain a "monoclonal/oligoclonal" population of high affinity binders starting from a "polyclonal" library (Nissim et al. 1994) (Fig.1.13).

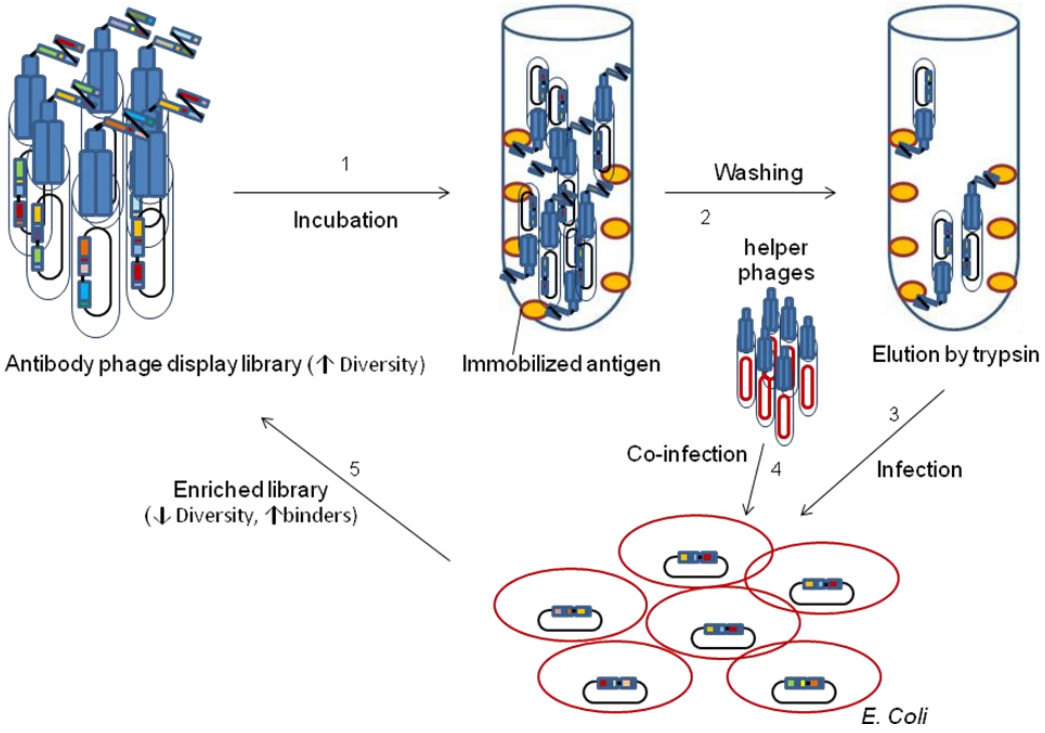

Figure 1.13 Antibody phage display selection: Obtained the library the scFv binding to the antigens of interest are selected biopanning the library on coated immunotubes (1). After washing away the aspecific phages (2), the retained binders are eluted by trypsin and can infect their bacterial host (3). The enriched library is then rescued by co-infection with helper phages and another round of selection can start (4-5).

1.4 Hypothesis and Objectives

Hypothesis: The analysis of B cell repertoire from MS brain infiltrates will shed light on the mechanism of B cell driven autoimmunity. Hence making phage display library from this repertoire will be a valuable source to identify potential autoantibodies in the MS and in the longer term help the development of targeted therapeutics.

My objectives were:

- To analyse the presence of immune infiltrates and follicle-like aggregates in the MS brain tissues
- To build an antibody phage display library from B cells infiltrating MS brain tissues
- To analyse the VH and VL repertoire represented in the B cells from MS brain tissues
- To perform a parallel selection using the newly built MS library and the *in house* synthetic library and to test the potential of the MS library as source of Abs against known autoantigens in MS

The objectives will be described and discussed in the following chapters.

Chapter 2: Materials and Methods

2.1 Patients

To evaluate the antigen-driven response of B cells infiltrating the brain I analysed 14 brain blocks from MS patients with primary (1), secondary (12) and relapsing (1) progressing MS and 2 control brains (patients not affected by neurological diseases). In the MS group the sex ratio (M:F) was 1:2.5, the average disease duration was 20 years and the median of age at death of 50.5 years (range=34-77y). The two controls were both male with an average age of 66 years (64 and 68y). The post mortem delay average was 17 hours for the MS and 24 hours for the control group (complete patients' details in table 2.1).

	Patient case	Sex	Age at death (years)	Disease duration (years)	Form of MS	Cause of death	Post Mortem delay (hrs)
1	103	F	77	21	SPMS	Pneumonia	7
2	154	F	34	11	SPMS	Pneumonia	12
3	160	F	44	16	SPMS	Aspiration pneumonia	18
4	179	F	70	21	SPMS	Aspiration pneumonia, sepsis	20
5	307	M	55	21	SPMS	Multiple Sclerosis	19
6	311	F	45	16	SPMS	Pneumonia	22
7	317	F	48	29	SPMS	Aspiration Pneumonia	21
8	325	M	51	5	PPMS	Bronchopneumonia	13
9	330	F	59	39	SPMS	Pneumonia	21
10	335	M	62	37	SPMS	Aspiration pneumonia, renal failure	22
11	341	F	52	22	RPMS	Aspiration Pneumonia	8
12	342	F	35	5	SPMS	Multiple Sclerosis	9
13	352	M	43	18	SPMS	Bronchopneumonia	26
14	377	F	50	23	SPMS	Aspiration Pneumonia	22
1control	Co14	M	64	N.A.	N.A.	Myocardial infarction	18
2control	Co36	M	68	N.A.	N.A.	Heart failure	30

Table 2.1 Details of MS patients and non neurological controls

2.2 Immunohistochemistry

Brain tissues from people with multiple sclerosis, screened for the presence of lymphoid follicle-like aggregates and provided by the UK Multiple Sclerosis Tissue Bank (ethics approved by Cambridgeshire 1 Research Ethics Committee, reference number 08/H0304/7), were used for this study. Snap frozen brain tissues were used to evaluate the expression of different lymphoid and myelin markers. Air dried, acetone fixed sequential cryosections 7-10 µm

thick were rehydrated with PBS and standard immunohistochemical staining procedures for frozen sections were performed making use of Vector laboratories consumables and detection kits. Briefly, the slides were labelled with a solvent resistant pen and demarcate with a hydrophobic barrier pen (*Vector Laboratories, Burlingame, Calif*). All the steps were performed at RT if not otherwise specified. Endogenous peroxidase activity was blocked by incubating the slides in 0.3% H_2O_2 solution in PBS for 10 minutes. The sections were then washed with PBS 5 minutes and blocked in normal horse serum 20 minutes. The excess of blocking solution was blotted and the slides incubated 30 minutes with primary antibody (Ab) diluted in buffer. All the primary and secondary Abs used in this study were diluted in PBS + 1% blocking serum. The optimal working concentration (dilution) of each primary antibody (list in table 3.1.1-3.1.3) was obtained by a titration experiment to determine the optimal antibody dilution for optimal results, i.e. high specific-staining signal and low background. After extensive washing with PBS, sections were incubated 30 minutes with the corresponding biotinylated secondary antibody. Washed with PBS the sections were incubated 30 minutes with avidin-biotin horseradish peroxidase complex (ABC), using the ABC Vectastain *Elite* kit (*Vector Laboratories, Burlingame, Calif*), according to the manufacturer's instructions followed by 3,3'-diaminobenzidine DAB (Vector Laboratories, Burlingame, Calif) as substrate for the HRP. As counterstain was used hematoxylin and then rinsed in water. All sections were sealed with Depex Polystyrene (DPX) and viewed with an OLYMPUS microscope*,* images were captured with a digital camera and an image software (CellP)*.* Negative controls included were obtained omitting of the primary Ab and/or using an aspecific primary antibody. Myelin staining was performed using hematoxylin and eosin (H&E) and Oil Red O following the standard operating procedures used in the Blizard Institute - Core Pathology, QMUL.

2.3 Laser capture microdissection

A 10 µm thick section was collected by PEN (polyethylene–naphthalate) membrane slides for microdissection from Zeiss, after UV treatment, picking up from the annular cryocassette the tissue by holding the slide just above the

section and angle the slide down to touch a portion of the tissue. Then the slides were fixed in ice cold ethanol and stained as little as possible to save time for the RNA extraction. A Zeiss Axiovert 200M inverted laser capture microscope was used to analyse the sections and a monitor using the PALM® RoboSoftware (Carl Zeiss Ltd., UK; P.A.L.M, Bernried, Germany) to visualize them. Lesions, vessels and follicle-like aggregates were identified and selectively laser microdissected (laser energy: 85mW; laser focus: 7.5µm - 75mW) from MS brain blocks supplied by Dr. Gusta Trillo-Pazos (Department of Virology and Department of Neuroinflammation, IoN, UCL, UK). Using the laser catapulting function (LPC), the dissected lymphoid aggregate was catapulted into separate specialised adhesive caps. From microdissected samples total RNA was extracted by RNeasy Micro extraction kit (Qiagen Ltd., UK) following the manufacturer's instructions and cDNA obtained as detailed previously.

2.4 Tissue homogenization, RNA extraction and cDNA synthesis

Snap frozen tissue blocks from 14 MS brains, 2 control brains, 1 control lymph node and 1 tonsil were used to extract RNA. A portion of tissue was weighed and ~ 30 mg were harvested with a sterile blade without allowing the tissue to thaw during the handling by performing the cut on dry ice. The piece of tissue harvested was put directly in a glass vessel and disrupted/homogenized by manual glass tissue grinder and pestle (KONTES, Kimble Chase LLC, USA) or in tubes with ceramic beads and processed by tissue homogenizer Precellys 24 (Bertin Technologies, France) using the protocol 2x15 seconds at 5000 rpm in both cases in presence of lysis buffer containing phenol and guanidine thiocyanate. Total RNA molecules longer than 200 bp were extracted by RNeasy Lipid tissue extraction kit (Qiagen Ltd., UK) following the manufacturer's instructions. The eluted RNA was divided in two samples of which one was stored at -80°C and the other further treated with Turbo™ DNase (Ambion, Life Technologies Ltd, UK) following the manufacturer's instructions. cDNA was obtained from the two different RNA stocks (untreated and Turbo treated) using 2 µg RNA in a total volume of 20 µl and retrotranscribed by ThermoScript™ reverse transcriptase (Invitrogen, Life

Technologies Ltd, UK) with a first step of denaturation at 65°C for 5 min, followed by 60 min at 55°C and 5 min at 85°C priming by oligo(dT)$_{20}$ and/or random hexamers. The residual RNA in the reaction was eliminated using RNaseH (Invitrogen, Life Technologies Ltd, UK) at RT for 20 min. The cDNA produced was stored at -20°C.

2.5 RT-PCR

My experiments of quantitative real time PCR (qPCR) were performed using the SYBR Green chemistry. The SYBR Green dye binds only to double-stranded (ds) DNA, thus providing a fluorescent signal that reflects the amount of dsDNA product generated during quantitative real time (RT)-PCR (Zipper et al. 2004). Primers of reference and target genes were designed using an *ad hoc* software such as Beacon Designer 7.9 (Premier Biosoft International, USA) (trial version). All primers were designed to anneal in gene regions of no secondary structure formation under the same temperature condition of 60°C and chosen to span one exon-exon boundary when possible (sequences of reference genes primers in table 2.2 and of target genes primers in table 2.3).

Reference Genes	Primer	Sequence	Primer bp	Amplicon length (bp)
DNMBP	For	GCAGATGGTGATTAAGGTCTC	21	117 bp
	Rev	CAGTAAATCTTGTATGTTCCCTCA	24	
ENOX1	For	CACCACAAATAACAAGCAGAA	21	176 bp
	Rev	AGGTCATCAGATTCTCAAAACT	22	
GAPDH	For	CAAGATCATCAGCAATGCCTCCT	23	92 bp
	Rev	TGAGTCCTTCCACGATACCAAAGT	24	
HMBS	For	ATGTCTGGTAACGGCAATG	19	66 bp
	Rev	GCGAATCACTCTCATCTTTGG	21	
NUMA1	For	TGGGAACAACTTTCTCTCAGGTT	23	78 bp
	Rev	CGTCTCATCTGGAACTGTGGG	21	
RNF20	For	CGACTCAACCGACACTTAGC	20	93 bp
	Rev	TGTGCCGCCATACAGACT	18	
RPL37A	For	CGTACAATACCACTTCCGCTGTCA	24	78 bp
	Rev	GGAGCGTCTACTGGTCTTTCAACT	24	
TBP	For	TGACCCAGCATCACTGTTTC	20	116 bp
	Rev	TGGAACTCGTCTCACTATTCAATT	24	
TTC1	For	GAGCGGACAAGGTTGAGAACAA	22	147 bp
	Rev	TTCCCTCCTCCTTTAGTCTAGTGC	24	
XDH	For	TGCTGTGGAGGAGATGGGAAT	21	72 bp
	Rev	CGAGAGGCTGACTGAGTGGT	20	

Table 2.2 Sequences and details of reference genes primers

Target Genes	Primer	Sequence	Primer bp	Amplicon length (bp)
AICDA	For	CCTTTTCACTGGACTTTGGTTATC	24	73 bp
	Rev	ATGTAGCGGAGGAAGAGCAAT	21	
CD20	For	ATCTCTGTTCTTGGGCATTTTGT	23	123 bp
	Rev	ACTATGTTAGATTTGGGTCTGGAG	24	
CD40	For	TTGTGCCAGCCAGGACAGAAACT	23	78 bp
	Rev	GCTTTCACCGCAAGGAAGGCATT	23	
CD40L	For	CAGAATCCTCAAATTGCGGCACAT	24	75 bp
	Rev	TTCAGCCCACTGTAACACAGATGT	24	
CXCL12	For	CGTCAAGCATCTCAAAATTCTCAA	24	119 bp
	Rev	GGTACTCCTGAATCCACTTTAGC	23	
CXCL13	For	TGAGGTGTAGATGTGTCCAA	20	127 bp
	Rev	GACTTGTTCTTCTTCCAGACTATG	24	
CXCR4	For	TACACTTCAGATAACTACACCGAG	24	60 bp
	Rev	TTCCTTCATGGAGTCATAGTCC	22	
CXCR5	For	CCTCACGCACCTCCCATCCTAATC	24	71 bp
	Rev	CTCCGTTGGCAAGGGCAGAAGTA	23	
CCR7	For	CTGGTGGTGGCTCTCCTTGTC	21	67 bp
	Rev	TGTAATCGTCCGTGACCTCATCTT	24	
CD77	For	CGCCTCCAGGATCGCACTCAT	21	90 bp
	Rev	TTGGTCAGGTTCCGCAGGTTCT	22	
LTbetaR	For	TGGAAGGGGAGGAAAATGGCAAGT	24	86 bp
	Rev	GCACGAGCGGCACGAGTTTAG	21	

Table 2.3 Sequences and details of target genes primers

As the thermal cycling conditions chosen were the same for all the genes evaluated further optimization of qPCR was obtained varying the primers concentrations by primers matrix to compensate for variations in primers melting temperature. The thermal profile was of 4 steps: 1) 50°C for 2min, 2) 95°C for 10min, 3) 40 cycles of 95°C for 15sec, 60°C for 30sec and 72°C for 30sec, 4) 1 cycle of 95°C for 15sec and 55°C for 15sec. The step 4 was used to design melting curves. Reaction mixtures were set using Power SYBR® Green PCR Master Mix (Applied Biosystems®, Life Technologies Ltd, UK) and adding template, primers and water to a final volume of 25 µl as detailed below:

Recipe	µl
Template cDNA	5
Master Mix	12.5
Water	6.5
Primer For	0.5
Primer Rev	0.5
Total volume	**25**

Plates of 96/384 wells were used depending on the pipetting method and each sample was measured in triplicates with cDNA levels analysed using the ABI 7900HT instrument (Applied Biosystems®, Life Technologies Ltd, UK). The data were collected by the SDS2.4 software supplied with the instrument.

All Real-time PCR experiments were compliant with the Minimum Information for Publication of Quantitative Real-Time PCR Experiments guidelines (MIQE) (Bustin et al. 2009) (Table 2.4).

ITEM TO CHECK	IMPORTANCE
EXPERIMENTAL DESIGN	
Definition of experimental and control groups	E
Number within each group	E
Assay carried out by core lab or investigator's lab?	D
Acknowledgement of authors' contributions	D
SAMPLE	
Description	E
Volume/mass of sample processed	D
Microdissection or macrodissection	E
Processing procedure	E
If frozen - how and how quickly?	E
If fixed - with what, how quickly?	E
Sample storage conditions and duration (especially for FFPE samples)	E
NUCLEIC ACID EXTRACTION	
Procedure and/or instrumentation	E
Name of kit and details of any modifications	E
Source of additional reagents used	D
Details of DNase or RNAse treatment	E
Contamination assessment (DNA or RNA)	E
Nucleic acid quantification	E
Instrument and method	E
Purity (A260/A280)	D
Yield	D
RNA integrity method/instrument	E
RIN/RQI or Cq of 3' and 5' transcripts	E
Electrophoresis traces	D
Inhibition testing (Cq dilutions, spike or other)	E
REVERSE TRANSCRIPTION	
Complete reaction conditions	E
Amount of RNA and reaction volume	E
Priming oligonucleotide (if using GSP) and concentration	E
Reverse transcriptase and concentration	E
Temperature and time	E
Manufacturer of reagents and catalogue numbers	D
Cqs with and without RT	D*
Storage conditions of cDNA	D
qPCR TARGET INFORMATION	
If multiplex, efficiency and LOD of each assay.	E
Sequence accession number	E
Location of amplicon	D
Amplicon length	E
In silico specificity screen (BLAST, etc)	E
Pseudogenes, retropseudogenes or other homologs?	D
Sequence alignment	D
Secondary structure analysis of amplicon	D
Location of each primer by exon or intron (if applicable)	E
What splice variants are targeted?	E

ITEM TO CHECK	IMPORTANCE
qPCR OLIGONUCLEOTIDES	
Primer sequences	E
RTPrimerDB identification Number	D
Probe sequences	D**
Location and identity of any modifications	E
Manufacturer of oligonucleotides	
Purification method	D
qPCR PROTOCOL	
Complete reaction conditions	E
Reaction volume and amount of cDNA/DNA	E
Primer, (probe), Mg++ and dNTP concentrations	E
Polymerase identity and concentration	E
Buffer/kit identity and manufacturer	E
Exact chemical constitution of the buffer	
Additives (SYBR Green I, DMSO, etc.)	E
Manufacturer of plates/tubes and catalog number	D
Complete thermocycling parameters	E
Reaction setup (manual/robotic)	D
Manufacturer of qPCR instrument	E
qPCR VALIDATION	
Evidence of optimisation (from gradients)	D
Specificity (gel, sequence, melt, or digest)	E
For SYBR Green I, Cq of the NTC	E
Standard curves with slope and y-intercept	E
PCR efficiency calculated from slope	E
Confidence interval for PCR efficiency or standard error	D
r2 of standard curve	E
Linear dynamic range	
Cq variation at lower limit	E
Confidence intervals throughout range	D
Evidence for limit of detection	E
If multiplex, efficiency and LOD of each assay.	E
DATA ANALYSIS	
qPCR analysis program (source, version)	E
Cq method determination	E
Outlier identification and disposition	E
Results of NTCs	
Justification of number and choice of reference genes	E
Description of normalisation method	E
Number and concordance of biological replicates	D
Number and stage (RT or qPCR) of technical replicates	E
Repeatability (intra-assay variation)	E
Reproducibility (inter-assay variation, %CV)	D
Power analysis	D
Statistical methods for result significance	E
Software (source, version)	E
Cq or raw data submission using RDML	D

MIQE checklist for authors, reviewers and editors. All essential information (E) must be submitted with the manuscript. Desirable information (D) should be submitted if available. If using primers obtained from RTPrimerDB, information on qPCR target, oligonucleotides, protocols and validation is available from that source.

*: Assessing the absence of DNA using a no RT assay is essential when first extracting RNA. Once the sample has been validated as RDNA-free, inclusion of a no-RT control is desirable, but no longer essential.

**: Disclosure of the probe sequence is highly desirable and strongly encouraged. However, since not all commercial pre-designed assay vendors provide this information, it cannot be an essential requirement. Use of such assays is advised against.

Table 2.4 MIQE checklist: Information necessary for evaluating qPCR experiments (Bustin et al. 2009)

2.6 Immune libraries construction

The MS libraries built had the plasmid frame of pIT2, a plasmid derived from pHEN1 and optimized for V gene cloning. A clone, named 1-11E, already in use in our laboratory encoding a scFv with binding specificity to native and modified collagen type II and known to have good expression was kindly supplied by Dr C. Hughes (Hughes et al. 2010). The 1-11E plasmid pre-existing inserts were replaced, by a sequential process of enzyme digestions and ligations, with the inserts of my interest, i.e. V genes from B cells infiltrating the brain tissue of patients with MS.

2.6.1 Inserts preparation

Two libraries containing immunoglobulin heavy (VH) and light (VL) chain variable (V) genes or VH genes only were prepared from lymphocytes infiltrating brain tissue of 14 MS patients by polymerase chain reaction (PCR) amplification. Sequential PCR reactions were performed with the obtained first cDNA strand as template and using as forward primer either an IgG or an IgM isotype constant region primer for the heavy chains, or a κ or λ constant region primer for the light chains and as reverse primer a VH or VL family specific primer designed according to Marks et al. (Marks et al. 1991) and the VBASE database (http://vbase.mrc-cpe.cam.ac.uk/). VH, Vκ and Vλ -genes were amplified separately in a nested PCR reaction changing only the forward primer (Fig.2.1). The primers used to amplify the V genes contained restriction sites compatible with the vector sites and precisely two different restriction sites for each VH and VL amplicon allowed to obtain a directional cloning. The restriction sites were specifically XhoI and NcoI for the VH insert with the back primer containing a NcoI site and with the internal forward primer in the nested PCR containing a XhoI site. The restriction site contained in the back primer of the VL inserts was a SalI site and a NotI site for the internal forward primer. The first step forward primer, annealing to the constant regions, of my nested PCR reactions did not contain any restriction site (Fig.2.1).

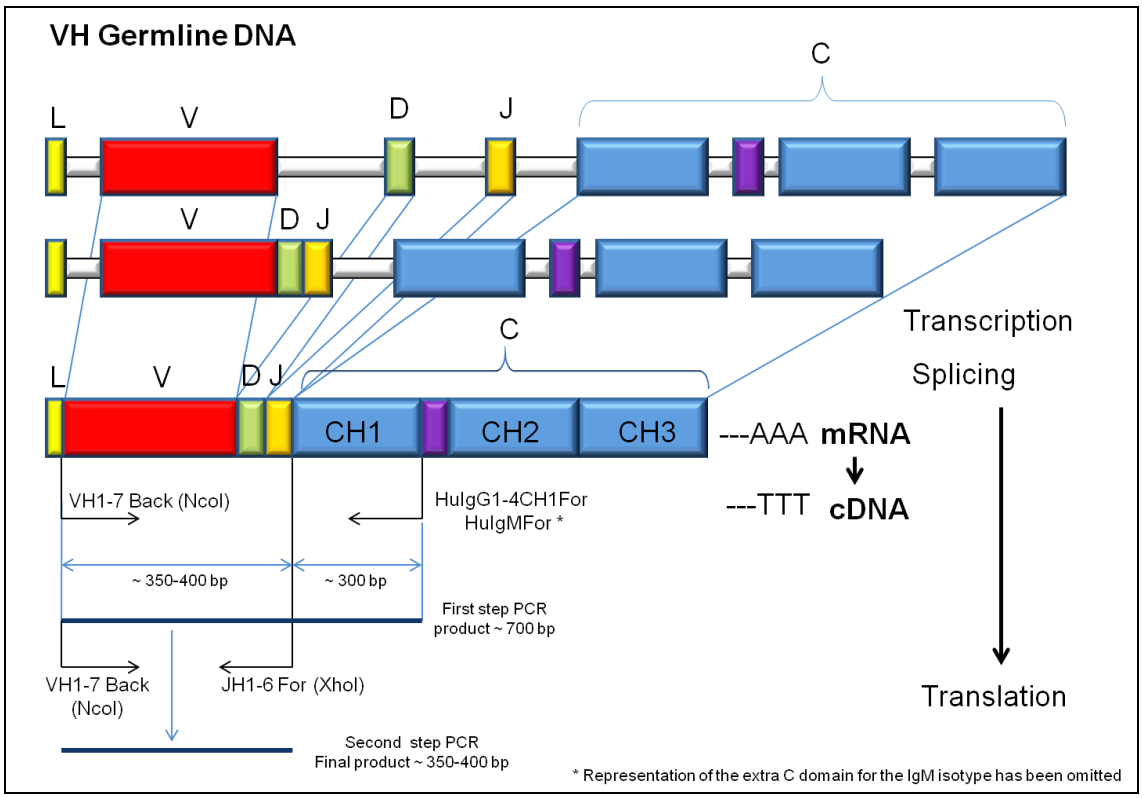

Figure 2.1 Schematic map of VH primers on mRNA: The primers used for my PCRs were designed to anneal specifically on VH sequence after splicing reducing the possibility of bias for DNA contamination. The scheme shows that my target sequence was obtained after 2 steps of amplification for both immunoglobulin heavy-chain isotypes considered (IgG and IgM are the isotypes found in the CSF of MS patients by isoelectrofocusing). MS cDNA was used as template to obtain amplicons of around 700 bp by use of an external primer annealing on the 3' end of the constant domain 1. The resulting amplicons were used as template for a further step of amplification performed with an inner forward primer annealing on the 3' end of the JH region. The final amplicon had a length of around 350-400 bp depending on the CDR3 length. The same steps were applied to amplify the light chains.

The amplification of the variable domains was conducted with an equimolar mixture of an appropriate family-based annealing reverse primer and a forward junction region annealing primer both incorporating restriction sites allowing to force-clone the insert in the vector for sequencing and expression (sequences in table 2.5-2.7).

VH	Restriction site inserted
Primers BACK VH	**NcoI**
VH1a	GTCCTCGCAACTGCGGCCAGCCGGCCATGGCCCAGG TGCAGCTGGTGCAG
VH2a	GTCCTCGCAACTGCGGCCCAGCCGGCCATGGCCCAG GTCAACTTAAGGGAG
VH3a	GTCCTCGCAACTGCGGCCCAGCCGGCCATGGCCGAG GTGCAGCTGGTGGAG
VH4a	GTCCTCGCAACTGCGGCCCAGCCGGCCATGGCCCAG GTGCAGCTGCAGGAG
VH5a	GTCCTCGCAACTGCGGCCCAGCCGGCCATGGCCCAG GTGCAGCTGTTGCAG
VH6a	GTCCTCGCAACTGCGGCCCAGCCGGCCATGGCCCAG GTACAGCTGCAGCAG
VH7a	GTCCTCGCAACTGCGGCCCAGCCGGCCATGGCCCAG GTCCAGCTGGTGCAA
Primers FOR VH	**XhoI**
JH1-2	GAGTCATTCTCGTCTCGAGACGGTGACCAGGGTGCC
JH3	GAGTCATTCTCGTCTCGAGACGGTGACCATTGTCCC
JH4-5	GAGTCATTCTCGTCTCGAGACGGTGACCAGGGTTCC
JH6	GAGTCATTCTCGTCTCGAGACGGTGACCGTGGTCCC
External Primers FOR VH nested PCR	**no restriction site**
HuIgG1-4CH1	GTCCACCTTGGTGTTGCTGGGCTT
HuIgM	TGGAAGAGGCACGTTCTTTTCTTT

Table 2.5 List of Primers for amplifications of human VH genes

VL	Restriction site inserted
Primers BACK Vk	**SalI**
Vk1	AACGGGTCGACGAACATCCAGATGACCCAG
Vk2	AACGGGTCGACGGTAATTGTGATGACCCAG
Vk3	AACGGGTCGACGGAAATTGTCTTGACACAG
Vk4	AACGGGTCGACGGACATCGTGATGACCCAG
Vk5	AACGGGTCGACGGAAACGACACTCACGCAG
Vk6	AACGGGTCGACGGAAATTGTGCTGACTCAG
Primers FOR Vk	**NotI**
Jk1	GAGTCATTCTCGACTTGCGGCCGCACGTTTGATTTCCA CCTTGGTCCC
Jk2	GAGTCATTCTCGACTTGCGGCCGCACGTTTGATCTCC AGCTTGGTCCC
Jk3	GAGTCATTCTCGACTTGCGGCCGCACGTTTGATATCCA CTTTGGTCCC
Jk4	GAGTCATTCTCGACTTGCGGCCGCACGTTTGATCTCC ACCTTGGTCCC
Jk5	GAGTCATTCTCGACTTGCGGCCGCACGTTTAATCTCCA GTCGTGTCCC
External Primer FOR Vk nested PCR	**no restriction site**
HuCkFOR	AGACTCTCCCCTGTTGAAGCTCTT

Table 2.6 List of Primers for amplifications of human Vk genes

VL	Restriction site inserted
Primers BACK Vλ	**SalI**
Vλ1a	AACGGGTCGACGCAGTCTGTGCTGACTCAG
Vλ2	AACGGGTCGACGCAGTCTGCCCTGACTCAG
Vλ3a	AACGGGTCGACGTCCTATGAGCTGACTCAG
Vλ3b	AACGGGTCGACGTCCTATGAGCTGACACAG
Vλ4	AACGGGTCGACGCAGCTTGTGCTGACTCAA
Vλ5	AACGGGTCGACGCAGGCTGTGCTGACTCAG
Vλ6	AACGGGTCGACGAATTTTATGCTGACTCAG
Primers FOR Vλ	**NotI**
Jλ1	GAGTCATTCTCGACTTGCGGCCGCACCTAGGACGGTG ACCTTGGTCCC
Jλ2-3	GAGTCATTCTCGACTTGCGGCCGCACCTAGGACGGTC AGCTTGGTCCC
Jλ4-5	GAGTCATTCTCGACTTGCGGCCGCACCTAAAACGGTG AGCTGGGTCCC
External Primer FOR Vλ nested PCR	**no restriction site**
HuCλFOR	TGAAGATTCTGTAGGGGCCACTGTCTT

Table 2.7 List of Primers for amplifications of human Vλ genes

The cDNA template was obtained by retrotranscription of RNA extracted from brain tissues as detailed in paragraph 2.3. PCR mixture and thermal conditions of the inserts amplification are reported below:

Recipe	µl
Template	5-7
dNTPs 10mM	1.25
Primer For 10µM	2
Primer Rev 10µM	2
KapaReady Mix	25
Water	x
Taq	0.5
Total volume	**50**

Cycles	Temperature	Time
1x	95°C	10 min
30x	95°C	1 min
	58°C	1 min
	72°C	1 min
1x	72°C	10 min

The products were analysed by running 10 µl volume in presence of 6x loading buffer on 1% agarose gels.

2.6.2 Cloning of V genes into vector

The cDNA used as template of my inserts was the result of pooling the same volume of each V gene PCR reaction. Considering the PCR efficiency the same for each reaction, my V gene inserts were resembling the same relative expression of VH and VL families as in the B cells infiltrating the brain. The PCR products were a reliable copy of the humoral immune response of the patients and I cloned the amplicons by digesting with NcoI and XhoI (for the heavy

chains) and NotI and SalI (for the light chains) overnight (O.N.) at 37°C followed by a boost of 1 µl of XhoI/NcoI or NotI/SalI for 2 hours as in the reaction detailed below:

Recipe	**µl**
Insert	30
XhoI	2
NcoI	2
10x Buffer	10
Water	55
BSA	1
Total volume	**100**

Digested PCR products were checked for presence of a single band, corresponding to approximately 400 bp, on 1% agarose gel to determine quantity and quality. The remaining volume was then run on a 0.8% low melting point preparative agarose gel and the band excised with a sterile blade being visualized by a UV transilluminator. The DNA was extracted using the QIAquick Gel extraction kit (Qiagen Ltd., UK).

2.6.2.1 Preparation of Vector

The bacterial growth media formulations were prepared as detailed in table 2.8. 2TY broth and TYE agar were prepared in double-distilled water and the pH adjusted to 7.4. The minimal media components were autoclaved separately except for the glucose and thiamine that were sterile filtered.

2TY broth	Tryptone	16 g/l	Biogene Ltd, Kimbolton, Cambs, UK
	Yeast Extract	10 g/l	Biogene Ltd.
	Sodium Chloride	5 g/l	BDH Laboratory Supplies (BDH), supplied by VWR International Ltd, Lutterworth, UK
TYE agar	Tryptone	10 g/l	Biogene Ltd.
	Yeast Extract	5 g/l	Biogene Ltd.
	Sodium Chloride	8 g/l	BDH
	Bacto-Agar	15 g/l	Biogene Ltd.
Minimal Salt (2x M9)	Na_2HPO_4	12g/l	NA
	KH_2PO_4	6g/l	NA
	NaCl	1g/l	NA
	NH_4Cl	2g/l	NA
Minimal Media	2x M9	500 ml	NA
	3% Agar	500 ml	NA
	20% Glucose	20 ml	NA
	$MgSO_4$ 1M	2 ml	NA
	$CaCl_2$ 1M	0.1 ml	NA
	Thiamine (10 mg/ml)	1 ml	NA

Table 2.8 Bacterial growth media formulations

The plasmid bacterial stock was cultured at 37°C O.N. in 10 ml 2xTY, 100µg/ml ampicillin, 1% glucose. Plasmid DNA was isolated using the Qiagen Plasmid Midiprep kit (Qiagen Ltd., UK). The plasmid was digested with NcoI and XhoI as detailed previously and run on a 0.8% low melting point agarose gel. The digested vector ~ 5Kb was excised out of the gel as for the inserts and extracted using the QIAquick Gel extraction kit (Qiagen Ltd., UK). An amount of 10 µl of DNA was run on a 1% agarose gel to determine quantity and purity.

The resulting DNA was purified by precipitation at -20°C for 15-20 min in a mixture of water, NH_4 acetate and 3x volume of ethanol. After the ethanol precipitation the sample was centrifuged at 4°C at max speed for 15 min. The pellet was washed with increasing concentrations of ethanol, left to dry and resuspended in water.

2.6.2.2 Ligation

To optimize the ratio for the ligation reaction, test ligations were performed in different ratios of insert to vector (1:1, 3:1, 5:1 and 10:1). To estimate the correct concentration of vector and insert, the preparations were run on agarose gel and quantified on an UV transilluminator. The desired ratio insert:vector was obtained adding the appropriate volumes to the test ligation reaction mixture in a total volume of 20 µl as reported below. Ligation reactions were incubated O.N. at 37°C. Large scale ligations were concentrated by ethanol precipitation.

Recipe	**µl**
Insert	x
Vector	x
Buffer	2
Water	x
T4 ligase	1
Total volume	**20**

2.6.2.3 Preparation of competent *E. coli* TG1

E. coli, TG1 strain, cells were cultured O.N. shaking in 2xTY medium and incubated at 37°C. The cultured bacteria were inoculated in baffled flasks and grown in a 37°C shaker, cooled on ice for 10 min before transferring to cold centrifuge bottles. The chilled culture was spun for 15 min at ~ 4500 rpm and the resulting pellet washed with multiple passages in HEPES solution. In the final step the pellet was resuspended in 10% glycerol. The cells were frozen as 100µl aliquots at -80°C or kept on ice for fresh use.

2.6.2.4 Transformation

The electrocompetent bacteria were thawed if necessary and mixed with 4 µl of ligated phagemid in a 0.2 cm electroporation cuvette. The cuvette with the mixture was placed in the electroporator Biorad MicroPulser (Bio-Rad Laboratories Ltd., UK) and pulsed following the manufacturer's instructions. The electroporated cultures were plated and incubated at 37°C O.N.. The plates were scraped and the library stock stored at -80°C.

2.6.2.5 Library size

The evaluation of the MS libraries size was obtained by plating serial dilutions of the libraries on agar plates containing ampicillin for colony counting.

2.6.2.6 Sequencing

Sanger sequencing

A small portion of the PCR products were cycle sequenced using the BigDye chemistry material kindly supplied by Dr Alex Pearson and then sent for sequencing to The Institute of Cancer Research, London, UK. The PCR product templates were prepared by half-reactions with 1μl PCR template per 20μl total volume, and the extension reaction performed by thermal cycler according to the following schedule:

Denaturation	3 minutes	96°C	1x
Denaturation	30 seconds	96°C	25x
Annealing	15 seconds	50°C	
Extension	4 minutes	60°C	

The remaining PCR products were sent for sequencing directly to The Genome Centre (WHRI, QMUL) and sequenced by BigDye 3.1 chemistry with visualization on the ABI 3730xl capillary sequencer.

The following primers were used in sequencing of the heavy and light chains of scFv from the MS antibody phage display libraries:

PHEN: 5'_CTATGCGGCCCCATTCA_3'
LMB3: 5'_CAGGAAACAGCTATGAC_3'

2.7 Libraries selection

The libraries were grown, rescued and screened following the methods described in Harrison et al. (Harrison et al. 1996) and following the protocol supplied with the Tomlinson library (MRC Centre for Protein Engineering, Cambridge, UK).

2.7.1 Rescue of MS and Tomlinson I libraries

2.7.1.1 Production of KM13 helper phage from stock

A volume of 200 µl of *E. coli* TG1 culture was infected in log phase with 10 µl of 100 fold serial dilutions of KM13 helper phage derived from stock 1 (stock concentration $>10^{13}$ plaque forming unit/ml, or pfu/ml) in a heated water bath at 37°C for 30 min. TYE plates with no antibiotics were then covered pouring a mixture of the infected TG1 culture and 3 ml of molten H-Top agar and allowed to set. The plates were incubated O.N. at 37°C. From areas with well separated plaques a single one was picked and used to infect a fresh 5 ml TG1 culture at log phase and grown at 37°C for 2 hours. The culture was then transferred into a large flask containing 500 ml 2xTY medium and grown for a further 1 hour at 37°C. The culture was then left growing at 30°C O.N. after adding 50 µg/ml kanamycin. The produced phages were recovered from the supernatant by 20% polyethylene glycol 2.5M NaCl (PEG/NaCl) precipitation on ice after spinning down the culture at 10.800g for 20 min. The PEG/NaCl solution was eliminated from the phage by repeated steps of centrifugation and the pellet finally resuspended in PBS with 15% glycerol and stored in aliquots at -80°C. The titration of the helper phage was performed for trypsin treated and non-treated phages by transduction of log phase TG1 cultures by 100-fold serial dilutions of 1 µl helper phage (trypsin treated and non-treated), added to 3 ml of molten H-Top agar and poured evenly onto TYE plates. The titer of the helper phage new stock and its trypsin sensitivity was evaluated counting as pfu/ml and the titer of the trypsin treated phage resulted 10^6 lower than for the non-trypsin treated phage (see results chapter 5).

2.7.1.2 Production of large quantities of phages

As described previously in 2.6.2.4 after scraping the plates the MS libraries stock was stored at -80°C. The Tomlison I library was supplied in phagemid form as bacterial stock. The same procedure was followed to grow all the libraries. An aliquot of the stock library was thawed and mixed with growing medium 2xTY supplemeted with 1% glucose and ampicillin 100 µg/ml. The library culture was grown until log phase, then $2x10^{11}$ KM13 helper phage were

added at a multiplicity of infection (MOI) of ~10:1 to 50 ml of the culture and incubated for 30 min without shaking in a heated water bath at 37°C. The infected culture was spun at 3600 rpm for 10 min and the bacterial pellet resuspended and transferred in a flask with 100 ml of medium 2xTY supplemeted with 0.1% glucose, ampicillin 100 µg/ml and kanamycin 50 µg/ml. The culture in the flask has then been grown shaking O.N. at 30°C. The produced library phages were recovered from the supernatant by adding 1 volume of 20% polyethylene glycol 2.5M NaCl (PEG/NaCl) to 4 volumes supernatant and precipitated for 1 hour on ice after spinning down the O.N. culture at 4000 rpm for 30 min. Bacterial debris and dregs of PEG/NaCl solution were eliminated from the phages by repeated steps of centrifugation and resuspension in PBS and the rescued phages finally resuspended in PBS and stored at 4°C or stored in aliquots at -80°C adding 15% glycerol.

2.7.2 Target Protein Analysis

2.7.2.1 SDS-Polyacrylamide Gel Electrophoresis (SDS-PAGE)

The proteins used in this study were supplied by colleagues: MP4 was obtained from Prof. David Baker and Dr. Gareth Pryce (Neuroimmunology group, ICMS), CIII was obtained in house from Dr. Assi Hendler and Dr. Rocky Strollo; human r-MOG1-125, Nf-L and CRYAB were obtained from Prof. Sandra Amor and Dr Fabiola Puentes (Neuroimmunology group, ICMS & Pathology department, Amsterdam, NL). The proteins of interest were separated mainly by their molecular weights using sodium dodecyl sulfate polyacrylamide gel electrophoresis (SDS-PAGE). The 10% resolving and 5% stacking gels were prepared based on the recipes reported in Sambrook and Russell 2001. The reducing gels were loaded with a mixture of the different samples and loading buffer in a ratio of 3:1 for each well and 10µl SeeBlue® Plus2 Pre-Stained Standard marker (Invitrogen) into a separate well of each gel used for visualization of protein molecular weight ranges during the electrophoretic run. Gels were exposed to 150V for 60 minutes by a Biorad power supply (Bio-Rad Laboratories Ltd., UK), after which they were removed from the casing and the separated proteins visualised by Coomassie Blue staining (see below).

2.7.2.2 Coomassie Blue Detection of Proteins

The SDS-PA gels were stained for detection of separated proteins by soaking in a Coomassie Brilliant Blue R-250 dye solution shaking gently on an orbital shaker at RT O.N.. The proteins were visualised from the background by repeated washes with destaining solution for 1 hour (recipes in table 2.9).

Buffer	Component	Concentration	Source
Running Buffer	Glycine	4g/l	Sigma-Aldrich
	Tris-HCl	3g/l	Sigma-Aldrich
	SDS	1g/l	Sigma-Aldrich
2x Reducing Sample Buffer	Tris-HCl, pH 6.8	1.25mM	NA
	Glycerol	20% (v/v)	NA
	β-mercaptoethanol	2% (v/v)	NA
	Bromophenol Blue	0.1% (w/v)	NA
	SDS	0.1% (w/v)	NA
Western Blotting Buffer	Glycine	2.96g/l	Sigma-Aldrich
	Tris (base)	5.82g/l	Sigma-Aldrich
	20% SDS solution	188µl/l	National Diagnostics (East Riding, Yorkshire, UK)
Destain solution	Methanol	30% (v/v)	Fisher Scientific (Loughborough, UK)
	Glacial Acetic Acid	10% (v/v)	BDH
Coomassie Stain	Coomassie Brilliant Blue R250	Saturated (est. 10-70 g/l)	Sigma-Aldrich

Table 2.9 Protein analysis buffer formulations: All buffers were prepared in deionised water, with the exception of Coomassie Stain which was prepared in Destain solution

The destained gels were scanned and saved as image files or dried between cellophane sheets and stored.

2.7.2.3 Protein concentration

The concentration of proteins when not supplied were evaluated by BCA Protein Assay (Thermo Fisher Scientific Inc., USA). The MBP-PLP fusion protein (MP4) concentration was evaluated by the reported assay.

2.7.3 Selection of antigen specific binders from phage libraries

All the procedures of selection and screening have to be considered performed in accordance with the protocol supplied with the Tomlinson I & J bacteriophage libraries (MRC HGMP Resource Centre; http://www.hgmp.mrc.ac.uk/geneservice/ reagents/products/datasheets/scFv/tomlinsonIJ.pdf) if not differently specified.

Isolation of antigen specific binders was obtained by subjecting the library phages to 3-4 rounds of selection on various antigens. Hydrophilic immunotubes (Nunc, Thermo Fisher Scientific, DK) were coated with each antigen at a concentration of 10 µg/ml in PBS and incubated O.N. at 4°C. Non-specific phage binding sites were inhibited by exposure for 2 hours to a blocking agent such as fat free milk powder 2% solution in PBS (MPBS). Around 1 ml MPBS solution containing phage was then poured in the immunotubes and allowed to bind for 2 hours at RT. The unbound phages were mechanically discarded and after the 1st round to favor the selection of high affinity antibodies PBS washing steps had increased stringency. The bound phages were eluted by proteolityc cleavage with trypsin, amplified by transduction into *E. coli* TG1 and successively plated on TYE plates containing 1% glucose and 100 µg/ml ampicillin. The further rounds of selection were performed rescuing the phages adding 5x10^{10} helper phage and following the protocol as in 2.7.1.2. The phages resulting from the first round were used for the following rounds repeating the above described selection on the same concentration of each immobilized antigen.

2.7.4 Screening by ELISA

Populations of phage after each round of selection were analysed by polyclonal and monoclonal ELISA. Summaries of these procedures will be outlined below.

2.7.4.1 ELISA with polyclonal and monoclonal phages

Polyclonal phage ELISAs were performed as follows.

The eluted phages from each round of selection were screened for binding specificity by ELISA to evaluate the enrichment of specific binders. 96 wells plates were coated overnight at 4°C with the same antigens used for the selection. The day after blocked with 2% MPBS and after washes serial dilutions of the precipitated phage pool were added to the plate wells. Similarly monoclonal phage ELISA was performed. Single colonies from a titration plate of the 3rd round of selection were inoculated into single wells of a 96-well plate containing 2xTY medium supplemented with 1% glucose and 100μg/ml ampicillin and grown shaking O.N. at 37°C. About 2 μl of the O.N. cultures were transferred to a new plate with each well containing 200 μl of the same supplemented medium as previously and grown shaking for 2 hours. The original plate was then stored at -80°C as glycerol stock adding 15% glycerol. After 2 hours all the new single cultures in the wells reached presumably the log phase and 25 μl of medium containing 10^9 helper phage were added and incubated shaking for a further hour. The single clones were spun down and the pellet resuspended in 200 μl 2xTY supplemented with 100μg/ml ampicillin and 50μg/ml kanamycin and grown O.N. at 30°C. In parallel a 96-well plate was coated with the same antigen and at the same concentration used for the selection and incubated O.N. at 4°C. The day after, the supernatant from the single wells containing the produced monoclonal phage antibodies was screened for binding by ELISA.

After polyclonal or monoclonal phage antibodies were added to the coated wells they were left for 1 hour to incubate and washed three times with PBS-0.1%

Tween 20. Detection of phages binding the coated antigen was obtained incubating 1 hour with peroxidase-conjugated anti-M13 (GE Healthcare) diluted 1:5000 in 2% MPBS, followed by three times washing with PBS-0.1% Tween 20. The level of binding was evaluated by a colour reaction of the peroxidase with the substrate solution containing tetramethylbenzidine (TMB) 100 μg/ml in 100 mM sodium acetate pH 6 and 1:5000 of 30% hydrogen peroxide. The reaction was stopped by adding 50 μl 1 M sulphuric acid and the OD signal read at 450 nm.

2.7.4.2 ELISA with soluble scFv antibody fragments

Individual clones of the VH+VL library were selected from the monoclonal phage ELISA of the last round of selection on MP4. The clones were grown and then used to infect exponentially growing HB2151 cells (a non-suppressor strain that allows expression of TAG codons as stop codons). The single colonies were grown O.N. at 37°C with the appropriate antibiotic. A small volume of the culture was then used to inoculate a larger volume (100ml-1L) and grown in low concentration of glucose (0.1%) at 37°C until the O.D.600 was approximately 0.9. Reached O.D. 0.9 the culture is induced adding isopropyl β-D-thiogalactoside (IPTG, final concentration 1 mM) and left to grow O.N. at 30°C. Supernatant and periplasmic preparations containing soluble antibody fragments were combined and used to evaluate the presence of the individual scFVs. The expression of a positive control clone 1-11E resulted at good levels as expected, confirming the correct execution of the process, but I did not obtain good expression from my clones (data not shown). Consequently I could not use scFv for ELISAs.

Chapter 3: Lymphoid network in MS brain tissues

Background:

The importance of B cells as main player in the pathogenesis of MS is not only based on their role of antibody secreting cells but also as key mediators of the humoral immune response, as innocent carrier of EBV latent infection in the CNS and as provider of continual LTβR signaling via LTαβ for the maintenance of the organization of the lymphoid stromal cell network (Mccarthy et al. 2006). B cells consequently appear to be an effective therapeutic target for monoclonal therapies (Dobson et al. 2011; Meier et al. 2012). As already discussed in chapter 1 the presence of oligoclonal bands in CSF and brain of PwMS led to search for a production site that could be as persistent (Allen et al. 2007) as the life-long intrathecal immunoglobulins presence. In the immune system the site of an oligoclonal response with antibody affinity maturation and generation of antibody secreting cells is the germinal centre (GC). In numerous autoimmune diseases the invading lymphoid tissue is known to organize itself at the level of specific peripheral organs resembling ectopically the lymphoid follicles as described in the meninges of secondary progressive MS cases (Aloisi and Pujol-Borrell 2006). The presence of ectopic lymphoid structures was described and studied in different autoimmune diseases such as myasthenia gravis (Roxanis et al. 2002), rheumatoid arthritis (Humby et al. 2009; Manzo et al. 2010), Sjogren's syndrome (Barone et al. 2008; Bombardieri et al. 2007), thyroiditis (Söderström and Biörklund 1974), and other autoimmune diseases. In fact, a correspondence can be found between secondary lymphoid organs and follicle-like structures. Lymphoid neogenesis can be considered one of the pathogenic mechanisms of brain damage in MS. Electron-microscopy studies have shown the presence of aggregates of lymphocytes in the perivascular spaces of chronic plaques confirming the persistence of the B cell response at the lesion site (Prineas 1979; Prineas and Wright 1978). These early histological observations of perivascular lymphoid infiltrates in MS brain lesions, named perivascular cuffs, were confirmed and further expanded recently with the description of ectopic B-cell follicles in leptomeninges of around 40% of

secondary progressive MS patients (Magliozzi et al. 2007). The organization of lymphoid follicles is based on different lymphoid cell types and chemokines and the follicle-like structures found in different autoimmune diseases show a variable grade of organization. The finding of ectopic lymphoid aggregates in the inflamed meninges fits exactly the term “adaptive” for the immune response found in MS brain as it seems that the immune system is adapting itself to the brain environment to be able to respond in the same way the lymphoid tissue does during inflammation and/or infection (Fig.3.1).

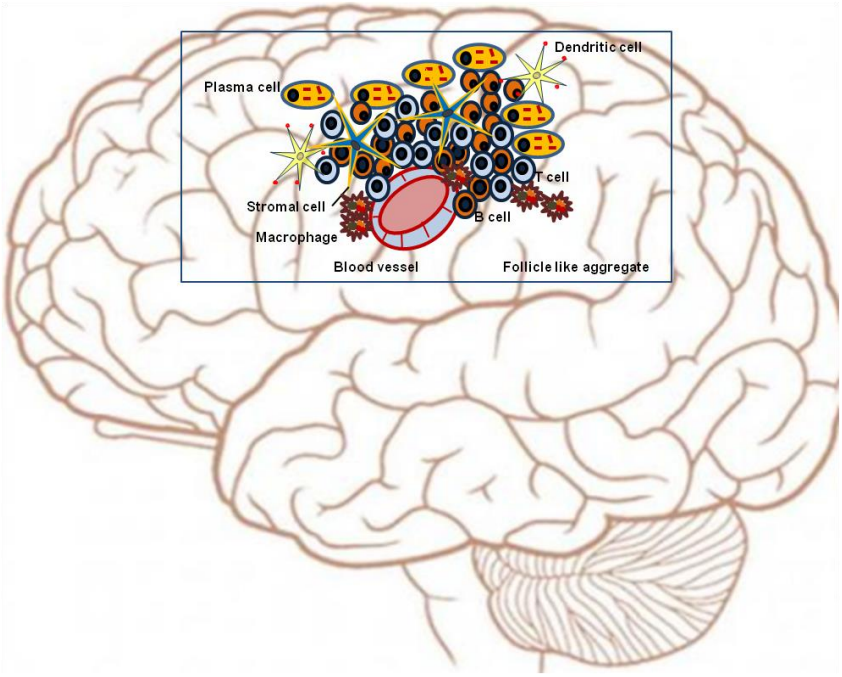

Figure 3.1.1 Follicle-like aggregate scheme: In many chronic inflammatory diseases the formation of ectopic lymphoid aggregates in peripheral target tissues is a common feature. Also, in a subset of patients with secondary progressive MS (SPMS) was described the presence of follicle-like aggregates formed by a network of immune cells. Each chronically inflamed tissue, though, develops a characteristic inflammatory process. In SPMS the lymphoid aggregates are found in the meninges entering the sulci in a perivascular location but not in the plaques and can be considered the anatomical correlate of the OCBs found in the CSF. The ectopic lymphoid follicles are found to contain macrophages, T-cells, B-cells, plasma cells and a network of follicular dendritic cells producing lymphoid chemokines, such as CXCL13.

Furthermore ectopic follicles were correlated with high inflammatory activity, early onset of disease and subpial type of cortical lesions, where the aggregates are usually found in close proximity causing a pial to white matter gradient of neuronal loss (Magliozzi et al. 2007; Magliozzi et al. 2010). The distribution of follicle-like aggregates is wide throughout the cerebral cortex and the cortical demyelination is significantly increased in follicle positive patients (F+) as shown by global measures of demyelination in complete coronal sections (Howell et al. 2011). Recently, the molecular analysis of B cell receptors from ectopic follicle-like aggregates B cells in comparison with B cells infiltrating the other brain compartments did show related B-cells populations undergoing clonal expansion, somatic mutations, isotype switching and skewed family usage (Lovato et al. 2011) resembling functionally a germinal centre reaction as described above and that I could define as an adaptive follicle formation.

Objective:

To evaluate the brain blocks used to build the Ab library for presence of immune cells

Specific aims:

- Histopathology: Brain blocks were screened by immunohistochemistry for presence of immune infiltrates and follicle-like structures

- qPCR: MS tissues and controls were used to determine the most stable reference genes and to evaluate levels of expression of chemokines

3.1 Histopathology of supplied tissues

Background

The characteristic feature of MS is the plaque found disseminated in the CNS and defined as “grey induration” corresponding “to one of the modes of primary chronic inflammation” by Charcot in one of his lectures at La Salpetriere (Charcot 1877). As well, the characteristic pathological feature of the sclerotic MS plaque is demyelination interesting grey and white matter. The chronic inflammation is fundamental part of the histology associated with the axonal damage as reported since the seventies and eighties and as described in chapter 1. Briefly, the demyelinating lesion is the result of myelin sheaths and oligodendrocytes destruction, following the autoimmune attack directed against myelin epitopes by cellular and humoral immunity proceeding respectively through phagocytosis or opsonisation by macrophages (Bruck 2005). Myelin stains and immunohistochemistry has to be used to highlight the differences in composition of grey and white matter lesions with different extent of lymphoid infiltrate with grey matter lesions lacking the inflammatory markers usually found in white matter plaques (Vercellino et al. 2005; Wegner et al. 2006). Localization of the cortical lesions can be described following one of the first studies correlating neuropathology and *in-vivo* MRI by Kidd and colleagues that divided the lesions by the type of cortical venous supply of the cortex (Kidd et al. 1999) or simply by localizing the lesions within the cortical layers (Peterson et al. 2001). These lesions may be circumscribed or involving multiple adjacent gyri, thus leading to a phenomenon termed “general subpial demyelination” (Bo et al. 2003). Among the three types of cortical lesions, namely cortico-subcortical (leukocortical) lesions, affecting cortex and adjacent white matter, small, purely intracortical lesions, and subpial lesions directly abutting on the subarachnoid space, the latter are the most extensive and frequent, followed by cortico-subcortical and purely intracortical lesions. Grey matter demyelination is not restricted to cerebral cortical areas, but also involves the deep grey matter nuclei (Huitinga et al. 2004). Considering the spinal cord, the grey matter is even more demyelinated than the white matter with no preponderance for the subpial lesions (Gilmore et al. 2006; Gilmore et al. 2009). Actually the findings

of meningeal ectopic follicle-like aggregates associated with high degree of meningeal inflammation and cortical lesions have evoked enormous interest and suggested that soluble factors diffusing from these structures could have a pathogenic role (Popescu and Lucchinetti 2012).

Methods:

In my study I tried to detect presence of inflammatory infiltrates, follicle-like aggregates and lesions by immunohistochemistry and different myelin stains to be able to screen the blocks and correlate the histopathology with molecular biology seeking for a functional correlation. The blocks were cut in sequential cryosections 7-10 µm thick by a microtome as detailed in chapter 2 and then stained to screen for lymphoid aggregates. In a preliminary work my specific immunohistochemistry staining used primary antibodies targeting inflammatory infiltrate, myelin antigens and EBV latent phase antigens as described in the literature for detection of MS lesions and demyelination. Immunohistochemistry was performed in collaboration with Dr. Gusta Trillo-Pazos and Prof. David Miller (Institute of Neurology, UCL) and the tissues stained with the markers detailed below (tables 3.1.1; 3.1.2; 3.1.3):

Cell lineage		Marker used
detection of B cells/B cell origin (with CD20)		CD79a
macrophage/monocytes (including Kupffer cells and microglia)		CD68
considered a pan B cell antigen and follicular dendritic cells		CD19
most B cells, also follicular dendritic cells		CD20
peripheral T cells, NK cells, thymocytes		CD3
mature B cells, follicular dendritic cells		CD21

Table 3.1.1 Primary antibody specificity targeting the lymphoid infiltrates

Cell type		Marker used
Astrocytes		GFAP
Neurons		MAP2
Oligodendrocytes		PLP
Oligodendrocytes		CNPase

Table 3.1.2 Primary antibody specificity targeting areas of demyelination

Latent Phase protein		
EBNA-1		Nuclear antigen
LMP-1 LMP-2		Membrane antigen

Table 3.1.3 Primary antibody specificity for EBV screening

A block labeled P1C3 from the internal capsule of case MS136 and a block labeled P2D2 from the thalamus of the case MS182 were used. The patients and blocks details are as follow:

	Patient case	Sex	Age at death (years)	Disease duration (years)	Form of MS	Cause of death	Post Mortem delay (hrs)
1	136	F	77	21	SPMS	Pneumonia	7
2	182	F	34	11	PPMS	Pneumonia	12

Results:

I was able to characterize structures resembling meningeal aggregates in 2 progressive cases (Institute of Neurology, UCL) one secondary progressive and one primary progressive (data not shown) and in my knowledge no cases containing ectopic follicles have been described before in primary progressive form and in the deep grey matter. The quality of the staining did not allow us to differentiate the different immune cells but presence of immune aggregates could be detected from the staining of the cells nuclei. The staining with anti-EBNA1 antibodies of a secondary progressive case did show nuclear staining (data not shown). No staining was present in the sections stained only with secondary antibody.

In a second set of experiments the cases used in the antibody library construction were stained by H&E and Oil Red O in collaboration with Christopher Evagora and Prof. Jo Martin (Blizard Institute Core Pathology, QMUL). The blocks presented immune infiltrates and aggregates as shown below in figure 3.1.2.

a')

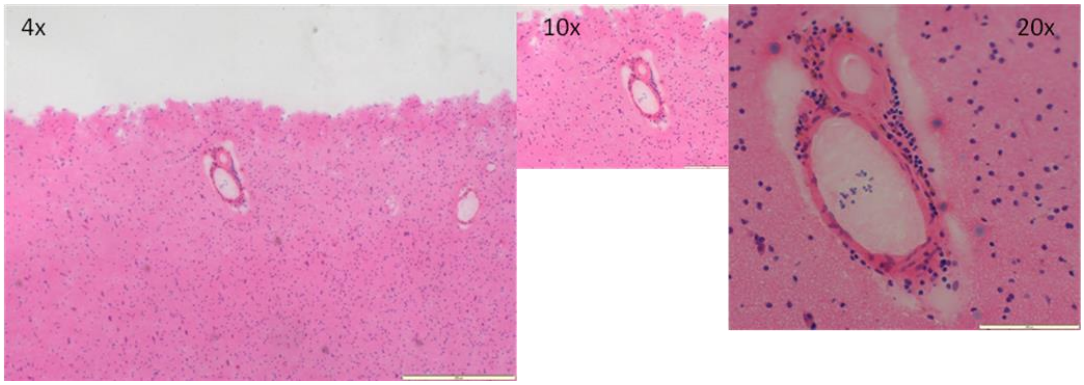

a'')

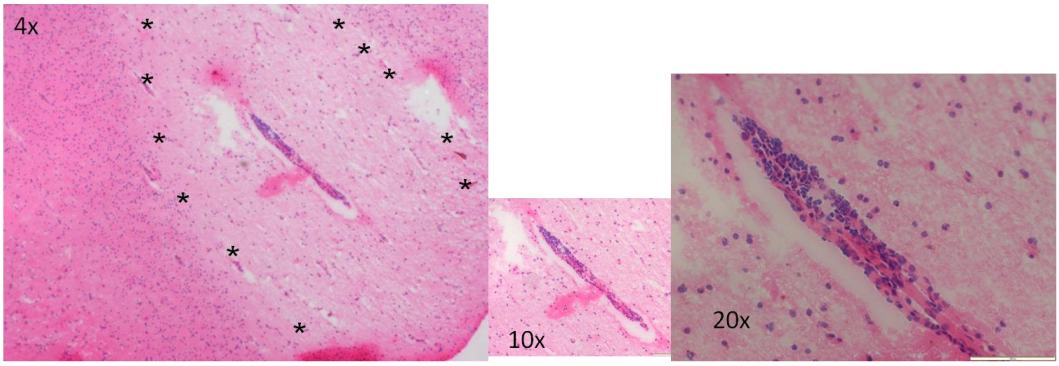

a''')

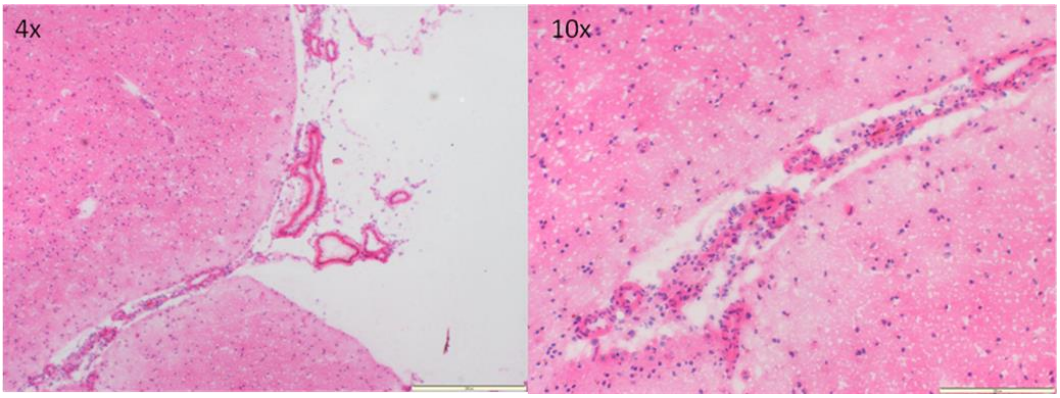

b)

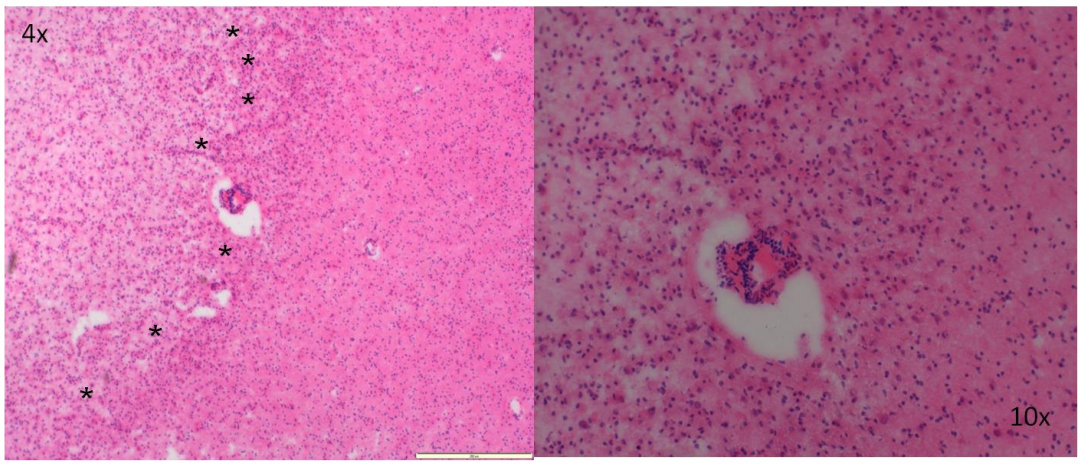

c)

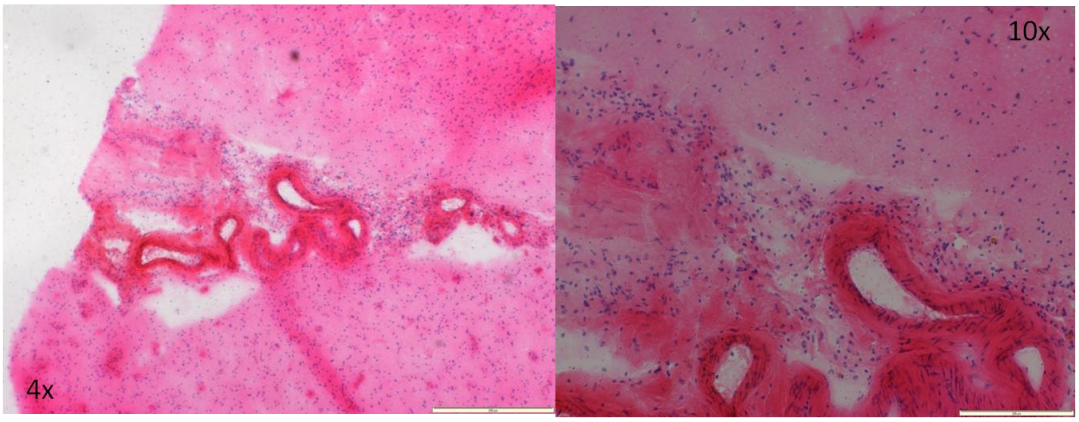

d)

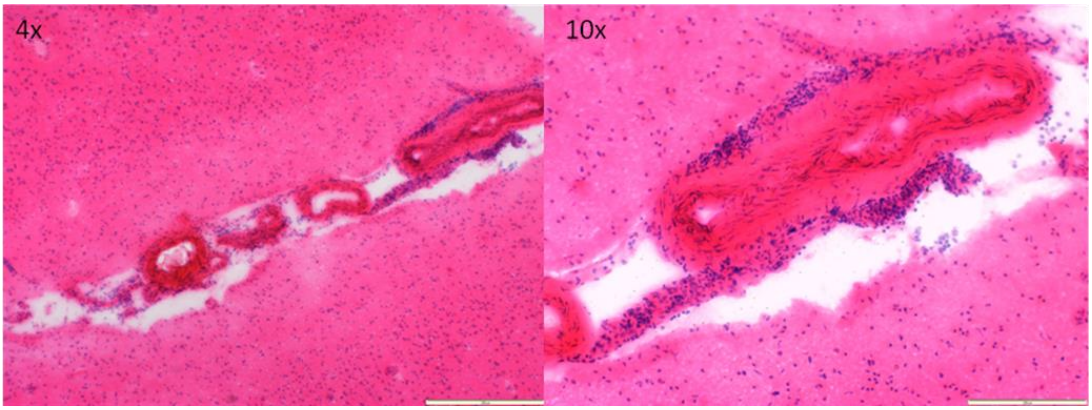

e’)

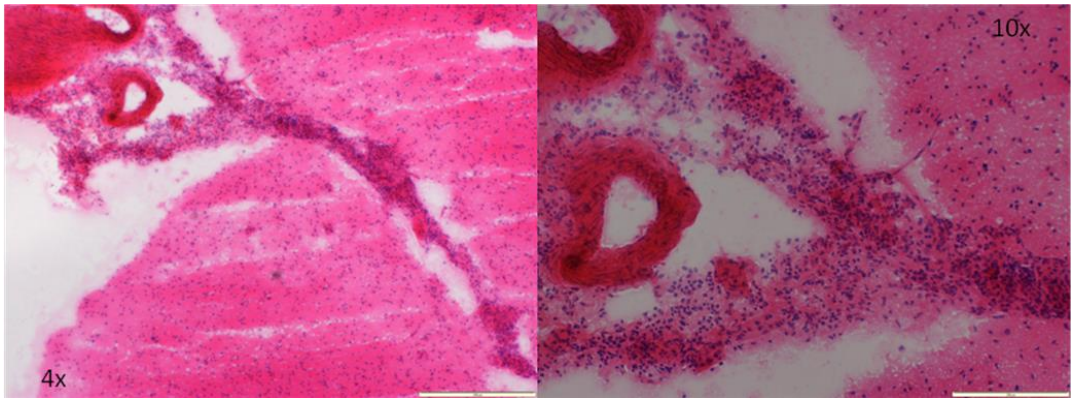

e’’)

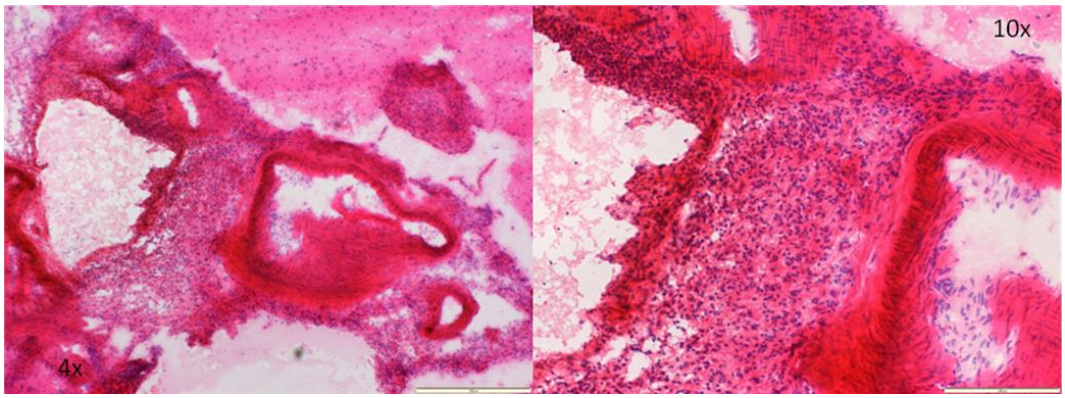

e’’’)

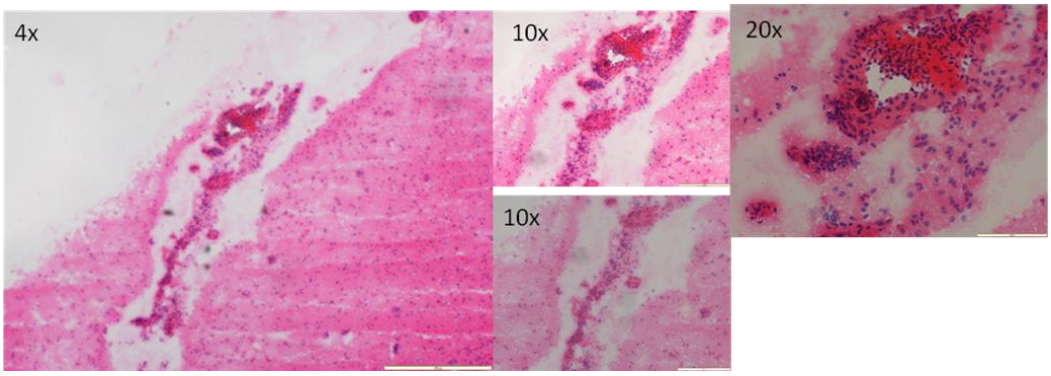

Figure 3.1.2 Examples of immune infiltrates and aggregates: MS330 frontal lobe a’) perivascular infiltrate, a’’) perivascular cuff surrounding a vessel in the centre of a lesion and a’’’) meningeal inflammation; MS342 frontal lobe: b) lesion edge and perivascular cuff on the lesion border; MS325 frontal lobe c) presence of meningeal inflammation and immune cells aggregate in a primary progressive case; MS103 frontal lobe d) presence of meningeal inflammation and lymphoid aggregate; MS160 frontal lobe e’+e’’+e’’’) different lymphoid aggregates along the sulci of a secondary progressive case (*=lesion edge; scale bar=200 µm)

From the follicle-like aggregate found in the SPMS case 136 in collaboration with Dr. Gusta Trillo-Pazos and Prof. David Miller (Institute of Neurology, UCL) I decided to use laser capture microdissection (figure 3.1.3) to isolate the follicle-like structure and extract RNA from this specific cellular network as detailed in chapter 2.

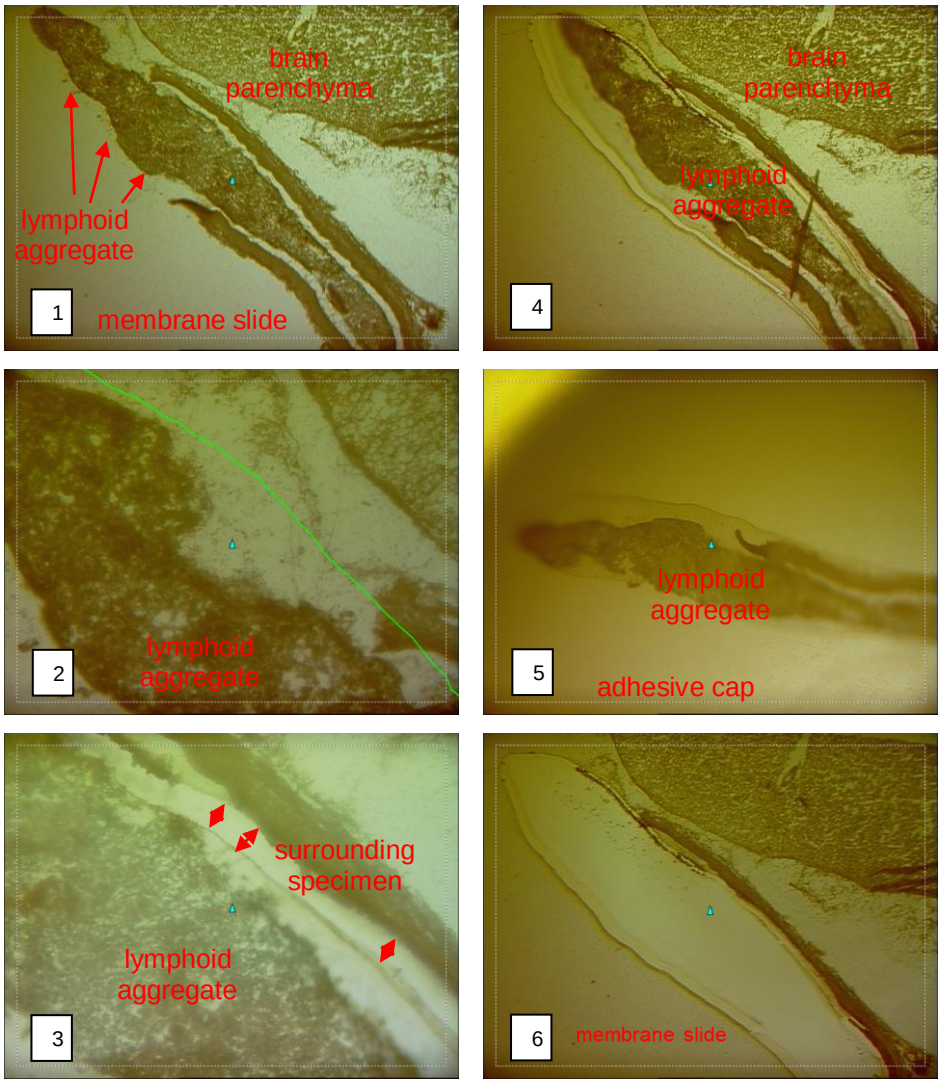

Figure 3.1.3 Sequence of events in laser capture microdissection: the follicle-like structure from SPMS case 136 was microdissected and catapulted onto the adhesive cap by laser beam. 1) Section containing the region of interest (ROI) was visualized utilizing the computer-controlled stage and a colour CCD camera; 2) a green line was drawn on the video image to outline the region to be microdissected; 3-4) the computer system automatically guided the UV laser to cut the ROI and separate it from the surrounding specimen; 5-6) the dissected lymphoid aggregate was catapulted onto a separate adhesive cap and on the membrane slide the area previously occupied by the lymphoid aggregate was left empty. Extraction of total RNA was then performed on the selected group of cells.

As the material available was very low, no evaluation of RNA integrity was performed for this sample and a single experiment was attempted to amplify VH1/3/4 genes (figure 3.1.4).

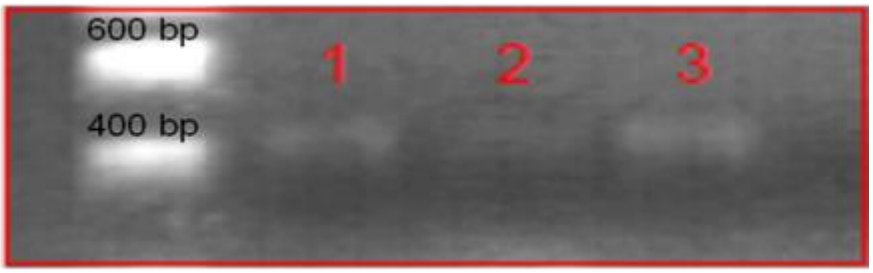

Figure 3.1.4 1% Agarose gel PCR products from microdissected lymphoid aggregate: I was able to amplify VH genes from microdissected lymphoid aggregate. Using 1) VH1a, 2) VH2a and 3) VH3a back primers and as common forward primer a sequence annealing on JH4. Amplification of a product with appropriate length (~ 350-400 bp) was obtained but no sequencing and analysis was performed (data in need of further experimental confirmation).

3.2 Gene Expression

Background

Physiologically lymphocytes encounter the processed or soluble antigen in the lymph node where chances of interaction among different immune cells are increased. High endothelial cells and lymphatic endothelium express CC-chemokine ligands, suc as CCL21 and CCL19, bound by the chemokine C receptor 7 (CCR7) present on lymphocytes and dendritic cells. Chemokines that start the homing cascade in secondary lymphoid organs and allow the immune-cells to interact (Von Andrian and Mempel 2003). From studies on murine GCs by laser-capture microdissection it was shown that the polarization into dark and light zone of the GC is dictated by expression of chemokines CXCL12 and CXCL13 or B-cell homing chemokine (BLC) and their receptors on GCs B cells CXCR4 and CXCR5 segregating centroblasts from centrocytes (Allen et al. 2004). The centroblasts from the dark zone after completing the cell cycle enter in the FDCs network of the light zone as centrocytes and are selected by their capacity to interact with the antigen held on the FDCs. After encountering the Ag the centroblast becomes itself an APC and follows its default fate dying by apoptosis or, in case of CD40/CD40L interactions, survives and induces expression on B cells of LTαβ with maintenance signal for the FDCs (Boulianne et al. 2012). The T-cells have one of the main roles in the germinal centre organization and expressing CXCR5, a receptor for CXCL13, draw the migration path for the B cells in the light zone. The result of a germinal centre reaction is the affinity maturation and germinal centre B cells express the enzyme activation-induced cytidine deaminase (AICDA), also called simply activation-induced deaminase (AID), leading to somatic hypermutation and class switch recombination (Victora and Nussenzweig 2012) (Fig.3.2.1).

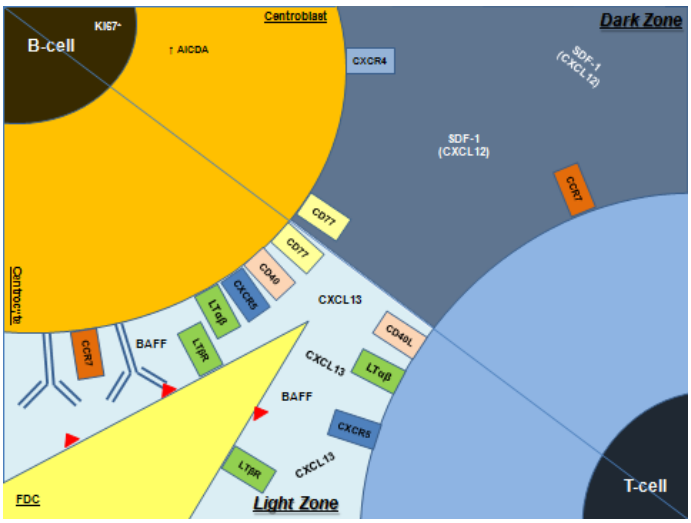

Figure 3.2.1 Cellular interactions in dark and light zone: Germinal centers (GCs) are the structures where affinity maturation takes place and B cells at this level express activation-induced cytidine deaminase (AICDA), enzyme involved in somatic hypermuation and class switch recombination. The most prominent anatomical feature of the GC is its compartmentalization in dark zone (DZ) and light zone (LZ). The DZ contains mainly fast dividing B cells positive for the proliferation marker Ki67. The cycling B cells express specifically the chemokine receptor CXCR4 responsible for retaining the centroblasts in the DZ where its ligand the stromal cell-derived factor 1 (SDF-1), also known as CXCL12, is highly expressed. In the LZ the B cells are interspersed among a network of follicular dendritic cells (FDC) and T cells. The LZ contains characteristically high density of CXCL13 directing the migration of centroblasts differentiated into centrocytes that then populate the LZ expressing the CXCR5 receptor. The GC reaction is also dependent on T cells in the LZ delivering a cognate help to B cells via CD40-CD40L interaction. The lymphoid microenvironment of the GC is maintained by the lymphotoxin axis and in this context the fate of B cells is sustained by the B cell activating factor (BAFF) playing an important role in survival and maturation so that GC-B cells can differentiate to plasmacells.

Chemokines constitutively expressed in secondary lymphoid organs have been found also in tissues that are targeted by chronic inflammatory processes. In particular, elevated levels of CXCL12 and CXCL13 are found in CSF and brain of MS patients. These chemokines are the link to the intracerebral homing of immune cells and development of lymphoid neogenesis (Aloisi et al. 2008; Aloisi and Pujol-Borrell 2006). In fact it was shown by immunohistochemistry that the inflamed meninges harbor follicle-like structures containing various degree of macrophages, $Ki67^+$ proliferating B cells, plasma cells, T cells and $CD35^+$ $CD21^+$ FDCs with expression of homing chemokines such as CXCL13 (Serafini et al. 2004).

Methods

To evaluate my samples for expression levels of different genes of interest (GOI) involved in inflammation and germinal centre reaction, minimum information for publication of quantitative real-time PCR experiments (MIQE) guidelines were followed during the experiments to make sure the results obtained could be reliable and the nomenclature appropriate as from the minimum information for biological and biomedical investigations (MIBBI) (Bustin et al. 2009; Kettner et al. 2010). The tissues examined were supplied by different tissue banks ("Amsterdam Pathology department", "Edinburgh Sudden Death Brain and Tissue Bank" and "The UK MS tissue bank") and before starting with my experiments I checked the quality of the material supplied. Total RNA was extracted from 14 postmortem brain blocks from MS patients (complete demographic characteristic in table 2.1) and from 2 lymph nodes from different sources (Amsterdam and Edinburgh source) as detailed in chapter 2.

The use of post-mortem human tissues and in particular brain tissues suffers several factors related with pre-mortem events (prolonged agonal state, hypoxia, acidosis fever and seizures) and with post-mortem events (delay between death and sample processing for storage and fixation or processing of frozen material) that can interfere with their utilization in molecular studies (Ferrer et al. 2008).

Characteristics of the tissues supplied were summarized below (table 3.2.1):

Parameters	Mean	Range	StDev
Age of death (years)	54	34-77	12.1
Post-mortem delay (h)	18.8	7-30	6.6
Brain pH (5 brain samples)	6.4	6.02-6.78	0.27

Table 3.2.1 Samples characteristics: Demographic and post-mortem events of 14 MS brain samples, 2 brain controls and 1 lymphoid tissue used in my study

To evaluate for RNA extraction yield, RNA quality and level of degradation different methods were used: agarose gel electrophoresis, electropherogram patterns and UV spectroscopy by classical spectrophotometer (Ultrospec II, LKB Biochrom, UK) with cuvettes and nanodrop spectrophotometer for small samples (Nanodrop 1000, Thermo scientific, UK).

Results

The RNA yield was analysed comparing the OD results from the two spectrophotometers obtaining a strong correlation between the measurements. Due to the strong correlation and to the lower amount of sample needed if not otherwise stated my RNA concentrations were measured by nanodrop with good relative measurements among samples (Fig.3.2.2).

a)

Samples:	ng/µl	260/280	260/230
MS103	753.1	2.12	2.17
MS154	973.8	2.13	1.97
MS179*	272.7	2.08	1.44
MS311	592.5	2.12	2.20
MS317	258.4	2.08	2.26
MS325	570.3	2.10	2.16

b)

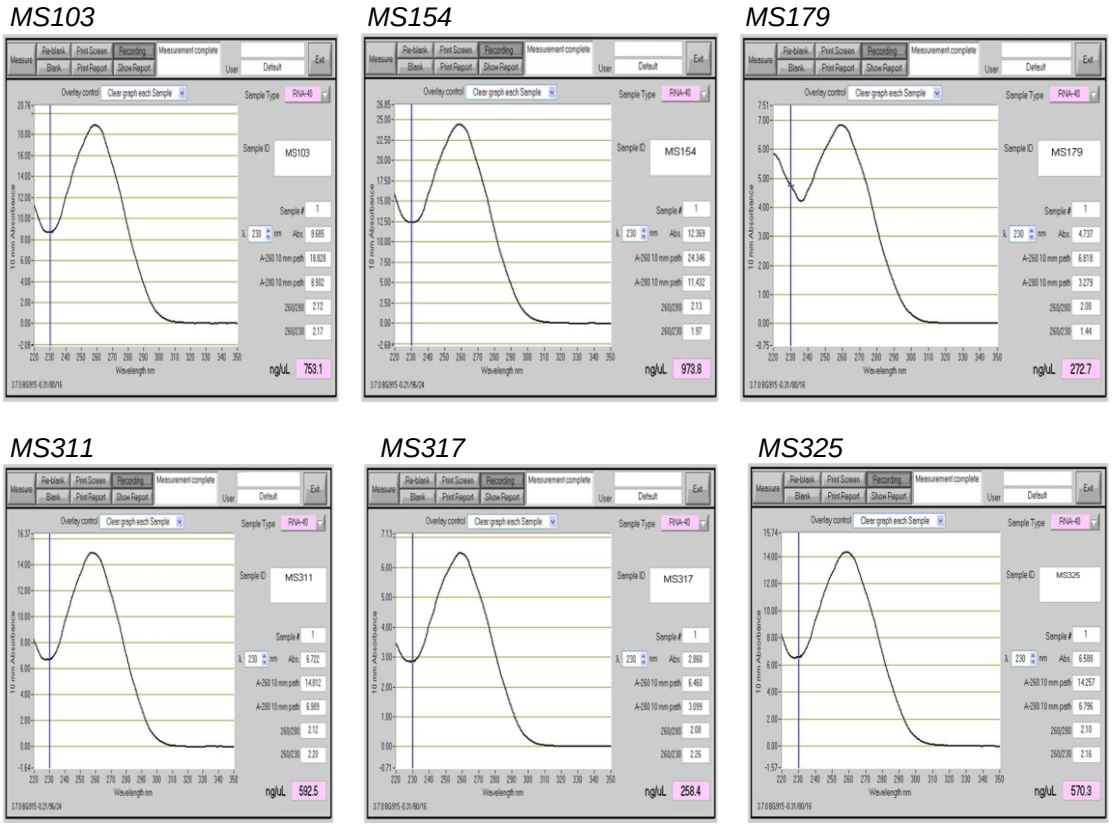

Fig.3.2.2 Nanodrop quantification and evaluation of RNA extraction: From each sample 1 µl RNA was measured to evaluate concentration and purity. a) The table shows the concentration in nanogram (ng)/microliter (µl), ratio of sample absorbance at 260 and 280 nm (260/280) and ratio of sample absorbance at 260 and 230 nm (260/230). Both ratio values are used to assess the purity of the sample or presence of proteins and other contaminats in the eluted sample. b) The absorbance spectra for the different samples show absorbance on the Y-axis and wavelength on the X-axis. Nanodrop results of some of MS samples, *=sample 179 gave a low value indicating some sort of contamination (the same sample gave the lowest RIN value as shown in table 3.2.2).

RNA degradation and DNA contamination were evaluated to obtain reliable results. The first method used to evaluate RNA degradation was agarose gel electrophoresis using RNA samples from healthy lymph node tissues, MS and control brain tissues. RNA was considered of high quality when the ratio of 28S:18S bands was about 2.0 and higher. My samples were treated with a two-step process to eliminate any possible DNA contamination (as my first experiment presented positive signal in the -RT control) and the RNAs obtained compared with different methods (Fig.3.2.3 and 3.2.4).

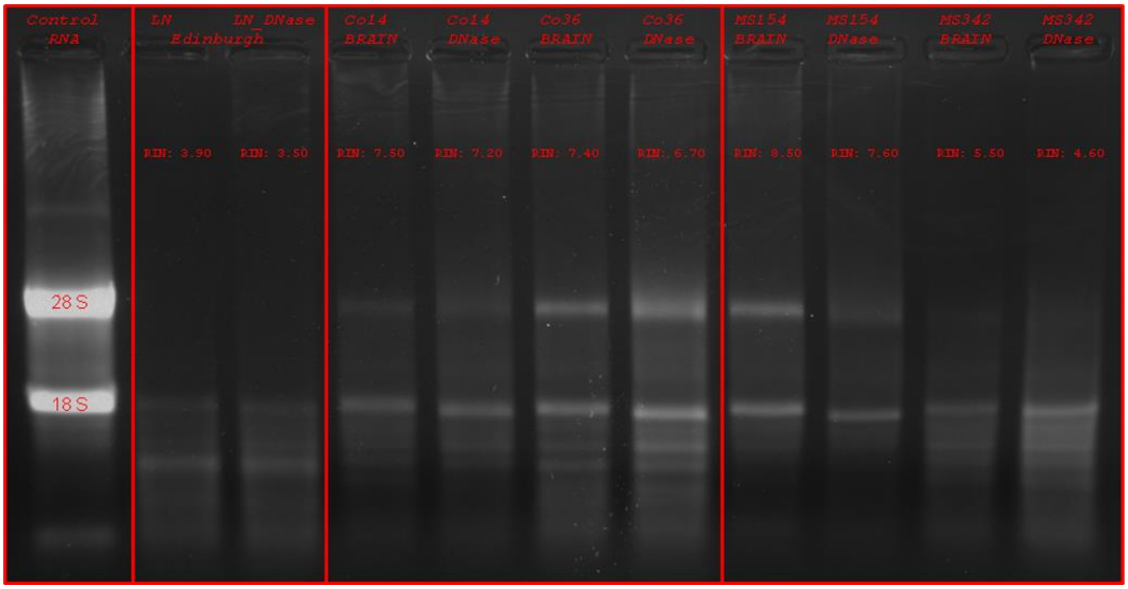

Figure 3.2.3 RNA quality checked by 1% denaturing agarose gel: All samples were DNase treated on column but for each samples are shown 2 lanes with on column treatment only and a further 2nd treatment with TurboTM DNase after on column treatment. The lanes were compared with RNA integrity number values of respective samples. Samples: LN=lymph node, Co=control brain, MS=MS brain, control RNA from Ambion.

The ribosomal RNA ratio values did not allow a consistent objective comparison of the results on the various samples and did not supply a consistent quantitative unambiguous cut off to be considered for downstream experiments. A large amount of RNA is needed for visualization using agarose gel electrophoresis and the assessment very subjective, consequently the classical agarose gel results expressed as ribosomal ratio of 28S:18S bands have not been considered for discriminating my samples. The following step was to test my samples by microcapillary electrophoretic RNA separation (Bioanalyser

2100 Agilent and RNA nano chip) to obtain an RNA integrity number (RIN). The RNA samples were separated based on their molecular weights in gel filled microchannels and detected by laser-induced fluorescence. The correlation of fluorescence units and the amount of RNA of a certain size was plotted and shown as electropherogram. Regions (such as the 28S region or the fast region, i.e. the region between the 5S region and the 18S region), peaks (such as presence or absence of the 18S peak) and ratios (such as the total RNA ratio corresponding to the fraction of the area in the region of 18S and 28S compared to the total area under the curve) are different features describing the curve of the electropherogram taken into consideration and that contribute to determine the RNA integrity. RIN values were obtained by application of a software algorithm trained with different levels of degraded RNA measurements based on these features and leading to a user-independent procedure for standardization of RNA quality control (Schroeder et al. 2006). My samples were then differentiated in integrity categories based on the results obtained with a RIN cut off value above >7 chosen to accept samples for further evaluation in qPCR experiments due to the significant correlation of high RIN values with good outcome of the experiments as reported in the literature (Schroeder et al. 2006). The RIN in my samples was evaluated on the RNAs just after on column DNase treatment elution and after a 2nd treatment with Turbo^{TM} DNase (Fig.3.2.4).

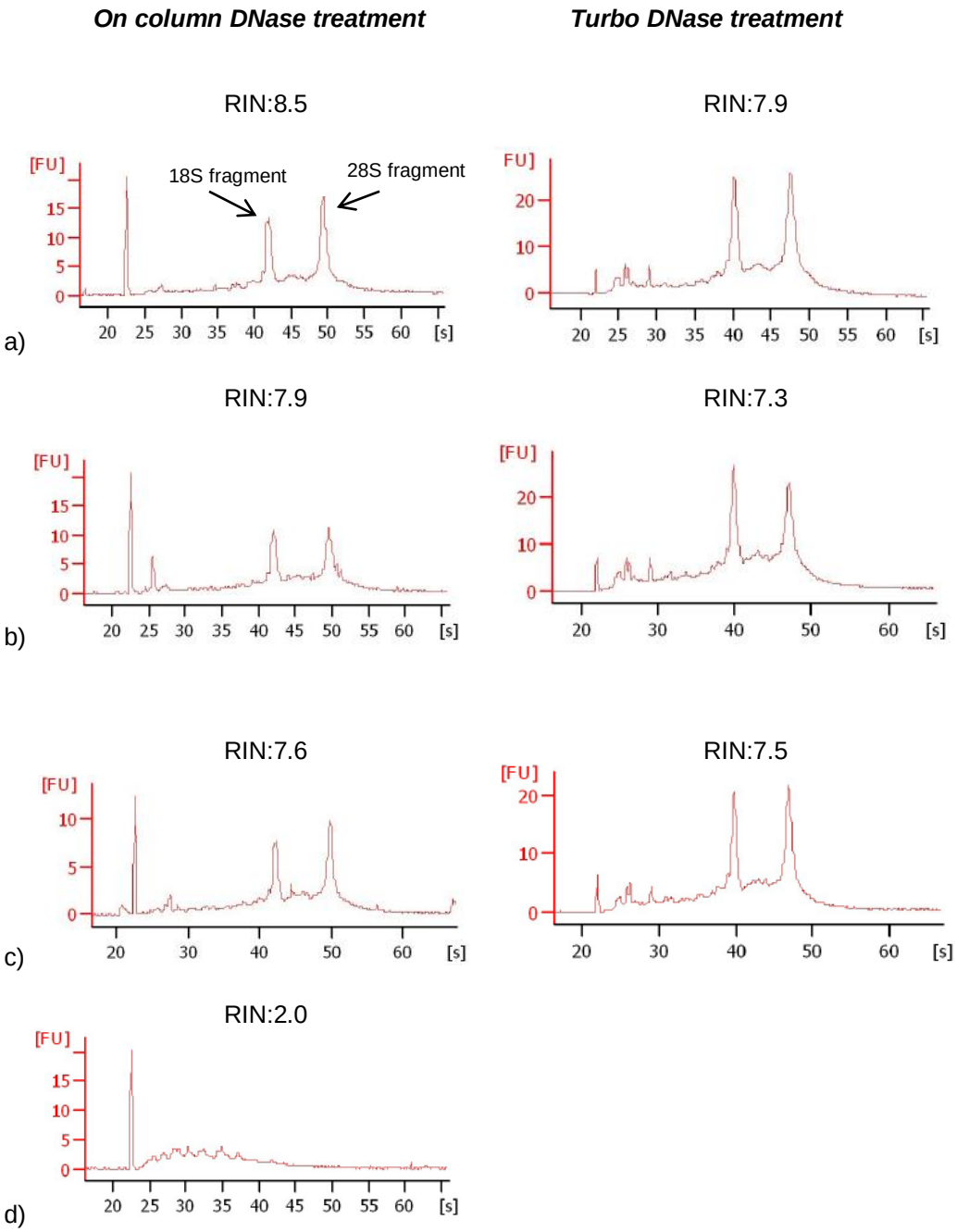

Figure 3.2.4 Examples of electropherogram by 2100 bioanalyser: electropherograms before and after Turbo™ DNase treatment of samples from different MS forms a) SPMS154; b)RPMS341; c)PPMS325; d)SPMS179 is one of the sample discarded from my analysis for low quality RNA (RIN=RNA integrity number). X-axis showing time and Y-axis showing fluorescence units.

The mean RIN for the MS brain samples was 6.93±1.76 with on column treatment and 6.96±0.89 after 2nd Turbo™ DNase treatment (Table 3.2.2).

	RNA Samples	Sex	Age at death	pH	Post mortem delay (h)	RIN (DNase on column)	RIN (Turbo DNase)	
a	SPMS103	F	77	6,78-6,73	7	8.1	7.8	√
	SPMS154	F	34	*	12	8.5	7.9	√
	SPMS160	F	44	6,37-6,31	18	NA	*	
	SPMS179	F	70	6,39-6,36	20	2	*	
	SPMS307	M	55	*	19	6.5	4.8	
	SPMS311	F	45	*	22	3.6	*	
	SPMS317	F	48	*	21	7.3	7.4	√
	PPMS325	M	51	*	13	7.6	7.5	√
	SPMS330	F	59	6,74-6,61	21	8.2	8.1	√
	SPMS335	M	62	*	22	8	7.6	√
	RPMS341	F	52	*	8	7.9	7.3	√
	SPMS342	F	35	*	9	7.1	6.5	
	SPMS352	M	43	*	26	6.8	6	
	SPMS377	F	50	*	22	6.5	6.5	
b	Co14	M	64	6,07-6,02	18	7.5	7.2	√
	Co36	M	68	*	30	7.4	6.7	√
c	TN_045/10_WHRI†	*	*	*	*	7.9	7.5	√
	TN_34.02_Amsterdam	*	*	*	*	6.5	5.7	
	LN_SD008/10_Edinburgh	M	61	*	47	3.1	*	

Table 3.2.2 Post-mortem parameters and respective RINs: a) 14 MS brain samples; b) control brain samples; c) lymphoid tissue samples († kindly provided by Dr B. Hands from Centre for Experimental Medicine and Rheumatology, WHRI; * not evaluated; NA=RNA extremely degraded) (samples selected for further experiments are ticked in the last column)

Some of my samples did not reach the RIN values requested despite all samples being processed in the same way. To understand the reason of this low level quality RNA I decided to evaluate peri and post-mortem events. Informations on agonal factors such as coma, hypoxia, pyrexia, seizures, dehydration, hypoglycemia, multiple organ failure, head injury, and ingestion of neurotoxic substances at time of death were missing. Alternatively, pH values as comprehensive result of these factors and post-mortem delay of the tissue blocks were taken into consideration. From the literature it is widely accepted that pH measurement is one of the most important parameters to correlate with RNA integrity (Atz et al. 2007; Durrenberger et al. 2010; Li et al. 2004; Mexal et al. 2006; Stan et al. 2006; Tomita et al. 2004). Average values of pH ranging

from 6.8 (6.5-7.1) to 6.3 (5.8–6.6) in control brains from various neuropathological collections have been described (Middleton et al. 2002; Torrey et al. 2000). In my samples the pH values were evaluated with two consecutive readings by an electronic pHmeter (Mettler Toledo MP220) after homogenizing 150 mg brain tissue in 1.5 ml ddH_2O (pH=7.0). The pH values of my MS samples were in the 6.3-6.7 range and within the normal range instead surprisingly the control sample showed an acidic pH ~ 6.0. The results obtained with the bioanalyser and the post-mortem delay in my samples showed a small negative linear dependence (Pearson's coefficient r=-0.24). A strong positive dependence (Pearson's coefficient r=0.96) was shown, instead, correlating RIN with pH in the MS samples. Correlation coefficient that was drastically reduced considering the control sample (Co14) values in the analysis, indicating the presence of some other factor influencing the RNA integrity in this sample (table 3.2.2; Fig.3.2.5).

a)

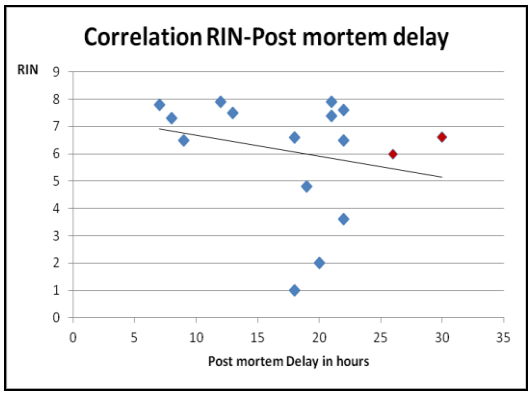

b)

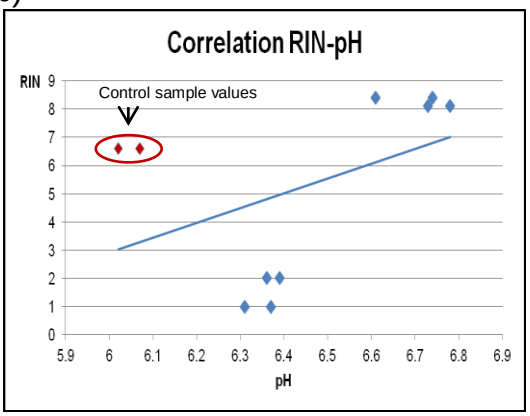

c)

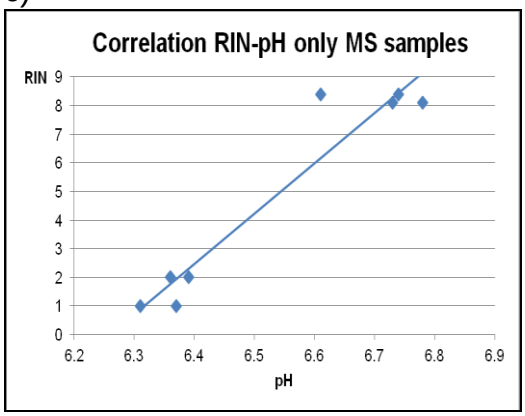

Figure 3.2.5 Correlation post-mortem parameters and RIN: a) almost no linear dependence was found between RIN values and post-mortem delay in MS (blu) and control (red) brain samples (r=-0.24); b) medium positive correlation between RIN and pH duplicates in all brain samples (r=0.43); c) strong positive correlation between RIN and pH duplicates when only MS brain samples without control sample (Co14) values were considered in the analysis (r=0.96).

The samples selected for high quality RNA were 7 MS brain samples, 2 controls and 1 lymphoid tissue, the latter used as positive control. cDNA was generated from total RNA as detailed in chaper 2. To standardize my data reference genes were required to be expressed at constant level in the MS and control brain samples and that could be useful for comparison with lymphoid tissue as well. In literature the choice of reference genes is usually related to genes involved in cell metabolism and maintenance of cell function, called “housekeeping”, expressed at constant level in different experimental conditions and able to eliminate the possible bias that could arise from sample processing changes

mistaken for gene expression level changes. The candidate reference genes identified in my study were selected checking the results of a DNA chip study, measuring expression levels of 7000 genes from a pool of whole organs, that identified 47 transcripts expressed at the same level in 11 human adult and fetal tissues (Warrington et al. 2000) and from other qPCR relevant studies utilizing human post-mortem brain tissues (Coulson et al. 2008; Koppelkamm et al. 2010). In a two step process I first identified the candidate genes and among the candidate genes I have selected 10 genes (Table 3.2.3), from different molecular pathways to avoid coregulation, for possible use in data normalization and examined the transcripts stability to determine the minimum number of genes required for reliable data normalization.

Gene Symbol	Full Name	Transcript variant	Pathway involved	Ref Seq
ENOX1	ecto-NOX disulfide-thiol exchanger 1	variant 1	plasma membrane transport	NM_017993.3
RNF20	ring finger protein 20	N.A.	ubiquitination	NM_019592.5
RPL37A	ribosomal protein L37a	N.A.	Subunit of ribosomal 60S	NM_000998.4
NUMA1	nuclear mitotic apparatus protein 1	N.A.	Mitotic regulation	NM_006185.2
TTC1	tetratricopeptide repeat domain 1	N.A.	molecular chaperones and protein folding	NM_003314.1
GAPDH	glyceraldehyde-3-phosphate dehydrogenase	N.A.	carbohydrate metabolism	NM_002046.3
HMBS	hydroxymethylbilane synthase	variant 1	heme biosynthetic pathway	NM_000190.3
TBP	TATA box binding protein	variant 1	Initiation of transcription	NM_003194.4
DNMBP	dynamin binding protein	N.A.	regulation of cell junctions	NM_015221.2
XDH	xanthine dehydrogenase	N.A.	oxidative metabolism of purines	NM_000379.3

Table 3.2.3 Endogenous reference genes analysed for data normalization: Genes expressed in brain and lymphoid tissues were chosen and different metabolic pathways were selected to avoid coregulation.

Once the genes were chosen, all primers were designed to anneal in gene regions of no secondary structure formation under the same temperature condition of 60°C and chosen to span one exon-exon boundary when possible. The 10 reference genes primers lengths were in the range of 18-24bp with a mean GC% content of 48% (range 36-60%) and a mean optimal annealing temperature of 58.8°C (range 57.2-60.5°C) compared with the 11 target genes primers lengths being in the range of 20-24 bp with a mean GC% content of 48.9% (range 37.5-61.9%) and a mean optimal annealing temperature of 57°C

(range 55-62.4°C). The mean amplification product length in the reference genes was 103 bp (range 66-176 bp) and 88 bp (range 60-127 bp) in the target genes to minimize any RNA degradation bias and all the products spanned at least one exon-exon boundary to minimize eventual amplification of contaminant DNA (primers sequences list in table A.5-A.6 and design examples in Fig.3.2.6). The primers were checked for specificity of target and transcript variant against a nucleotide sequence database such as BLAST using Primer-BLAST tool (Ye et al. 2012) (Fig.3.2.7).

✓ NM_017993.3

Homo sapiens ecto-NOX disulfide-thiol exchanger 1 (ENOX1), transcript variant 1, mRNA

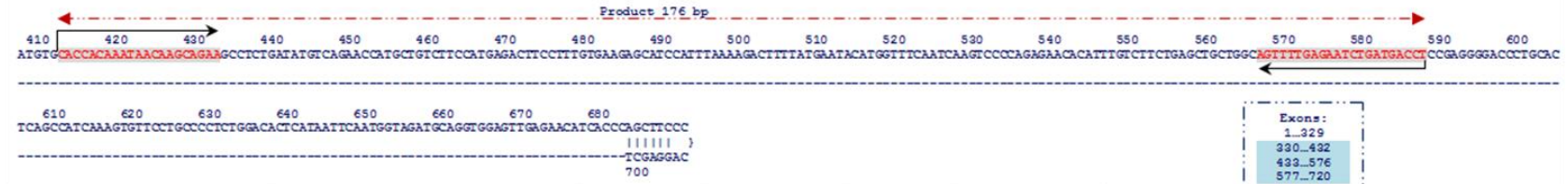

ENOX1	SEQUENCE	POSITION	LENGTH BP	Tm °C	Ta OPT °C
Sense Primer	CACCACAAATAACAAGCAGAA	414	21	61.1	
Anti-sense Primer	AGGTCATCAGATTCTCAAAACT	589	22	61.3	
Product			176	77.8	57.9

✓ NM_019592.5

Homo sapiens ring finger protein 20 (RNF20), mRNA

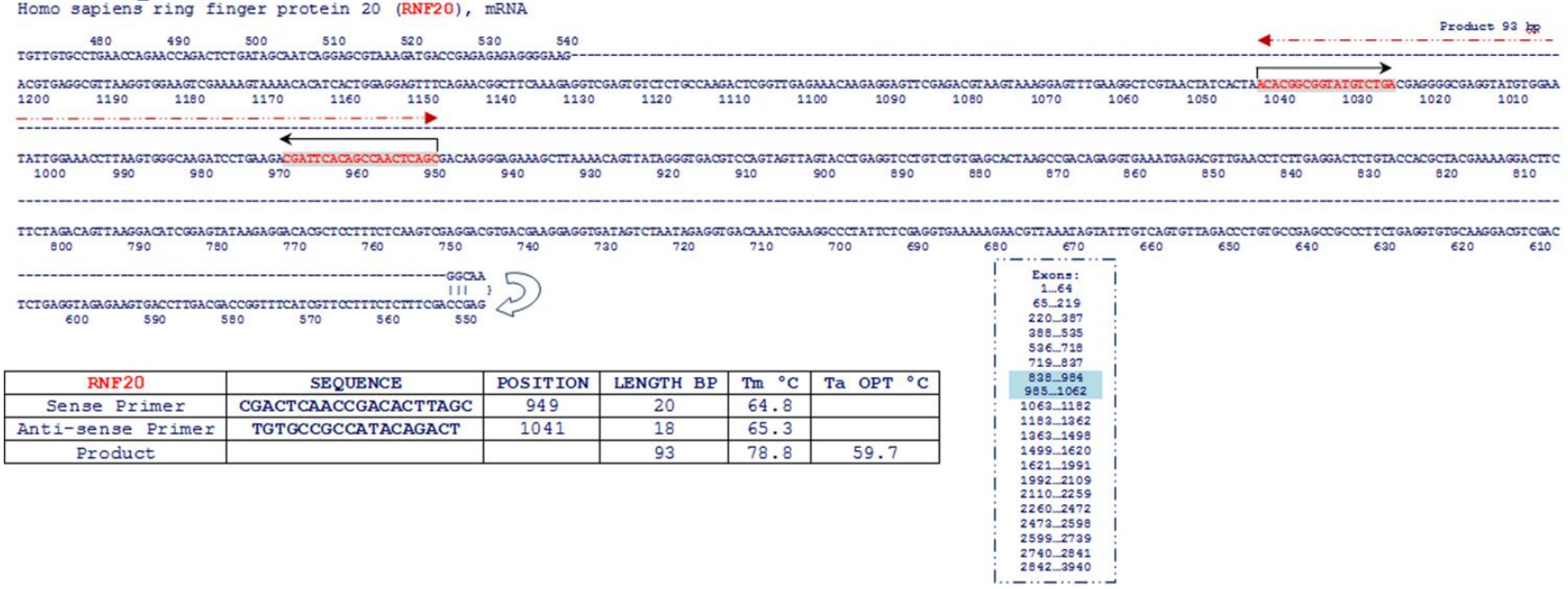

RNF20	SEQUENCE	POSITION	LENGTH BP	Tm °C	Ta OPT °C
Sense Primer	CGACTCAACCGACACTTAGC	949	20	64.8	
Anti-sense Primer	TGTGCCGCCATACAGACT	1041	18	65.3	
Product			93	78.8	59.7

✓ NM_002046.3

Homo sapiens glyceraldehyde-3-phosphate dehydrogenase (GAPDH), mRNA

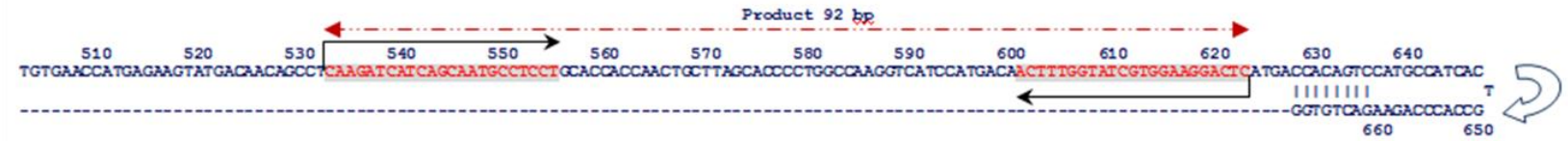

GAPDH	SEQUENCE	POSITION	LENGTH BP	Tm °C	Ta OPT °C
Sense Primer	CAAGATCATCAGCAATGCCTCCT	534	23	67.1	
Anti-sense Primer	TGAGTCCTTCCACGATACCAAAGT	625	24	67.6	
Product			92	79	60.5

Exons:
1…79
80…131
132…231
232…338
339…429
430…545
546…627
628…1040
1041…1310

✓ NM_000190.3

Homo sapiens hydroxymethylbilane synthase (HMBS), transcript variant 1, mRNA

HMBS	SEQUENCE	POSITION	LENGTH BP	Tm °C	Ta OPT °C
Sense Primer	ATGTCTGGTAACGGCAATG	158	19	62.3	
Anti-sense Primer	GCGAATCACTCTCATCTTTGG	223	21	63.2	
Product			66	76.4	57.2

Exons:
1…190
191…244
245…317
318…367
368…423
424…501
502…579
580…655
656…769
770…808
809…928
929…982
983…1069
1070…1509

✓ NM_015221.2

Homo sapiens dynamin binding protein (DNMBP), mRNA

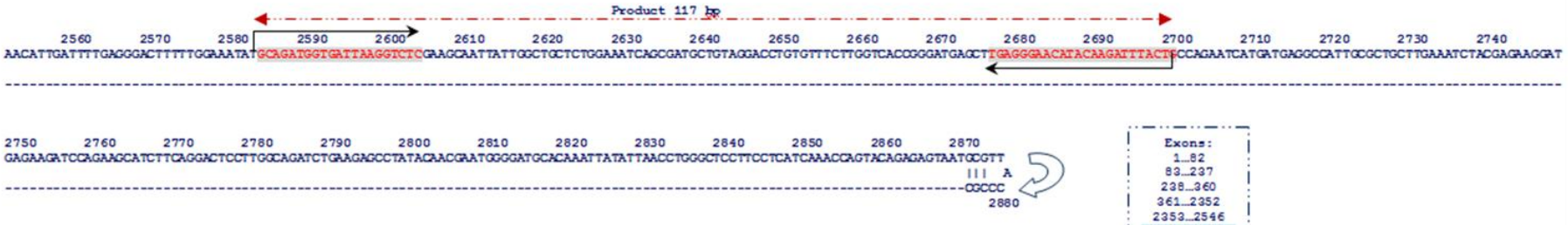

DNMBP	SEQUENCE	POSITION	LENGTH BP	Tm °C	Ta OPT °C
Sense Primer	GCAGATGGTGATTAAGGTCTC	2585	21	62.3	
Anti-sense Primer	CAGTAAATCTTGTATGTTCCCTCA	2701	24	62.4	
Product			117	78.4	58.7

Exons:
1…82
83…237
238…360
361…2352
2353…2546
2547…2646
2647…2794
2795…2812
2813…3012
3013…3143
3144…3248
3249…3377
3378…3710
3711…3890
3891…4089
4090…4640
4641…6400

✓ NM_003314.1

Homo sapiens tetratricopeptide repeat domain 1 (TTC1), mRNA

TTC1	SEQUENCE	POSITION	LENGTH BP	Tm °C	Ta OPT °C
Sense Primer	GAGCGGACAAGGTTGAGAACAA	274	22	67.2	
Anti-sense Primer	TTCCCTCCTCCTTTAGTCTAGTGC	420	24	67.2	
Product			147	76.2	58.6

Exons:
1…21
22…380
381…441
442…554
555…591
592…740
741…795
796…1407

✓ NM_006185.2

Homo sapiens nuclear mitotic apparatus protein 1 (NUMA1), mRNA (could be used for the ratio 3′:5′)

Product toward the 5′ end

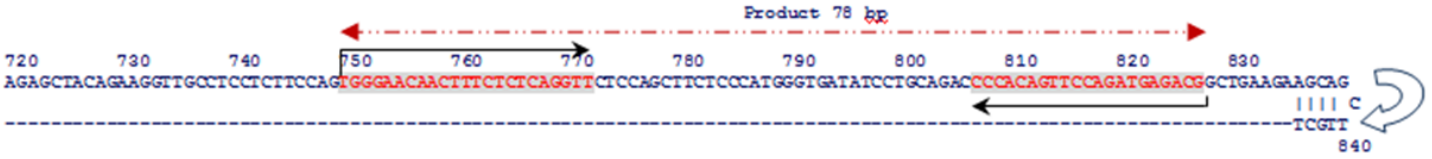

NUMA1	SEQUENCE	POSITION	LENGTH BP	Tm °C	Ta OPT °C
Sense Primer	TGGGAACAACTTTCTCTCAGGTT	748	23	66	
Anti-sense Primer	CGTCTCATCTGGAACTGTGGG	825	21	66.6	
Product			78	77.8	59.4

Exons:
1…70
71…140
141…214
215…300
301…380
381…463
464…544
545…632
633…756
757…914
915…1032
1033…1150
1151…1291
1292…1414
1415…4780
4781…4822
4823…4891
4892…5011
5012…5230
5231…5388
5389…5635
5636…5864
5865…6001
6002…6178
6179…6295
6296…6508
6509…7182

✓ NM_003194.4

Homo sapiens TATA box binding protein (TBP), transcript variant 1, mRNA

TBP	SEQUENCE	POSITION	LENGTH BP	Tm °C	Ta OPT °C
Sense Primer	TGACCCAGCATCACTGTTTC	124	20	64.5	
Anti-sense Primer	TGGAACTCGTCTCACTATTCAATT	239	24	63.9	
Product			116	77.5	58.5

Exons:
1…131
132…333
334…776
777…864
865…956
957…1124
1125…1219
1220…1904

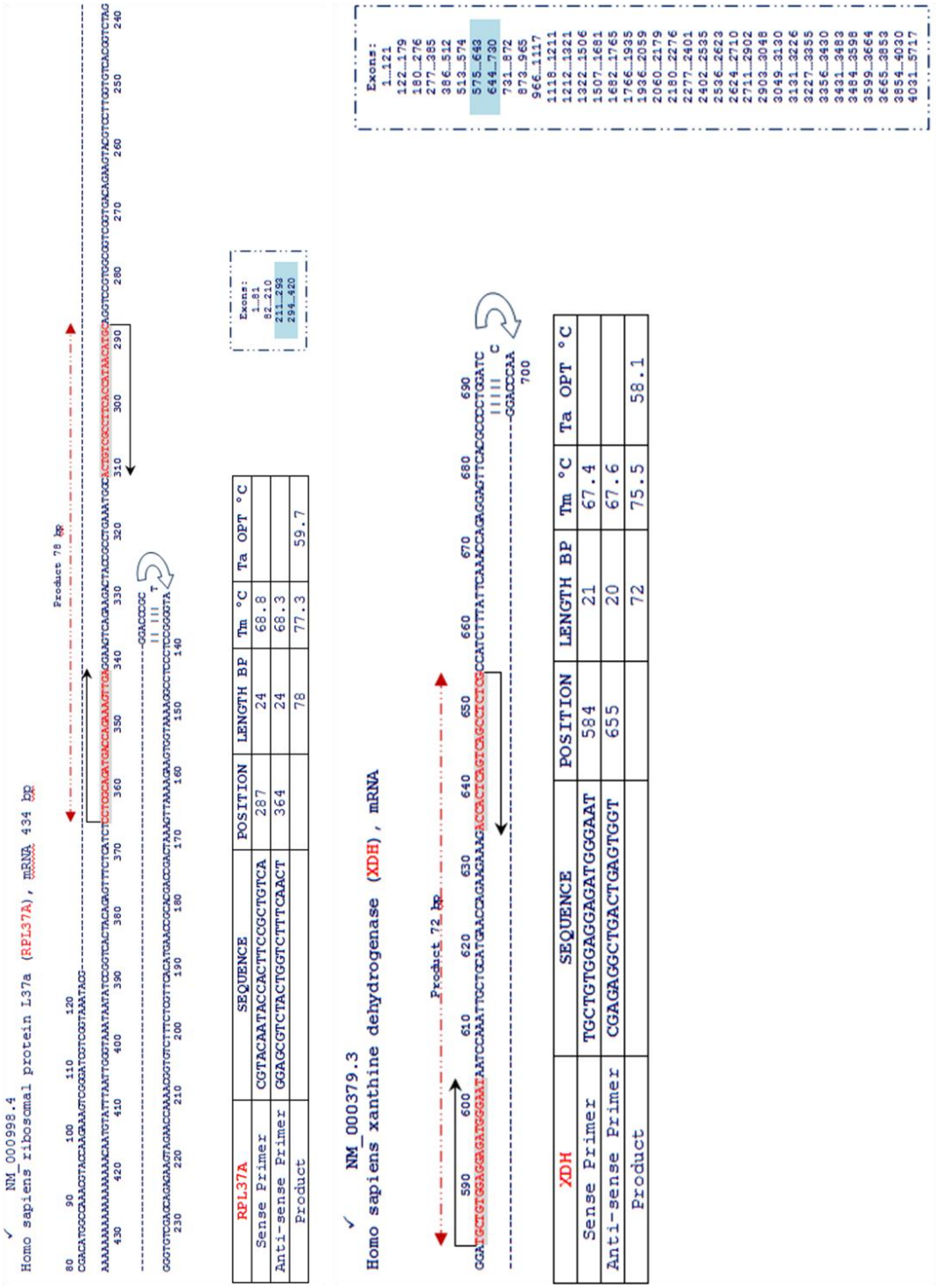

Figure 3.2.6 Reference genes primers design for SYBR Green chemistry: I overcame the lower level of specificity due to the lack of fluorescent specific probe as in the TaqMan assays designing my primers in a very stringent way. The examples of the two reference genes reported show sequences targeted and their secondary structures at 60°C (temperature chosen for the annealing step), positions of exons within the gene, primers sequences and summary of amplicon length, melting temperatures (Tm) and optimal annealing temperatures (Ta OPT).

a)

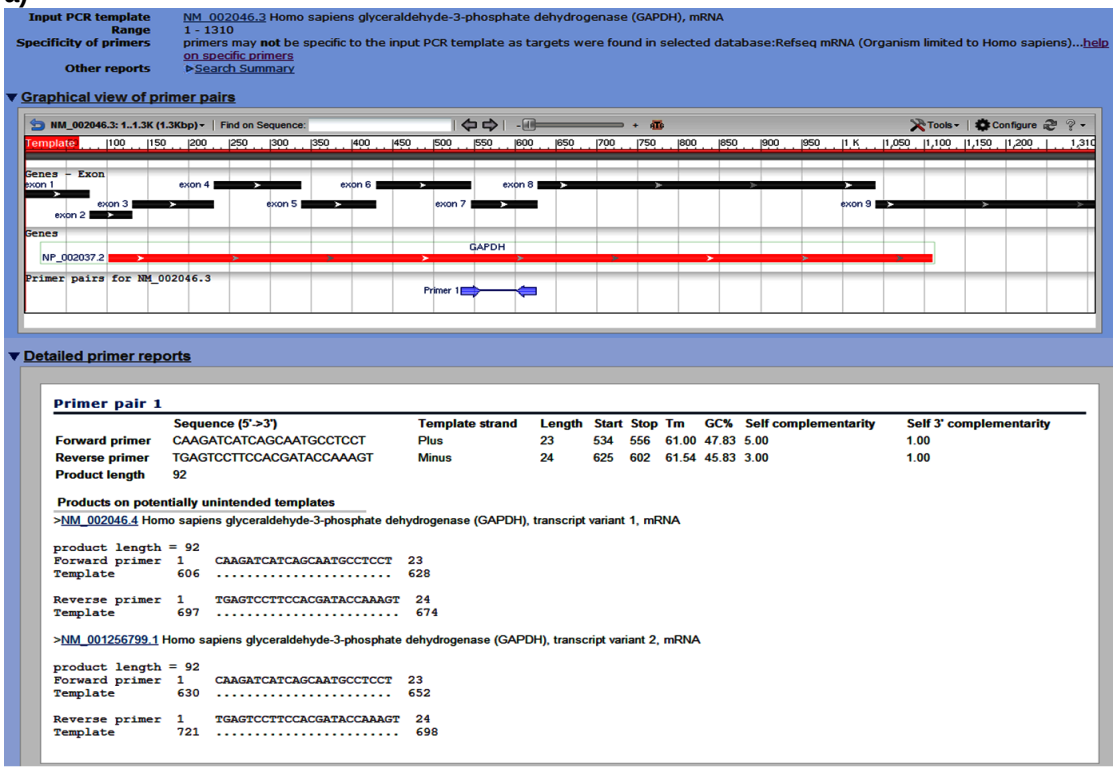

b)

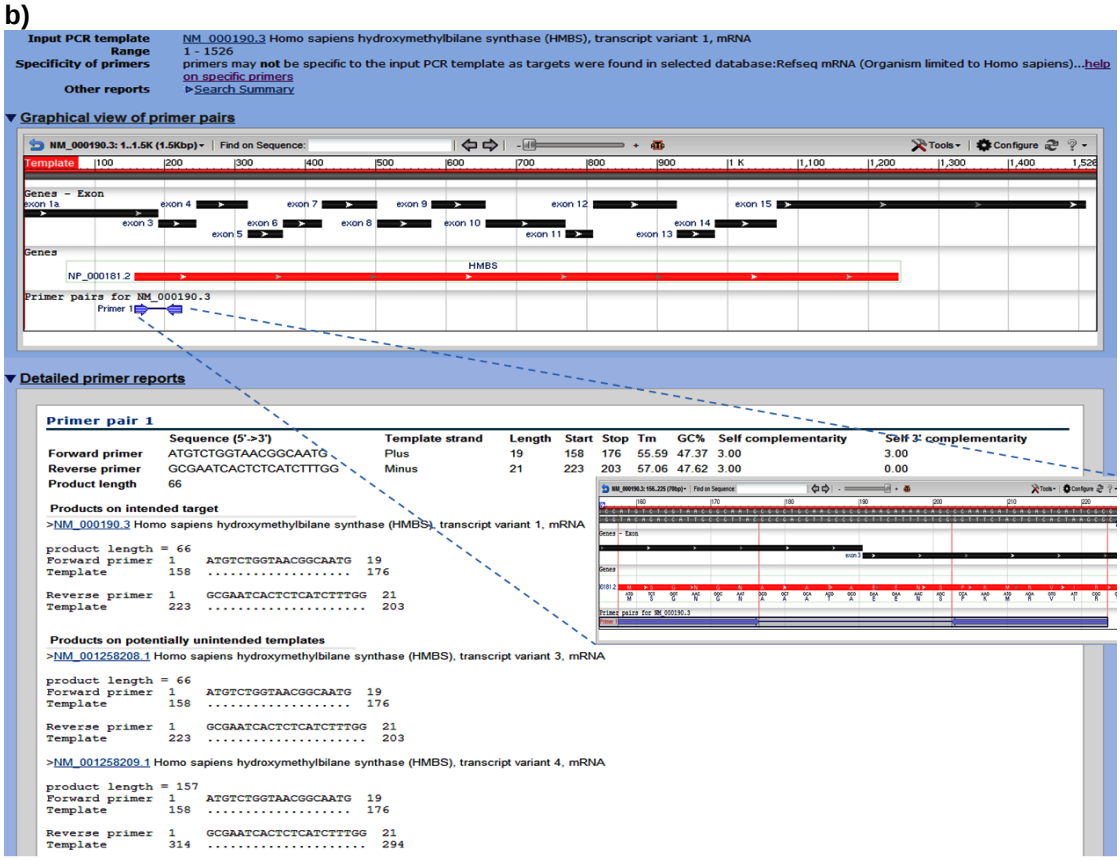

Figure 3.2.7 GAPDH and HMBS primers check against BLAST database: The GAPDH and HMBS primers were the only ones to retrieve multiple products. a) GAPDH primers amplified the same product from 2 variant transcripts of the target gene. b) HBMS primers amplified 3 variant transcripts from the target gene with 2 different products (inset: zoom primer sequence).

Primers concentration was investigated by an optimization matrix considering three different concentrations, 100 nM, 200 nM and 300 nM, and their combinations for the forward and reverse primers leaving the other conditions constant (Table 3.2.4 and Fig.3.2.8).

Matrix	[nM]
a1	100/100
a2	100/200
b1	200/100
a3	100/300
c1	300/100
b2	200/200
b3	200/300
c2	300/200
c3	300/300

Table 3.2.4 Optimization matrices for primers concentration: Matrix optimization with different primer combinations for reference genes.

Quantification cycle (Cq) lowest values for the reference genes were obtained at primers concentration of 300/300 nM (Fig.3.2.8) and this concentration was used in setting my reactions (Fig.3.2.9).

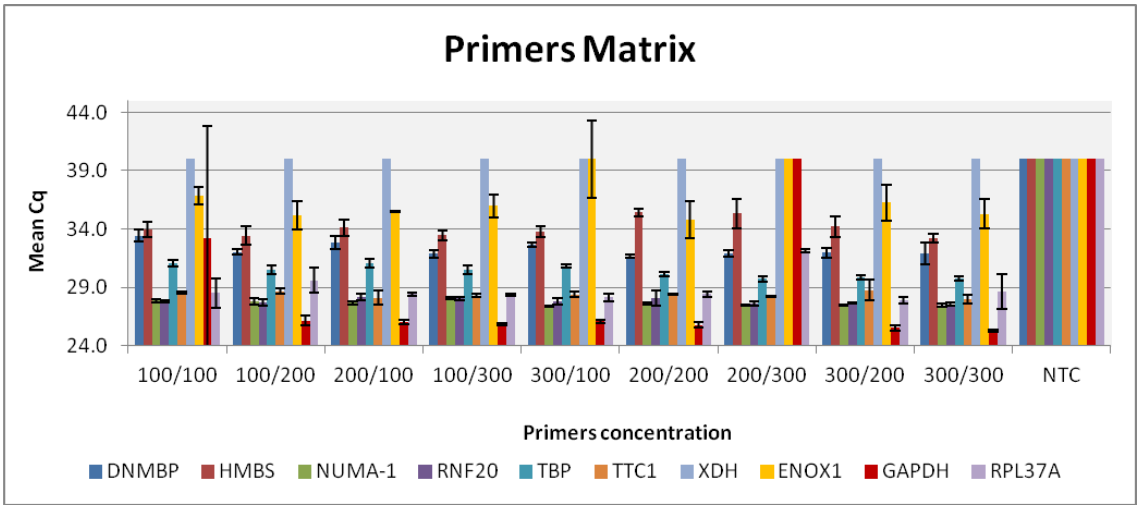

Figure 3.2.8 Optimization matrices results: Distribution of the mean Cq values of triplicates from different primer concentration combinations obtained for the different reference genes tested under identical thermal cycling conditions. The optimal primer concentration combination (lowest Cq value and no primer dimers) resulted 300/300 nM for the majority of the reference genes. NTC=no template control (undetermined values were represented with a Cq value=40). Error bars showing standard deviation of triplicates. Primer concentration combinations are given in nmol/L.

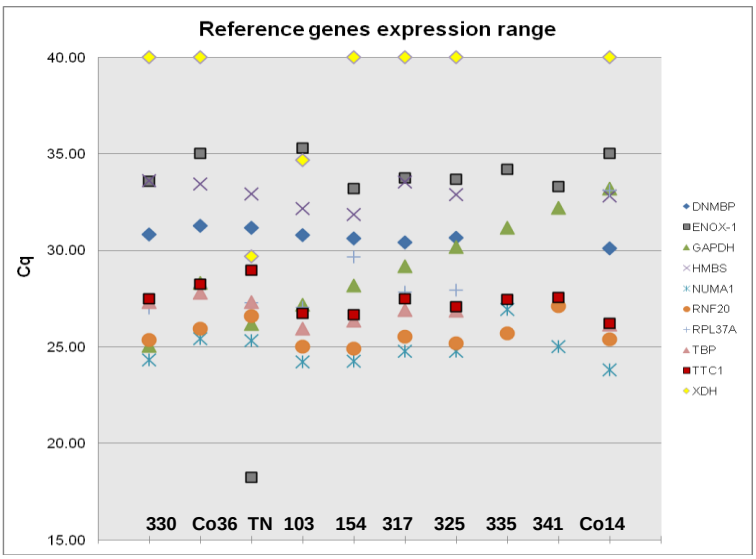

Figure 3.2.9 Reference genes expression range: cDNA from different MS (330, 103, 154, 317, 325, 335, 341), control (Co14, Co36) and lymphoid tissue (tonsil=TN) samples were used to set up multiple qPCR reactions for each of the reference genes on the same plate using the 300/300 combination. Plot showing the mean Cq from triplicate samples with primers combination of 300/300 under the same thermal parameters. The XDH gene resulted undetermined in most of the samples (plotted as Cq=40).

No double peaks of primer dimers by melting curves and no other products than the expected length amplicons by gel electrophoresis analysis were found confirming the specificity of the primers (Fig.3.2.10).

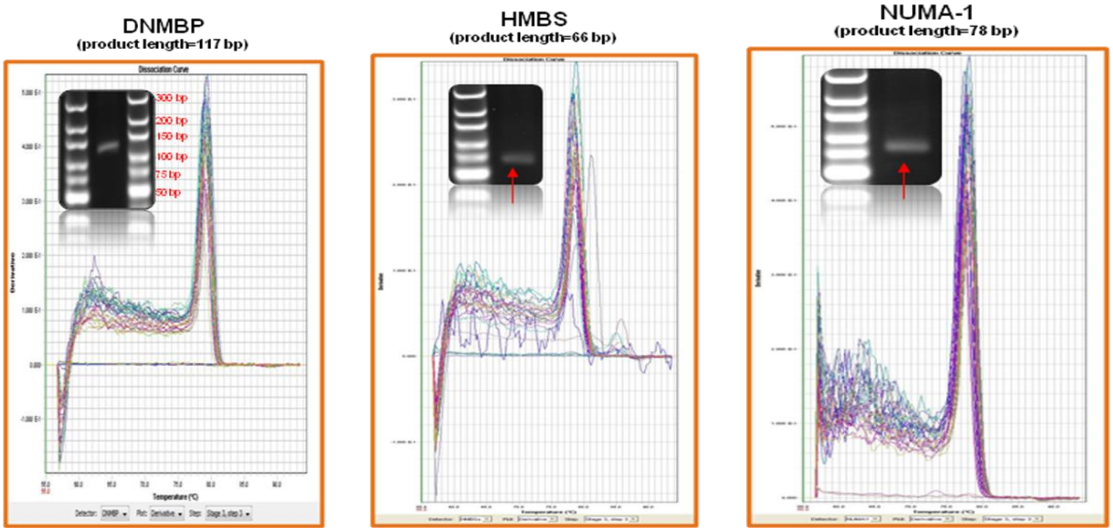

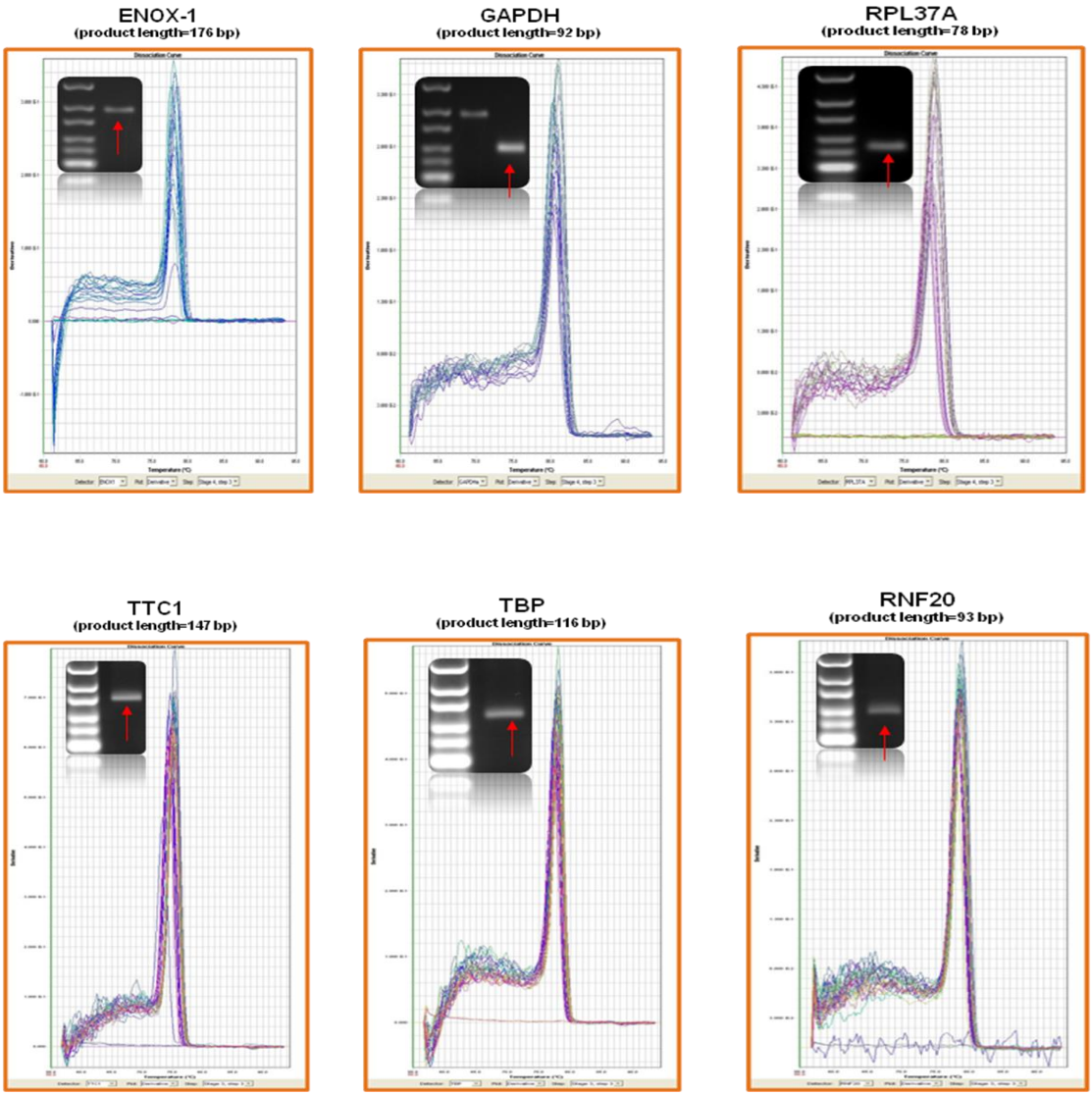

Figure 3.2.10 Reference genes dissociation curves and 2% agarose gel bands: Presence of primer dimers formation and additional non-specific bands were evaluated with dissociation curves and gel electrophoresis. At the end of the amplification cycles a thermal denaturation profile of the complex nucleic acid mixture was generated plotting the temperature on the X-axis versus the derivative of the fluorescence on the Y-axis. Gel wells were then loaded with the qPCR reactions from the plate. The dissociation curves are shown with the image of the relative qPCR amplicon generated and run on 2% agarose gel. All the reactions showed a single specific band of correct size (red arrow). Amplicon sizes are given in base pairs=bp. Marker molecular weight bands range of 300-50 bp was the same in all the samples. (XDH gene not represented has it didn't amplify in any of my samples).

To identify the best reference genes the web-based RefFinder tool was used allowing to integrate different methods such as the model-based, NormFinder (Andersen et al. 2004), the pair-wise correlation, BestKeeper (Pfaffl et al. 2004) and Genorm (Vandesompele et al. 2002), and ΔCt approach (Silver et al. 2006). Considering 5 of the MS samples with highest RIN values, 2 control brain samples and a tonsil sample as positive control, and comparing the different approaches the best genes for stability value resulted slightly different depending on the method. The best candidate gene by comprehensive ranking resulted DNMBP (Table 3.2.5).

	Delta CT	BestKeeper	NormFinder	Genorm	Comprehensive ranking
Most stable genes	TBP	DNMBP	HMBS	DNMBP/NUMA1	DNMBP
	NUMA1	RNF20	DNMBP		NUMA1
	DNMBP	NUMA1	TBP	TBP	TBP
	HMBS	HMBS	NUMA1	RNF20	HMBS
RANKING ORDER	RNF20	TBP	RNF20	TTC1	RNF20
	TTC1	TTC1	TTC1	HMBS	TTC1
	RPL37A	RPL37A	RPL37A	RPL37A	RPL37A
	GAPDH	GAPDH	GAPDH	GAPDH	GAPDH
Least stable genes	XDH	XDH	XDH	XDH	XDH
	ENOX1	ENOX1	ENOX1	ENOX1	ENOX1

Table 3.2.5 Candidate reference genes analysed with different methods

Chapter discussion

The immune system has evolved to optimize the encounter of the antigen-presenting dendritic cells of the innate immunity with the antigen specific T and B cells of the adaptive immunity in structures called secondary lymphoid organs (SLOs) such as lymph nodes (LNs) and spleen that are organized in well defined areas rich in T or B cells. After birth such events can be resembled in the form of tertiary lymphoid organs (TLOs) in transplant rejection, autoimmune diseases and infections where persistence of the source of antigen leads to continuous need of leukocytes extravasation. The degree of internal

organization of an inflammation that becomes chronic differentiate between a chronic infiltrate organized as structured lesion such as a granuloma or as a TLO with defined areas rich in T or B cells. The presence of antigen specific B cells, T cells and dendritic cells in the TLOs can function as lymphoid tissue inducer cells and function as adaptive response to an increased demand of localized immune response (Neyt et al. 2012). The histopathology work in my study demonstrated the presence of lymphoid aggregates in some of the tissues supplied and led me to take the work further and utilize these samples to build my phage display library. Hence, additional work will need to address if the aggregates found in the SPMS cases and in the PPMS cases contain the same cell types or if a different network is organized leading to define a functional TLO or another form of chronic inflammatory infiltrate. Better understanding of the environment in which the lymphoid cells can create their niches will provide possible targets for disrupting the inflammatory site. Furthermore, the micro-dissection experiments did show that it is possible to identify and isolate the lymphoid structure for further downstream applications such as RNA extraction for building antibody libraries or for qPCR. Apart from the ability to evaluate the quality of each sample used, this technique will allow better stratification of the tissues and will reduce the bias inserted in the library, for example in the library construction by exclusively pooling cDNA derived from the lymphoid structure of a similar form of disease. The use of a selected area will make the chances of obtaining a correct pairing of VH and VL much higher. The experiments performed showed that DNMBP is the most stable reference gene that can be used for brain and lymphoid samples. Nevertheless, in the current study I was unable to highlight increased gene expression of molecules required for specific lymphoid follicles processes (data not shown). The design of my qPCR experiments needs to be improved to better delineate the type of cytokines involved in the organization of the lymphoid network in the chronic lymphoid infiltrate and in the different types of disease.

Chapter 4: Immune phage-displayed libraries from B cells of MS patients' brains

Background:

The phage display is one of the most successful technologies in generating antibodies of different specificities. The encounter of a naïve antigen-binding B cell with the target antigen, in some cases even in absence of $CD4^+$ T cell signals, initiates the humoral immune response and leads to antibody production. B cells, after encountering an antigen, are subject to mutations, selection processes and clonal expansion constituting the molecular signature of an antigen-driven response as found in specific infections but also in tumors and autoimmune diseases of the nervous system and characterizing the B cell response in MS. Therefore, phage display human antibody generated from rearranged V-genes of the peripheral blood lymphocytes of immunised humans (Barbas et al. 1992; Mullinax et al. 1990) or from humans with disease will greatly enrich for the V-genes encoding antibodies complementary to the immunogen; thereby leading to the isolation of antibodies with excellent binding affinities (Barbas et al. 1994; Chester et al. 1994; Clackson et al. 1991). Indeed, antibody libraries from patients' B cells were built to raise antibodies with high affinity. For example antibody libraries were built in systemic lupus erythematosus (SLE) (Zampieri et al. 2003), coeliac disease (CD) (Rhyner et al. 2003) as well as in MS (Gabibov et al. 2011) and recombinant antibodies with specificity corresponding to natural autoAbs have also been raised.

The novelty of this study was to analyse by use of phage display technique the type of repertoire present in the target diseased tissue: the brain

The objective of my study was to construct immune phage antibody libraries from the B cells infiltrating the brain tissues of MS patients. My basic hypothesis was that MS auto-immune response is antigen driven. It is not clear what the triggers are but there are speculations that some viral infections, such as EBV

infection, are involved. It is known from two other brain infectious diseases of the nervous system: subacute sclerosing panencephalitis (SSPE) and chronic varicella zoster virus (VZV) vasculopathy, that the Igs found in the CSF are directed against the respective causative agents, i.e. measles virus and VZV, with a typical signature of an antigen-driven immune response also present (Burgoon et al. 2003; Burgoon et al. 2005; Owens et al. 2001). Similarly, in germinomas, germ cell brain tumors, and in inflammatory myopathies the infiltrating B cells organize themselves in extranodal lymphoid follicles and after molecular characterization the results showed the molecular signature of an antigen-driven response (Bradshaw et al. 2007; Willis et al. 2009). In MS however, the exact causative agent is not known and the auto-immunity is possibly against multiple autoantigens. Building and analyzing the antibody repertoire from the MS brain could: a) shed light on the type of antibody repertoire and b) help us to further understand the relevant target by using these repertoires for selection against potential autoantigens.

Objective:

To analyse the Ig repertoire derived from B cells present in the brain of MS patients searching for molecular characteristics of an antigen-driven immune response utilizing the phage display technique and comparing my results with the literature.

Specific aims:

a. *Analysis of the VH repertoire:* Family usage analysis was based on the knowledge that the heavy chain variable region (VH) segments can be classified into seven families, VH1-VH7, with a homology of at least 80% at nucleotide sequence level within the same family (Cook and Tomlinson 1995). The human immunoglobulin (VH) locus is located on three different chromosomes (Ch) respectively Ch14q32.3, Ch15q11.2 and Ch16p11.2, with the total number of VH segments in the human genome of 119 derived from 95 segments on Ch14, 8 segments on Ch15 and 16 segments on Ch16 (Cook et al. 1994; Tomlinson et al. 1994). The 7 families present 51 rearranged ORF genes (Cook and Tomlinson 1995) with different updates in the years so that 40 transcribed functional genes (Matsuda et al. 1998) and lately from 45 to 60 functional IGHV genes, due to allelic variants, were described (Boyd et al. 2010). The D locus is divided into 27 D segments that can be grouped in 7 families with four functional members in each family whilst the seventh has a unique functional segment, resulting in 25 functional genes (Corbett et al. 1997). In the JH locus were identified 6 genes (Ravetch et al. 1981; Ruiz et al. 1999).

b. Analysis of the *VL repertoire:* Family usage analysis was based on the knowledge that the Vk locus is composed of 51 potentially functional IGKV genes divided into 7 families and 3 clans (Barbie and Lefranc 1998). The Vk locus contains a joining region with 5 functional genes and a unique IGKC gene. The Vλ locus was described to contain 51 genes with 30 functional ones organized into 10 families and 7 Jλ segments. Four of the joining genes are functional Jλ1, Jλ2, Jλ3, and Jλ7, the others

are non-functional (Williams et al. 1996). In the last few decades new genes have been described (Kawasaki et al. 1997) and at the moment the potential repertoire is composed of 73-74 genes divided into 11 subgroups belonging to five clans with 33 functional genes (Pallares et al. 1998).

c. *Somatic hypermutations:* V genes were analysed for presence, type and site of mutations within complementary determining regions (CDRs) and frameworks (FRs). The way in which B cells found in brain tissue can adapt to the antigen encountered is based on the process of affinity maturation. The B cell ability to recognize any possible antigen relies on two processes: during maturation on combinatorial diversity and junctional diversity due to somatic recombination; after antigen encounter on somatic hypermutation affecting the binding specificity and affinity of the receptor.

d. *Clonal expansion:* Evaluation of clonally related sequences was performed by analysis of V genes rearrangements and comparison of CDR3 amino acid sequences. The antigen pressure selects the B cell clones able to survive with resulting clonal expansion of the precursors that have the highest affinity.

Methods:

Samples were cut into pieces of 30 mg of brain tissue from each patient, homogenized and total RNA extracted by a single step protocol and first strand cDNA synthesized with oligo-dT (see Chapter 2 for further details). Briefly from the RNAs extracted a first cDNA pool of 3 patients was created and used as a source of VH gene fragments to construct the first antibody library. By cloning the PCR amplified VH gene into the pIT2 vector I first created a VH only library. This library was then used as a vector for cloning the light chain V regions from a cDNA pool of 14 patients to make the VH+VL library. In addition, the VH repertoire was expanded by including B cells from the additional 11 patients. In summary, I built two libraries of MS B cells one with VH repertoire only from 14 MS patients and the other library with VH+VL repertoire from 3 and 14 patients, respectively (Fig.4.1).

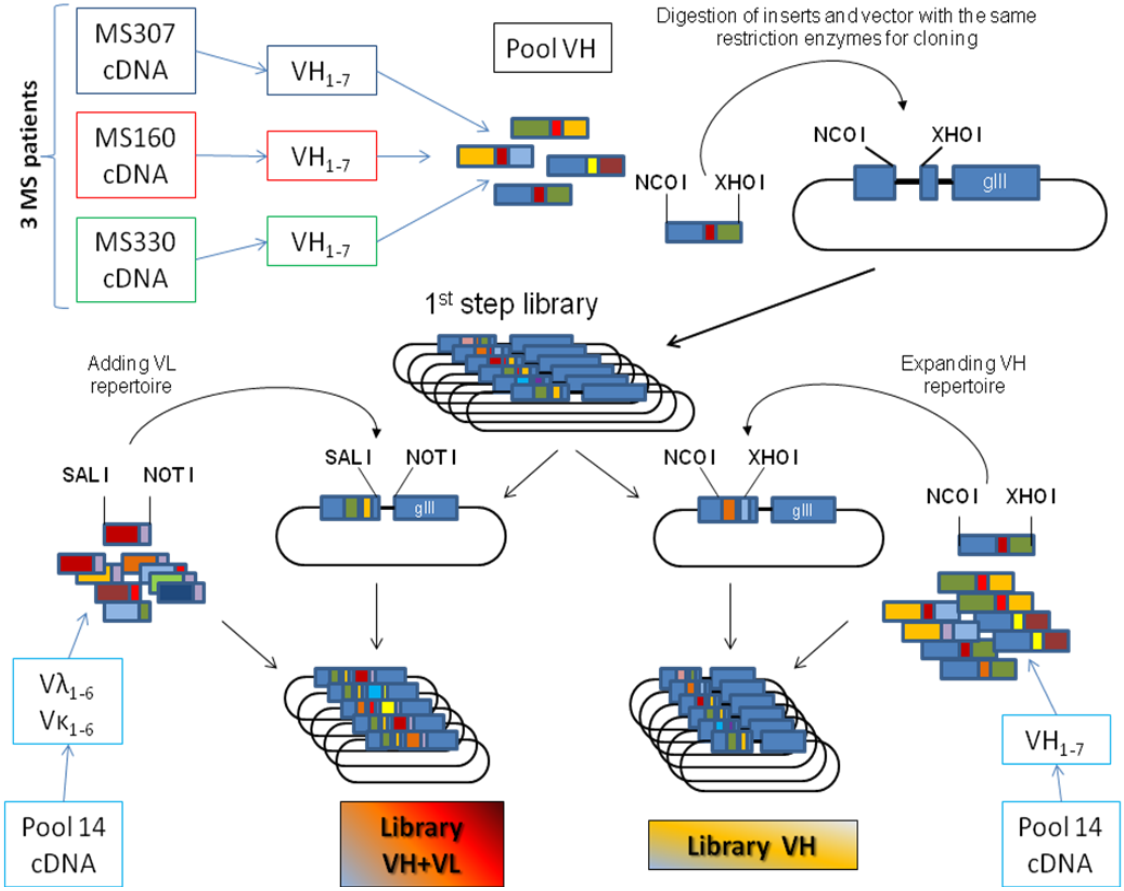

Figure 4.1 Strategy of library construction: The library and consequently the repertoire analysed was built starting from cDNA of a pool of 3 MS patients heavy chain genes amplified and cloned in the *in house* vector 1-11E (pIT2) (supplied by Dr C. Hughes) using appropriate restriction sites. This first library was enriched with a pool of light or heavy chains from 14 MS patients obtaining 2 distinct libraries: library VH+VL and library VH only.

The V genes were amplified using a nested PCR approach and then cloned into the linearised plasmid after digestion with the appropriate enzymes: NcoI/XhoI for the VH inserts and SalI/NotI for the VL inserts. Initially, the VH region was amplified by a reverse family specific (VH1-7) primer in combination with an external μ or γ isotype specific forward primer. The VH insert to be cloned was then obtained amplifying the obtained PCR product with the family specific primer and with a different JH1-6 specific forward primer at the 3' end. Both the primers contained the sequence for the restriction sites. Similarly, the Vλ and Vk and Jk1-5 and Jλ1-5 light chain specific primers were used to amplify Vk1-6 and Vλ1-6 families. The PCR products obtained were then digested and ligated into

the vector. After the libraries were built, clones were then sequenced by specific primers (details in chapter2 and fig.2.1)

All the sequences obtained were compared with their respective germlines using the IMGT, the international ImMunoGeneTics database (Lefranc et al. 1999; Lefranc et al. 2009; Ruiz et al. 2000), currently the most updated but, when necessary, checked with the databases VBase (http://vbase.mrc-cpe.cam.ac.uk/) - compiled manually by analysing all human immunoglobulin variable gene segments and excluding all somatic mutations but not updated after 1997- and VBase2 (Retter et al. 2005). The VH and VL regions were analysed as nucleotide and amino acid sequences. Sequences were considered clonally related if they originated from the same VH gene segment and the amino acid sequence of the CDR3 was identical or different by only one amino acid even in presence of different somatic mutations in the VH region. The large amount of replacement mutations in the FRs was analysed taking into consideration the quality of the replaced aa residues (Zuckerman et al. 2010) and following the IMGT ranking of aa substitutions from very similar to very different. The results obtained analyzing my libraries were compared mainly with two data sets available from the literature: the expected repertoires (data distribution inferred from the germline genes if randomly expressed) and the observed repertoires. The latter was obtained by analyzing the transcriptome of healthy controls of different age groups with a view to reproduce the increased antigen challenge of the immune system with development.

Statistics:

The frequencies of V family usage observed in my library were compared by χ^2 goodness-of-fit test with the frequencies expected by random usage from the functional genes in the genome and from healthy controls finding significantly different distributions. The Student t-test was applied to evaluate differences in CDR3 lengths and two-tailed Fisher's exact test for the same data binned. The difference in median CDR3 length and the number of somatic mutations per base pair were evaluated by two-tailed Mann-Whitney test. P-values equal to or less than 0.05 were considered significant. All the calculations were performed

with Excel analysis tools (Office 2007, Microsoft Corporation, USA) or PASW Statistics 18 (SPSS Inc., IBM software, USA).

Results:

V genes amplification

The VH and VL products obtained by nested PCR reactions as detailed in paragraph 2.6.1 were analysed by running 10 µl volume in presence of 6x loading buffer on a 1% agarose gels (Fig. 4.2-4.5). The resulted amplicons had a length of around 350-400 bp depending on the CDR3 length. The same steps were applied to amplify the light chains.

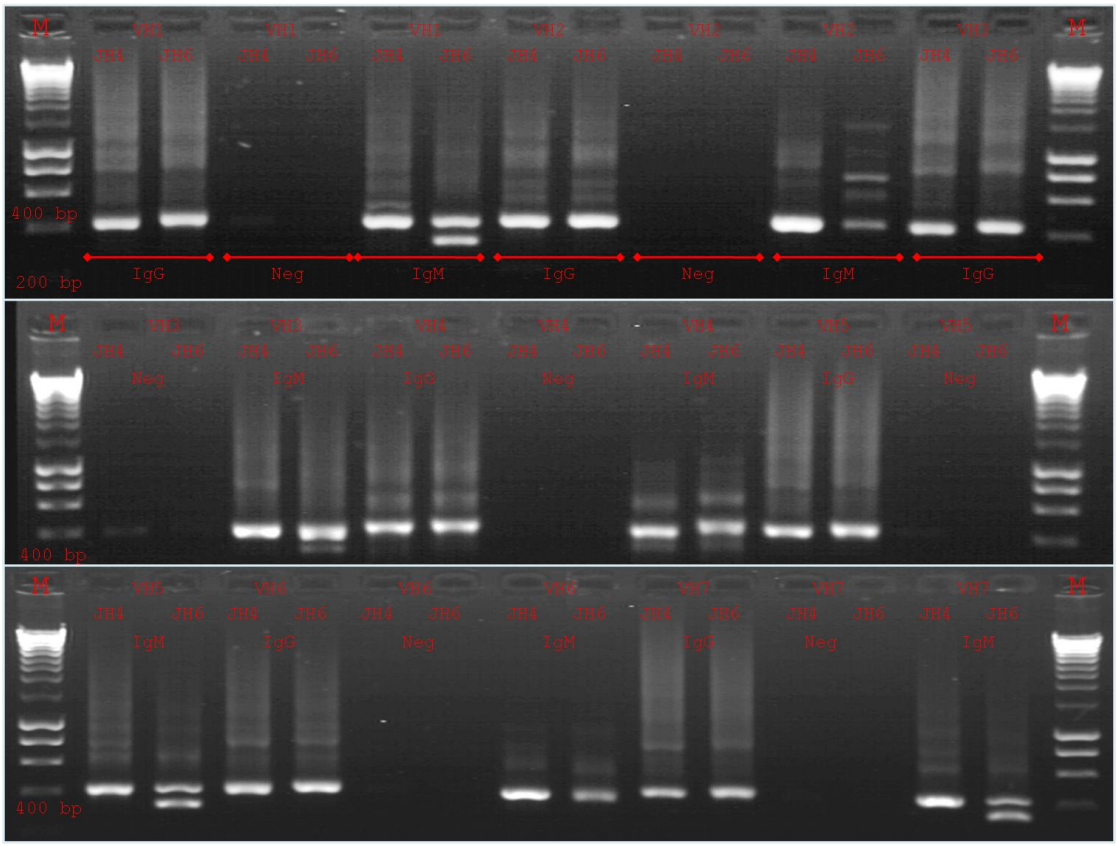

Figure 4.2 1% Agarose of VH PCR products: 1 µg total RNA extracted from each of the 14 MS samples were pooled together and cDNA retrotranscribed starting from 2 µg of the pooled RNA. In a 2 step nested PCR reaction a first product of ~ 700 bp was obtained using an external primer amplifying the constant region (IgM or IgG), subsequentely the product was reamplified with a primer annealing to the JH region obtaining my target product of ~ 350-400 bp. In the photos 1% agarose gel electrophoresis run of 10 µl PCR products from the second step of the reactions for the VH family 1-7 and for IgM and IgG

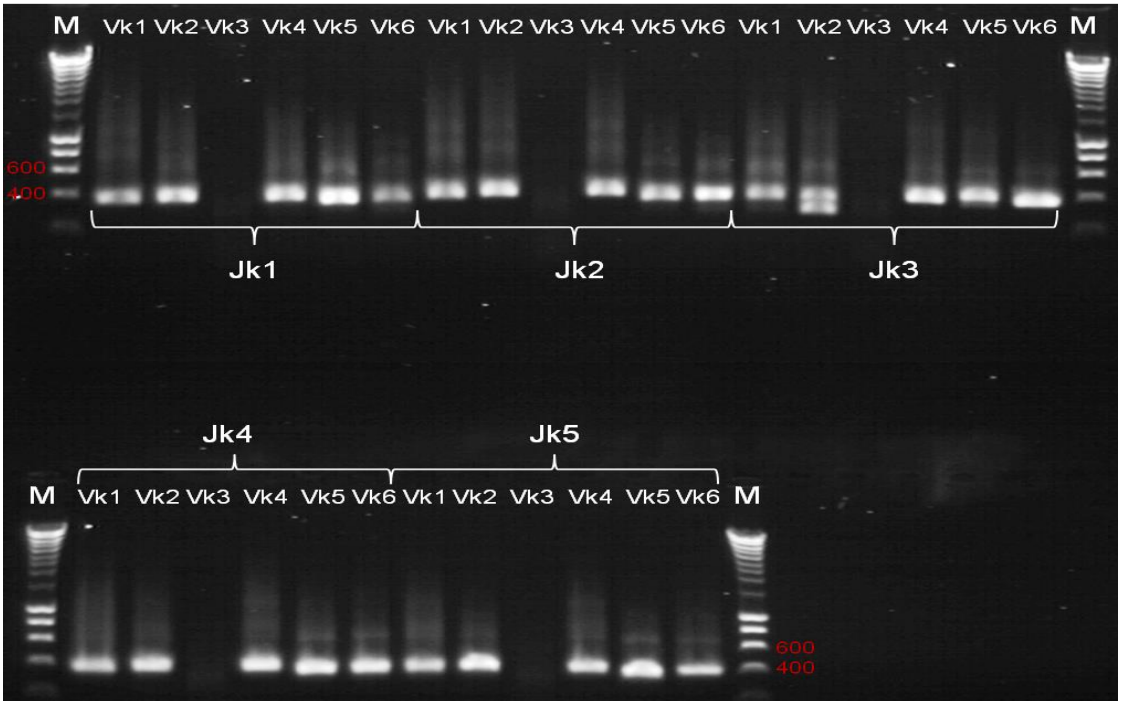

Figure 4.3 1% Agarose gel of Vk PCR products: Amplicon length for the kappa variable region amplified with a family specific primer and a junction region primer was around 350 bp. The reactions in the lanes labelled Vk3 were repeated as I obtained negative results.

a)

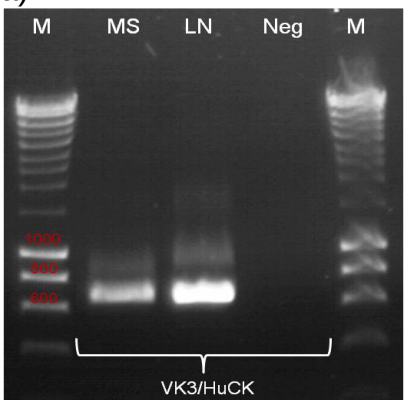

b)

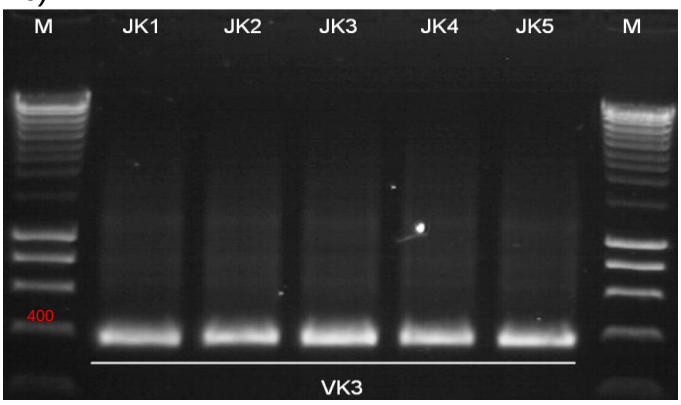

Figure 4.4 1% Agarose gel of Vk3 PCR products: a) amplification of Vk3 segments with external forward primer HuCk and b) nested with the Jk1-5 primers (MS). The amplicon length decreased as expected from around 700bp to 350-400bp.

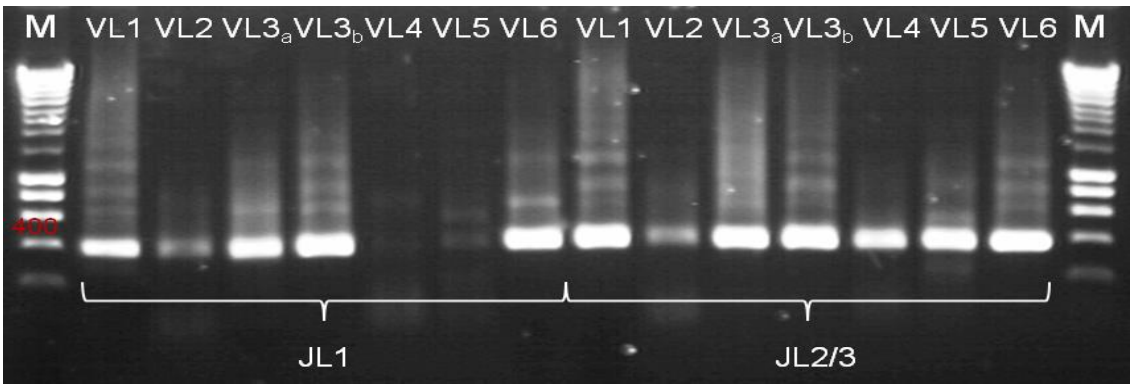

Figure 4.5 1% Agarose gel of Vλ PCR products: Lambda variable region amplification by family specific and junction specific primers. Amplicon length expected around 350 bp.

The attempt to amplify V genes from control brain samples gave negative results. The V genes amplified from the MS cases were used to build my antibody libraries and the diversity of the final VH+VL library was ~$5.8*10^7$ with an insert percentage of 82%.

Analysis of the heavy chain repertoire:

A total of 85 clones were picked for sequence analysis. The V genes were amplified and the PCR products derived from IgM and IgG variable regions analysed. After removal of duplicate sequences 47 unique sequences remained. All the sequences but one were productive (table 4.1).

a)

ID	IGVH gene	FR1 (1-26)	CDR1 (27-38)	FR2 (39-55)	CDR2 (56-65)	
1	1-24*01	QVQLVQSGA.EVKKPGASVKVSCKVS	GYTL....TDLS	MHWVRQAPGKGLEWMGS	FDPE..DGET	>
2	4-30-4*01	RCSCCESGP.GLVKPSQTLSLTCTVS	GGSIS..SGDYY	WSWIRQSPTKGLEWIGY	IYYS...GST	>
3	1-46*01	QVQLLRSGA.EVKKPGASLKIYCKSS	GNTF....TAYY	MHWVRQAPGQGLEWMGV	INPS..GGDT	>
4	1-69*02	QVQLVQSGA.EVKKPGSSVKVSCKAS	GGTF....SSYI	LIWVRQAPGQGLEWMGR	IIPM..LNIP	>
5	1-69*10	QVQLVQSGA.EVKKPGASVKVSCKAS	GATF....SSYA	ISWVRQAPGQGLEWMGW	VIPI..PHMP	>
6	1-69*06	QVQLVQSGA.EVQKPGSSVKISCKTS	GYTF....SDYA	ISWVRQAPGQGLEWMGG	IIPV..FGTP	>
7	1-2*02	QVQLVQSGA.EVKKPGASVKVSCQAS	GHTF....TAYY	IHWVRQAPGQGLVWMGW	INPD..GRGT	>
8	1-69*06	QVQLLQSGA.EVKKPGSSVKVSCKTS	GGTF....SSYG	FSWVRQAPGQGLEWMGG	IIPM..FGTS	>
9	1-69*04	QVQLVQSGA.EVKKPGSSVKVSCKSS	GDTF....RTYA	ISWVRQAPGQGLEWMGR	IIPV..LGIA	>
10	1-69*02	QVQLVQSGA.EVKKPGSSVKVSCKAS	GGTF....STYT	FSWVRQAPGQGLEWMGR	IIPI..LGIT	>
11	1-46*01	QVQLLRSGA.EMKKPGASVKLSCKAS	GYTF....IDHQ	IHWVRRAPGQGLEWMGA	INPR..GSTT	>
12	1-8*01	QVQLVQSGA.EVKKPGATVKLSCKAS	GYTF....TSYD	LNWVRQATGQGLEWMGW	MIPN..NGNT	>
13	1-8*01	EVQLVQSGA.EVKKPGASVKVSCKAS	GYTL....TSYD	INWVRQASGQGLEWMGW	INPN..TADT	>
14	2-70*01	QVNLRESGP.ALVKPKQTLTLTCTVS	GFSLS..TSGMC	VSWIRQPPGKALEWLAR	IDWD...DDK	>
15	2-70*01	QVNLRESGP.ALVKPTQTLTLTCTFS	GFSLS..TSGMC	VSWIRQPPGKALEWLAR	IDWD...DDK	>
16	2-5*01	QITLKESGP.TLVKPTQTLTLTCTFS	GFSLS..TSGVG	VGWIRQPPGKALEWLAL	IYWN...DDF	>
17	2-5*10	QITLKESGP.TLVKPTQSLTLTCSFS	GFSLS..ATGLG	VGWIRQPPGRPLEWLAV	IYWD...DEK	>
18	3-49*05	EVQLVESGG.GLVKPGRSLRLSCTAS	GFTF....GDFS	MSWFRQAPGKGLEWVGF	IRSKTYGGTT	>
19	3-23*01	QVQLLRSGG.GSVQPGESLRLSCAVS	GFTV....GSYA	MSWVGQAPGKGLEWVSV	ISGG..AGTT	>
20	3-33*01	EVQLVESGG.GVVQPGSSLRLSCAVS	GFTF....SDYG	MHWVRQAPGKGLEWVAV	IWYD..GSHE	>
21	3-7*02	EVQLVESGG.DLVQPGGSLRLSCAAS	GFTF....NTFW	MTWVRQAPGRGLEWVAN	INQD..EYER	>
22	3-11*05	QVQLVESGG.GLVKPGGSLRLSCAAS	GFTF....SDYY	MSWFRQAPGKGLEWLSY	MSGN..SNYT	>
23	3-7*01	EVQLVESGG.GLVQPGGSLRLSCAAS	GFAF....SGYW	MSWVRQAPGKGLEWVAS	IKQD..AGEK	>
24	3-11*01	EVQLVESGG.GLVKPGGSLRLSCAAS	GFTF....DDYY	MSWIRQVPGKGLECVSY	IGHS..GDIV	>
25	3-30*03	EVQLVESGG.GVVQPGRSLRLSCAAS	GFTF....ISYG	MHWVRQAPGKGLEWVAV	ISYD..GSIK	>
26	3-7*02	EVQLVESGG.GLVQPGGSLRLSCAAS	GFTF....SSTW	MSWVRQAPGKGLEWVAN	IKSD..GSAK	>
27	3-49*04	QVQLVESGG.GLVQPGRSLRLSCKAS	GFAF....GGYA	MTWVRQAPGKGLEWVGL	IRSKAYGGTT	>
28	1-69*04	QVQLVQSGS.EVKKPGSSVKVSCKAS	GATF....SSYA	ISWVRQAPGQGLEWMGW	VIPI..PHMP	>
29	3-23*01	EVQLLESGG.GLVQPGGSLRLSCAAS	GFTF....SSYA	MSWVRQAPGKGLEWVSD	ISAS..GGYT	>
30	3-7*02	EVQLVESGG.GLVQPGGSLRLSCVAS	GVMF....SRQW	MSWVRQAPGKGLEWVAN	IKED..GSER	>
31	3-43*01	EVQLVESGG.VVVPPGGSLRLSCAAS	GFIF....DDYT	MHWARQGPEKGLEWVSL	ISWD..SGFT	>
32	3-23*04	QVQLVESGG.GLAQPGESLRLSCVAS	GFAL....NNFI	MSWVRQAPGKGLEWVSS	ITES...GNI	>
33	4-59*08	QVQLQESGP.GLLKPSETLSLTCTVS	GGSI....SSDY	WSWIRQPPGQTLEYIGY	VYHS...GAT	>
34	4-59*01	QVQLQQSGP.GLVSPSETLFLTCSIS	GGSM....KNFY	WNWIRQSPGRGLEWIGH	IYYS...GST	>
35	4-4*02	QVQLQESGP.GLVKPSGTLSLTCDVF	GGSID...STYW	WSWVRQPPGKGLEWIGE	IYHS...GST	>
36	4-31*06	QVQLLQSGP.GLVKPSQTLSLTCTVS	GGSIS..SGTYY	WSWIRQHPGKGLECIGY	IYDG...GST	>
37	3-23*01	QVQLLRSGG.GSVQPGESLRLSCAVS	GFTV....GSYA	MSWVRQAPGKGLEWVSV	ISGG..AGTT	>
38	4-31*03	QVQLQESGP.GLVKPAQTLSLTCTVS	GVSIS..TGGYY	WTWIRQHPGKGLEWIGN	IYYS...GRT	>
39	4-61*02	.VQLQESGP.RLVKPSQTLSLSCTVS	GDSIT..SGSHF	WTWIRQPAGKGLEWIGR	LHTS...GST	>
40	1-69*02	QVQLVQSGA.EVKKPGSSVKVSCKAS	GGTF....STYS	FSWVRQAPGQGLEWMGR	IIPI..LGIT	>
41	4-34*01	QVQLQQWGA.GLLKPSETLSLTCGVY	GGSL....SGYF	WSWIRQPPGKGLEWIGE	IKES...GTT	>
42	4-31*03	QVQLQESGP.GLVKPSETLSLTCSVS	GGSIS..NGDYY	WSWIRQHPGKGLEWIGY	ISYS...GST	>
43	3-7*02	EVQLVESGG.GLVQPGGSLRLSCAAS	GFTF....SSTW	MSWVRQAPGKGLEWVAN	IKSD..GSAK	>
44	6-1*01	QVQLQQSGP.GLVMPSQTLSLTCAIS	GDRVS..SNTAA	WNWIRQSPSRGLEWLGR	TYHRS.KWSN	>
45	6-1*01	QVQLQQSGP.GLVKPSQTLSLTCAIS	GDSVS..STSAA	WTWVRQSPSRGLEWLGR	TYYRS.TWFN	>
46	5-51*03	EVQLVQSGA.EVKKPGESLEISCKTS	GYTF....ITHW	IAWVRQMPGKGLEWVGV	IYPG..DTDT	>
‡	1-2*02	QVQLLRSGA.EVKKPGASVKVSCKTF	GYTF....TKYY	MHWVRQAPGQGLEWMGW	IDPS..SGDT	>

b)

	ID	V gene and allele	FR3 (66-104)	CDR3 (105-117)
>	1	IGHV1-24*01	IYAQKLQ.GRITMTEDRATDTAYMELSSLRSEDTAVYYC	ARGMGYLIRYFDL
>	2	IGHV4-30-4*01	SYNPSLQ.SRATISVDTSKNNFSLKLRSVTAADSARYYC	VRGGYEVGRSGSVYGMDV
>	3	IGHV1-46*01	RYTQKFQ.GRVAMTGDTSTSTVSLELTRLTSEDTAMYFC	ASEVERRLVFDN
>	4	IGHV1-69*02	NYAQKFE.GRVTLTADKSTSTAYMELRSLTSEDTAVYYC	AGFCGTPNCDDV
>	5	IGHV1-69*10	NYAQKFQ.GRVTIMADKSTDTAYLELSSLGSDDTAVYYC	AYSQYYYDTSGPDSDFYYSYFMDV
>	6	IGHV1-69*06	NYAQKFQ.GRVTIRADRSTTTVYMELSSLRSEDTAMYYC	ARDPTRFTLFGRGEYYYGLEV
>	7	IGHV1-2*02	NYVKKFQ.GRVTMTRDTSISTAYMELSSLRSDDTAVYYC	ARGGASGGYDRPIDY
>	8	IGHV1-69*06	NYAQKFR.DRVTISADKSTSTAYMELSSLRSEDTAVYYC	ARGPLEFLWGSYRYEVFDH
>	9	IGHV1-69*04	NYALKFQ.GRLTITADKATTTAYMALTSLGSEDTAVYFC	ARDRDTSGSNDVFDI
>	10	IGHV1-69*02	NYAQKFQ.GRVTITADKSTTTVYMDLSSLRSEDTAVYYC	ASIGDNTGYFREAFTYYFDY
>	11	IGHV1-46*01	TYAQKFQ.GRVTLTTDPSTTTVYMELSRLMSEDTARYIC	ARATPYTIFGVSTYYRYFMDV
>	12	IGHV1-8*01	GYAPKFQ.GRVAMTRDTSISTAYMELSSLTSEDTAVYYC	VRGQFGYCSSPSCPEY
>	13	IGHV1-8*01	DYAQNFR.GRVTMTTNSSIDTAYMVLSSLTFEDTAVYYC	ARGGHIVGSTTDYYYALDV
>	14	IGHV2-70*01	FYSTPLK.TRLTVSRDSSNNQVVLTMTDMDPVDTGTYYC	ARMGPDNRAWYRFDY
>	15	IGHV2-70*01	YYTTSLK.TRLTISKDTSKNQVVLTMTNMNPVDTGTYYC	ARLIWFGESVFPTRGMDV
>	16	IGHV2-5*01	HYSPSLK.SRLTITKDTSKNQVVLTLTNMDPVDTATYYC	ARRLSHRYCSRGSCPNWFDP
>	17	IGHV2-5*10	HYSSSLR.NRVSIVKDTSENHVVLTLTNVDPVDTATYYC	ARLNVVVAPRFDR
>	18	IGHV3-49*05	EYAASVK.DRFTISRDDSKSIAYLEMSSLKTEDTAIYYC	ARVLKAPQGYSGSWYPVHY
>	19	IGHV3-23*01	YYADSVK.GRFTISRDKSKNTLFLEISSLRAEDTAVYYC	ASHGDYVRHYYFHMDV
>	20	IGHV3-33*01	YYADSVK.GRFTISRDNSKNTLYLQMNSLRAEDTAVYYC	AKVGDSDWGTSFFDY
>	21	IGHV3-7*02	YYVDSVK.GRFTISRDNDRNSLYLEMNSLTADDTAVYYC	VRQSGYLYSSSWGLHNYMWYLDV
>	22	IGHV3-11*05	NYADSVK.GRFTLSRDNAKKLLYLQMNSLRAEDTALYYC	ARNLYSSTWTGVGDY
>	23	IGHV3-7*01	YYVDSVK.GRFAISRDNAKNSLYLQMNSLRGEDTAVYYC	ARVRDNISIVGVVLNIGAFDI
>	24	IGHV3-11*01	YYADSVR.GRFTISRDNANNSLFLQMNSLRAEDTAVYYC	VRLIYAYGRDY
>	25	IGHV3-30*03	YYADSVK.GRFTISRDNSKNTLFLQMNSLRAEDTAVYYC	AKDHYYDSSVPAYYFDY
>	26	IGHV3-7*02	DYVDSVR.GRFTISRDNAENSLSLQMNSLRAEDTAVYYC	ARGYL
>	27	IGHV3-49*04	DYAASVK.GRFSISRDDSKSLAYLQMNSLTTEDTAVYYC	TRVLGYTYDKLDYFDS
>	28	IGHV1-69*04	NYAQKFQ.GRVTIMADKSTDTAYLELSSLGSDDTAVYYC	AYSQYYYDTSGPDSDFYYSYFMDV
>	29	IGHV3-23*01	AYADSVK.GRFTISRDNSKNTLYLQMNSLRAEDTAVYYC	AKSYSAFDY
>	30	IGHV3-7*02	SHAGSVE.GRFTISRDNAKNSLYLQMNSLRAEDTAVYYC	ALGPY
>	31	IGHV3-43*01	YYADSVK.GRFTISRDNTKNSLSLQMDSLKTEDSGLYYC	GKGISIGAVADAVDV
>	32	IGHV3-23*04	FYADSVR.GRFTISRDISMNTLYLQMNNLRAEDTARYYC	VPRRTASWFDP
>	33	IGHV4-59*08	NYNPSLK.SRVSISIDTSKNQFSLRLTSVTAADTAFYYC	ARRRAGAHLYGDYQNWFDP
>	34	IGHV4-59*01	NYNPSLK.SRVTISLDASNRQLSLRLASVTAADTAVYYC	AGGTSPWSSEYYFYF
>	35	IGHV4-4*02	NYNPSLK.SRVTIPIDKSNNQFFLKMSSVTAADTAIYYC	ARIQYCTDITCFYDWFDP
>	36	IGHV4-31*06	YYNPSLM.SRATISIDTSKNQFSLKLSFVTAADTAVYYC	ARGKWSGSYKGDAFDI
>	37	IGHV3-23*01	YYADSVK.GRFTISRDKSKNTLFLEISSLRAEDTAVYYC	ASHGDYVRHYYFHMDV
>	38	IGHV4-31*03	NYNPSLK.SRVTVSVDTSKNQFSLRLTSVTAADTAMYYC	ARDSSGHFEALNI
>	39	IGHV4-61*02	NYNPSLK.SRVSISMDASKNQFSLNVSSVTAEDTAVYYC	AGEGYCRSSTCYNKIHTNWFDL
>	40	IGHV1-69*02	NYAQKFQ.GRVTITADKSTTTVYMDLSSLRSEDTAVYYC	ASIGDNTGYFREAFTYYFDY
>	41	IGHV4-34*01	NYNPSLK.SRVSISEDTPKNQFSLHLRSVTAADTAVYYC	ARGYTGVVADY
>	42	IGHV4-31*03	YYNPSLK.SRVTISVDTSKNQFSLKLSSVTAADTAVYYC	ARSEELDY
>	43	IGHV3-7*02	DYVDSVR.GRFTISRDNAENSLSLQMNSLRAEDTAVYYC	ARGYL
>	44	IGHV6-1*01	DYAVSVK.SRIAISPDTSKNQFSLQLNSVTPEDTAVYYC	ARHGNWASNFDS
>	45	IGHV6-1*01	DYAVSVK.SRATIKSDTSNNQFSLHLKSVTPEDTAVYYC	AREVRNSWYDP
>	46	IGHV5-51*03	RYSPSFQ.GQVSISVDRSTATAYLRWVRLKASDTAMYYC	ARQPYDTAGYFATGDKWYGMDV
>	‡	IGHV1-2*02	KIHRSFR.AGSP*PGTRPSARPTWS*TD*LLTTRPFITV	RGPPRVRHMT

Table 4.1 VH amino acid sequences: the table shows the 47 amino acid sequences of the VH clones analysed in my study. a) amino acid sequences of the FR1, CDR1, FR2 and CDR2; b) amino acid sequences of FR3 and CDR3. IMGT numbering was followed and amino acid changes with the closest germline are highlighted in red. The non productive sequence is shown with a grey background.

The amplified VH sequences showed an identity with their respective germlines in the range of 85.42-97.94% and the JH segments an average of 84% identity (range 68.3-97.4%). The degree of identity found leads one to think that the majority of the sequences were derived from an immune rather than a naïve repertoire. The usage of VH families was analysed and compared with the expected usage from randomly expressed germline genes and with studies describing the observed usage in the transcriptome of healthy controls. In fact, the analysis of healthy individuals Ig repertoire of different age groups and derived from different B cell populations by various techniques did show that the different subgroups are not used randomly. From all the studies available I have compared my repertoire with the frequencies of the VBase expected germlines detecting significantly different distributions ($p \leq 0.05$) (Fig.4.6).

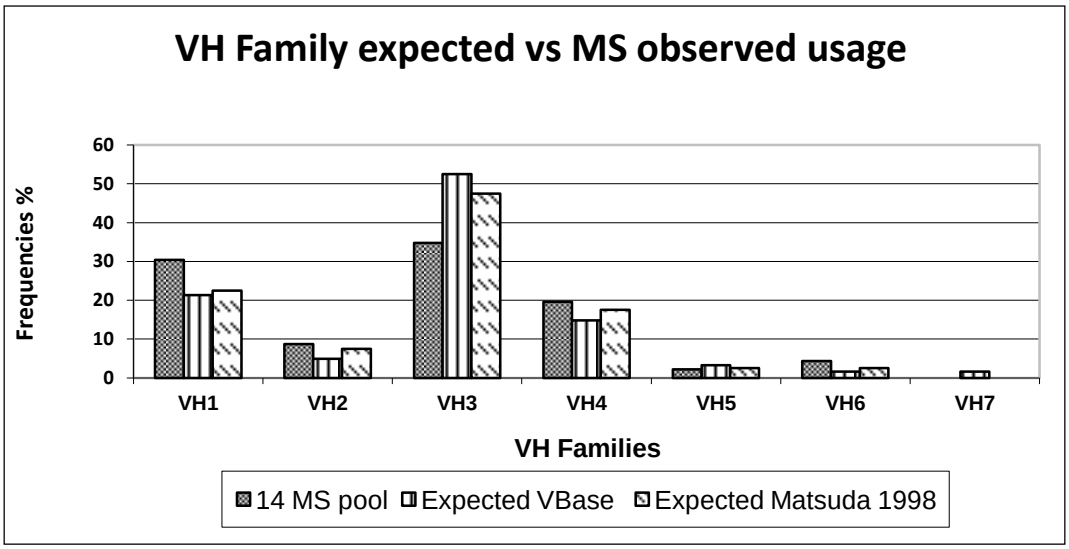

Figure 4.6 VH usage observed vs expected: The frequency of each family was calculated and compared with that of previously reported studies and to expected values as well. VH genes usage in brain samples and as expected from germline genes inferred randomly expressed (data adapted from Matsuda et al. 1998 and from VBase database). The distribution was significantly different from the VBase expected germline usage ($p \leq 0.05$) but not from the usage described in Matsuda's paper.

My repertoire was also compared with the existing literature data obtained from peripheral blood of 11 healthy adults and from cord blood of 2 healthy newborns transcriptomes (Boyd et al. 2010; Prabakaran et al. 2012) (Fig.4.7).

Past studies have analysed VH family usage from peripheral blood of 1 young (25y) and 5 elderly individuals (≥65y) by construction of cDNA libraries from IgM and IgG variable regions (Wang and Stollar 1999), by cDNA libraries from IgM of 2 adults (Huang et al. 1992), from 3 adults by anchored PCR-Elisa (Rassenti et al. 1995), from 1 female donor by single-cell PCR (Brezinschek et al. 1995), by *in-situ* hybridization (Zouali and Theze 1991), and lately from 11 healthy individuals (Boyd et al. 2010) and 2 newborns cord blood (Prabakaran et al. 2012) by high-throughput DNA sequencing. My pool of 14 MS patients had a different distribution from the expected germline distribution ($p \leq 0.05$) but also from the adults ($p \leq 0.001$; VH7 was not considered in the test as it was equal to zero in both distributions) and newborns' ($p=4.2E-181$) transcriptomes distribution (Fig.4.7).

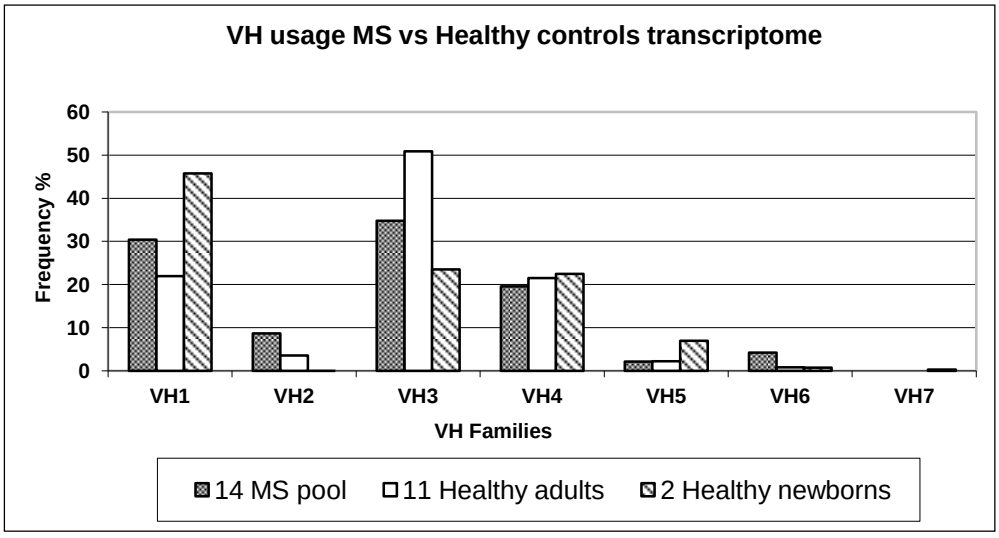

Figure 4.7 VH usage MS vs Healthy Controls transcriptome: VH family distributions in productive sequences of brain samples and of 11 healthy adults PBLs and 2 newborns cord blood (data adapted from Boyd et al. 2010 and Prabakaran et al. 2012); statistically significant differences were observed between adults ($p \leq 0.001$), newborns ($p=4.2E-181$) and MS repertoires.

Continuing on the loop 3 of the heavy chain variable domain I analysed the D segments. In my sample I have identified 19 different D segments out of the 25 functional D segments. D3 was used in more than 30% of the sequences analysed, it is significantly higher than expected from germline random expression ($p \leq 0.001$) (Fig.4.8 and Fig.4.9): D3-22 (16%), D2-2 (11%), D3-3 (9%) and D6-13 (9%) and in just one sequence I identified D7-27 the only member of the D7 family.

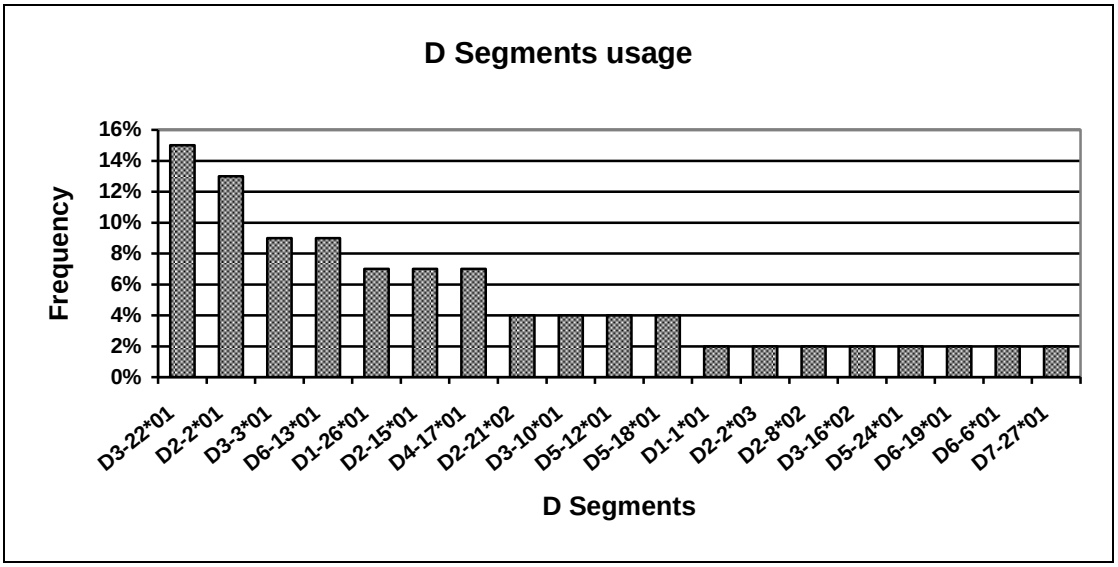

Figure 4.8 D segments usage: The most used segment in my pool was D3-22 (15% of recombinations) especially used in conjunction with VH1 family

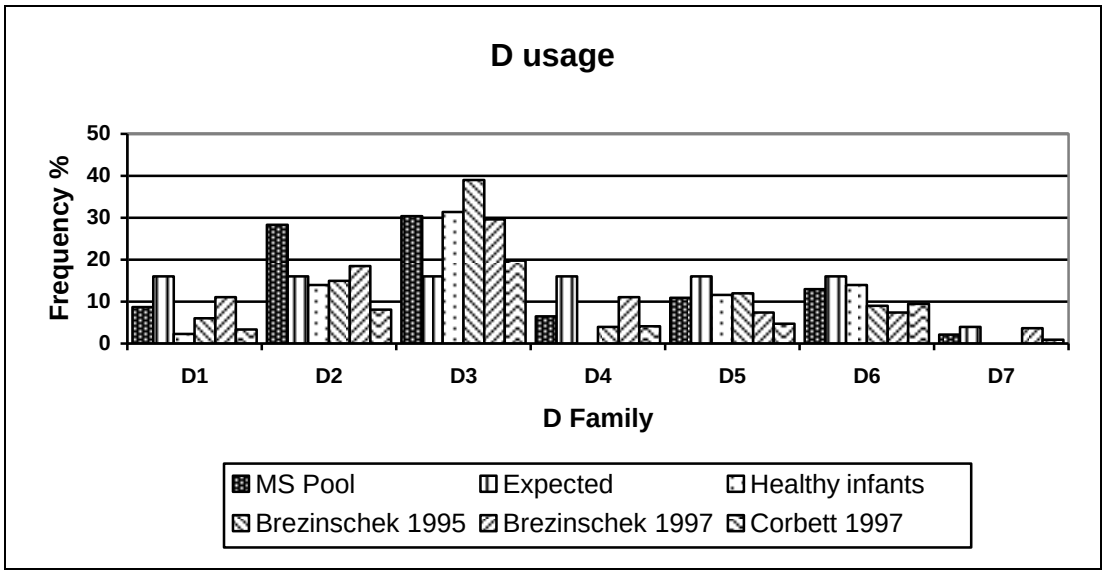

Figure 4.9 D Usage: The rearranged sequences of the MS pool presented a significantly different utilization from the expected distribution based on the germline genes of D genes with D3 and D2 being the most represented ($p \leq 0.001$)

The last locus that interacts in the rearrangement of the CDR3 of the immunoglobulin antigen binding site is the JH. The segment is divided into six families with as many functional genes. The analysis of the usage of these segments from PBLs of adult and infant controls has shown a preferential utilization of the JH4 family (Minegishi et al. 1994; Yamada et al. 1991). The same bias was found in my pool with an usage of JH4 in almost half of the sequences analysed (48.9%), JH6 (22.2%), JH5 (17.8%) and JH3 (11.1%). I did not find any sequence using JH1 or JH2 in my VDJ rearrangement (Fig.4.10).

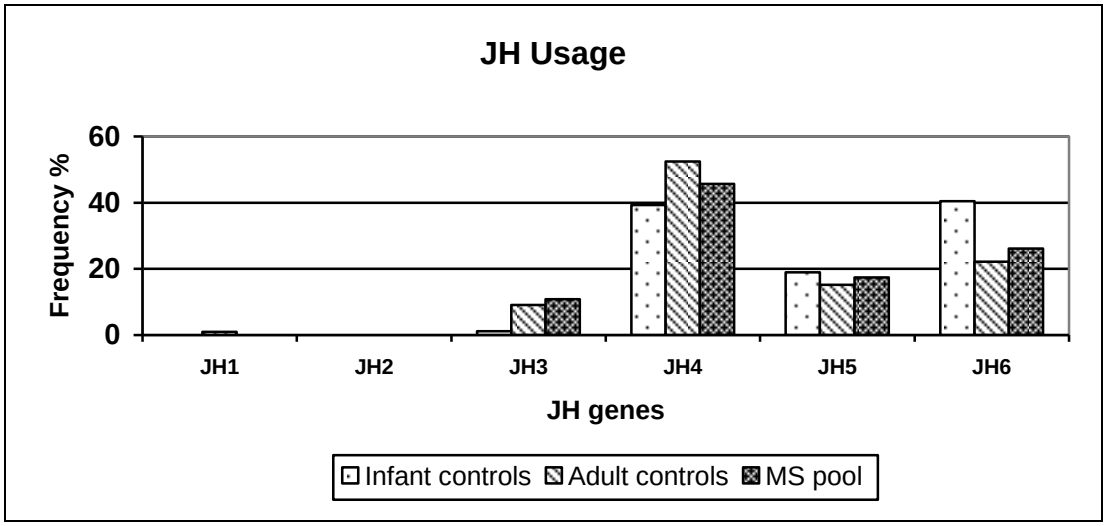

Figure 4.10 JH Usage: The JH usage of the pool was biased towards the specific utilization of JH4 gene as well as in the controls.

Analysis of the light chains repertoire:

In my analysis I have sequenced 40 light chains amplicons of which 30 were kappa and 10 lambda. After removal of duplicate sequences of the kappa ones 15 unique functional sequences and 1 pseudogene (IGKV2-29*01 P) remained (table 4.2).

a)

ID	Vk gene	FR1 (1-26)	CDR1 (27-38)	FR2 (39-55)	CDR2 (56-65)	
1	IGKV6-21*01	EIVLTQSPDFQSVPPKETVTITCRAS	QSV.....GGS	LHWYQQKSGQSPKLLIR	YG.....S	>
2	IGKV1-39*01	DIQMTQSPSSLSASVGDRVTITCRAS	QSI.....SSY	LNWYQQRPGRAPKLLIY	AA.....S	>
3	IGKV1-39*01	NIQMTQSPSSLSASVGDRITITCQAS	QDI.....YNY	LNWYQQQPGKAPNLLIY	AA.....S	>
4	IGKV2-28*01	EIVLTQSPLSLPVTPGEPASISCRSS	QSLLHS.SGYNF	LDWYLQRPGQSPQLLIY	LG.....S	>
5	IGKV2D-29*01	.EIVLTQPLSLSVTPGQPASISCRSS	QSLLHS.DGKTY	LYWYLQRPGQAPQLLIY	EV.....S	>
6	IGKV4-1*01	DIVMTQSPDSLAVSLGERATINCRSS	QSVL.....YSS	LAWYQQKSGQPPKMLIY	GA.....S	>
7	IGKV5-2*01	ETTLTQSPAFMSATPGDKVNISCKAS	QDI.....DDD	MNWYQQKPGEAAIFIIQ	EA.....T	>
8	IGKV2-29*02	DIVMTQTPLSLSVTPGQPASISCKSS	QSLLHS.DGKTY	LFWYLQKPGQSPQLLIY	EV.....S	>
9	IGKV1-39*01	DIQMTQSPSSLSASVGDRVTITCRAS	QSI.....SSY	LNWYQQKPGKAPKLLIY	YA.....S	>
10	IGKV2-30*01	EIVLTQSPLSLPVTLGQPASFSCRSS	QSLVFS.DGNTY	LNWFQQRPGQSPRRLIH	KV.....S	>
11	IGKV5-2*01	ETTLTQSPAFMSATPGDKVNISWKAS	QDI.....DDD	INWNQQKPGEGAIFIIQ	EA.....T	>
12	IGKV1-12*01	DIQMTQSPSSLSASVGDRVTITCRAS	QGI.....SSW	LGWYQQKPGKVPKLLIY	AA.....S	>
13	IGKV4-1*01	DIVMTQSPDSLAVSLGERATINCKSS	QSVFSSSSNKNY	LAWYQQIPGQPPKLLIY	WA.....S	>
14	IGKV1-33*01	NIQMTQSPPSLSASVGDRVTITCQAS	QDM.....SDH	LNWYQQKPGKVPKLLIS	DA.....S	>
15	IGKV2-28*01	DIVMTQSPLSLPVTPGEPASISCRSS	QSLLHT.NGYNY	LDWYLQRPGQSPQLLIY	LG.....S	>
‡	IGKV2-29*01 P	DIVMTQTPLSLSVTPGQPASISCKSS	QTLLHS.DGKTY	LYWYLQKPGQSPQLLIY	EV.....S	>

b)

	ID	Vk gene	FR3 (66-104)	CDR3 (105-117)
>	1	IGKV6-21*01	QSFSGVP.SRFSGSR..SGTDFTLTISGLEAEDAATYFC	HQSSSLPFT
>	2	IGKV1-39*01	NLQSGVP.SRFSGSG..SGTDFTLTISSLQPEDFATYYC	QQYKSYSLT
>	3	IGKV1-39*01	TLQSGVP.SRFSGSG..SGTDFTLTISSLQPEDFATYYC	QQSYSTPLT
>	4	IGKV2-28*01	NRASGVP.DRFSGSG..SGTDFTLKISRVEAEDVGVYYC	MQALQTPQVT
>	5	IGKV2D-29*01	NRFSGVP.ARFSGSG..SGTDFTLKISRVEAEDVGVYYC	MQSIQDPLFT
>	6	IGKV4-1*01	SRESGVT.DRFSGSG..SGTDFTLTISSLQAEDVAVYYC	QQYYTAPRT
>	7	IGKV5-2*01	TLVPGIP.PRFSGSG..YGTDFTLTINNIESEDAAYYFC	LQHDNFPIT
>	8	IGKV2-29*02	SRFSGVP.DRFSGSG..SGTDFTLRISRVEAEDVGVYYC	MQGVHLPLT
>	9	IGKV1-39*01	SLQSGVP.SRFSGSG..SGTDFTLTISSLQPEDFATYYC	QQAANYPNT
>	10	IGKV2-30*01	DRDSGVP.DRFSGSG..SGTDFTLKISRVEAEDVGVYYC	MQGTHWPPS
>	11	IGKV5-2*01	ILVPGIS.PRFSGSG..YGTDFTLTINNIESEDAAYYFC	LQHDNFPFT
>	12	IGKV1-12*01	SLQSGVP.SRFSGSG..SGTDFTLTISSLQAEDSATYYC	QQADSFPT
>	13	IGKV4-1*01	TRDSGVP.DRFSGSG..SGADFTLTISSLQAEDVAVYYC	QQYFSIPLT
>	14	IGKV1-33*01	TLETGVP.SRFGGRG..SGTEFNFTISRLQPEDIATYYC	QQSDKLPLT
>	15	IGKV2-28*01	NRASGVP.DRFSGSG..SGTDFTLKIGRVEAEDVGIYYC	MQGLRAPWT
>	‡	IGKV2-29*01 P	SRFSGVP.DRFSGSG..SGTDFTLKVSRVEAEDVGVYY*	MQPIHLPIT

Table 4.2 Vk amino acid sequences: The table shows the 15 amino acid sequences of the Vk clones analysed in my study and 1 pseudogene. a) amino acid sequences of the FR1, CDR1, FR2 and CDR2; b) amino acid sequences of FR3 and CDR3. IMGT numbering was followed and amino acid changes with the closest germline are highlighted in red. The pseudogene sequence is shown with a grey background

A VJ rearrangement contained a rarely seen A26 functional gene and no VK3 family members were found. With the limitations of the low number of

sequences analysed my pool differed from the expected germline distribution and from the adult and neonatal repertoire as Vk2, Vk4 and Vk5 occurred significantly more frequently ($p \leq 0.001$) (Fig.4.11 and Fig.4.12).

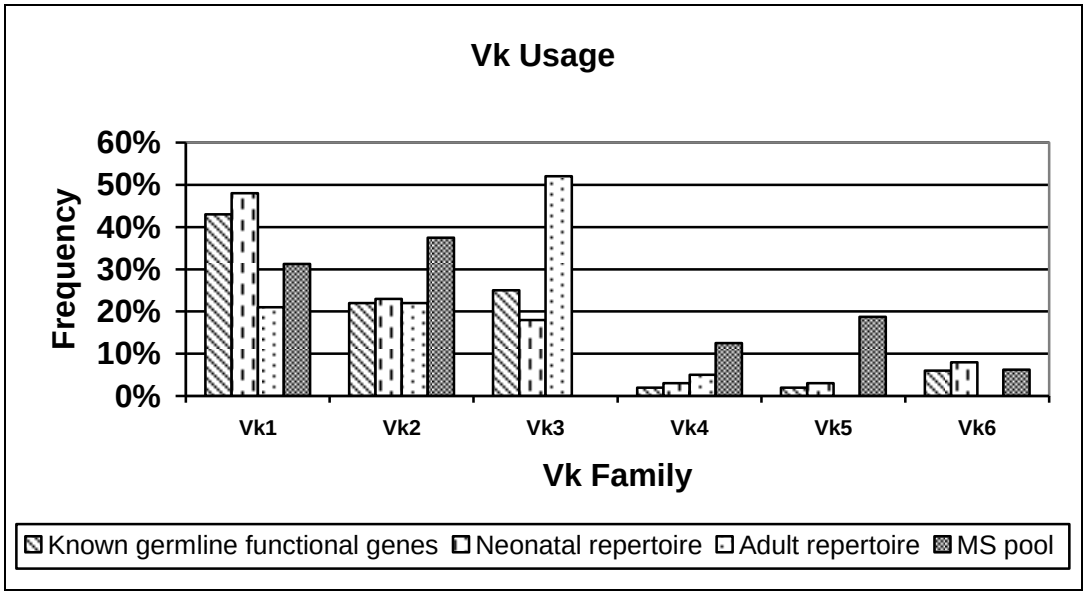

Figure 4.11 Vk Usage: In the MS pool the family Vk3 was not found compared with an expected high expression in the adult repertoire; significantly more frequent were the Vk2, Vk4 and Vk5 families (p=1.1E-48, df=5).

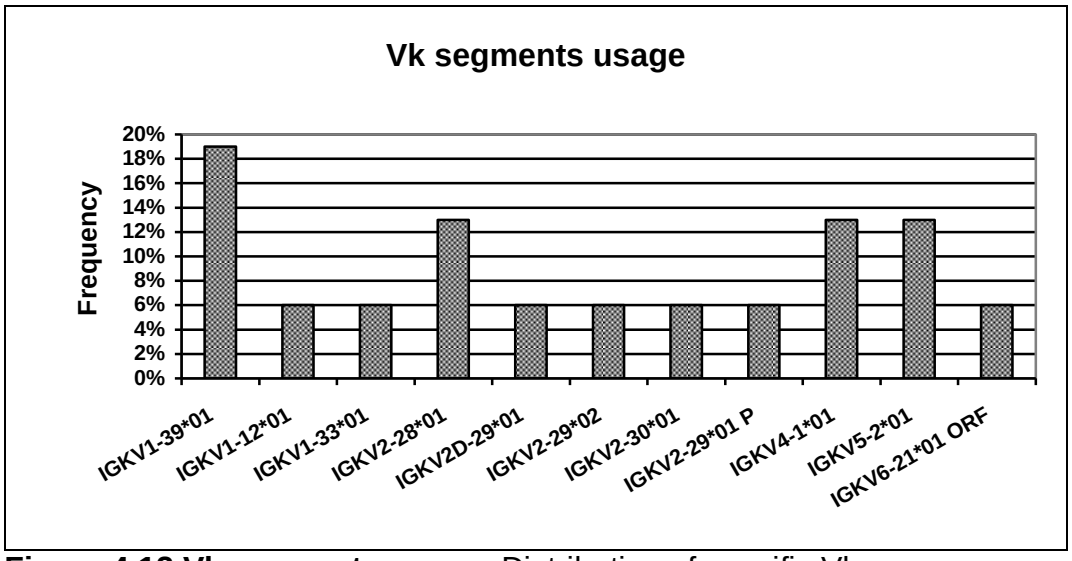

Figure 4.12 Vk segments usage: Distribution of specific Vk genes

The sequence analysed presented joining segments of all 5 families with JK4 being the most represented and Jk3 the least expressed (Juul et al. 1997; Klein and Zachau 1995). Jk4 and Jk5 were more frequent compared with the previous literature (Fig.4.13).

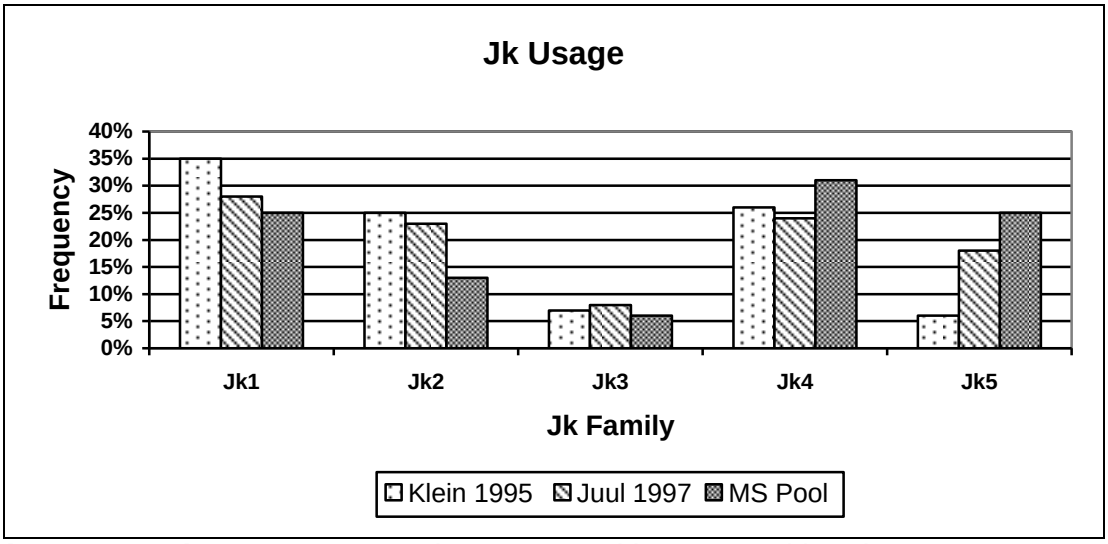

Figure 4.13 Jk Usage: MS pool JK usage with JK4 resulting the most frequent

The 10 different Vλ clones analysed were all functional (Table 4.3).

a)

ID	Vlambda gene	FR1 (1-26)	CDR1 (27-38)	FR2 (39-55)	CDR2 (56-65)	
1	V6-57*01	NFMLTQPHS.VSESPGKTVTISCTGS	SGSI....ASNY	VLWYQQRPGSAPITIIY	ED.....N	>
2	IGLV1-51*01	QSVLTQPPS.LSAAPGQRVTISCSGD	SSNI....GNAY	VSWYQKFPGAAPRLLIY	DN.....N	>
3	IGLV6-57*01	NFMLTQPHS.VSESPGKTVTISCTGS	SGSI....ASNY	VQWYQQRPGSAPTTVIY	ED.....N	>
4	IGLV1-40*01	QSVLTQPPS.VSGAPGQRVTIACTGS	SSNI....GTYD	VHWYQQLPGTAPKLLIH	SN.....T	>
5	IGLV6-57*01	NFMLTQPHS.VSESPGKTVTISCTRS	SGSI....ASDY	VQWYQQRPGSSPSTIIY	ED.....V	>
6	IGLV3-21*01	QAVLTQPSS.VSVAPGQTAKVTCGGD	NIW.....SKS	VHWYQQKPGQAPVLVIH	YD.....K	>
7	IGLV4-69*01	QVILTQPPS.ASASLGASVKLTCTLS	SGHS.....NSA	VAWHQQLPERGPRYLMN	VNSD...GSH	>
8	IGLV1-47*01	SYVLTQPPS.ASGTPGQRVTISCSGS	RSNI....GSNY	VCWYQQLPGAAPKLLIY	NS.....D	>
9	IGLV6-57*01	NFMLTQPHS.VSESPGKTVTISCTRS	SGSI....ASYY	VQWYQQRPGSSPTTVIY	ED.....N	>
10	IGLV3-19*01	SSQLTQDPA.VSVALGQTVRITCQGD	SLR.....SYS	ASWYQQKPGQAPLLVIY	GE.....N	>

b)

	ID	Vlambda gene	FR3 (66-104)	CDR3 (105-117)
>	1	IGLV6-57*01	QRPSGVP.DRFSGSIDSSSNSASLTISGLKTEDEADYYC	QSYDSSNHWV
>	2	IGLV1-51*01	KRASGIP.ARFSGSK..SGTSATLAITGLQTGDEADYYC	GTWDSSLSV
>	3	IGLV6-57*01	QRPSGVP.DRFSGSIDSSSNSASLIISRLKTEDEADYYC	QSYDSANLWV
>	4	IGLV1-40*01	NRPSGVP.DRFSGSK..SGTSASLAITGVQAEDEADYYC	QSYDSSLSGSRV
>	5	IGLV6-57*01	RRPSGVP.ARFSGSIDRSSNSASLTISGLKTEDEADYYC	QSYDSSTYV
>	6	IGLV3-21*01	ERPSGIP.ERFSGSN..SEDTATLTISGVESGDEADYYC	QVWDSDYDHRV
>	7	IGLV4-69*01	NKGDGIP.DRFSGSS..SGAERYLIISRLQSEDEADYYC	QTWDTGTV
>	8	IGLV1-47*01	HRPSGVP.DRFSGSR..SGTSASLAISGLRSEDEADYYC	AAWDDSLSGHWV
>	9	IGLV6-57*01	HRPSGVP.DRFSGFIDSSSNSASLTISALKTEDEADYYC	QSYDSNNQV
>	10	IGLV3-19*01	DRPSGIP.DRLSGSR..SGNTASLTITGAQAEDEADYYC	NSRDSSTIHLI

The Vλ6 family represented half of the sequences analysed which is a subgroup rarely seen in previous PBLs studies; these studies include analysis of 5 cDNA libraries from 4 healthy adults (Ignatovich et al. 1997) or by single-cell PCR in 2 adults (Farner et al. 1999) and 3 newborns (Richl et al. 2008) where Vλ1 and Vλ2 are the families most prominent. Comparing the frequencies of Vλ usage observed in my library with the frequencies expected by random usage from the functional genes in the genome I found significantly higher frequencies Vλ6 and no expression of Vλ2 (Fig.4.14). The JL3 family was represented in 6 unique functional sequences out of 10.

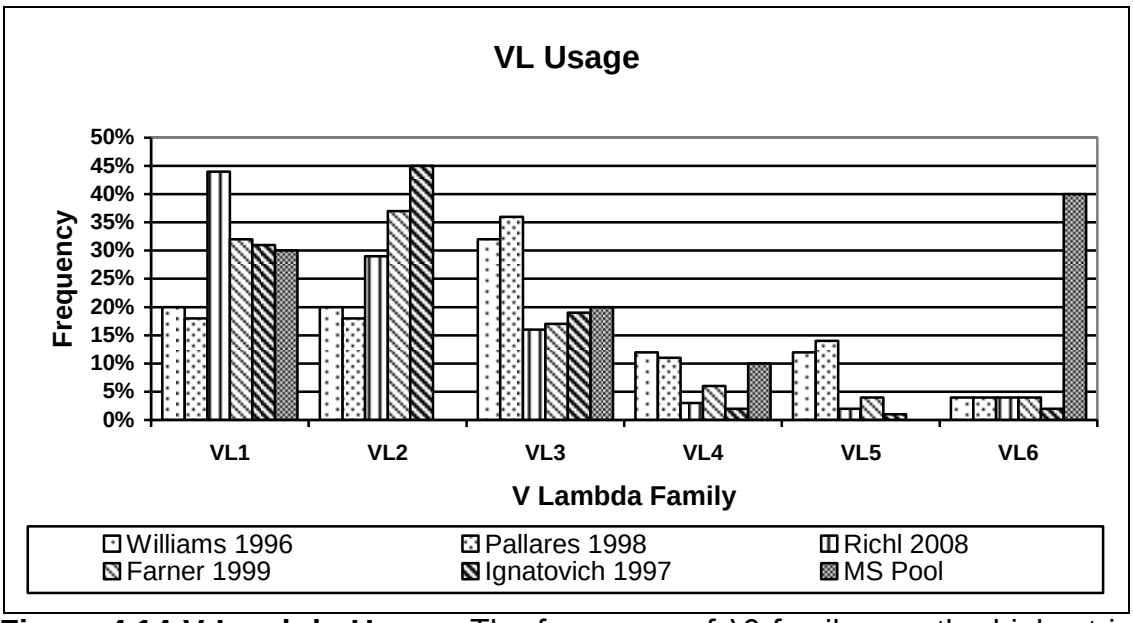

Figure 4.14 V Lambda Usage: The frequency of λ6 family was the highest in my MS pool compared with functional known germline genes (p=4.8E-78) and previous studies on adult and newborn PBLs (no other calculations were performed due to the low number of sequences analysed).

- Analysis of mutation and substitution patterns

Heavy chain CDR3 mutation analysis

The VH-CDR3s were analysed for length diversity, amino acid (aa) composition and net charge according to the IMGT unique numbering (positions considered 105-117).

ID	CDR3 (105-117)	ID	CDR3 (105-117)
26	ARGYL	19	ASHGDYVRHYYFHMDV
30	ALGPY	27	TRVLGYTYDKLDYFDS
43	ARGYL	36	ARGKWSGSYKGDAFDI
42	ARSEELDY	37	ASHGDYVRHYYFHMDV
29	AKSYSAFDY	25	AKDHYYDSSVPAYYFDY
24	VRLIYAYGRDY	2	VRGGYEVGRSGSVYGMDV
32	VPRRTASWFDP	15	ARLIWFGESVFPTRGMDV
41	ARGYTGVVADY	35	ARIQYCTDITCFYDWFDP
45	AREVRNSWYDP	8	ARGPLEFLWGSYRYEVFDH
3	ASEVERRLVFDN	13	ARGGHIVGSTTDYYYALDV
4	AGFCGTPNCDDV	18	ARVLKAPQGYSGSWYPVHY
44	ARHGNWASNFDS	33	ARRRAGAHLYGDYQNWFDP
1	ARGMGYLIRYFDL	10	ASIGDNTGYFREAFTYYFDY
17	ARLNVVVAPRFDR	16	ARRLSHRYCSRGSCPNWFDP
38	ARDSSGHFEALNI	40	ASIGDNTGYFREAFTYYFDY
7	ARGGASGGYDRPIDY	6	ARDPTRFTLFGRGEYYYGLEV
9	ARDRDTSGSNDVFDI	11	ARATPYTIFGVSTYYRYFMDV
14	ARMGPDNRAWYRFDY	23	ARVRDNISIVGVVLNIGAFDI
20	AKVGDSDWGTSFFDY	39	AGEGYCRSSTCYNKIHTNWFDL
22	ARNLYSSTWTGVGDY	46	ARQPYDTAGYFATGDKWYGMDV
31	GKGISIGAVADAVDV	21	VRQSGYLYSSSWGLHNYMWYLDV
34	AGGTSPWSSEYYFYF	5	AYSQYYYDTSGPDSDFYYSYFMDV
12	VRGQFGYCSSPSCPEY	28	AYSQYYYDTSGPDSDFYYSYFMDV

The VH-CDR3 lengths varied in the range of 15 and 72 bp (mean 47.4 bp) representing 5 to 24 aa residues, with an average of 16 ± 6 aa residues (Fig.4.15). The 67.4% of the VH-CDR3s resulted having a length >15 aa. Comparing my data with the repertoire of a female healthy control (Brezinschek et al. 1995) the average CDR3 lengths resulted significantly different between the repertoires: 48 base pairs (bp) ±14 (mean±SD), compared with the healthy control repertoire, 41bp±13 (p=0.02; two-tailed distribution). Ranking the VH-CDR3 lengths, there was a statistically significant difference between the MS pool and the healthy control repertoire (p=0.021). The usage of CDR3 lengths in the range of 60-72 was significantly higher (p=0.007) in the MS pool supporting

the bias towards longer CDR3 found in autoimmune diseases (Yurasov et al. 2005) (Fig.4.16).

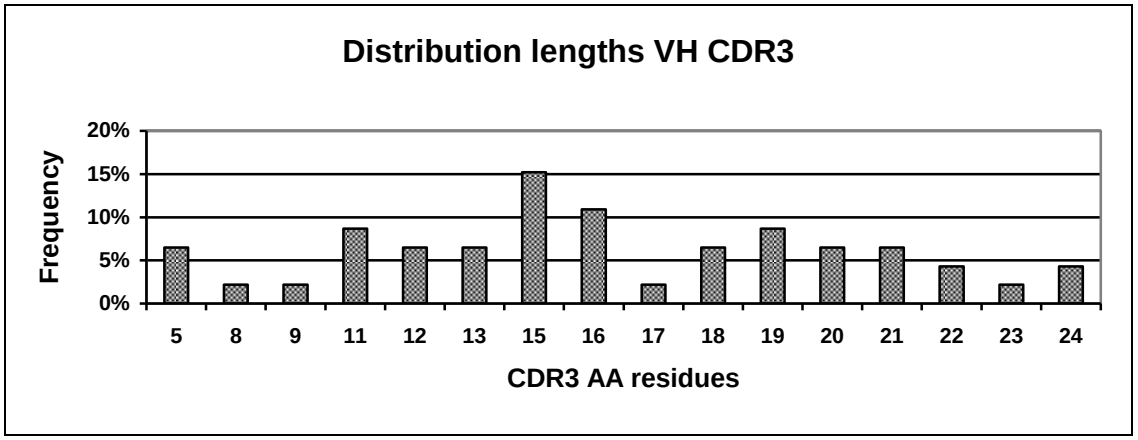

Figure 4.15 Distribution lengths VH CDR3: CDR3 lengths spectrum derived from the sequences analysed. The distribution of the CDR3 lengths was almost the same between the CDR3 ≤ 15 aa (47.8%) and the CDR3 > 15 aa (52.2%).

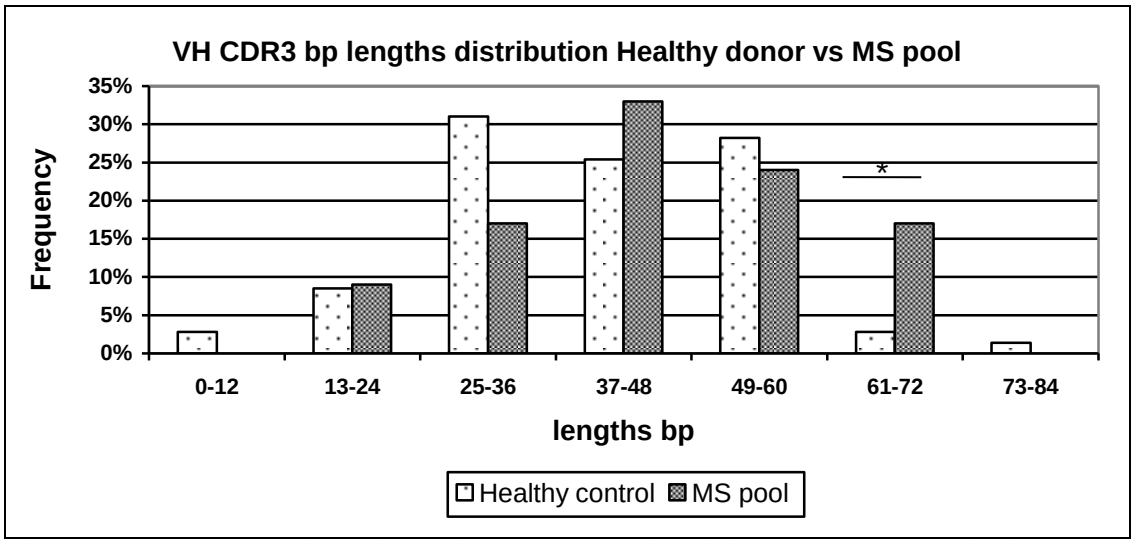

Figure 4.16 Comparison lengths VH CDR3 healthy vs MS: The distribution of the CDR3 lengths in bp of 46 productive sequences from my MS pool was compared with the distribution derived from 71 productive sequences of a female healthy donor PBLs (data adapted from Brezinschek HP 1995). The range 61-72 bp was statistically higher than control *(binned data analysed by two-tailed Fisher's exact test; p=0.007).

Furthermore, the status of mutations in my rearrangements from the MS pool was analysed. In my unique rearrangements I analysed 12990 nt and found 860 total mutations with a total frequency (mutations/bp) of 6.62% of which 75% were replacement mutations and a replacement to silent mutation ratio (R/S) of 2.96. The mutation frequency observed in my sample was significantly higher ($p \leq 0.001$; Yates correction applied) than the expected frequency of a VH gene (Insel et al. 1995) and from the frequency observed in PBLs from healthy controls (Harp et al. 2007). The comparison of the number of total and replacement mutations per base pair in the CDRs was significantly higher than in the FRs (respectively $p \leq 0.001$; $p \leq 0.001$). The overall distribution of the mutations across the genes showed that the majority were concentrated within the CDR2 (11.8%) and CDR1 (10%) compared with the FR average (5.4%) and with the highest ratio detected in the CDR2 (R/S=6.6). The sequences of the VH3 family presented the highest R/S ratio among the other families having a CDR R/S (CDR1+CDR2) equal to 10.12 compared to a FR R/S (FR1+FR2+FR3) equal to 1.78 (Fig.4.17).

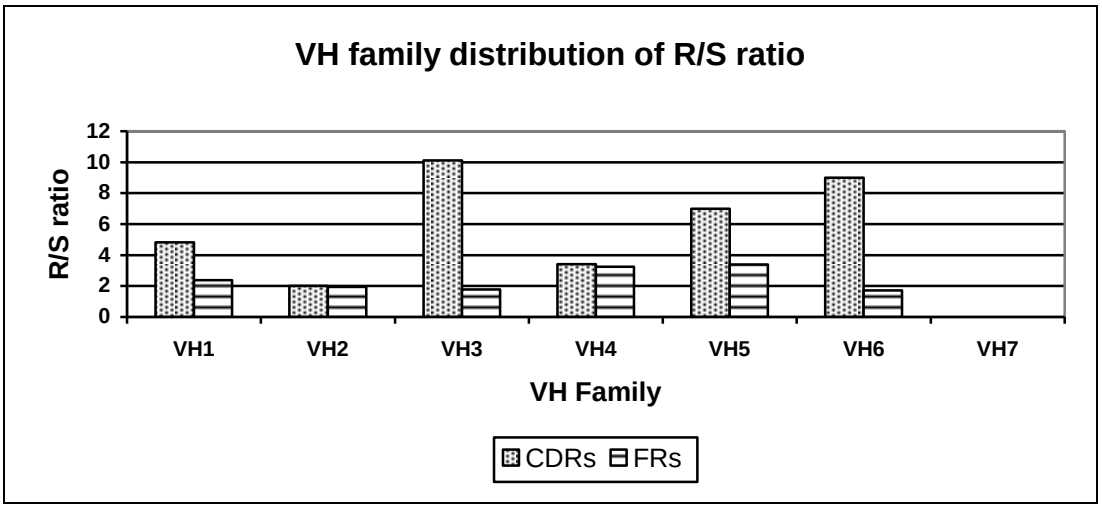

Figure 4.17 VH family distribution of R/S ratio: The distribution in the different families was heterogeneous with VH2 and VH4 having almost the same silent replacement ratio in CDRs and FRs.

In VH-CDR3 the amino acid usage was mainly tyrosine (13%), asparagine (10%), glycine (9.57%), alanine and arginine (8.71%) with more than 30% hydrophobic residues. The net charge composition of the VH-CDR3 was calculated (protein calculator 3.3) at pH=7.36 and the majority (73%) of the rearrangements had an acidic charge, range from -0.1 to -4.2. The range found was the same range of mature PBLs from controls and of previous studies on CSF B cells from PwMS (Harp et al. 2007). The distribution showed only a slight negative asymmetric tail (Fig.4.18).

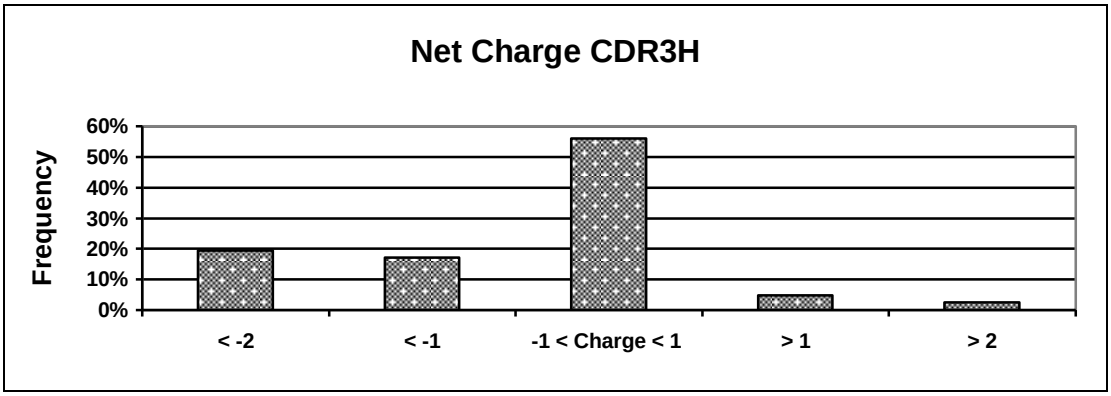

Figure 4.18 Net Charge VH CDR3: In the sequences derived from the MS pool the vast majority of the CDR3s were neutrally charged or slightly charged (56%).

The somatic hypermutation process is a two step process with AID activity for C/G followed by DNA polymerase η for A/T. The non-random targeting of the hypermutational machinery has also been shown to have preferential nucleotide sequence motifs, i.e. RGYW/WRCY (R=A/G, Y=C/T, W=A/T) and WA/TA (Dorner et al. 1998; Rogozin et al. 2001). In my study I analysed CDRs and FRs of the heavy chain repertoire for non-silent mutations and the vast majority of mutations were within the classical targeting motifs with around 52% of all replacement mutations of the CDRs and around 43% of the FRs. The intact targeting of the typical hotspots in the RGYW/WRCY motifs have been described previously (Harp et al. 2007) in MS CSF B cell repertoires (Fig.4.19). The percentage of mutations targeting the motifs were determined for CDRs and FRs in the clones analysed. The mutations in the CDRs were: 27% WA,

26% TW, 35% RGYW and 18% WRCY; in the FRs the percentages were: 20% WA, 10% TW, 23% RGYW and 20% WRCY.

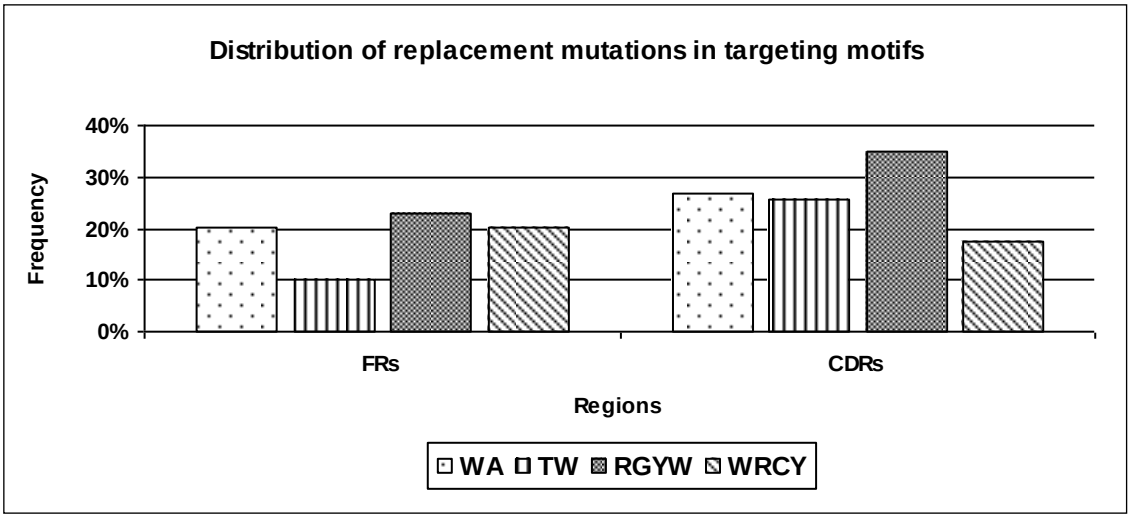

Figure 4.19 Mutations: In my heavy chain repertoire the majority of replacement mutations within CDRs (~52%) and FRs (~43%) targeted the RGYW/WRCY motifs with no significant differences between the two regions.

Furthermore, an antigen driven selection can determine an antibody gene mutation pattern. In MS a mutation pattern has been found when analysing the VH4 family which is known to be over utilized by CSF B cells. The analysis revealed 14 codons with an increased number of mutations in hot spots 31b, 32, 40, 56, 57, 60, 81 and 89 or a decreased number of mutations in cold spots 30, 43, 52, 77, 82, 82a and representing a potential mutational signature of conversion from CIS to CDMS (Cameron et al. 2009). My libraries were built from patients with progressive MS so I wanted to test the mentioned VH4 mentioned codons for mutations. As seen in Fig.4.20 no preferential mutations were present in the hotspots regions.

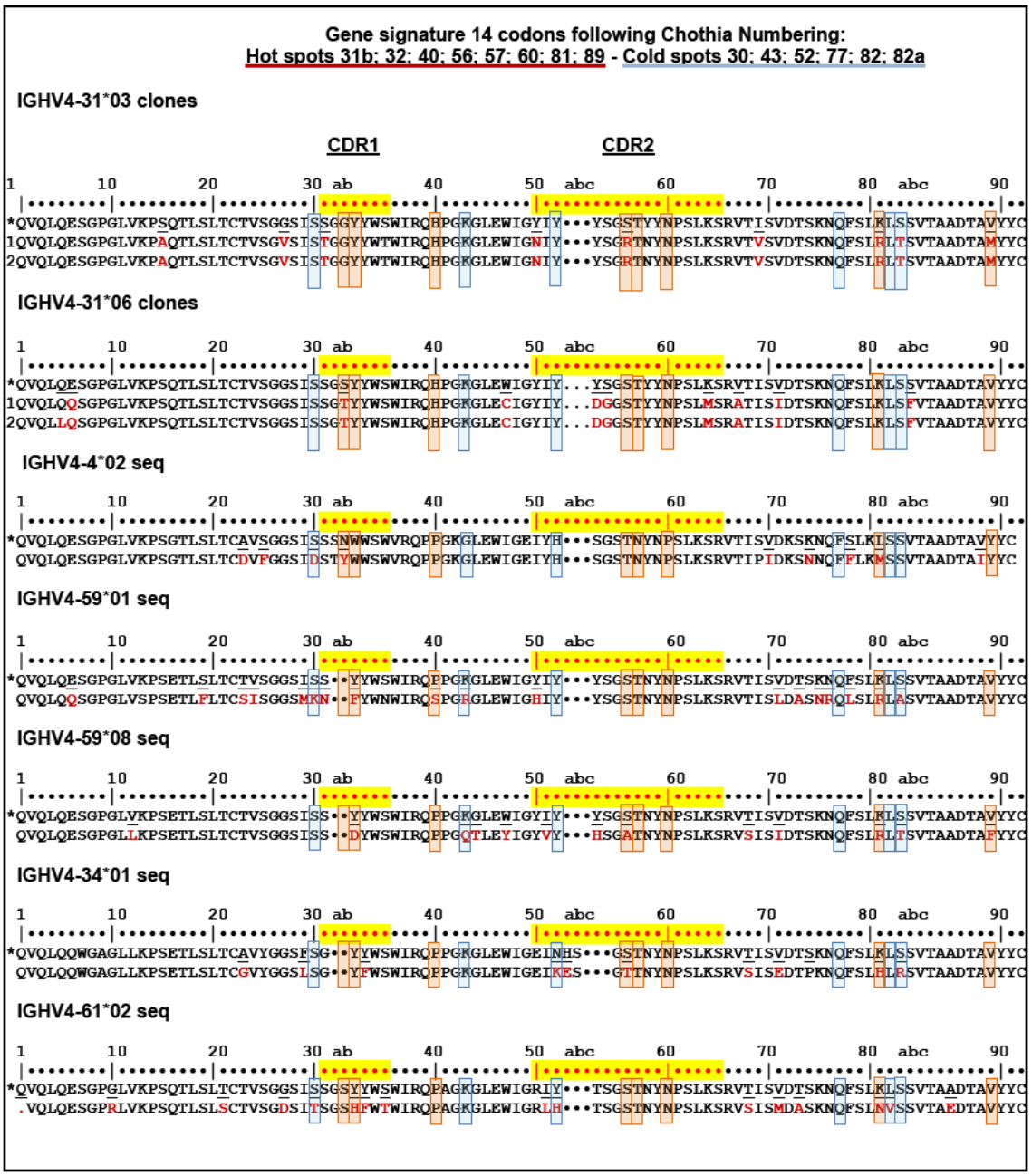

Figure 4.20 Gene signature in the VH4 clones: VH4 amino acid sequences evaluated for the presence of an unique antibody gene signature. (*=germline - top sequence; highlighted in yellow CDRs).

The results showed that among all the replacement mutations found the codon 81 (Chothia numbering) had the highest frequency of mutations but the spots considered couldn't be divided into hot or cold spots as similar frequencies were present (Fig.4.21).

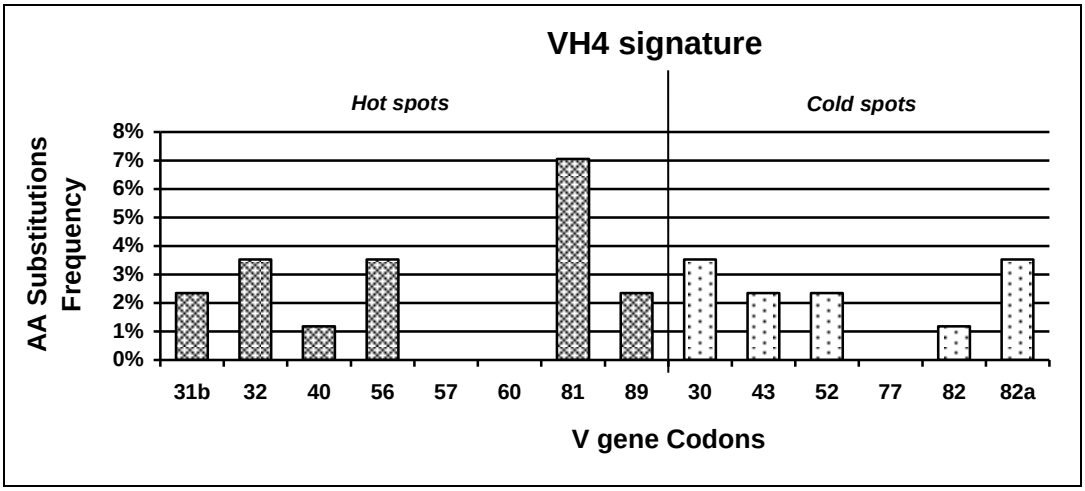

Figure 4.21 Hot and Cold spots of VH4 gene signature: Distribution of amino acid residue substitutions in V gene codons, as from Chothia numbering, in VH4 sequences derived from 14 patients with MS

Nevertheless, it is possible that a larger number of sequences needs to be analysed to be able to perform a proper analysis. In fact, the possibility to have a molecular signature of conversion in MS could be of extreme value as a prognostic biomarker and helpful in making therapeutic decisions.

After the analysis of the somatic hypermutation I analysed the aa substitutions given that the physical properties of the translated sequences can change based on the replacement mutation (a mutation yielding an aa replacement). A replacement mutation can give rise to a very similar but also a very different aa substitution compared with the respective germline. Surprisingly in my sample, I found that the very different replacement mutation was the one preponderant in the FRs mutations (Fig. 4.22).

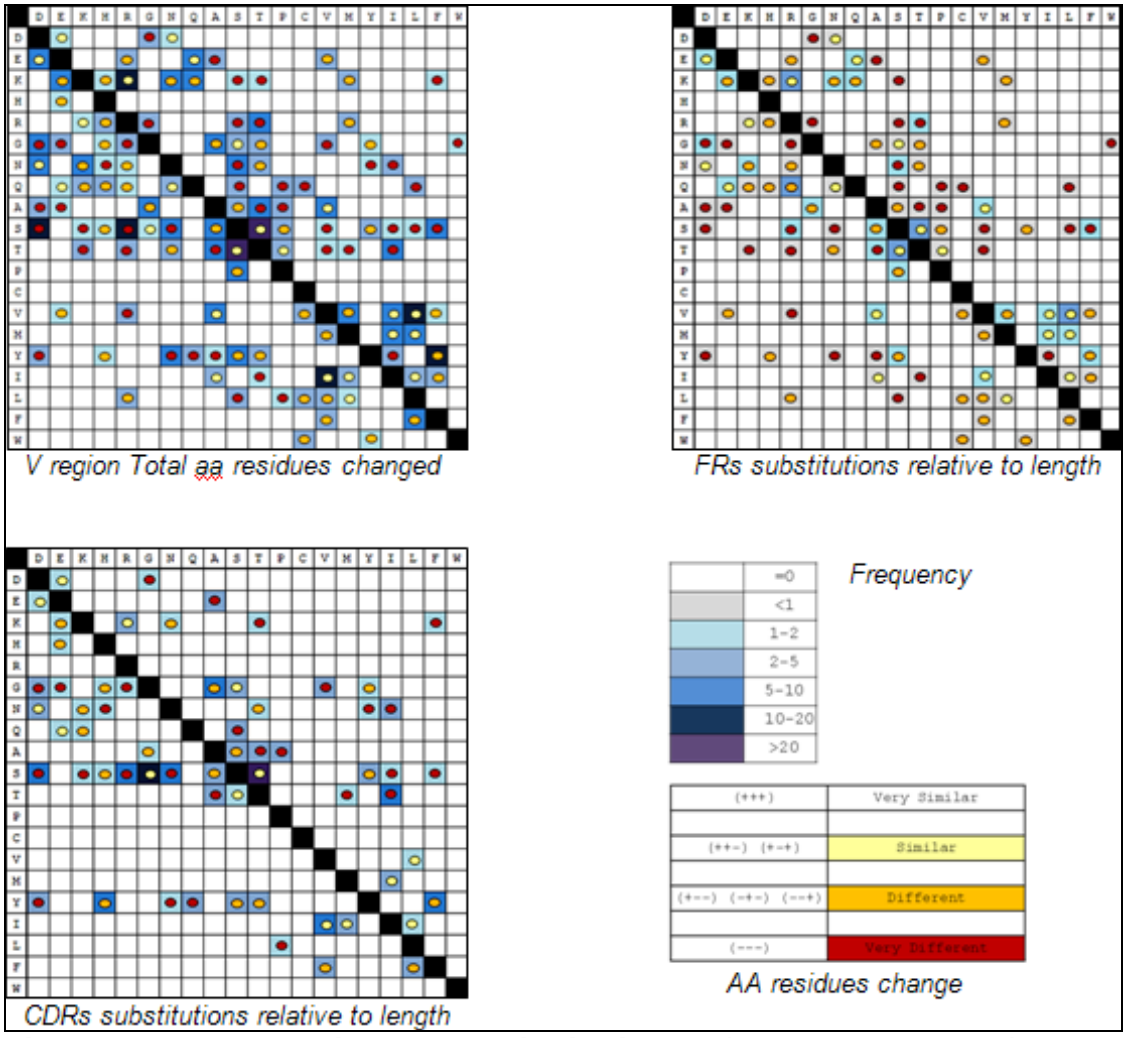

Figure 4.22 CDRs and FRs AA substitutions: The frequency of replacement mutations was higher in CDRs than FRs but interestingly the type of replacement was predominantly very different in the FRs (graphs adapted from Zuckerman NS et al. 2010)

Light chain CDR3 mutation analysis

More than 80% of the unique sequences in the Vk had CDR3 lengths of 27 bp whereas the average number of residues in the Vλ was 30 bp; this represents an average of 9 ± 0.4 and 10 ± 1.4 aa residues respectively. Of the 177 residues in the Vk sequences almost 50% of them were glycine (15%), phenylalanine (13%), threonine (11%) and proline (10%), compared to the 121 residues in the Vλ sequences where 55% were constituted of serine (20%), asparagine (11%) and equal amounts of cysteine, valine and phelynalanine (8%). The calculated net charge at pH=7.36 of the Vk rearrangements had an average acidic charge of -0.24 (range 0.8 to -1.3) and of the Vλ rearrangements it was -1.16 (range -0.1 to -2.1). The status of mutations in the light chains was analysed for 4356 nt of unique Vk and 2932 nt of unique Vλ rearrangements and in total 181 and 155 mutations respectively. This corresponds to a frequency of 4% and 5% of which 64% and 72% were replacement mutations. The R/S ratio was 1.78 for Vk and 2.7 for Vλ. The CDR1 and CDR2 had the highest percentage of mutations (6.8%, 6.7% for Vk and 6.7%, 15.7% for Vλ). Across the Vk and Vλ genes the CDR1 had the highest R/S ratio of 2.1 and 6.5 respectively. The total R/S ratio of 4.5 in the Vk FRs was higher than the ratio of 3.4 found in the CDRs; in the Vλ the total R/S ratio of CDRs was 9.5 compared with the 7.5 of FRs.

- Clonal expansion

After exclusion of the identical sequences the remaining sequences originated from the same VH with an identical VH CDR3 or a CDR3 with one mutation: they can therefore be considered related sequences. Nevertheless, as the library was made from a pool of B cells from 14 patients I could not be sure these sequences were derived from the same donor. Examples of clonal expansion found in my samples are reported below:

1)

IMGT Numbering	FR1	CDR1	FR2	CDR2	>
Germline	(1-26)	(27-38)	(39-55)	(56-65)	>
IGHV4-31*03	~GLVKPSQTLSLTCTVS	GGSIS..SGGYY	WSWIRQHPGKGLEWIGY	IYYS…GST	>
Clone 1	~GLVKPAQTLSLTCTVS	GVSIS..TGGYY	WTWIRQHPGKGLEWIGN	IYYS...GRT	>
Clone 2	~GLVKPAQTLSLTCTVS	GVSIS..TGGYY	WTWIRQHPGKGLEWIGN	IYYS...GRT	>

IMGT Numbering	FR3	CDR3	% identity	N. mutations	
Germline	(66-104)	(105-117)		Nt	AA
IGHV4-31*03	YYNPSLK.SRVTISVDTSKNQFSLKLSSVTAADTAVYYC				
Clone 1	NYNPSLK.SRVTVSVDTSKNQFSLRLTSVTAADTAMYYC	ARDSSGHFEALNI	94.5	16	11
Clone 2	NYNPSLK.SRVTVSVDTSKNQFSLRLTSVTAADTAMYYC	ARDSSGHFEALNI	94.16	17	11

2)

IMGT Numbering	FR1	CDR1	FR2	CDR2	>
Germline	(1-26)	(27-38)	(39-55)	(56-65)	>
IGHV4-31*06	~QESGP.GLVKPSQTLSLTCTVS	GGSIS..SGSYY	WSWIRQHPGKGLEWIGY	IYYS...GST	>
Clone 1	~QQSGP.GLVKPSQTLSLTCTVS	GGSIS..SGTYY	WSWIRQHPGKGLECIGY	IYDG...GST	>
Clone 2	~LQSGP.GLVKPSQTLSLTCTVS	GGSIS..SGTYY	WSWIRQHPGKGLECIGY	IYDG...GST	>

IMGT Numbering	FR3	CDR3	% identity	N. mutations	
Germline	(66-104)	(105-117)		Nt	AA
IGHV4-31*06	YYNPSLK.SRVTISVDTSKNQFSLKLSSVTAADTAVYYC				
Clone 1	YYNPSLM.SRATISIDTSKNQFSLKLSFVTAADTAVYYC	*ARGKWSGSYKG*	93.45	19	9
Clone 2	YYNPSLM.SRATISIDTSKNQFSLKLSFVTAADTAVYYC	*ARGKWSGSYKG*	93.10	20	10

3)

IMGT Numbering	FR1	CDR1	FR2	CDR2	>
Germline	(1-26)	(27-38)	(39-55)	(56-65)	>
IGHV1-69*02	~KAS	GGTF....SSYT	ISWVRQAPGQGLEWMGR	IIPI..LGIA	>
Clone 1	~KAS	GGTF....STYT	FSWVRQAPGQGLEWMGR	IIPI..LGIT	>
Clone 2	~KAS	GGTF....STYS	FSWVRQAPGQGLEWMGR	IIPI..LGIT	>

IMGT Numbering	FR3	CDR3	% identity	N. mutations	
Germline	(66-104)	(105-117)		Nt	AA
IGHV1-69*02	NYAQKFQ.GRVTITADKSTSTAYMELSSLRSEDTAVYYC				
Clone 1	NYAQKFQ.GRVTITADKSTTTVYMDLSSLRSEDTAVYYC	*ASIGDNTGYFR*	96.18	11	6
Clone 2	NYAQKFQ.GRVTITADKSTTTVYMDLSSLRSEDTAVYYC	*ASIGDNTGYFR*	95.83	12	7

4)

IMGT Numbering	FR1	CDR1	FR2	CDR2	>
Germline	(1-26)	(27-38)	(39-55)	(56-65)	>
IGHV3-23*01	EVQLLESGG.GLVQPGGSLRLSCAAS	GFTF....SSYA	MSWVRQAPGKGLEWVSA	ISGS..GGST	>
Clone 1	QVQLLRSGG.GSVQPGESLRLSCAVS	GFTV....GSYA	MSWVRQAPGKGLEWVSV	ISGG..AGTT	>
Clone 2	QVQLLRSGG.GSVQPGESLRLSCAVS	GFTV....GSYA	MSWVGQAPGKGLEWVSV	ISGG..AGTT	>

IMGT Numbering	FR3	CDR3	% identity	N. mutations	
Germline	(66-104)	(105-117)		Nt	AA
IGHV3-23*01	YYADSVK.GRFTISRDNSKNTLYLQMN SLRAEDTAVYYC				
Clone 1	YYADSVK.GRFTISRDKSKNTLFLE I S SLRAEDTAVYYC	*ASHGDYVRHYY*	93,40	19	16
Clone 2	YYADSVK.GRFTISRDKSKNTLFLE I S SLRAEDTAVYYC	*ASHGDYVRHYY*	92,36	22	17

5)

IMGT Numbering	FR1	CDR1	FR2	CDR2	>
Germline	(1-26)	(27-38)	(39-55)	(56-65)	>
IGHV3-7*02	EVQLVESGG.GLVQPGGSLRLSCAAS	GFTF....SSYW	MSWVRQAPGKGLEWVAN	IKQD..GSEK	>
Clone 1	EVQLVESGG.GLVQPGGSLRLSCAAS	GFTF....SSTW	MSWVRQAPGKGLEWVAN	IKSD..GSAK	>
Clone 2	EVQLVESGG.GLVQPGGSLRLSCAAS	GFTF....SSTW	MSWVRQAPGKGLEWVAN	IKSD..GSAK	>

IMGT Numbering	FR3	CDR3	% identity	N. mutations	
Germline	(66-104)	(105-117)		Nt	AA
IGHV3-7*02	YYVDSVK.GRFTISRDNAKNSLYLQMNSLRAEDTAVYYC				
Clone 1	DYVDSVR.GRFTISRDNAENSLSLQMNSLRAEDTAVYYC	*ARGYLWGKGTT*	95.49	13	7
Clone 2	DYVDSVR.GRFTISRDNAENSLSLQMNSLRAEDTAVYYC	*ARGYLWGKGTT*	95.14	14	7

(Differences of even 1 nucleotide in the VDJ recombination of each sequence were assumed to be due to somatic hypermutation as the error rate of the high-fidelity DNA polymerase used in my experiment was of 1 error per 3.6x10^6 nucleotides incorporated and the nucleotides inserted for each sequence analysed were in the range of ~10^4 - ~350bp for each insert analysed, multiplied 2x30 PCR cycles before ligation -).

Chapter Discussion

The antibody phage display technology generates high affinity and specificity recombinant antibodies against a variety of antigens. The process outcome selects antigen-specific antibody fragments that can be used as therapeutics and diagnostic reagents with different tissue penetration based on the fragment type. In my work the phage display technology was applied to study the immune repertoire of MS patients and at the same time also to isolate fragments specific to known MS autoantigens. The formation of a pool containing cDNA derived from 3 patients, and from 14 patients in the second step, did allow to obtain a larger repertoire to be used for antigen selection. The construction of the library gave me the possibility to study the VH and VL family usage, analyse the sequences and evaluate their specificity as expressed auto-antibodies. The sequence analysis of the variable regions did confirm an antigen-driven response. The nature of the eliciting antigen (self or foreign) remains, though, elusive in MS and as next step the library was panned against known antigens involved in MS pathogenesis. The strategy used to build the library did raise also some limitations:

a) VH and VL family usage analysis

The evaluation of the VH and VL family usage did not take into consideration the efficiency of the different pair of primers used to amplify the different families and also the possible bias during the cloning process due to the different length of amplicons inserted was not considered. A different approach, such as deep sequencing would have overcome this limitation as the analysis of the whole RNA isolated from a sample could be achieved without the need to design primers and thus any knowledge of the relative expression of each family gene. Comparing the data obtained with this method before and after the cloning process will help in identifying any possible bias.

b) Library was not exclusive from TLOs

During an immune response against a pathogen the affinity for the target antigens increases radically with time, in a phenomenon known as affinity maturation. Affinity maturation takes place in SLOs in structures known as

germinal centres (GCs). GCs provide the environment to fine tune the Igs to be able to bind with high affinity by the combination of somatic hypermutation (SHM) and iterative rounds of affinity based selection. In different autoimmune diseases such as autoimmune thyroiditis and diabetes data suggest that the Ag-driven somatic hypermutation and selection does not occur in the SLOs but locally at the inflammation site. In my sequence analysis the construction of the library from the B cells present in the brain with no separation among perivascular cuffs, brain infiltrates or ectopic lymphoid aggregates did not give the possibility to differentiate if the skewing of the repertoire found was derived from an Ag-driven selection in a germinal center (GC)-like reaction supported in the organized chronic infiltrate. Furthermore, the use of the whole tissue will not allow to differentiate from B cells infiltrating the brain and the ones derived from the peripheral blood eventually contained in the brain vessels. Similarly, B cells could undergo Ag-driven somatic hypermutation externally to the infiltrated tissue and then invade the brain, but not having the possibility to compare my findings with the repertoire found in the SLOs draining the brain of MS patients I could not ascribe the source of the mutations found to any of the compartments. Therefore the presence of an Ag-driven selection in the repertoire analysed is supported in my work but the germinal centre reaction cannot be ascribed positively to the lymphoid aggregates identified. The development of the laser capture experiments described in the previous chapter could help to answer these open questions as well.

c) Library was done as pool and not derived from a single patient or single cell

The library was constructed as a pool derived from cDNA of different MS patients. In my study, increasing the amount of possible VH and VL combinations decreased the probability to obtain a correct pairing by random combination. The possibility to work on a single patient at the time will give me the possibility to delineate if the VH and VL usage is patient specific or disease specific. The different contribution of each patient to the amount of each VH and VL family couldn't be evaluated as well as the contribution to the diversity found in the library. Furthermore, the strategy used to build the library did not

differentiate between IgG or IgM repertoire and the two repertoires could not be analysed separately. Selection of a more restricted amount of cells by laser capturing singly the inflammatory infiltrates will increase my chances to obtain a correct pairing. Eventually the possibility to evaluate the VH and VL pairing by single cell laser capturing will allow to identify the exact pairing of the VH and VL of the B cells involved in the ectopic lymphoid aggregates. A study analysing the single-cell repertoire by cell sorting in RRMS patients has shown that in the CSF the repertoire is derived from clonally expanded B cell populations (Owens et al. 2003). It has also been shown that antigen experienced B cell clones are shared among CSF, meningeal aggregates and corresponding parenchyma (Lovato et al. 2011; Obermeier et al. 2011). In this study, clonal variants have been identified but they could not be ascribed to the IgG or IgM repertoire or to the same patient. The laser capture technique should be further used to improve the analysis of the VH and VL family usage in MS patients in a faithful manner.

Chapter 5: MP4 specific scFv raised from the MS library

Background:

To the best of my knowledge the only antibody phage display that has been constructed from MS patients was from PBL of eight RRMS patients. The authors selected the library on MBP (native and treated) and raised multiple anti-MBP scFVs that bound to either linear MBP epitopes, native MBP or both. Interestingly, one of the scFv cross-reacted with EBV latent membrane protein 1 (LMP1) supporting the molecular mimicry hypothesis of MS pathogenesis (Gabibov et al. 2011). These results showed the possibility of using an antibody phage display library built from MS B cells to make recombinant antibodies with specificity that may mimic natural autoAbs. In my study the specificities of the synthetic library and the two newly built MS libraries, containing VH only and VH+VL gene segments, were tested for their ability to be a source of antibodies against known MS autoantigens. Hence, the performance of the newly built libraries was compared to *in house* human synthetic library (De Wildt et al. 2000). In addition, pre-selection with the synthetic library was done with all auto-antigens available to test their performance as target proteins for selection.

Objective:

In my study I screened my antibody libraries to identify binders that could resemble the specificity of B cells found in MS brain infiltrates.

Specific aims:

- To biopan the Tomlinson I antibody phage display library on known autoantigens

- To biopan the libraries built from V genes derived from MS patients on a fusion protein, MP4, carrying epitopes of MBP and PLP.

Methods:

The libraries were built in a pIT2 phagemid vector, and the choice of a phagemid vector implied the need for a helper phage in different steps of the process; specifically in the rescue of the starting library and in the amplification of the eluted phages after a round of selection (see chapter 1.4.2 for details). The strategy to select specific binders from my libraries followed a two step process. I started my screenings enriching the *in house* Tomlinson I library as a positive control for the process that I was going to perform, and after positive results, I then performed panning with the MS libraries. The Tomlinson I library has a size of $1.47x10^8$ with diversified side chains in 18 different amino acid positions between heavy and light chain antigen binding sites and it was used successfully in selecting a vast variety of antigens, including native or denatured proteins, impure antigens, and whole-cell extracts (De Wildt et al. 2000). The Tomlinson I library was biopanned on immunotube immobilised antigens and after each round of selection the output of eluted phages was analysed by polyclonal phage ELISA and by monoclonal phage ELISA mainly after the 3rd round. In my experiments the proteins for selection were chosen because they had been identified as potential autoantigens and targets of CSF OCBs in the literature (see chapter1). The proteins were kindly provided by colleagues and were analysed by SDS-PAGE (Fig.5.2). I considered antigens spanning among the possible myelin epitopes, axonal epitopes and matrix epitopes. These include: MP4, a recombinant fusion protein including portions of myelin basic protein (MBP) and proteolipid protein (PLP), the recombinant extracellular domain 1-125 of myelin-oligodendrocyte glycoprotein (MOG_{1-125}) and αβ-crystallin (CRYAB), axonal cytoskeletal protein neurofilament light (Nf-L) as a neuronal antigen and collagen type III (CIII) as an extracellular matrix protein. Below is the description of the MP4 fusion protein that I used as a target autoantigen for selection using both the synthetic and the newly built MS libraries.

MP4 fusion protein

MBP 160 aa (protein sequence)

```
1    masqkrpsqr hgskylatas tmdharhgfl prhrdtgild sigrffggdr gapkrgsgkd
61   shhpartahy gslpqkshgr tqdenpvvhf fknivtprtp ppsqgkgaeg qrpgfgyggr
121  asdyksahkg fkgvdaqgtl skifklggrd srsgspmarr
```

PLP 274 aa (protein sequence)

```
1    mglleccarc lvgapfaslv atglcffgva lfcgcgheal tgtekliety fsknyqdyey
61   linvihafqy viygtasfff lygalllaeg fyttgavrqi fgdykticg kglsatvtgg
121  qkgrgsrgqh qahslervch clgkwlghpd kityaltvvw llvfacsavp vyiyfntwtt
181  cqsiafpskt sasigslcad armygvlpwn afpgkvcgsn llsicktaef qmtfhlfiaa
241  fvgaaatlvs lltfmiaaty nfavlklmgr gtkf
```

(underlined the sequences used in the fusion protein)

ΔPLP4 (PLP residues 35–69, 87–154 and 177–237)
Junction: llggledp

MP4 (MBP+Junction+ΔPLP4) (protein sequence)

```
masqkrpsqr hgskylatas tmdharhgfl prhrdtgild sigrffggdr gapkrgsgkd
shhpartahy gslpqkshgr tqdenpvvhf fknivtprtp ppsqgkgaeg qrpgfgyggr
asdyksahkg fkgvdaqgtl skifklggrd srsgspmarr llggledpgh ealtgtekli
etyfsknyq dyeylinvi hafqlaegf yttgavrqi fgdykttic gkglsatvt
ggqkgrgsr gqhqahsle rvchclgkw lghpdkity wttcqsiaf psktsasig
slcadarmy gvlpwnafp gkvcgsnll sicktaefq mtfhlf
```

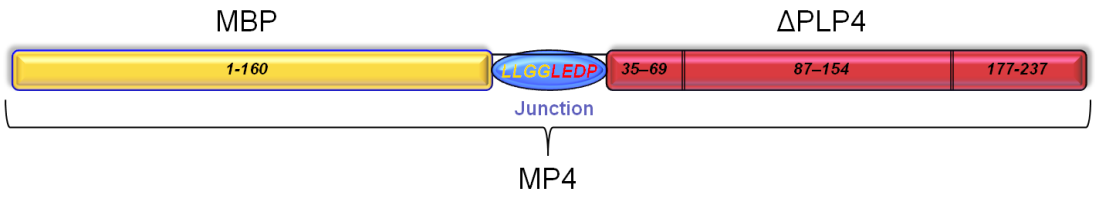

Figure 5.1 Fusion protein MP4 schematic drawing

Results:

a. Validation of the helper phage

As elution was done by trypsin digestion, I first tested the sensitivity of the helper phage to the trypsin digestion. After trypsin digestion a reduction in phage infectivity was expected with a corresponding reduction in phage titer (see also chapter1.4.2) expressed as plaque forming units/ml (pfu/ml). I observed a 10^6 fold decrease in infectivity (Fig.5.2) showing the high trypsin sensitivity of my helper phage working stocks.

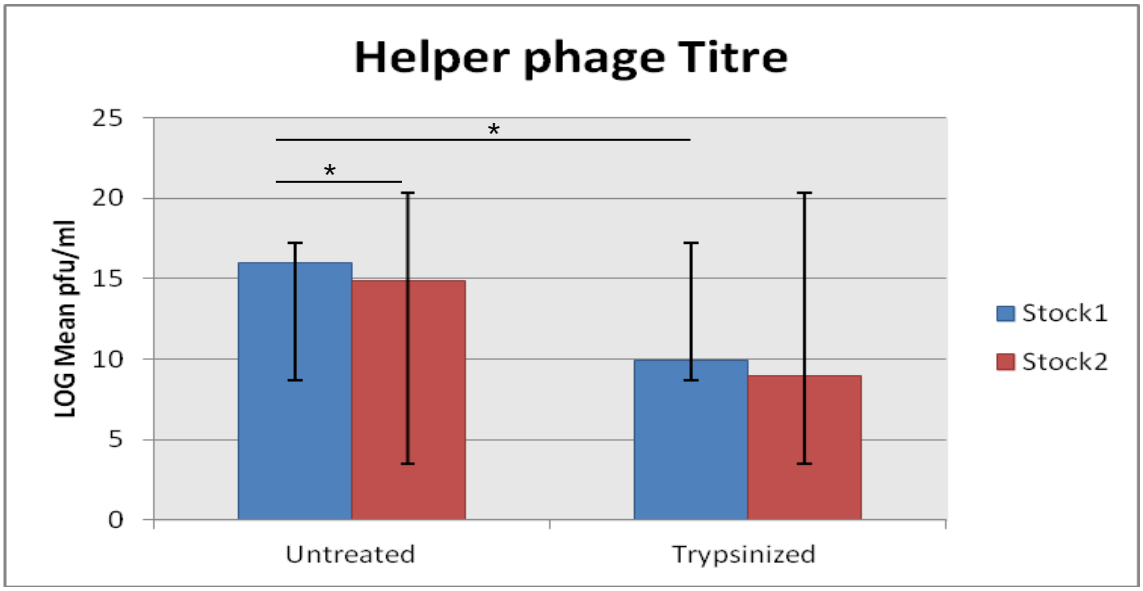

Figure 5.2 Helper phage titer: The initial stocks were labelled stock 1 and stock 2. The titers of the helper phage expressed as plaque forming units (pfu)/ml were significantly different between the untreated and treated groups. The result of the titration plates evaluated in duplicates show a decrease of 10^6 fold in both stocks after trypsin treatment. The data show mean±2SD; descriptive error bars show 2SD. *$p<0.05$ ($p=0.033$ for stock1 untreated vs treated and $p=0.039$ for comparison of the untreated stocks) (Welch's test).

Stock 1 was used to produce my own stock following the protocol as in chapter2.

b. Evaluation of proteins used for biopanning

The proteins used for biopanning and ELISAs were run by SDS-PAGE electrophoresis (Fig.5.3)

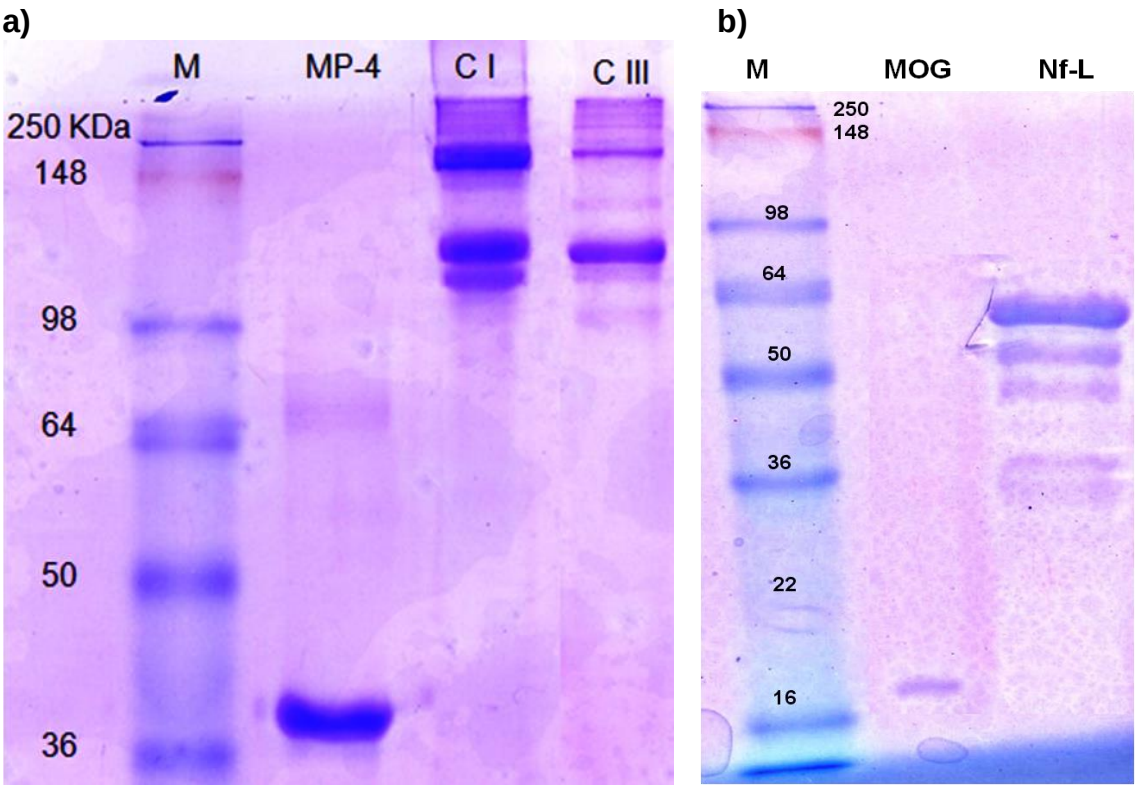

Figure 5.3 SDS-PAGE analysis of the proteins used for selections and ELISAs: Samples were combined with 4x reducing loading buffer and run in 10% SDS-PAGE gels. After separation by electrophoresis, protein bands were visualised by staining with Coomassie Blue. a) MP4 ~40 KDa fusion protein CIII ~140 KDa; b) human r-MOG_{1-125} ~14.2 kDa, Nf-L ~61 KDa (68 KDa).

c. Selection using *in house* synthetic library

C1- polyclonal phage analysis

Selection was done using antigen coated immunotubes. I performed three rounds of panning on candidate autoantigens using 10^{12}-10^{13} phage particles from the Tomlinson I library. All the antigens tested showed an increase of the eluted phage titer following each round of panning. In particular after 3 rounds of selection the library panned on rMOG resulted in a 6.4 fold titer increase although the final titer was the lowest of all other selections ($<10^4$). The panning on MP4 provided a 2 fold titer increase, on Nf-L a 33.3 fold titer increase, on CRYAB a $5x10^3$ fold titer increase and on CIII a 13 fold titer increase (Fig.5.4).

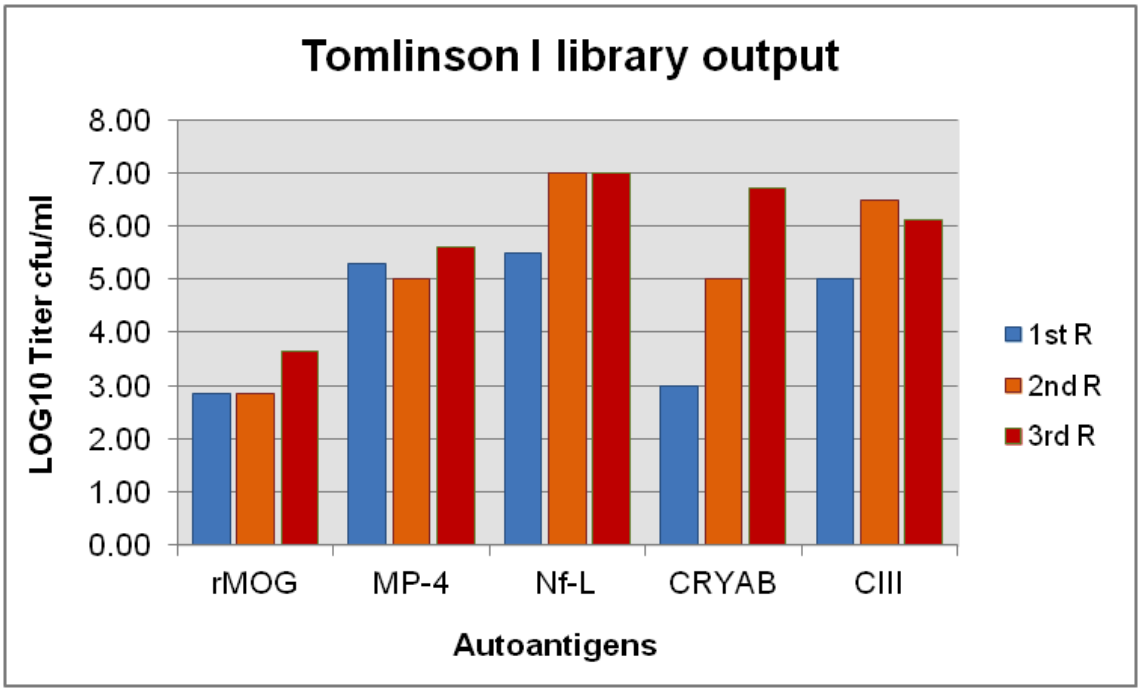

Figure 5.4 Tomlinson I library output after each round of selection: The library was biopanned on the autoantigens with very different results ranging from 2 fold (MP4) to $5x10^3$ fold (CRYAB) increase in titer after 3 rounds. The titer of the eluted phages after each round is expressed as the mean LOG10 of the number of colony forming units/ml of duplicate plates.The output of the phage titer panned on rMOG was low.

After titration the eluted phage pool was analysed by polyclonal phage ELISA

a) MP4 polyclonal phage ELISA:

It is possible that specific polyclonal phages were cross-reacting with MOG secondary to mimicry between the two proteins or multispecificity mediated by conformational diversity

a)

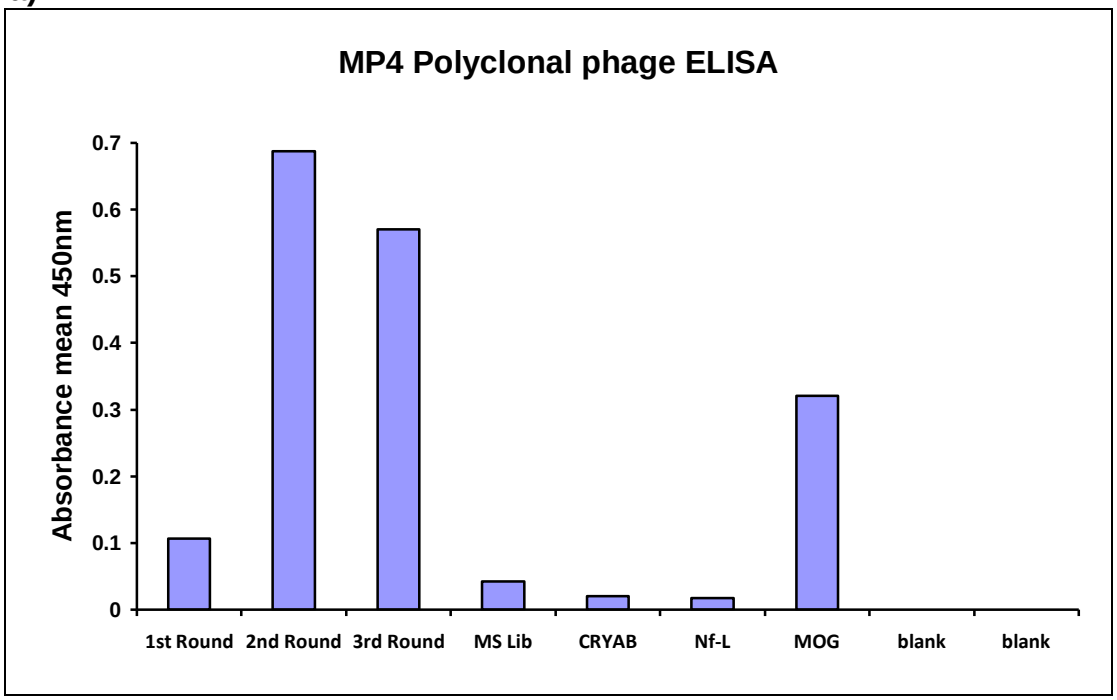

b)

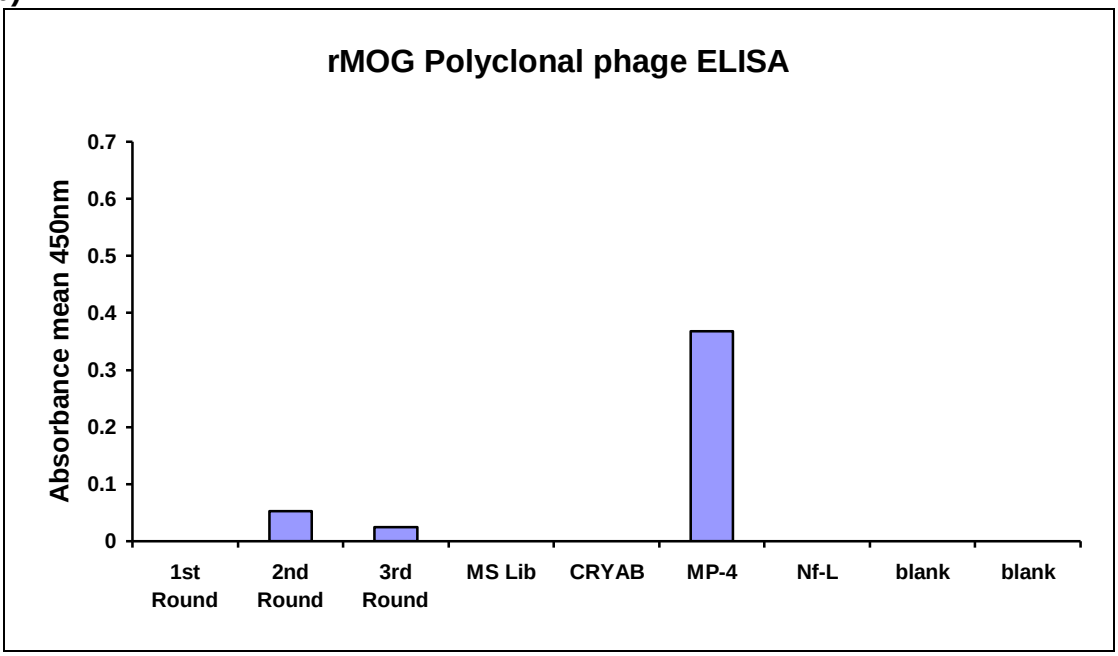
rMOG Polyclonal phage ELISA
Absorbance mean 450nm
0.7
0.6
0.5
0.4
0.3
0.2
0.1
0
1st Round
2nd Round
3rd Round
MS Lib
CRYAB
MP-4
Nf-L
blank
blank

c)

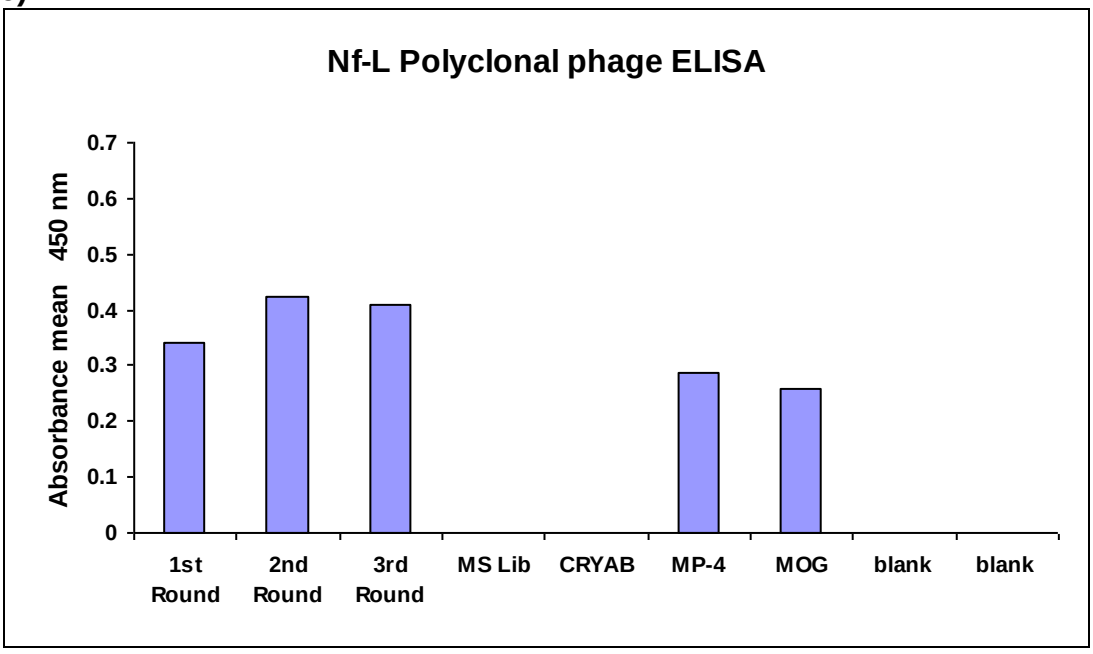
Nf-L Polyclonal phage ELISA
Absorbance mean 450 nm
0.7
0.6
0.5
0.4
0.3
0.2
0.1
0
1st Round
2nd Round
3rd Round
MS Lib
CRYAB
MP-4
MOG
blank
blank

d)

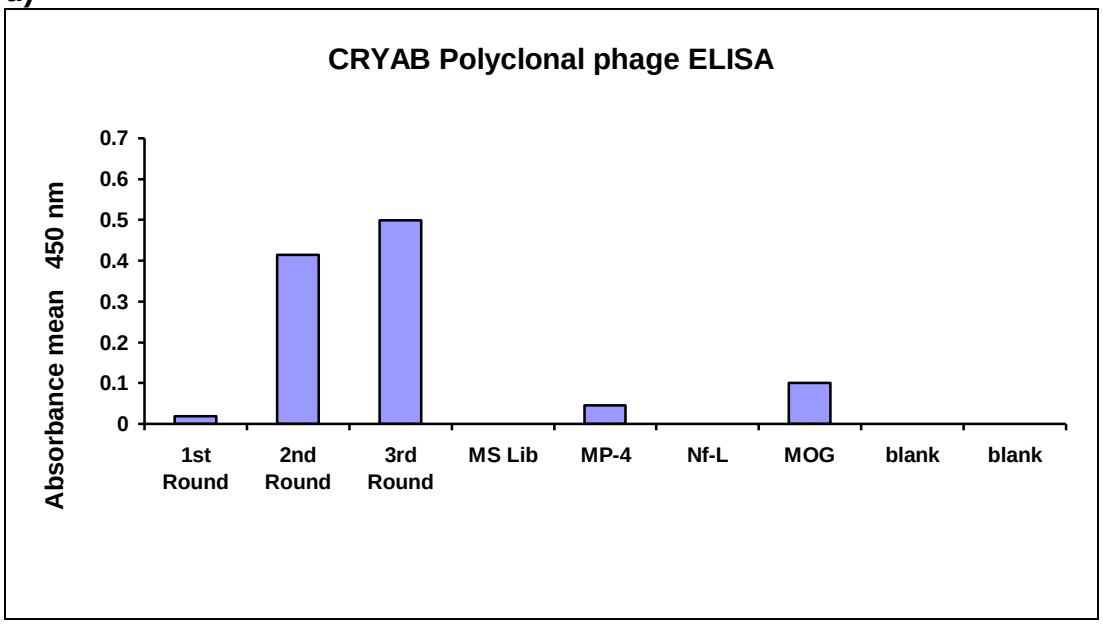

Figure 5.5 Polyclonal phage ELISAs: ELISA plates were coated with the same autoantigen used for biopanning. Binding specificity of the eluted phages was checked after each round of selection. The phage from the 3rd round was also tested for cross-reactivity. 3rd round eluted phages against MP4 and rMOG both showed reciprocal cross-reactivity in both the selections. The 3rd round eluted phage against Nf-L cross-reacted with MP4 and rMOG. No clear cross-reactivity was present for the eluted phage selected against CRYAB. The absorbance values shown were corrected for the background value. Detection of phage binders was obtained by an HRP-conjugated anti-M13 antibody.

C2-monoclonal phage ELISA

From the 3rd round individual phage antibody fragments were prepared in 96 well microtiter plates and the induced phages were used for monoclonal phage ELISA (Fig.5.7). Clones were sequenced if they showed binding, expressed as elevated O.D.450nm values.

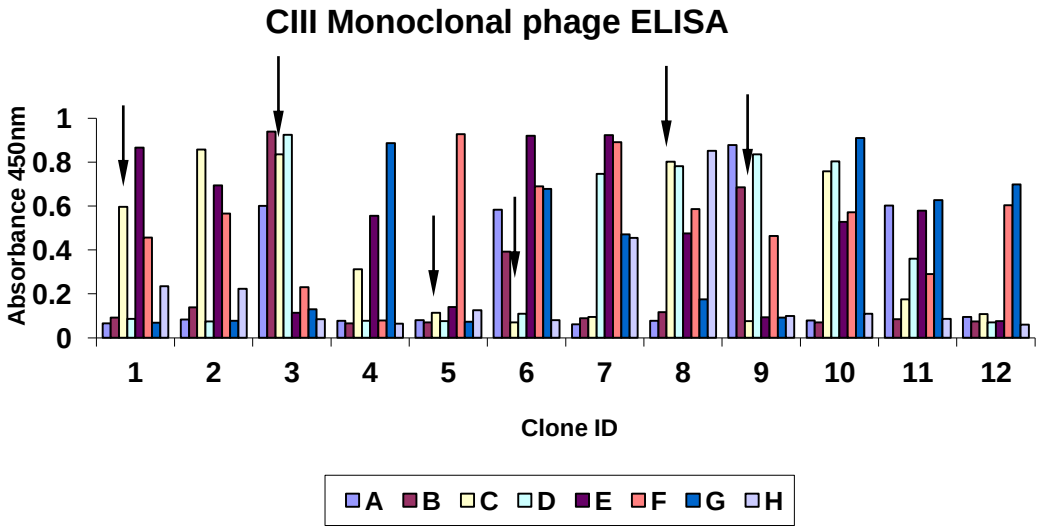

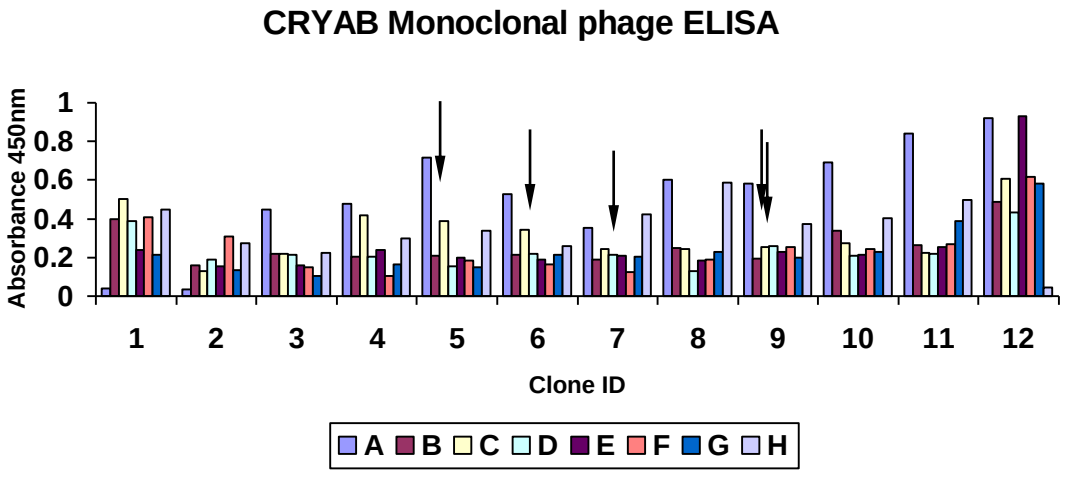

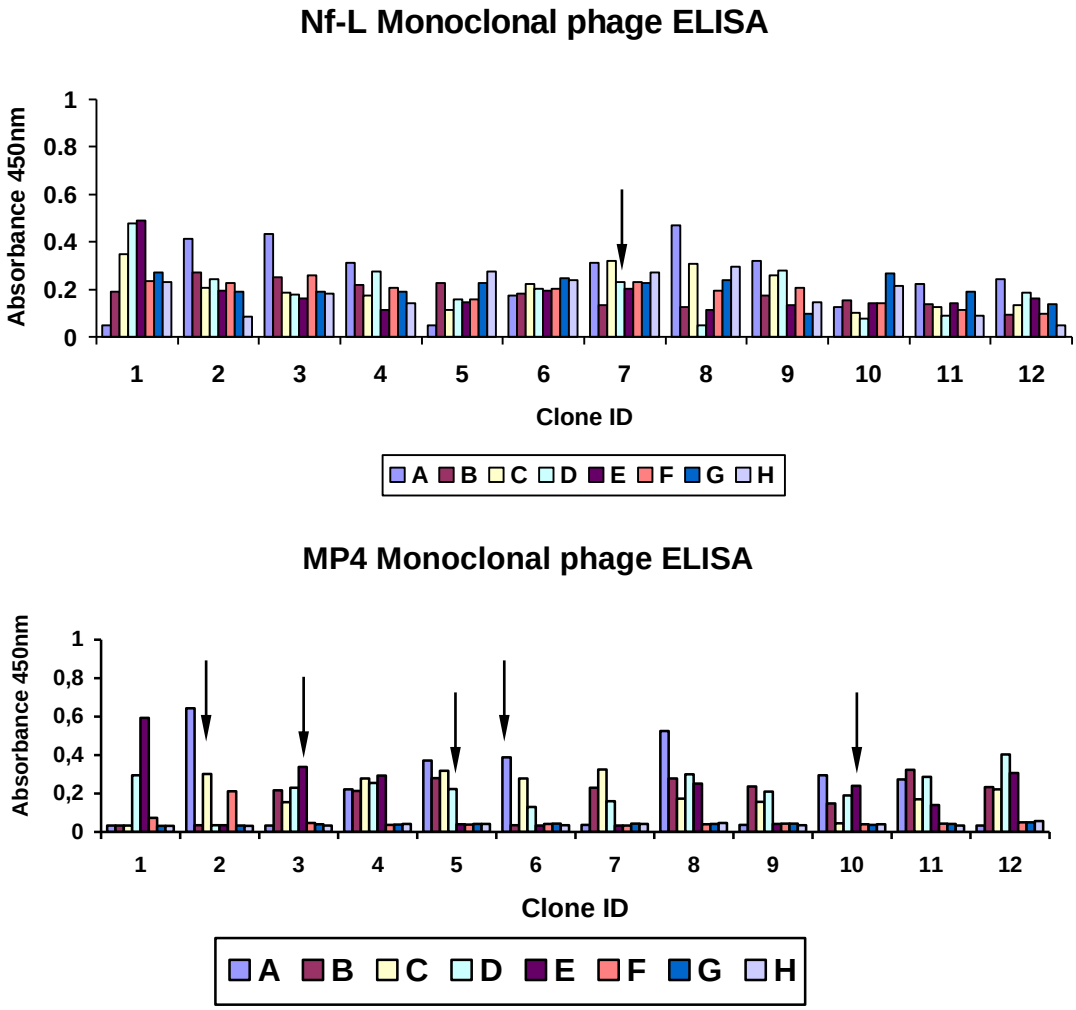

Figure 5.6 Tomlinson I library monoclonal phage ELISAs: The individual colonies from the 3rd round titration plates of CIII, CRYAB, Nf-L and MP4 were amplified in 96 wells plates and antibody phages used for ELISA. The clone ID resembles the alphanumeric position of the phage clones in the 96 well plate with numbers and colours on the X axis of the histograms. Arrows indicate the clones chosen for sequencing. Mean $O.D._{450nm}$ CIII=0.37; CRYAB=0.3; Nf-L=0.2; MP4=0.15 (control wells: A1, D6, H12)

Clones which were positive in ELISA were taken forward for sequencing. Unique sequences from each selection are shown in Table 5.1. The sequences all belonged to the VH3-23/DP47 family as expected and all the CDR3s had a slightly negative net charge (mean= -0.42 at pH=7.36) (charge=-1.3 or charge=-0.3) (Table 5.2).

Antigen	Clone	V gene	CDR3
CIII	C3	IGHV3-23*01	CAKGDATFDYW
	C5	IGHV3-23*01	CAKNYSDFDYW
	C6	IGHV3-23*01	CAKNGNTFDYW
	C8, C9	IGHV3-23*01	CAKSYSYFDYW
	C1	IGHV3-23*01	CAKTTGSFDYW
CRYAB	C6	IGHV3-23*01	CAKTSSSFDYW
	D7, B5, C9, B9	IGHV3-23*01	CAKYGTSFDYW
MP4	C2, A6, E3, E10, D5	IGHV3-23*01	CAKGAASFDYW
Nf-L	D7	IGHV3-23*05	CAKNAYAFDYW

Table 5.1 Sequences of the 3rd round clones: From the 3rd round of selection against various autoantigens individual colonies were amplified and screened by monoclonal phage ELISA. The clones with highest O.D. in the monoclonal phage ELISA were sequenced. Each autoantigen group contained 1 (MP4 antigen) or few clones.

Since selection with this library was just to validate the protein antigen as well as the selection technique I decided not to proceed for soluble ELISA with this library.

D. Selection using the newly built MS library

I compared selection using the VH only library versus the VH+VL library on MP4 as a target. The selection with the synthetic library resulted in only one unique clone for MP4. It would therefore be interesting to use MP4 as the first antigen for biopanning to see if I get more diversity of MP4 specific scFv.

Around 10^{12}-10^{13} of resuspended phage was pooled and used as input for all the rounds. The results showed a $3.8x10^{2}$-fold enrichment of the eluted phage output from the VH only library against MP4 after 3 rounds of selection. The VH+VL library presented a $4.4x10^{3}$ enrichment against MP4 (Fig.5.7).

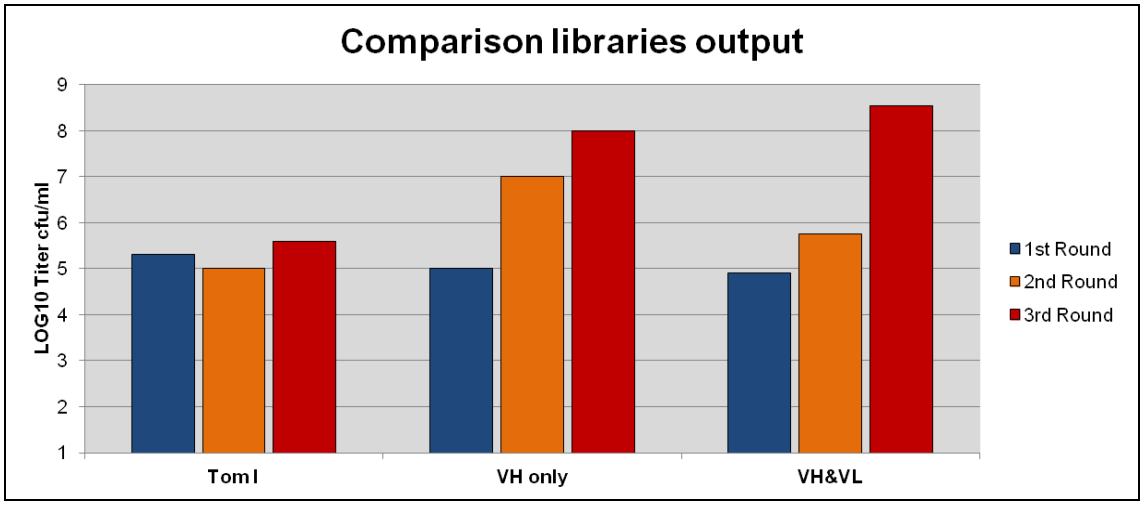

Figure 5.7 MS antibody libraries output after each round of selection: Around 10^{12}-10^{13} phage of the two libraries was used as input for each round and checked for specificity against immunotubes coated with MP4 (this protein could show eventual nonspecific binding and explain low levels of specific reactivity in the ELISA analysis). The titer of the eluted phage after each round is expressed as mean LOG10 of the number of colony forming units/ml of duplicate plates and shows increased binders' titer in each round.

As these libraries were newly built and are from patients, I firstly wanted to monitor randomly the sequence diversity of phage clones through the selection process of the VH only library on MP4 (Table 5.2).

As shown in the table sequences that appear in the first round are still present in the third round so there was a selection and enrichment process of specific clones

Round of selection	Sequence ID	V-GENE and allele	AA JUNCTION (IMGT Numbering)
1st Round	1	IGHV4-61*02	CAREYSSAWSPRYNYYNYMDVW
	2	IGHV5-51*01	CARRLCSSTSCYFGGLDWFDPW
	3	IGHV1-69*06	CARELF*QWIYYYCTLDVW
	4	IGHV3-53*01	CARGGYSYFLDYW
	5	IGHV1-8*01	CVRGQFGYCSSPSCPEYW
	6	IGHV2-5*01	CARRLSHRYCSRGSCPNWFDPW
	7	IGHV1-8*01	CVRGQFGYCSSPSCPEYW
	8	IGHV3-7*02	CALGPYW
	9	IGHV6-1*01	CARQASSGWYLSYAMDVW
2nd Round	1	IGHV3-72*01	CARDYFDSGRYFPDVW
	2	IGHV5-51*03	CARRGCSSTSCYLGLDWFDPW
	3	IGHV3-53*01	CARGGYSYFLDYW
	4	IGHV1-69*11	CARGRSGSGAFAWGPKRTFNYGLDVW
	5	IGHV1-2*02	CARDETQRPAQTWYISECDPNYFYFYGMDVW
	6	IGHV4-39*01	CVRHGGGRFYCTGGSCFSAYYFDSW
	7	IGHV2-5*01	CARRLSHRYCSRGSCPNWFDPW
	8	IGHV5-51*03	CARRGCSSTSCYLGLDWFDPW
3rd Round	1	IGHV3-72*01	CARDYFDSGRYFPDVW
	2	IGHV3-66*01	CATPRGYRAW
	3	IGHV4-61*02	CARGDYGDFFDYW
	4	IGHV5-51*03	CARRGCSSTSCYLGLDWFDPW
	5	IGHV2-5*10	CVHRPREDFWSGWDYYYGLDVW
	6	IGHV1-2*02	CARDETQRPAQTWYISECDPNYFYFYGMDVW
	7	IGHV6-1*01	CAREVRNSWYDPW
	8	IGHV1-2*02	CARDETQRPAQTWYISECDPNYFYFYGMDVW
	9	IGHV3-66*01	CATPRGYRAW
	10	IGHV2-5*01	CVHRPREDFWSGWDYYYGLDVW

Table 5.2 Enrichment on MP4 of the phage antibodies pool derived from VH only library: All the sequences resulted in frame and productive but one in the 1st round (highlighted in red), not found in the following rounds. The same sequences found in different rounds were labelled with the same background colours.

D2: polyclonal and monoclonal ELISA

The phage pool from the different rounds of selections was also analysed by polyclonal and monoclonal ELISA. The resulted mean absorbance of the pool of individual phage antibody fragments analysed by monoclonal ELISA was 2.5 fold higher in the VH+VL derived phages compared to the VH only library and 3.2 fold higher compared to the Tomlinson I derived ones. This result indicates a stronger binding for the VH+VL library fragments (Fig.5.8 and 5.9).

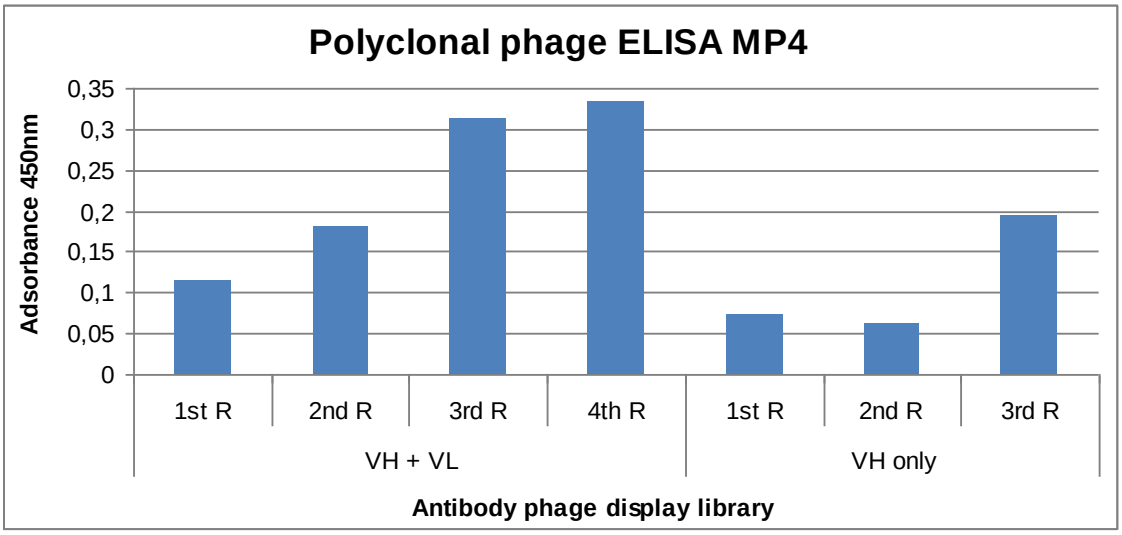

Figure 5.8 MP4 Polyclonal phage ELISA: VH only and VH+VL libraries were biopanned against immobilized MP4. Phages eluted from each round of selection were analysed for binding in polyclonal phage ELISA. An extra round of selection was performed (4th round) with VH+VL derived phage but only a weak increase in absorbance was observed indicating that 3 rounds were satisfactory for a good level of enrichment. The level of absorbance was calculated as the mean of different dilutions (1:2; 1:4, 1:8). Detection was obtained by an HRP-conjugated anti-M13.

a)

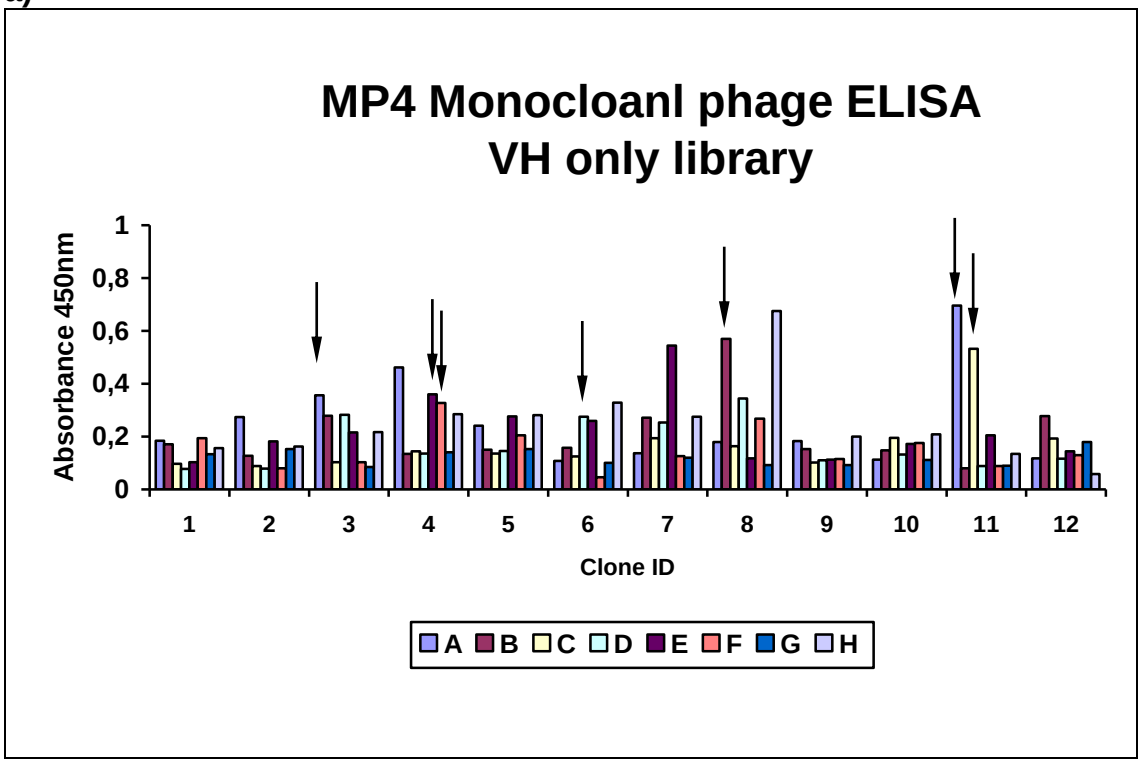

b)

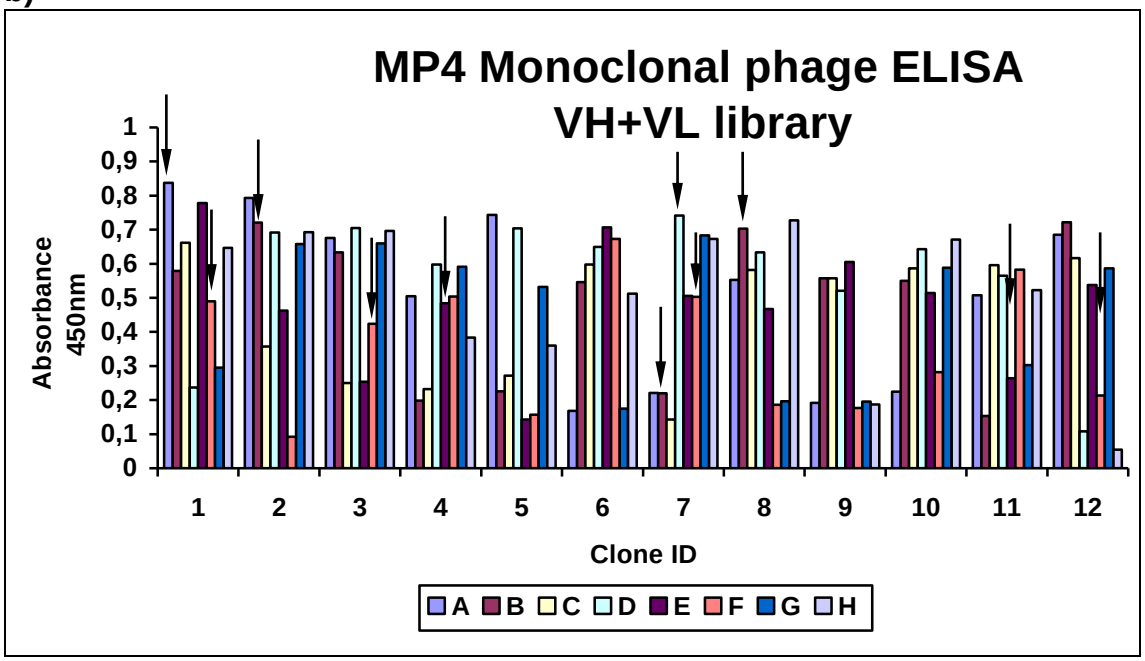

Figure 5.9 MP4 Monoclonal phage ELISAs: a) VH only library and b) VH+VL library derived phage antibody fragments analysed by monoclonal phage ELISA. The mean absorbance of the VH+VL library derived phage antibody fragments resulted in 0.48 compared with the mean absorbance of 0.19 of the VH only library derived phage antibody fragments and with the mean absorbance of 0.15 of the Tomlinson I derived phage antibody fragments.

Sequencing analysis of monoclonal phage clones

As final step in the selection I analysed the sequence of phage binders as seen by the monoclonal ELISA clones from the pool of selected phages comparing the two VH only and VH+VL libraries. To determine if the phages were derived from different or identical clones I sequenced 7 of the clones from the VH only monoclonal phage ELISA and 11 clones from the VH+VL monoclonal phage ELISA. The resulted sequences showed 3 and 7 unique clones for VH and VH+VL library, respectively (Table 5.3).

a) VH only

VH gene	N. of clones	Clones ID	CDR1	CDR2	CDR3	Light chain
IGHV2-5*10	1	HF4	GFSLSTSGVG	IFWDDDK	VHRPREDFWSGWDYYYGLDV	**(IGKV1-39*01)**
IGHV2-5*01	3	HA11, HB8, HC11	GFSLSTSGVG	SYWNDDK	VHRPREDFWSGWDYYYGLDV	
IGHV1-69*06	3	HD6, HE4, HA3	GGTFTRYA	IIPLFGTT	ARDQDADFWSIYRQYYYYGMDV	

b) VH+VL (random pairing)

	V genes	N. of clones	Clones ID	CDR1	CDR2	CDR3
VH	IGHV3-11*03	2	HLA1; HLE4	GFTFSDYY	ISSSGSYT	ARDLGRDYGLNWFDP
VL	IGLV5-45*03			SGINVAAYR	YKSDSDR	VIWHNSAWV
VH	IGHV3-11*03	2	HLB2; HLD7	GFTFSDYY	MSGNSNYT	ARNLYSSTWTGVGDY
VL	IGLV2-11*01			SSDVGGFDY	DVS	CAYAGSDTYV
VH	IGHV1-69*01	1	HLB7	GGSFSSDF	IIPLFGTP	ARSPISYYNSGSYFDL
VL	IGKV4-1*01			QSVLNSSNNKNY	WAS	QQYYSSLLT
VH	IGHV3-23*04	5	HLB8; HLE11; HLF1; HLF7; HLF12	GFALNNFI	ITESGNI	VPRRTASWFDP
VL	IGLV1-51*01			SSNIGNAY	DNN	GTWDSSLSV
VH	IGHV3-23*04	1	HLF3	GFALNNFI	ITESGNI	VPRRTASWFDP
VL	IGLV1-51*01			QSVFYMSHNKNS	WAS	QQYYTTPFT

Table 5.3 Sequences from the 3rd round of selection of VH only and 4th round of VH+VL libraries: Clones from the last round of selection with high absorbance cut-off were analysed. 7 colonies for the VH only library and 11 colonies for VH+VL library were selected. The analysis of the sequences revealed 3 different clones in the VH only library and 5 clones in the VH+VL library.

In summary the MS library may represent a better source of MP4 specific antibodies:

a) The 3 rounds of selection performed with the synthetic library on MP4 show only a 2 fold increase of titer compared with a 10^2 and 10^3 increase in titer respectively of VH only and VH+VL MS biased libraries respectively.

b) In the polyclonal ELISA I saw an increase in level of absorbance from the 1st to the 3rd round. Although the synthetic library had higher polyclonal ELISA O.D the sequence implied that only one clone was enriched. In addition, the monoclonal ELISA showed 88% of binders (O.D.>0.2) in the VH+VL library compared to 42% in the synthetic library. The average O.D. of the monoclonal ELISA wells was 0.14 in the synthetic library compared to 0.47 in the VH+VL library. Furthermore, I observed at least 7 unique clones in the VH+VL library while in the synthetic library I identified only one sequence.

Chapter discussion

An important question raised from the presence of lymphoid aggregates: what is the Ag(s) targeted in the enrichment of the B cells carrying auto-reactive specific receptors found in the aggregates? The study of B cells specificities via biopanning of the library resulted in isolation of target-specific antibody fragments to known MS autoantigens, thus indicating that VH-VL pairing was functional and possibly resembled the in vivo pairing. In fact, the presence of OCBs in the CSF of MS patients and their relation with B cells infiltrating the brain tissue imply a specific immune response restricted to the CNS and raised against persistent epitopes. Attempts to identify the specificity of the CSF antibodies using a faithful pairing of VH and VL derived from CSF B cells during different stages of the disease via the production of recombinant mAbs showed myelin staining at the edge of demyelinating lesions but no reactivity was demonstrated against the expected myelin antigens such as MOG, PLP or MBP (Owens et al. 2009; Von Budingen et al. 2008). The panel of recombinant mAbs expressed in my library could be representative of the whole antibody repertoire in the patients analysed. If this is the case, the pooled antibody phage display

strategy used in my study increases the viability of antibody specificities from MS patients that can be analysed at the same time. But it is not possible to exclude that other autoantigens play an important role in MS pathogenesis supporting the view that each patient could develop an his/her own autoreactivity against CNS antigens. Nevertheless, the specificity of the antibodies in MS patient is still an open debate as MBP specific antibodies were found in another study analysing the CSF B cell specificity from RRMS patients as Fab fragments (Lambracht-Washington et al. 2007). These results have been supported also from the results of a study using a phage display library of scFvs constructed from blood B cells of RRMS patients that showed clones selected against MBP (Gabibov et al. 2011). Both latter studies have shown that the antibodies studied were polyreactive. In my study the VH+VL library panned on MP4 resulted in binders specific for myelin antigens that could correspond to natural autoantibodies from progressive MS patients even though with the limitations imposed by the random pairing of VH and VL from different patients. The fusion protein MP4 used for selection using my libraries raised different specific binders which may further be characterised for their specific target epitope(s).

Chapter 6: Discussion

MS is a chronic inflammatory autoimmune disease with involvement of different immune cells in the pathogenesis targeting the brain of PwMS. Identification of the causative agent of MS was the aim of many studies but, so far, no specific trigger agent(s) has been uncovered. The presence of immune cells infiltrating the brain tissue points to an ongoing autoimmune reactivity of some type. In a subset of secondary progressive cases of MS (40%) the infiltrated immune cells tend to organize themselves in aggregates resembling lymph nodal follicles. Follicle-like aggregates were described in the meninges along and in depth of cerebral sulci mainly of the temporal, cingulate, insula and frontal cortex (Howell et al. 2011; Magliozzi et al. 2004; Magliozzi et al. 2007).

- Lymphoid network

In my work follicle-like aggregates were detected not only in secondary progressive but also in primary progressive cases. The location of the lymphoid aggregates was meningeal in frontal and temporal lobes but also in the deep grey matter at level of the thalamus and internal capsule. My findings show a diffuse involvement of the brain not only at cortical level with presence of lymphoid neogenesis in the progressive forms of MS. The areas touched by the CSF could be the main sites where the immune cells can organize themselves and aggregate. The tissues used for the library construction were analysed by qPCR and stable reference genes were determined. The lymphoid infiltrates and aggregates found in my samples, however, are being currently characterized by measuring inflammatory and germinal centre cytokines expression levels.

- Library construction and analysis

The novelty of the phage display technique is the link between the displayed proteins and their coding genes. Different antigen and antibody phage display libraries were built with the intent to reproduce and analyse the variety of the possible target antigens and specific functional reactive antibodies in numerous

systemic and organ specific autoimmune as well as in infectious diseases. In fact, the use of the phage display technology in infectious diseases of the nervous system facilitated the identification of the causative agent that triggers the specific humoral immune response. Panning of phage display Ag library built from SSPE brain identify the measles virus (MV) epitope recognised by the natural antibodies extracted from the infected brain (Burgoon et al. 2001; Owens et al. 1997). Similarly in VZV vasculopathy the CSF OCBs react specifically with VZV antigens (Burgoon et al. 2003). The mentioned studies demonstrated that the natural Igs found in patients affected by infectious diseases are reactive specifically against the viral agent involved. At the same time the Igs sequences expressed in SSPE brain were analysed and showed reduced identity with their closest germline and high R/S ratio in their CDRs as result of affinity maturation and pointing to an Ag-driven response. The same SSPE brain derived Ig sequences were cloned and functional transfectoma-derived monoclonal antibodies have been obtained confirming the high specificity against their corresponding disease related MV Ags (Burgoon et al. 1999).

- Restricted VH and VL usage

Numerous studies have described an Ag-driven response also in autoimmune diseases. Reviewing the past literature regarding the cells producing antibody in brain and CSF of MS patients, it has been shown that the VH genes from the cells infiltrating the brain and found at CSF level have the same molecular features of an Ag-driven response characterized by presence of somatic mutations, CDRs increased R/S mutations ratio and restricted use of VH family germlines. A skewed VH family usage pattern has been described and confirmed by different studies analysing the V genes CSF repertoire. The analysis of V genes derived from different B cells populations (CD19+ and CD138+) from CSF of MS patients with different forms of disease has shown a consistent VH4 family bias (Owens et al. 2007; Qin et al. 1998). The altered distribution of the VH family usage has been described to be already detectable after the first clinical presentation and strongly correlates with conversion to MS in the next 6 months (Bennett et al. 2008). The skewed VH gene family usage

and in some studies even the same segments have been described analysing the repertoire of the B cells infiltrating all the brain areas, including meninges, plaques, NAWM and CSF (Baranzini et al. 1999; Lovato et al. 2011). Striking usage (60%) of the VH4 family was described in a MS brain with acute plaques and half of the different VH4 sequences being represented by the VH4-39 segment (Owens et al. 1998). In my analysis of V genes derived from B cells infiltrating the brain tissue of a pool of 14 MS cases, I found significantly different VH1 (30%) and VH2 (9%) family usage compared with PBL of adult healthy individuals (respectively 22% and 4%), but no biased VH4 usage was observed (20% MS pool vs 22% for the healthy controls). My data differ from the previously reported literature but an increased usage of VH1 and VH2 families has also been described. In fact, it was shown that not only the VH4 but also the VH2 family in one-third of cases is biased (Bennett et al. 2008). A patient specific VH biased immune response was identified also in a NMO brain with the VH2 family resulting overrepresented (Owens et al. 2001). Furthermore, my results are consistent with another study highlighting an increase in VH1 and VH4 usage, specifically of VH1-69, VH4-34 and VH4-39 (Baranzini et al. 1999). My data derive from 14 MS cases pooled and the results obtained derive from a mixture of patient specific VH bias. Consistent with my data the results of a study describing a unique skewed repertoire in the brains of MS and SSPE patients, confirming the common Ag-driven response in both the diseases (Smith-Jensen et al. 2000). Nevertheless, it should be considered that may be the number of sequences analysed were not enough to show the real pattern and analysis of a larger number of sequences before cloning could be ideal to this purpose. No peripheral blood from the same patients was available for analysis and it has not been possible to confirm that the biased detected family usage was restricted to the brain. The analysis of the D showed a broad utilization, with 80% D segments represented, and confirming previous literature data of overuse of specific D segments (D3-22, D2-2, D3-3 and D6-13 constituted ~45% of the D segments) in MS (Baranzini et al. 1999) as well as in the general population (!!! INVALID CITATION !!!). Similarly, the analysis of the JH segment usage highlighted a significant over-representation of the JH4 family compared with the expected germline frequencies (MS pool vs expected

germline JH usage: p=7E-20). The over-representation of JH4 has already been described in other autoimmune diseases, in MS and in healthy individuals (Baranzini et al. 1999). Hence the results found for D and JH highlight a bias not related to the specific immune response but to molecular mechanisms. In the analysis of the light chains was found an abnormal k/λ light-chain ratio as previously described in the MS literature (Jenkins et al. 2001), but the low number of sequences analysed does not allow to evaluate properly the entity of this finding in the brain. Among the kappa families Vk2, Vk4 and Vk5 were the most represented. The Vk3 family, usually constituting more than 50% of the kappa adult healthy individual repertoire, was not found in my repertoire. Among the lambda families Vλ6 represented more than the 50% of the sequences analysed. The usage of the light chains families confirm a restricted family usage.

- Somatic hypermutation analysis

Once activated by the target antigen the immunoglobulin loci of the B cells undergo mutations at an extremely high rate compared to most somatic cells to improve the antigen binding of the receptor. The mentioned mechanism known as hypermutation occurs typically in strategic positions that are away from residues essential for V gene folding (cold spots) within FRs and preferring residues that give an advantage in affinity maturation (hot spots) within the CDRs (Jolly et al. 1996). The presence of mutations in FRs and CDRs was evaluated and the number of replacement mutations in the CDRs resulted significantly higher than in the FRs ($p \leq 0.001$). Typically germinal centres B cells present somatically hypermutated V genes and the presence of this molecular event in B cells obtained from MS brain tissue is consistent with the described presence of ectopic germinal centre-like reactions occurring in the CNS of MS patients behaving as a germinal centre-like environment (Corcione et al. 2004; Serafini et al. 2004). The overall and replacement mutations identified in the study had the typical molecular characteristic of a GC reaction with high mutational frequencies targeting the CDRs but presented as well no difference in the mutational targeting of the classical RGYW/WRCY motifs suggesting an independent clonal expansion from the classical GCs. The results confirm the

hypothesis that brain of MS patients could represent an immunological niche where B cells, GC-derived, undergo an upregulation of recombination activating genes (RAGs) and atypical mutations process that do not target the RGYW/WRCY motifs. Thus indicating that MS brain's GC-like reactions are not classical ones (Monson et al. 2005).

In the early phases of B cell development the majority of antibody produced are self-reactive and display long and positively charged VH CDR3 (Wardemann et al. 2003). The same characteristics were described in MS and other autoimmune diseases. The VH CDR3 from the pool analysed showed a length > 15 aa consistent with autoreactive B cells but a charge composition similar to mature B cells. My data are consistent with the data previously reported in MS (Harp et al. 2007).

From a diagnostic point of view the analysis of the mutations in the B cell population V genes was proposed as potential marker for disease conversion from CIS to CDMS. The targeting of particular residues in the general affinity maturation concept can be narrowed to the possibility of finding cold spots and hot spots in a specific antigen response as in different infectious disease and in MS. The described prevalence of VH4 usage in patients with MS has induced to search a possible marker of definite MS conversion in CIS patients. A unique pattern was shown from the mutation analysis of VH4 genes in MS rearranged sequences derived from CSF B cells compared with peripheral blood ones from healthy controls. The unique pattern of mutations in VH4 genes recognizes 8 hot spots and 4 cold spots depending on the frequency of replacement mutations in the codons considered and the higher or lower frequency compared with that of the B cells from the blood. The predictivity of this signature was explored in CIS patients with the possibility to identify the ones that would convert to clinically defined MS within 5-18 months from their first demyelinating event and identifying the antigen specificity of the antibodies derived from the CSF B cells signature-enriched may reveal antigens involved in the initiation of the humoral response (Cameron et al. 2009). The analysis of VH family usage in my repertoire did not highlight a VH4 bias and the analysis

of the mutation frequencies in the VH4 sequences did not show differences between hot and cold spots.

- Clonal expansion

Another aspect of the antigen-driven immune response is the clonal expansion. The presence of CSF OCBs, a diagnostic hallmark of MS, is the result of the B cells clonal expansion present in the CNS of patients with MS. Numerous studies have described the overlap of CSF proteome and IgG transcriptomes from B cells at different levels such as CSF, brain parenchyma and meningeal aggregates (Obermeier et al. 2011; Obermeier et al. 2008). After CSF analysis the isoelectrically focused proteins, visualized as oligoclonal bands, are the result of antibody producing cells clonally expanded, with a B cell clone defined as 2 or more single B cells from the same donor having the same heavy and light chain rearrangements resulting in an identical amino acid sequence of the CDR3 region (Harp et al. 2007; Owens et al. 2003). Confirmation of identity between oligoclonal bands and antibodies produced by B cell clones was given by studies utilizing monoclonal antibodies derived from these cells (Von Budingen et al. 2008) and from studies applying rabbit anti-idiotypic antibodies against clonally expanded plasma cells antibodies able to recognize specific VH-CDR3 idiotopes and at the same time able to cross-react with OCBs (Von Budingen et al. 2010). Different studies have further confirmed that the B-cell clones producing the immunoglobulins found in the CSF travel among different brain anatomical areas such as parenchymal infiltrates, extraparenchymal lymphoid tissue aggregates and CSF directing their products against brain tissue constituents (Lovato et al. 2011; Obermeier et al. 2011). In my study the related sequences identified in clonal populations were 10 out of 46 sequences analysed. My cases were progressive MS and I would expect to see clonal expansion. This was previously described IgG repertoire of MS CSF B cells population, especially in late phases, but not in IgM (Owens et al. 2003). My repertoire was composed of IgM and IgG derived sequences and did not allow us a precise differentiation of the two isotype derived repertoires.

- Selection

In the second phase of my study I used the built antibody phage display MS libraries for selection against MP4. MP4 is a fusion protein presenting multiple epitopes from MBP and PLP. In the animal model MP4 reactive serum transferred in MP4-immunized B cell deficient mice induce EAE showing a pathogenic role for the auto-Abs (Kuerten et al. 2011). In PwMS auto-reactivity to MBP and PLP have been shown in matched serum and CSF with patient-specific specificity (Quintana et al. 2012). In my study I was able to raise anti-MP4 specific antibody fragments using either VH or VH+VL MS library. The VH library was paired with synthetic VL so I did not expect it to resemble the natural antigen driven selection. Although the VH+VL was built from the natural repertoire only, the combined VH and VL might not be identical to the natural auto-antibodies as I did not build the library by single cell PCR approach. Nevertheless, I could see Ag driven selection as VH3 was predominant in the anti-MP4 clones raised rather than VH2 and VH1 in the library. The number of clones analysed was too small to assess clonal expansion. In addition, it was quite obvious that the VH+VL library performed better than the VH and the synthetic library: a) much higher increase in titer (10^3 fold enrichment of the VH+VL library vs 10^2 and 2 fold enrichment) and b) diversity of selected clones.

Summary

In this project I was able to build an antibody phage display library from B cells infiltrating the brain of progressive MS patients. The library was a single-pot human scFv library built from IgG and IgM repertoire. The analysis of the repertoire cloned in the library did show a biased usage of the VH and VL family germlines. The most represented VH families were the VH1 and VH2. The VH4 family was reported to be the most represented one in PwMS from the past literature. Finding not confirmed in my analysis. Presence of an antigen driven immune response was confirmed. Furthermore I did build an intermediate VH only library from the same repertoire. Both the libraries were screened against MP4, a fusion protein containing epitopes of MBP and PLP. As comparison a synthetic library, Tomlinson I, was used an screened against the same antigen. Different level of enrichment were present in the libraries screened with the

VH+VL library presenting the highest affinity binders. The possibility of pairing, even if randomly, the VH and VL could have given a binding advantage to this library. The clones identified in the library could resemble what happens in the patients and support the presence of autoantibodies against MBP or PLP epitopes involved in MS pathogenesis.

Further work

The antigenic target of the OCBs and the target responsible for MS onset have yet to be established. The possibility to build antibody phage display libraries directly from the B cells infiltrating the target organ, the brain, of the immune response could lead to identify such targets and help to develop diagnostic means and therapeutics. An individual differentiation of the repertoire cloned and an increase of the library diversity by increasing the number of patients' repertoires could delineate a better view of the antigens involved in the pathogenic process. The possibility to identify and dissect specific B cells could improve further the characterization of the immune process. The comparison of the organ specific with peripheral blood libraries could help to find useful biomarkers for disease progression. Furthermore the possibility to compare progressive form with acute form of disease could further elucidate the timing of the immune response. The present work is just the tip of an iceberg of possibilities that I would like to explore.

References

(!!! INVALID CITATION !!!).

Allen C. D., Ansel K. M., Low C., Lesley R., Tamamura H., Fujii N. and Cyster J. G. (2004). Germinal center dark and light zone organization is mediated by CXCR4 and CXCR5. *Nat Immunol* **5**,943-52.

Allen C. D., Okada T. and Cyster J. G. (2007). Germinal-center organization and cellular dynamics. *Immunity* **27**,190-202.

Aloisi F., Columba-Cabezas S., Franciotta D., Rosicarelli B., Magliozzi R., Reynolds R., Ambrosini E., Coccia E., Salvetti M. and Serafini B. (2008). Lymphoid chemokines in chronic neuroinflammation. *J Neuroimmunol* **198**,106-12.

Aloisi F. and Pujol-Borrell R. (2006). Lymphoid neogenesis in chronic inflammatory diseases. *Nat Rev Immunol* **6**,205-17.

Alotaibi S., Kennedy J., Tellier R., Stephens D. and Banwell B. (2004). Epstein-Barr virus in pediatric multiple sclerosis. *JAMA* **291**,1875-9.

Alt F. W., Yancopoulos G. D., Blackwell T. K., Wood C., Thomas E., Boss M., Coffman R., Rosenberg N., Tonegawa S. and Baltimore D. (1984). Ordered rearrangement of immunoglobulin heavy chain variable region segments. *EMBO J* **3**,1209-19.

Andersen C. L., Jensen J. L. and Orntoft T. F. (2004). Normalization of real-time quantitative reverse transcription-PCR data: a model-based variance estimation approach to identify genes suited for normalization, applied to bladder and colon cancer data sets. *Cancer Res* **64**,5245-50.

Andersson M., Alvarez-Cermeno J., Bernardi G., Cogato I., Fredman P., Frederiksen J., Fredrikson S., Gallo P., Grimaldi L. M., Gronning M. et al. (1994). Cerebrospinal fluid in the diagnosis of multiple sclerosis: a consensus report. *J Neurol Neurosurg Psychiatry* **57**,897-902.

Aravalli R. N., Peterson P. K. and Lokensgard J. R. (2007). Toll-like receptors in defense and damage of the central nervous system. *J Neuroimmune Pharmacol* **2**,297-312.

Archelos J. J., Trotter J., Previtali S., Weissbrich B., Toyka K. V. and Hartung H. P. (1998). Isolation and characterization of an oligodendrocyte precursor-derived B-cell epitope in multiple sclerosis. *Ann Neurol* **43**,15-24.

Arnadottir T., Reunanen M. and Salmi A. (1982). Intrathecal synthesis of virus antibodies in multiple sclerosis patients. *Infect Immun* **38**,399-407.

Ascherio A. and Munger K. L. (2007a). Environmental risk factors for multiple sclerosis. Part I: the role of infection. *Ann Neurol* **61**,288-99.

Ascherio A. and Munger K. L. (2007b). Environmental risk factors for multiple sclerosis. Part II: Noninfectious factors. *Ann Neurol* **61**,504-13.

Atz M., Walsh D., Cartagena P., Li J., Evans S., Choudary P., Overman K., Stein R., Tomita H., Potkin S. et al. (2007). Methodological considerations for gene expression profiling of human brain. *J Neurosci Methods* **163**,295-309.

Babbe H., Roers A., Waisman A., Lassmann H., Goebels N., Hohlfeld R., Friese M., Schroder R., Deckert M., Schmidt S. et al. (2000). Clonal expansions of CD8(+) T cells dominate the T cell infiltrate in active multiple sclerosis

lesions as shown by micromanipulation and single cell polymerase chain reaction. *J Exp Med* **192**,393-404.

Bajramovic J. J., Plomp A. C., Goes Av, Koevoets C., Newcombe J., Cuzner M. L. and van Noort J. M. (2000). Presentation of alpha B-crystallin to T cells in active multiple sclerosis lesions: an early event following inflammatory demyelination. *J Immunol* **164**,4359-66.

Baker D., O'Neill J. K., Gschmeissner S. E., Wilcox C. E., Butter C. and Turk J. L. (1990). Induction of chronic relapsing experimental allergic encephalomyelitis in Biozzi mice. *J Neuroimmunol* **28**,261-70.

Ballenthin P. A. and Gardinier M. V. (1996). Myelin/oligodendrocyte glycoprotein is alternatively spliced in humans but not mice. *J Neurosci Res* **46**,271-81.

Banwell B., Krupp L., Kennedy J., Tellier R., Tenembaum S., Ness J., Belman A., Boiko A., Bykova O., Waubant E. et al. (2007). Clinical features and viral serologies in children with multiple sclerosis: a multinational observational study. *Lancet Neurol* **6**,773-81.

Bar-Or A., Calabresi P. A., Arnold D., Markowitz C., Shafer S., Kasper L. H., Waubant E., Gazda S., Fox R. J., Panzara M. et al. (2008). Rituximab in relapsing-remitting multiple sclerosis: a 72-week, open-label, phase I trial. *Ann Neurol* **63**,395-400.

Bar-Or A., Fawaz L., Fan B., Darlington P. J., Rieger A., Ghorayeb C., Calabresi P. A., Waubant E., Hauser S. L., Zhang J. et al. (2010). Abnormal B-cell cytokine responses a trigger of T-cell-mediated disease in MS? *Ann Neurol* **67**,452-61.

Baranzini S. E., Jeong M. C., Butunoi C., Murray R. S., Bernard C. C. and Oksenberg J. R. (1999). B cell repertoire diversity and clonal expansion in multiple sclerosis brain lesions. *J Immunol* **163**,5133-44.

Barbas C. F., 3rd, Bjorling E., Chiodi F., Dunlop N., Cababa D., Jones T. M., Zebedee S. L., Persson M. A., Nara P. L., Norrby E. et al. (1992). Recombinant human Fab fragments neutralize human type 1 immunodeficiency virus in vitro. *Proc Natl Acad Sci U S A* **89**,9339-43.

Barbas C. F., 3rd, Hu D., Dunlop N., Sawyer L., Cababa D., Hendry R. M., Nara P. L. and Burton D. R. (1994). In vitro evolution of a neutralizing human antibody to human immunodeficiency virus type 1 to enhance affinity and broaden strain cross-reactivity. *Proc Natl Acad Sci U S A* **91**,3809-13.

Barbie V. and Lefranc M. P. (1998). The human immunoglobulin kappa variable (IGKV) genes and joining (IGKJ) segments. *Exp Clin Immunogenet* **15**,171-83.

Barkhof F. and van Walderveen M. (1999). Characterization of tissue damage in multiple sclerosis by nuclear magnetic resonance. *Philos Trans R Soc Lond B Biol Sci* **354**,1675-86.

Barnett M. H. and Prineas J. W. (2004). Relapsing and remitting multiple sclerosis: pathology of the newly forming lesion. *Ann Neurol* **55**,458-68.

Barnett M. H. and Sutton I. (2006). The pathology of multiple sclerosis: a paradigm shift. *Curr Opin Neurol* **19**,242-7.

Barone F., Bombardieri M., Rosado M. M., Morgan P. R., Challacombe S. J., De Vita S., Carsetti R., Spencer J., Valesini G. and Pitzalis C. (2008). CXCL13, CCL21, and CXCL12 expression in salivary glands of patients

with Sjogren's syndrome and MALT lymphoma: association with reactive and malignant areas of lymphoid organization. *J Immunol* **180**,5130-40.

Bartos A., Fialova L., Soukupova J., Kukal J., Malbohan I. and Pitha J. (2007). Antibodies against light neurofilaments in multiple sclerosis patients. *Acta Neurol Scand* **116**,100-7.

Barun B. and Bar-Or A. (2012). Treatment of multiple sclerosis with anti-CD20 antibodies. *Clin Immunol* **142**,31-7.

Ben-Hur T., Abramsky O. and River Y. (1996). The clinical significance of a single abnormal immunoglobulin band in cerebrospinal fluid electrophoresis. *J Neurol Sci* **136**,159-61.

Bennett J. L., Haubold K., Ritchie A. M., Edwards S. J., Burgoon M., Shearer A. J., Gilden D. H. and Owens G. P. (2008). CSF IgG heavy-chain bias in patients at the time of a clinically isolated syndrome. *J Neuroimmunol* **199**,126-32.

Berger T., Rubner P., Schautzer F., Egg R., Ulmer H., Mayringer I., Dilitz E., Deisenhammer F. and Reindl M. (2003). Antimyelin antibodies as a predictor of clinically definite multiple sclerosis after a first demyelinating event. *N Engl J Med* **349**,139-45.

Bielekova B., Sung M. H., Kadom N., Simon R., McFarland H. and Martin R. (2004). Expansion and functional relevance of high-avidity myelin-specific CD4+ T cells in multiple sclerosis. *J Immunol* **172**,3893-904.

Bitsch A., Schuchardt J., Bunkowski S., Kuhlmann T. and Bruck W. (2000). Acute axonal injury in multiple sclerosis. Correlation with demyelination and inflammation. *Brain* **123 (Pt 6)**,1174-83.

Bo L., Vedeler C. A., Nyland H. I., Trapp B. D. and Mork S. J. (2003). Subpial demyelination in the cerebral cortex of multiple sclerosis patients. *J Neuropathol Exp Neurol* **62**,723-32.

Boggs J. M. (2006). Myelin basic protein: a multifunctional protein. *Cell Mol Life Sci* **63**,1945-61.

Bombardieri M., Barone F., Humby F., Kelly S., McGurk M., Morgan P., Challacombe S., De Vita S., Valesini G., Spencer J. et al. (2007). Activation-induced cytidine deaminase expression in follicular dendritic cell networks and interfollicular large B cells supports functionality of ectopic lymphoid neogenesis in autoimmune sialoadenitis and MALT lymphoma in Sjogren's syndrome. *J Immunol* **179**,4929-38.

Boppana S., Huang H., Ito K. and Dhib-Jalbut S. (2011). Immunologic aspects of multiple sclerosis. *Mt Sinai J Med* **78**,207-20.

Boulianne B., Porfilio E. A., Pikor N. and Gommerman J. L. (2012). Lymphotoxin-sensitive microenvironments in homeostasis and inflammation. *Front Immunol* **3**,243.

Boyd S. D., Gaeta B. A., Jackson K. J., Fire A. Z., Marshall E. L., Merker J. D., Maniar J. M., Zhang L. N., Sahaf B., Jones C. D. et al. (2010). Individual variation in the germline Ig gene repertoire inferred from variable region gene rearrangements. *J Immunol* **184**,6986-92.

Bradshaw E. M., Orihuela A., McArdel S. L., Salajegheh M., Amato A. A., Hafler D. A., Greenberg S. A. and O'Connor K. C. (2007). A local antigen-driven humoral response is present in the inflammatory myopathies. *J Immunol* **178**,547-56.

Breij E. C., Brink B. P., Veerhuis R., van den Berg C., Vloet R., Yan R., Dijkstra C. D., van der Valk P. and Bo L. (2008). Homogeneity of active demyelinating lesions in established multiple sclerosis. *Ann Neurol* **63**,16-25.

Brennan K. M., Galban-Horcajo F., Rinaldi S., O'Leary C. P., Goodyear C. S., Kalna G., Arthur A., Elliot C., Barnett S., Linington C. et al. (2011). Lipid arrays identify myelin-derived lipids and lipid complexes as prominent targets for oligoclonal band antibodies in multiple sclerosis. *J Neuroimmunol* **238**,87-95.

Brettschneider J., Tumani H., Kiechle U., Muche R., Richards G., Lehmensiek V., Ludolph A. C. and Otto M. (2009). IgG antibodies against measles, rubella, and varicella zoster virus predict conversion to multiple sclerosis in clinically isolated syndrome. *PLoS One* **4**,e7638.

Brezinschek H. P., Brezinschek R. I. and Lipsky P. E. (1995). Analysis of the heavy chain repertoire of human peripheral B cells using single-cell polymerase chain reaction. *J Immunol* **155**,190-202.

Brilot F., Dale R. C., Selter R. C., Grummel V., Kalluri S. R., Aslam M., Busch V., Zhou D., Cepok S. and Hemmer B. (2009). Antibodies to native myelin oligodendrocyte glycoprotein in children with inflammatory demyelinating central nervous system disease. *Ann Neurol* **66**,833-42.

Bruck W. (2005). The pathology of multiple sclerosis is the result of focal inflammatory demyelination with axonal damage. *J Neurol* **252 Suppl 5**,v3-9.

Burgoon M. P., Hammack B. N., Owens G. P., Maybach A. L., Eikelenboom M. J. and Gilden D. H. (2003). Oligoclonal immunoglobulins in cerebrospinal fluid during varicella zoster virus (VZV) vasculopathy are directed against VZV. *Ann Neurol* **54**,459-63.

Burgoon M. P., Keays K. M., Owens G. P., Ritchie A. M., Rai P. R., Cool C. D. and Gilden D. H. (2005). Laser-capture microdissection of plasma cells from subacute sclerosing panencephalitis brain reveals intrathecal disease-relevant antibodies. *Proc Natl Acad Sci U S A* **102**,7245-50.

Burgoon M. P., Owens G. P., Carlson S., Maybach A. L. and Gilden D. H. (2001). Antigen discovery in chronic human inflammatory central nervous system disease: panning phage-displayed antigen libraries identifies the targets of central nervous system-derived IgG in subacute sclerosing panencephalitis. *J Immunol* **167**,6009-14.

Burgoon M. P., Owens G. P., Smith-Jensen T., Walker D. and Gilden D. H. (1999). Cloning the antibody response in humans with inflammatory central nervous system disease: analysis of the expressed IgG repertoire in subacute sclerosing panencephalitis brain reveals disease-relevant antibodies that recognize specific measles virus antigens. *J Immunol* **163**,3496-502.

Bustin S. A., Benes V., Garson J. A., Hellemans J., Huggett J., Kubista M., Mueller R., Nolan T., Pfaffl M. W., Shipley G. L. et al. (2009). The MIQE guidelines: minimum information for publication of quantitative real-time PCR experiments. *Clin Chem* **55**,611-22.

Cameron E. M., Spencer S., Lazarini J., Harp C. T., Ward E. S., Burgoon M., Owens G. P., Racke M. K., Bennett J. L., Frohman E. M. et al. (2009).

Potential of a unique antibody gene signature to predict conversion to clinically definite multiple sclerosis. *J Neuroimmunol* **213**,123-30.

Campagnoni A. T. and Skoff R. P. (2001). The pathobiology of myelin mutants reveal novel biological functions of the MBP and PLP genes. *Brain Pathol* **11**,74-91.

Cao L., Goodin R., Wood D., Moscarello M. A. and Whitaker J. N. (1999). Rapid release and unusual stability of immunodominant peptide 45-89 from citrullinated myelin basic protein. *Biochemistry* **38**,6157-63.

Cepok S., Rosche B., Grummel V., Vogel F., Zhou D., Sayn J., Sommer N., Hartung H. P. and Hemmer B. (2005a). Short-lived plasma blasts are the main B cell effector subset during the course of multiple sclerosis. *Brain* **128**,1667-76.

Cepok S., Zhou D., Srivastava R., Nessler S., Stei S., Bussow K., Sommer N. and Hemmer B. (2005b). Identification of Epstein-Barr virus proteins as putative targets of the immune response in multiple sclerosis. *J Clin Invest* **115**,1352-60.

Charcot J. M. . (1877). Lectures on the Diseases of the Nervous System, Delivered at La Salpetriere. . *London: New Sydenham Society*.

Chaudhuri A. (2012). Ocrelizumab in multiple sclerosis: risks and benefits. *Lancet* **379**,1196-7; author reply 1197.

Chester K. A., Begent R. H., Robson L., Keep P., Pedley R. B., Boden J. A., Boxer G., Green A., Winter G., Cochet O. et al. (1994). Phage libraries for generation of clinically useful antibodies. *Lancet* **343**,455-6.

Clackson T., Hoogenboom H. R., Griffiths A. D. and Winter G. (1991). Making antibody fragments using phage display libraries. *Nature* **352**,624-8.

Cohen J. A., Barkhof F., Comi G., Hartung H. P., Khatri B. O., Montalban X., Pelletier J., Capra R., Gallo P., Izquierdo G. et al. (2010). Oral fingolimod or intramuscular interferon for relapsing multiple sclerosis. *N Engl J Med* **362**,402-15.

Colombo M., Dono M., Gazzola P., Roncella S., Valetto A., Chiorazzi N., Mancardi G. L. and Ferrarini M. (2000). Accumulation of clonally related B lymphocytes in the cerebrospinal fluid of multiple sclerosis patients. *J Immunol* **164**,2782-9.

Comabella M. and Khoury S. J. (2012). Immunopathogenesis of multiple sclerosis. *Clin Immunol* **142**,2-8.

Compston A. and Coles A. (2008). Multiple sclerosis. *Lancet* **372**,1502-17.

Cook G. P. and Tomlinson I. M. (1995). The human immunoglobulin VH repertoire. *Immunol Today* **16**,237-42.

Cook G. P., Tomlinson I. M., Walter G., Riethman H., Carter N. P., Buluwela L., Winter G. and Rabbitts T. H. (1994). A map of the human immunoglobulin VH locus completed by analysis of the telomeric region of chromosome 14q. *Nat Genet* **7**,162-8.

Corbett S. J., Tomlinson I. M., Sonnhammer E. L., Buck D. and Winter G. (1997). Sequence of the human immunoglobulin diversity (D) segment locus: a systematic analysis provides no evidence for the use of DIR segments, inverted D segments, "minor" D segments or D-D recombination. *J Mol Biol* **270**,587-97.

Corcione A., Casazza S., Ferretti E., Giunti D., Zappia E., Pistorio A., Gambini C., Mancardi G. L., Uccelli A. and Pistoia V. (2004). Recapitulation of B

cell differentiation in the central nervous system of patients with multiple sclerosis. *Proc Natl Acad Sci U S A* **101**,11064-9.

Cortese I., Capone S., Luchetti S., Cortese R. and Nicosia A. (2001). Cross-reactive phage-displayed mimotopes lead to the discovery of mimicry between HSV-1 and a brain-specific protein. *J Neuroimmunol* **113**,119-28.

Cortese I., Capone S., Luchetti S., Grimaldi L. M., Nicosia A. and Cortese R. (1998a). CSF-enriched antibodies do not share specificities among MS patients. *Mult Scler* **4**,118-23.

Cortese I., Capone S., Tafi R., Grimaldi L. M., Nicosia A. and Cortese R. (1998b). Identification of peptides binding to IgG in the CSF of multiple sclerosis patients. *Mult Scler* **4**,31-6.

Cortese I., Tafi R., Grimaldi L. M., Martino G., Nicosia A. and Cortese R. (1996). Identification of peptides specific for cerebrospinal fluid antibodies in multiple sclerosis by using phage libraries. *Proc Natl Acad Sci U S A* **93**,11063-7.

Cotton F., Weiner H. L., Jolesz F. A. and Guttmann C. R. (2003). MRI contrast uptake in new lesions in relapsing-remitting MS followed at weekly intervals. *Neurology* **60**,640-6.

Cottrell D. A., Kremenchutzky M., Rice G. P., Koopman W. J., Hader W., Baskerville J. and Ebers G. C. (1999). The natural history of multiple sclerosis: a geographically based study. 5. The clinical features and natural history of primary progressive multiple sclerosis. *Brain* **122 (Pt 4)**,625-39.

Coulson D. T., Brockbank S., Quinn J. G., Murphy S., Ravid R., Irvine G. B. and Johnston J. A. (2008). Identification of valid reference genes for the normalization of RT qPCR gene expression data in human brain tissue. *BMC Mol Biol* **9**,46.

Cree Bruce A. C. (2010). Diagnosis and differential diagnosis of multiple sclerosis *Continuum Lifelong Learning Neurol* **16**,19-36.

Cross A. H., Stark J. L., Lauber J., Ramsbottom M. J. and Lyons J. A. (2006). Rituximab reduces B cells and T cells in cerebrospinal fluid of multiple sclerosis patients. *J Neuroimmunol* **180**,63-70.

Cross A. H. and Waubant E. (2011). MS and the B cell controversy. *Biochim Biophys Acta* **1812**,231-8.

Cruz M., Olsson T., Ernerudh J., Hojeberg B. and Link H. (1987). Immunoblot detection of oligoclonal anti-myelin basic protein IgG antibodies in cerebrospinal fluid in multiple sclerosis. *Neurology* **37**,1515-9.

Davenport R. D. and Keren D. F. (1988). Oligoclonal bands in cerebrospinal fluids: significance of corresponding bands in serum for diagnosis of multiple sclerosis. *Clin Chem* **34**,764-5.

Davies G., Keir G., Thompson E. J. and Giovannoni G. (2003). The clinical significance of an intrathecal monoclonal immunoglobulin band: a follow-up study. *Neurology* **60**,1163-6.

de Wildt R. M., Mundy C. R., Gorick B. D. and Tomlinson I. M. (2000). Antibody arrays for high-throughput screening of antibody-antigen interactions. *Nat Biotechnol* **18**,989-94.

Deisenhammer F., Bartos A., Egg R., Gilhus N. E., Giovannoni G., Rauer S. and Sellebjerg F. (2006). Guidelines on routine cerebrospinal fluid analysis. Report from an EFNS task force. *Eur J Neurol* **13**,913-22.

Delbecq S. P. and Klevit R. E. (2013). One size does not fit all: The oligomeric states of alphaB crystallin. *FEBS Lett*.

Dhib-Jalbut S. and Marks S. (2010). Interferon-beta mechanisms of action in multiple sclerosis. *Neurology* **74 Suppl 1**,S17-24.

Di Pauli F., Mader S., Rostasy K., Schanda K., Bajer-Kornek B., Ehling R., Deisenhammer F., Reindl M. and Berger T. (2011). Temporal dynamics of anti-MOG antibodies in CNS demyelinating diseases. *Clin Immunol* **138**,247-54.

Di Perri C., Battaglini M., Stromillo M. L., Bartolozzi M. L., Guidi L., Federico A. and De Stefano N. (2008). Voxel-based assessment of differences in damage and distribution of white matter lesions between patients with primary progressive and relapsing-remitting multiple sclerosis. *Arch Neurol* **65**,236-43.

Dobson R., Giovannoni G. and Ramagopalan S. (2012). The month of birth effect in multiple sclerosis: systematic review, meta-analysis and effect of latitude. *J Neurol Neurosurg Psychiatry*.

Dobson R., Meier U. C. and Giovannoni G. (2011). More to come: humoral immune responses in MS. *J Neuroimmunol* **240-241**,13-21.

Dobson R., Ramagopalan S., Davis A. and Giovannoni G. (2013). Cerebrospinal fluid oligoclonal bands in multiple sclerosis and clinically isolated syndromes: a meta-analysis of prevalence, prognosis and effect of latitude. *J Neurol Neurosurg Psychiatry*.

Dorner T., Foster S. J., Farner N. L. and Lipsky P. E. (1998). Somatic hypermutation of human immunoglobulin heavy chain genes: targeting of RGYW motifs on both DNA strands. *Eur J Immunol* **28**,3384-96.

Durrenberger P. F., Fernando S., Kashefi S. N., Ferrer I., Hauw J. J., Seilhean D., Smith C., Walker R., Al-Sarraj S., Troakes C. et al. (2010). Effects of antemortem and postmortem variables on human brain mRNA quality: a BrainNet Europe study. *J Neuropathol Exp Neurol* **69**,70-81.

Dybwad A., Flrre O. and Sioud M. (1997). Probing for cerebrospinal fluid antibody specificities by a panel of random peptide libraries. *Autoimmunity* **25**,85-9.

Ebers G. C., Sadovnick A. D. and Risch N. J. (1995). A genetic basis for familial aggregation in multiple sclerosis. Canadian Collaborative Study Group. *Nature* **377**,150-1.

Ehling R., Lutterotti A., Wanschitz J., Khalil M., Gneiss C., Deisenhammer F., Reindl M. and Berger T. (2004). Increased frequencies of serum antibodies to neurofilament light in patients with primary chronic progressive multiple sclerosis. *Mult Scler* **10**,601-6.

Eikelenboom M. J., Petzold A., Lazeron R. H., Silber E., Sharief M., Thompson E. J., Barkhof F., Giovannoni G., Polman C. H. and Uitdehaag B. M. (2003). Multiple sclerosis: Neurofilament light chain antibodies are correlated to cerebral atrophy. *Neurology* **60**,219-23.

Elliott E. A., McFarland H. I., Nye S. H., Cofiell R., Wilson T. M., Wilkins J. A., Squinto S. P., Matis L. A. and Mueller J. P. (1996). Treatment of

experimental encephalomyelitis with a novel chimeric fusion protein of myelin basic protein and proteolipid protein. *J Clin Invest* **98**,1602-12.

Esiri M. M. (1977). Immunoglobulin-containing cells in multiple-sclerosis plaques. *Lancet* **2**,478.

Esiri M. M. (1980). Multiple sclerosis: a quantitative and qualitative study of immunoglobulin-containing cells in the central nervous system. *Neuropathol Appl Neurobiol* **6**,9-21.

Esiri M. M. (1983). Immunohistological studies of immunoglobulin-containing cells and viral antigens in some inflammatory diseases of the nervous system. *Prog Brain Res* **59**,209-19.

Farner N. L., Dorner T. and Lipsky P. E. (1999). Molecular mechanisms and selection influence the generation of the human V lambda J lambda repertoire. *J Immunol* **162**,2137-45.

Farrell M. A., Kaufmann J. C., Gilbert J. J., Noseworthy J. H., Armstrong H. A. and Ebers G. C. (1985). Oligoclonal bands in multiple sclerosis: clinical-pathologic correlation. *Neurology* **35**,212-8.

Farrell R. A., Espasandin M., Lakdawala N., Creeke P. I., Worthington V. and Giovannoni G. (2011). Incorporation of an interferon-beta neutralizing antibody assay into routine clinical practice. *Mult Scler* **17**,1333-40.

Farrell R. A., Marta M., Gaeguta A. J., Souslova V., Giovannoni G. and Creeke P. I. (2012). Development of resistance to biologic therapies with reference to IFN-beta. *Rheumatology (Oxford)* **51**,590-9.

Fernando M. M., Stevens C. R., Walsh E. C., De Jager P. L., Goyette P., Plenge R. M., Vyse T. J. and Rioux J. D. (2008). Defining the role of the MHC in autoimmunity: a review and pooled analysis. *PLoS Genet* **4**,e1000024.

Ferrer I., Martinez A., Boluda S., Parchi P. and Barrachina M. (2008). Brain banks: benefits, limitations and cautions concerning the use of post-mortem brain tissue for molecular studies. *Cell Tissue Bank* **9**,181-94.

Fisniku L. K., Brex P. A., Altmann D. R., Miszkiel K. A., Benton C. E., Lanyon R., Thompson A. J. and Miller D. H. (2008). Disability and T2 MRI lesions: a 20-year follow-up of patients with relapse onset of multiple sclerosis. *Brain* **131**,808-17.

Fortini A. S., Sanders E. L., Weinshenker B. G. and Katzmann J. A. (2003). Cerebrospinal fluid oligoclonal bands in the diagnosis of multiple sclerosis. Isoelectric focusing with IgG immunoblotting compared with high-resolution agarose gel electrophoresis and cerebrospinal fluid IgG index. *Am J Clin Pathol* **120**,672-5.

Frederiksen J. L. and Sindic C. J. (1998). Intrathecal synthesis of virus-specific oligoclonal IgG, and of free kappa and free lambda oligoclonal bands in acute monosymptomatic optic neuritis. Comparison with brain MRI. *Mult Scler* **4**,22-6.

Freedman M. S., Thompson E. J., Deisenhammer F., Giovannoni G., Grimsley G., Keir G., Ohman S., Racke M. K., Sharief M., Sindic C. J. et al. (2005). Recommended standard of cerebrospinal fluid analysis in the diagnosis of multiple sclerosis: a consensus statement. *Arch Neurol* **62**,865-70.

Frohman E. M., Racke M. K. and Raine C. S. (2006). Multiple sclerosis--the plaque and its pathogenesis. *N Engl J Med* **354**,942-55.

Fuhr P. and Kappos L. (2001). Evoked potentials for evaluation of multiple sclerosis. *Clin Neurophysiol* **112**,2185-9.

Fujimori J., Nakashima I., Fujihara K., Misu T., Sato S. and Itoyama Y. (2011). Epitope analysis of cerebrospinal fluid IgG in Japanese multiple sclerosis patients using phage display method. *Mult Scler Int* **2011**,353417.

Gabibov A. G., Belogurov A. A., Jr., Lomakin Y. A., Zakharova M. Y., Avakyan M. E., Dubrovskaya V. V., Smirnov I. V., Ivanov A. S., Molnar A. A., Gurtsevitch V. E. et al. (2011). Combinatorial antibody library from multiple sclerosis patients reveals antibodies that cross-react with myelin basic protein and EBV antigen. *FASEB J* **25**,4211-21.

Gafson A. R. and Giovannoni G. (2012). Towards the incorporation of lumbar puncture into clinical trials for multiple sclerosis. *Mult Scler*,3.

George A. J., Lee L. and Pitzalis C. (2003). Isolating ligands specific for human vasculature using in vivo phage selection. *Trends Biotechnol* **21**,199-203.

Gilden D. H. (2005). Infectious causes of multiple sclerosis. *Lancet Neurol* **4**,195-202.

Gilden D. H., Devlin M. E., Burgoon M. P. and Owens G. P. (1996). The search for virus in multiple sclerosis brain. *Mult Scler* **2**,179-83.

Gilmore C. P., Bo L., Owens T., Lowe J., Esiri M. M. and Evangelou N. (2006). Spinal cord gray matter demyelination in multiple sclerosis-a novel pattern of residual plaque morphology. *Brain Pathol* **16**,202-8.

Gilmore C. P., DeLuca G. C., Bo L., Owens T., Lowe J., Esiri M. M. and Evangelou N. (2009). Spinal cord neuronal pathology in multiple sclerosis. *Brain Pathol* **19**,642-9.

Giovannoni G., Cutter G. R., Lunemann J., Martin R., Munz C., Sriram S., Steiner I., Hammerschlag M. R. and Gaydos C. A. (2006). Infectious causes of multiple sclerosis. *Lancet Neurol* **5**,887-94.

Giovannoni G. and Nath A. (2011). After the storm: neurofilament levels as a surrogate endpoint for neuroaxonal damage. *Neurology* **76**,1200-1.

Greer J. M., Csurhes P. A., Muller D. M. and Pender M. P. (2008). Correlation of blood T cell and antibody reactivity to myelin proteins with HLA type and lesion localization in multiple sclerosis. *J Immunol* **180**,6402-10.

Greer J. M., Denis B., Sobel R. A. and Trifilieff E. (2001). Thiopalmitoylation of myelin proteolipid protein epitopes enhances immunogenicity and encephalitogenicity. *J Immunol* **166**,6907-13.

Greer J. M. and Lees M. B. (2002). Myelin proteolipid protein--the first 50 years. *Int J Biochem Cell Biol* **34**,211-5.

Greter M., Heppner F. L., Lemos M. P., Odermatt B. M., Goebels N., Laufer T., Noelle R. J. and Becher B. (2005). Dendritic cells permit immune invasion of the CNS in an animal model of multiple sclerosis. *Nat Med* **11**,328-34.

Haas J., Bekeredjian-Ding I., Milkova M., Balint B., Schwarz A., Korporal M., Jarius S., Fritz B., Lorenz H. M. and Wildemann B. (2011). B cells undergo unique compartmentalized redistribution in multiple sclerosis. *J Autoimmun* **37**,289-99.

Haase C. G., Guggenmos J., Brehm U., Andersson M., Olsson T., Reindl M., Schneidewind J. M., Zettl U. K., Heidenreich F., Berger T. et al. (2001). The fine specificity of the myelin oligodendrocyte glycoprotein

autoantibody response in patients with multiple sclerosis and normal healthy controls. *J Neuroimmunol* **114**,220-5.

Hafler D. A., Compston A., Sawcer S., Lander E. S., Daly M. J., De Jager P. L., de Bakker P. I., Gabriel S. B., Mirel D. B., Ivinson A. J. et al. (2007). Risk alleles for multiple sclerosis identified by a genomewide study. *N Engl J Med* **357**,851-62.

Hafler D. A., Kent S. C., Pietrusewicz M. J., Khoury S. J., Weiner H. L. and Fukaura H. (1997). Oral administration of myelin induces antigen-specific TGF-beta 1 secreting T cells in patients with multiple sclerosis. *Ann N Y Acad Sci* **835**,120-31.

Harauz G., Ladizhansky V. and Boggs J. M. (2009). Structural polymorphism and multifunctionality of myelin basic protein. *Biochemistry* **48**,8094-104.

Harp C., Lee J., Lambracht-Washington D., Cameron E., Olsen G., Frohman E., Racke M. and Monson N. (2007). Cerebrospinal fluid B cells from multiple sclerosis patients are subject to normal germinal center selection. *J Neuroimmunol* **183**,189-99.

Harrison J. L., Williams S. C., Winter G. and Nissim A. (1996). Screening of phage antibody libraries. *Methods Enzymol* **267**,83-109.

Haubold K., Owens G. P., Kaur P., Ritchie A. M., Gilden D. H. and Bennett J. L. (2004). B-lymphocyte and plasma cell clonal expansion in monosymptomatic optic neuritis cerebrospinal fluid. *Ann Neurol* **56**,97-107.

Hauser S. L., Waubant E., Arnold D. L., Vollmer T., Antel J., Fox R. J., Bar-Or A., Panzara M., Sarkar N., Agarwal S. et al. (2008). B-cell depletion with rituximab in relapsing-remitting multiple sclerosis. *N Engl J Med* **358**,676-88.

Hawker K., O'Connor P., Freedman M. S., Calabresi P. A., Antel J., Simon J., Hauser S., Waubant E., Vollmer T., Panitch H. et al. (2009). Rituximab in patients with primary progressive multiple sclerosis: results of a randomized double-blind placebo-controlled multicenter trial. *Ann Neurol* **66**,460-71.

Hawker Kathleen. (2010). Primary Progressive Multiple Sclerosis. *Continuum Lifelong Learning Neurol* **16**,211-225.

Hedegaard C. J., Chen N., Sellebjerg F., Sorensen P. S., Leslie R. G., Bendtzen K. and Nielsen C. H. (2009). Autoantibodies to myelin basic protein (MBP) in healthy individuals and in patients with multiple sclerosis: a role in regulating cytokine responses to MBP. *Immunology* **128**,e451-61.

Hedstrom A. K., Baarnhielm M., Olsson T. and Alfredsson L. (2009). Tobacco smoking, but not Swedish snuff use, increases the risk of multiple sclerosis. *Neurology* **73**,696-701.

Hellings N., Gelin G., Medaer R., Bruckers L., Palmers Y., Raus J. and Stinissen P. (2002). Longitudinal study of antimyelin T-cell reactivity in relapsing-remitting multiple sclerosis: association with clinical and MRI activity. *J Neuroimmunol* **126**,143-60.

Henderson A. P., Barnett M. H., Parratt J. D. and Prineas J. W. (2009). Multiple sclerosis: distribution of inflammatory cells in newly forming lesions. *Ann Neurol* **66**,739-53.

Henriksson A., Kam-Hansen S. and Link H. (1985). IgM, IgA and IgG producing cells in cerebrospinal fluid and peripheral blood in multiple sclerosis. *Clin Exp Immunol* **62**,176-84.

Hoogenboom H. R., Griffiths A. D., Johnson K. S., Chiswell D. J., Hudson P. and Winter G. (1991). Multi-subunit proteins on the surface of filamentous phage: methodologies for displaying antibody (Fab) heavy and light chains. *Nucleic Acids Res* **19**,4133-7.

Howell O. W., Reeves C. A., Nicholas R., Carassiti D., Radotra B., Gentleman S. M., Serafini B., Aloisi F., Roncaroli F., Magliozzi R. et al. (2011). Meningeal inflammation is widespread and linked to cortical pathology in multiple sclerosis. *Brain* **134**,2755-71.

Huang C., Stewart A. K., Schwartz R. S. and Stollar B. D. (1992). Immunoglobulin heavy chain gene expression in peripheral blood B lymphocytes. *J Clin Invest* **89**,1331-43.

Hughes C., Faurholm B., Dell'Accio F., Manzo A., Seed M., Eltawil N., Marrelli A., Gould D., Subang C., Al-Kashi A. et al. (2010). Human single-chain variable fragment that specifically targets arthritic cartilage. *Arthritis Rheum* **62**,1007-16.

Huitinga I., Erkut Z. A., van Beurden D. and Swaab D. F. (2004). Impaired hypothalamus-pituitary-adrenal axis activity and more severe multiple sclerosis with hypothalamic lesions. *Ann Neurol* **55**,37-45.

Huizinga R., van der Star B. J., Kipp M., Jong R., Gerritsen W., Clarner T., Puentes F., Dijkstra C. D., van der Valk P. and Amor S. (2012). Phagocytosis of neuronal debris by microglia is associated with neuronal damage in multiple sclerosis. *Glia* **60**,422-31.

Humby F., Bombardieri M., Manzo A., Kelly S., Blades M. C., Kirkham B., Spencer J. and Pitzalis C. (2009). Ectopic lymphoid structures support ongoing production of class-switched autoantibodies in rheumatoid synovium. *PLoS Med* **6**,e1.

Idiman E., Ozakbas S., Dogan Y. and Kosehasanogullari G. (2009). The significance of oligoclonal bands in multiple sclerosis: relevance of demographic and clinical features, and immunogenetic backgrounds. *J Neuroimmunol* **212**,121-4.

Ignatovich O., Tomlinson I. M., Jones P. T. and Winter G. (1997). The creation of diversity in the human immunoglobulin V(lambda) repertoire. *J Mol Biol* **268**,69-77.

Imrell K., Landtblom A. M., Hillert J. and Masterman T. (2006). Multiple sclerosis with and without CSF bands: clinically indistinguishable but immunogenetically distinct. *Neurology* **67**,1062-4.

Insel R. A., Varade W. S., Chu Y. W., Marin E., Fuleihan R. and Geha R. S. (1995). Somatic mutation of human immunoglobulin V genes: bias, rate, and regulation. *Ann N Y Acad Sci* **764**,158-69.

Jenkins M. A., Cheng L. and Ratnaike S. (2001). Multiple sclerosis: use of light-chain typing to assist diagnosis. *Ann Clin Biochem* **38**,235-41.

Johns T. G. and Bernard C. C. (1999). The structure and function of myelin oligodendrocyte glycoprotein. *J Neurochem* **72**,1-9.

Jolivet-Reynaud C., Perron H., Ferrante P., Becquart L., Dalbon P. and Mandrand B. (1999). Specificities of multiple sclerosis cerebrospinal fluid and serum antibodies against mimotopes. *Clin Immunol* **93**,283-93.

Jolly C. J., Wagner S. D., Rada C., Klix N., Milstein C. and Neuberger M. S. (1996). The targeting of somatic hypermutation. *Semin Immunol* **8**,159-68.

Joseph F. G., Hirst C. L., Pickersgill T. P., Ben-Shlomo Y., Robertson N. P. and Scolding N. J. (2009). CSF oligoclonal band status informs prognosis in multiple sclerosis: a case control study of 100 patients. *J Neurol Neurosurg Psychiatry* **80**,292-6.

Juul L., Hougs L., Andersen V., Svejgaard A. and Barington T. (1997). The normally expressed kappa immunoglobulin light chain gene repertoire and somatic mutations studied by single-sided specific polymerase chain reaction (PCR); frequent occurrence of features often assigned to autoimmunity. *Clin Exp Immunol* **109**,194-203.

Kabat E. A., Moore D. H. and Landow H. (1942). An Electrophoretic Study of the Protein Components in Cerebrospinal Fluid and Their Relationship to the Serum Proteins. *J Clin Invest* **21**,571-7.

Kappos L., Li D., Calabresi P. A., O'Connor P., Bar-Or A., Barkhof F., Yin M., Leppert D., Glanzman R., Tinbergen J. et al. (2011). Ocrelizumab in relapsing-remitting multiple sclerosis: a phase 2, randomised, placebo-controlled, multicentre trial. *Lancet* **378**,1779-87.

Kappos L., Radue E. W., O'Connor P., Polman C., Hohlfeld R., Calabresi P., Selmaj K., Agoropoulou C., Leyk M., Zhang-Auberson L. et al. (2010). A placebo-controlled trial of oral fingolimod in relapsing multiple sclerosis. *N Engl J Med* **362**,387-401.

Karni A., Abraham M., Monsonego A., Cai G., Freeman G. J., Hafler D., Khoury S. J. and Weiner H. L. (2006). Innate immunity in multiple sclerosis: myeloid dendritic cells in secondary progressive multiple sclerosis are activated and drive a proinflammatory immune response. *J Immunol* **177**,4196-202.

Kawasaki K., Minoshima S., Nakato E., Shibuya K., Shintani A., Schmeits J. L., Wang J. and Shimizu N. (1997). One-megabase sequence analysis of the human immunoglobulin lambda gene locus. *Genome Res* **7**,250-61.

Kettner Carsten, Field Dawn, Sansone Susanna, Taylor Chris, Aerts Jan, Binns Nigel, Black Andrew, Britten Cedrik M., de Marco Ario, Fostel Jennifer et al. (2010). *Meeting Report from the Second "Minimum Information for Biological and Biomedical Investigations"• (MIBBI) workshop*.

Kidd D., Barkhof F., McConnell R., Algra P. R., Allen I. V. and Revesz T. (1999). Cortical lesions in multiple sclerosis. *Brain* **122 (Pt 1)**,17-26.

Kingwell E., van der Kop M., Zhao Y., Shirani A., Zhu F., Oger J. and Tremlett H. (2012). Relative mortality and survival in multiple sclerosis: findings from British Columbia, Canada. *J Neurol Neurosurg Psychiatry* **83**,61-6.

Kitley J., Woodhall M., Waters P., Leite M. I., Devenney E., Craig J., Palace J. and Vincent A. (2012). Myelin-oligodendrocyte glycoprotein antibodies in adults with a neuromyelitis optica phenotype. *Neurology* **79**,1273-7.

Klein R. and Zachau H. G. (1995). Expression and hypermutation of human immunoglobulin kappa genes. *Ann N Y Acad Sci* **764**,74-83.

Koch M., Kingwell E., Rieckmann P., Tremlett H. and Neurologists Ubc Ms Clinic. (2010). The natural history of secondary progressive multiple sclerosis. *J Neurol Neurosurg Psychiatry* **81**,1039-43.

Koppelkamm A., Vennemann B., Fracasso T., Lutz-Bonengel S., Schmidt U. and Heinrich M. (2010). Validation of adequate endogenous reference genes for the normalisation of qPCR gene expression data in human post mortem tissue. *Int J Legal Med* **124**,371-80.

Kostulas V. K., Link H. and Lefvert A. K. (1987). Oligoclonal IgG bands in cerebrospinal fluid. Principles for demonstration and interpretation based on findings in 1114 neurological patients. *Arch Neurol* **44**,1041-4.

Kristensen P. and Winter G. (1998). Proteolytic selection for protein folding using filamentous bacteriophages. *Fold Des* **3**,321-8.

Kroenke M. A., Carlson T. J., Andjelkovic A. V. and Segal B. M. (2008). IL-12- and IL-23-modulated T cells induce distinct types of EAE based on histology, CNS chemokine profile, and response to cytokine inhibition. *J Exp Med* **205**,1535-41.

Kuerten S., Pauly R., Rottlaender A., Rodi M., Gruppe T. L., Addicks K., Tary-Lehmann M. and Lehmann P. V. (2011). Myelin-reactive antibodies mediate the pathology of MBP-PLP fusion protein MP4-induced EAE. *Clin Immunol* **140**,54-62.

Kuhle J., Leppert D., Petzold A., Regeniter A., Schindler C., Mehling M., Anthony D. C., Kappos L. and Lindberg R. L. (2011). Neurofilament heavy chain in CSF correlates with relapses and disability in multiple sclerosis. *Neurology* **76**,1206-13.

Kuhle J., Pohl C., Mehling M., Edan G., Freedman M. S., Hartung H. P., Polman C. H., Miller D. H., Montalban X., Barkhof F. et al. (2007). Lack of association between antimyelin antibodies and progression to multiple sclerosis. *N Engl J Med* **356**,371-8.

Kurtzke J. F. (1993). Epidemiologic evidence for multiple sclerosis as an infection. *Clin Microbiol Rev* **6**,382-427.

Lalive P. H., Menge T., Delarasse C., Della Gaspera B., Pham-Dinh D., Villoslada P., von Budingen H. C. and Genain C. P. (2006). Antibodies to native myelin oligodendrocyte glycoprotein are serologic markers of early inflammation in multiple sclerosis. *Proc Natl Acad Sci U S A* **103**,2280-5.

Lambracht-Washington D., O'Connor K. C., Cameron E. M., Jowdry A., Ward E. S., Frohman E., Racke M. K. and Monson N. L. (2007). Antigen specificity of clonally expanded and receptor edited cerebrospinal fluid B cells from patients with relapsing remitting MS. *J Neuroimmunol* **186**,164-76.

Lampasona V., Franciotta D., Furlan R., Zanaboni S., Fazio R., Bonifacio E., Comi G. and Martino G. (2004). Similar low frequency of anti-MOG IgG and IgM in MS patients and healthy subjects. *Neurology* **62**,2092-4.

Lande R., Gafa V., Serafini B., Giacomini E., Visconti A., Remoli M. E., Severa M., Parmentier M., Ristori G., Salvetti M. et al. (2008). Plasmacytoid dendritic cells in multiple sclerosis: intracerebral recruitment and impaired maturation in response to interferon-beta. *J Neuropathol Exp Neurol* **67**,388-401.

Lassmann H., Bruck W. and Lucchinetti C. (2001). Heterogeneity of multiple sclerosis pathogenesis: implications for diagnosis and therapy. *Trends Mol Med* **7**,115-21.

Lassmann H., Raine C. S., Antel J. and Prineas J. W. (1998). Immunopathology of multiple sclerosis: report on an international meeting held at the

Institute of Neurology of the University of Vienna. *J Neuroimmunol* **86**,213-7.

Lechner-Scott J., Spencer B., de Malmanche T., Attia J., Fitzgerald M., Trojano M., Grand'Maison F., Gomez J. A., Izquierdo G., Duquette P. et al. (2012). The frequency of CSF oligoclonal banding in multiple sclerosis increases with latitude. *Mult Scler* **18**,974-82.

Lefranc M. P., Giudicelli V., Ginestoux C., Bodmer J., Muller W., Bontrop R., Lemaitre M., Malik A., Barbie V. and Chaume D. (1999). IMGT, the international ImMunoGeneTics database. *Nucleic Acids Res* **27**,209-12.

Lefranc M. P., Giudicelli V., Ginestoux C., Jabado-Michaloud J., Folch G., Bellahcene F., Wu Y., Gemrot E., Brochet X., Lane J. et al. (2009). IMGT, the international ImMunoGeneTics information system. *Nucleic Acids Res* **37**,D1006-12.

Lennon V. A., Wingerchuk D. M., Kryzer T. J., Pittock S. J., Lucchinetti C. F., Fujihara K., Nakashima I. and Weinshenker B. G. (2004). A serum autoantibody marker of neuromyelitis optica: distinction from multiple sclerosis. *Lancet* **364**,2106-12.

Leocani L. and Comi G. (2008). Neurophysiological markers. *Neurol Sci* **29 Suppl 2**,S218-21.

Li J. Z., Vawter M. P., Walsh D. M., Tomita H., Evans S. J., Choudary P. V., Lopez J. F., Avelar A., Shokoohi V., Chung T. et al. (2004). Systematic changes in gene expression in postmortem human brains associated with tissue pH and terminal medical conditions. *Hum Mol Genet* **13**,609-16.

Link H. and Tibbling G. (1977a). Principles of albumin and IgG analyses in neurological disorders. II. Relation of the concentration of the proteins in serum and cerebrospinal fluid. *Scand J Clin Lab Invest* **37**,391-6.

Link H. and Tibbling G. (1977b). Principles of albumin and IgG analyses in neurological disorders. III. Evaluation of IgG synthesis within the central nervous system in multiple sclerosis. *Scand J Clin Lab Invest* **37**,397-401.

Lourenco P., Shirani A., Saeedi J., Oger J., Schreiber W. E. and Tremlett H. (2013). Oligoclonal bands and cerebrospinal fluid markers in multiple sclerosis: associations with disease course and progression. *Mult Scler* **19**,577-84.

Lovato L., Willis S. N., Rodig S. J., Caron T., Almendinger S. E., Howell O. W., Reynolds R., O'Connor K. C. and Hafler D. A. (2011). Related B cell clones populate the meninges and parenchyma of patients with multiple sclerosis. *Brain* **134**,534-41.

Lucchinetti C., Bruck W., Parisi J., Scheithauer B., Rodriguez M. and Lassmann H. (2000). Heterogeneity of multiple sclerosis lesions: implications for the pathogenesis of demyelination. *Ann Neurol* **47**,707-17.

Ludwin S. K. (2000). Understanding multiple sclerosis: lessons from pathology. *Ann Neurol* **47**,691-3.

Lunemann J. D., Kamradt T., Martin R. and Munz C. (2007). Epstein-barr virus: environmental trigger of multiple sclerosis? *J Virol* **81**,6777-84.

Magliozzi R., Columba-Cabezas S., Serafini B. and Aloisi F. (2004). Intracerebral expression of CXCL13 and BAFF is accompanied by formation of lymphoid follicle-like structures in the meninges of mice with

relapsing experimental autoimmune encephalomyelitis. *J Neuroimmunol* **148**,11-23.

Magliozzi R., Howell O., Vora A., Serafini B., Nicholas R., Puopolo M., Reynolds R. and Aloisi F. (2007). Meningeal B-cell follicles in secondary progressive multiple sclerosis associate with early onset of disease and severe cortical pathology. *Brain* **130**,1089-104.

Magliozzi R., Howell O. W., Reeves C., Roncaroli F., Nicholas R., Serafini B., Aloisi F. and Reynolds R. (2010). A Gradient of neuronal loss and meningeal inflammation in multiple sclerosis. *Ann Neurol* **68**,477-93.

Manzo A., Bombardieri M., Humby F. and Pitzalis C. (2010). Secondary and ectopic lymphoid tissue responses in rheumatoid arthritis: from inflammation to autoimmunity and tissue damage/remodeling. *Immunol Rev* **233**,267-85.

Mao C., Liu A. and Cao B. (2009). Virus-based chemical and biological sensing. *Angew Chem Int Ed Engl* **48**,6790-810.

Marks J. D., Hoogenboom H. R., Bonnert T. P., McCafferty J., Griffiths A. D. and Winter G. (1991). By-passing immunization. Human antibodies from V-gene libraries displayed on phage. *J Mol Biol* **222**,581-97.

Marta M., Meier U. C. and Lobell A. (2009). Regulation of autoimmune encephalomyelitis by toll-like receptors. *Autoimmun Rev* **8**,506-9.

Matsuda F., Ishii K., Bourvagnet P., Kuma K., Hayashida H., Miyata T. and Honjo T. (1998). The complete nucleotide sequence of the human immunoglobulin heavy chain variable region locus. *J Exp Med* **188**,2151-62.

Mattson D. H., Roos R. P., Hopper J. E. and Arnason B. G. (1982). Light chain composition of CSF oligoclonal IgG bands in multiple sclerosis and subacute sclerosing panencephalitis. *J Neuroimmunol* **3**,63-76.

Mayo L., Quintana F. J. and Weiner H. L. (2012). The innate immune system in demyelinating disease. *Immunol Rev* **248**,170-87.

McCarthy D. D., Summers-Deluca L., Vu F., Chiu S., Gao Y. and Gommerman J. L. (2006). The lymphotoxin pathway: beyond lymph node development. *Immunol Res* **35**,41-54.

McLaurin J., Hashim G. and Moscarello M. A. (1992). An antibody specific for component 8 of myelin basic protein from normal brain reacts strongly with component 8 from multiple sclerosis brain. *J Neurochem* **59**,1414-20.

Mehraein Y., Lennerz C., Ehlhardt S., Remberger K., Ojak A. and Zang K. D. (2004). Latent Epstein-Barr virus (EBV) infection and cytomegalovirus (CMV) infection in synovial tissue of autoimmune chronic arthritis determined by RNA- and DNA-in situ hybridization. *Mod Pathol* **17**,781-9.

Mehta P. D., Patrick B. A. and Miller J. A. (1984). Absence of oligoclonal IgA in CSF and serum of multiple sclerosis patients. *J Neuroimmunol* **6**,67-9.

Meier U. C., Giovannoni G., Tzartos J. S. and Khan G. (2012). Translational Mini-Review Series on B cell subsets in disease. B cells in multiple sclerosis: drivers of disease pathogenesis and Trojan horse for Epstein-Barr virus entry to the central nervous system? *Clin Exp Immunol* **167**,1-6.

Mero I. L., Gustavsen M. W., Saether H. S., Flam S. T., Berg-Hansen P., Sondergaard H. B., Jensen P. E., Berge T., Bjolgerud A., Muggerud A. et

al. (2013). Oligoclonal band status in Scandinavian multiple sclerosis patients is associated with specific genetic risk alleles. *PLoS One* **8**,e58352.

Mexal S., Berger R., Adams C. E., Ross R. G., Freedman R. and Leonard S. (2006). Brain pH has a significant impact on human postmortem hippocampal gene expression profiles. *Brain Res* **1106**,1-11.

Middleton F. A., Mirnics K., Pierri J. N., Lewis D. A. and Levitt P. (2002). Gene expression profiling reveals alterations of specific metabolic pathways in schizophrenia. *J Neurosci* **22**,2718-29.

Miller D., Barkhof F., Montalban X., Thompson A. and Filippi M. (2005a). Clinically isolated syndromes suggestive of multiple sclerosis, part I: natural history, pathogenesis, diagnosis, and prognosis. *Lancet Neurol* **4**,281-8.

Miller D., Barkhof F., Montalban X., Thompson A. and Filippi M. (2005b). Clinically isolated syndromes suggestive of multiple sclerosis, part 2: non-conventional MRI, recovery processes, and management. *Lancet Neurol* **4**,341-8.

Minegishi Y., Okawa H., Sugamura K. and Yata J. (1994). Preferential utilization of the immature JH segment and absence of somatic mutation in the CDR3 junction of the Ig H chain gene in three X-linked severe combined immunodeficiency patients. *Int Immunol* **6**,1709-15.

Mirzaei F., Michels K. B., Munger K., O'Reilly E., Chitnis T., Forman M. R., Giovannucci E., Rosner B. and Ascherio A. (2011). Gestational vitamin D and the risk of multiple sclerosis in offspring. *Ann Neurol* **70**,30-40.

Mohan H., Krumbholz M., Sharma R., Eisele S., Junker A., Sixt M., Newcombe J., Wekerle H., Hohlfeld R., Lassmann H. et al. (2010). Extracellular matrix in multiple sclerosis lesions: Fibrillar collagens, biglycan and decorin are upregulated and associated with infiltrating immune cells. *Brain Pathol* **20**,966-75.

Monson N. L., Brezinschek H. P., Brezinschek R. I., Mobley A., Vaughan G. K., Frohman E. M., Racke M. K. and Lipsky P. E. (2005). Receptor revision and atypical mutational characteristics in clonally expanded B cells from the cerebrospinal fluid of recently diagnosed multiple sclerosis patients. *J Neuroimmunol* **158**,170-81.

Montalban X., Tintore M., Swanton J., Barkhof F., Fazekas F., Filippi M., Frederiksen J., Kappos L., Palace J., Polman C. et al. (2010). MRI criteria for MS in patients with clinically isolated syndromes. *Neurology* **74**,427-34.

Mullinax R. L., Gross E. A., Amberg J. R., Hay B. N., Hogrefe H. H., Kubitz M. M., Greener A., Alting-Mees M., Ardourel D., Short J. M. et al. (1990). Identification of human antibody fragment clones specific for tetanus toxoid in a bacteriophage lambda immunoexpression library. *Proc Natl Acad Sci U S A* **87**,8095-9.

Naismith R. T., Piccio L., Lyons J. A., Lauber J., Tutlam N. T., Parks B. J., Trinkaus K., Song S. K. and Cross A. H. (2010). Rituximab add-on therapy for breakthrough relapsing multiple sclerosis: a 52-week phase II trial. *Neurology* **74**,1860-7.

Neyt K., Perros F., GeurtsvanKessel C. H., Hammad H. and Lambrecht B. N. (2012). Tertiary lymphoid organs in infection and autoimmunity. *Trends Immunol* **33**,297-305.

Nissim A., Hoogenboom H. R., Tomlinson I. M., Flynn G., Midgley C., Lane D. and Winter G. (1994). Antibody fragments from a 'single pot' phage display library as immunochemical reagents. *EMBO J* **13**,692-8.

O'Connor K. C., Appel H., Bregoli L., Call M. E., Catz I., Chan J. A., Moore N. H., Warren K. G., Wong S. J., Hafler D. A. et al. (2005). Antibodies from inflamed central nervous system tissue recognize myelin oligodendrocyte glycoprotein. *J Immunol* **175**,1974-82.

Obermeier B., Lovato L., Mentele R., Bruck W., Forne I., Imhof A., Lottspeich F., Turk K. W., Willis S. N., Wekerle H. et al. (2011). Related B cell clones that populate the CSF and CNS of patients with multiple sclerosis produce CSF immunoglobulin. *J Neuroimmunol* **233**,245-8.

Obermeier B., Mentele R., Malotka J., Kellermann J., Kumpfel T., Wekerle H., Lottspeich F., Hohlfeld R. and Dornmair K. (2008). Matching of oligoclonal immunoglobulin transcriptomes and proteomes of cerebrospinal fluid in multiple sclerosis. *Nat Med* **14**,688-93.

Owens G. P., Bennett J. L., Lassmann H., O'Connor K. C., Ritchie A. M., Shearer A., Lam C., Yu X., Birlea M., DuPree C. et al. (2009). Antibodies produced by clonally expanded plasma cells in multiple sclerosis cerebrospinal fluid. *Ann Neurol* **65**,639-49.

Owens G. P., Burgoon M. P., Anthony J., Kleinschmidt-DeMasters B. K. and Gilden D. H. (2001). The immunoglobulin G heavy chain repertoire in multiple sclerosis plaques is distinct from the heavy chain repertoire in peripheral blood lymphocytes. *Clin Immunol* **98**,258-63.

Owens G. P., Burgoon M. P., Devlin M. E. and Gilden D. H. (1997). Extraction and purification of active IgG from SSPE and MS brain. *J Virol Methods* **68**,119-25.

Owens G. P., Kraus H., Burgoon M. P., Smith-Jensen T., Devlin M. E. and Gilden D. H. (1998). Restricted use of VH4 germline segments in an acute multiple sclerosis brain. *Ann Neurol* **43**,236-43.

Owens G. P., Ritchie A. M., Burgoon M. P., Williamson R. A., Corboy J. R. and Gilden D. H. (2003). Single-cell repertoire analysis demonstrates that clonal expansion is a prominent feature of the B cell response in multiple sclerosis cerebrospinal fluid. *J Immunol* **171**,2725-33.

Owens G. P., Winges K. M., Ritchie A. M., Edwards S., Burgoon M. P., Lehnhoff L., Nielsen K., Corboy J., Gilden D. H. and Bennett J. L. (2007). VH4 gene segments dominate the intrathecal humoral immune response in multiple sclerosis. *J Immunol* **179**,6343-51.

Pallares N., Frippiat J. P., Giudicelli V. and Lefranc M. P. (1998). The human immunoglobulin lambda variable (IGLV) genes and joining (IGLJ) segments. *Exp Clin Immunogenet* **15**,8-18.

Patsopoulos N. A., Esposito F., Reischl J., Lehr S., Bauer D., Heubach J., Sandbrink R., Pohl C., Edan G., Kappos L. et al. (2011). Genome-wide meta-analysis identifies novel multiple sclerosis susceptibility loci. *Ann Neurol* **70**,897-912.

Pearce J. M. (2005). Historical descriptions of multiple sclerosis. *Eur Neurol* **54**,49-53.

Pellkofer H. L., Krumbholz M., Berthele A., Hemmer B., Gerdes L. A., Havla J., Bittner R., Canis M., Meinl E., Hohlfeld R. et al. (2011). Long-term follow-up of patients with neuromyelitis optica after repeated therapy with rituximab. *Neurology* **76**,1310-5.

Pender M. P., Csurhes P. A., Greer J. M., Mowat P. D., Henderson R. D., Cameron K. D., Purdie D. M., McCombe P. A. and Good M. F. (2000). Surges of increased T cell reactivity to an encephalitogenic region of myelin proteolipid protein occur more often in patients with multiple sclerosis than in healthy subjects. *J Immunol* **165**,5322-31.

Petereit H. F., Moeller-Hartmann W., Reske D. and Rubbert A. (2008). Rituximab in a patient with multiple sclerosis--effect on B cells, plasma cells and intrathecal IgG synthesis. *Acta Neurol Scand* **117**,399-403.

Peterson J. W., Bo L., Mork S., Chang A. and Trapp B. D. (2001). Transected neurites, apoptotic neurons, and reduced inflammation in cortical multiple sclerosis lesions. *Ann Neurol* **50**,389-400.

Pette M., Fujita K., Kitze B., Whitaker J. N., Albert E., Kappos L. and Wekerle H. (1990). Myelin basic protein-specific T lymphocyte lines from MS patients and healthy individuals. *Neurology* **40**,1770-6.

Petzold A. (2005). Neurofilament phosphoforms: surrogate markers for axonal injury, degeneration and loss. *J Neurol Sci* **233**,183-98.

Pfaffl M. W., Tichopad A., Prgomet C. and Neuvians T. P. (2004). Determination of stable housekeeping genes, differentially regulated target genes and sample integrity: BestKeeper--Excel-based tool using pair-wise correlations. *Biotechnol Lett* **26**,509-15.

Pfender N. A., Grosch S., Roussel G., Koch M., Trifilieff E. and Greer J. M. (2008). Route of uptake of palmitoylated encephalitogenic peptides of myelin proteolipid protein by antigen-presenting cells: importance of the type of bond between lipid chain and peptide and relevance to autoimmunity. *J Immunol* **180**,1398-404.

Pittock S. J., McClelland R. L., Achenbach S. J., Konig F., Bitsch A., Bruck W., Lassmann H., Parisi J. E., Scheithauer B. W., Rodriguez M. et al. (2005). Clinical course, pathological correlations, and outcome of biopsy proved inflammatory demyelinating disease. *J Neurol Neurosurg Psychiatry* **76**,1693-7.

Pohl D., Krone B., Rostasy K., Kahler E., Brunner E., Lehnert M., Wagner H. J., Gartner J. and Hanefeld F. (2006). High seroprevalence of Epstein-Barr virus in children with multiple sclerosis. *Neurology* **67**,2063-5.

Poljak R. J., Amzel L. M., Avey H. P., Chen B. L., Phizackerley R. P. and Saul F. (1973). Three-dimensional structure of the Fab' fragment of a human immunoglobulin at 2,8-A resolution. *Proc Natl Acad Sci U S A* **70**,3305-10.

Polman C. H., Reingold S. C., Banwell B., Clanet M., Cohen J. A., Filippi M., Fujihara K., Havrdova E., Hutchinson M., Kappos L. et al. (2011). Diagnostic criteria for multiple sclerosis: 2010 revisions to the McDonald criteria. *Ann Neurol* **69**,292-302.

Poole B. D., Templeton A. K., Guthridge J. M., Brown E. J., Harley J. B. and James J. A. (2009). Aberrant Epstein-Barr viral infection in systemic lupus erythematosus. *Autoimmun Rev* **8**,337-42.

Popescu B. F. and Lucchinetti C. F. (2012). Meningeal and cortical grey matter pathology in multiple sclerosis. *BMC Neurol* **12**,11.

Poser C. M., Paty D. W., Scheinberg L., McDonald W. I., Davis F. A., Ebers G. C., Johnson K. P., Sibley W. A., Silberberg D. H. and Tourtellotte W. W. (1983). New diagnostic criteria for multiple sclerosis: guidelines for research protocols. *Ann Neurol* **13**,227-31.

Poskanzer D. C., Walker A. M., Yonkondy J. and Sheridan J. L. (1976). Studies in the epidemiology of multiple sclerosis in the Orkney and Shetland Islands. *Neurology* **26**,14-7.

Prabakaran P., Chen W., Singarayan M. G., Stewart C. C., Streaker E., Feng Y. and Dimitrov D. S. (2012). Expressed antibody repertoires in human cord blood cells: 454 sequencing and IMGT/HighV-QUEST analysis of germline gene usage, junctional diversity, and somatic mutations. *Immunogenetics* **64**,337-50.

Pribyl T. M., Campagnoni C. W., Kampf K., Kashima T., Handley V. W., McMahon J. and Campagnoni A. T. (1993). The human myelin basic protein gene is included within a 179-kilobase transcription unit: expression in the immune and central nervous systems. *Proc Natl Acad Sci U S A* **90**,10695-9.

Prineas J. W. (1979). Multiple sclerosis: presence of lymphatic capillaries and lymphoid tissue in the brain and spinal cord. *Science* **203**,1123-5.

Prineas J. W. and Graham J. S. (1981). Multiple sclerosis: capping of surface immunoglobulin G on macrophages engaged in myelin breakdown. *Ann Neurol* **10**,149-58.

Prineas J. W. and Wright R. G. (1978). Macrophages, lymphocytes, and plasma cells in the perivascular compartment in chronic multiple sclerosis. *Lab Invest* **38**,409-21.

Pugliatti M., Sotgiu S. and Rosati G. (2002). The worldwide prevalence of multiple sclerosis. *Clin Neurol Neurosurg* **104**,182-91.

Qin Y., Duquette P., Zhang Y., Talbot P., Poole R. and Antel J. (1998). Clonal expansion and somatic hypermutation of V(H) genes of B cells from cerebrospinal fluid in multiple sclerosis. *J Clin Invest* **102**,1045-50.

Quintana F. J., Farez M. F., Izquierdo G., Lucas M., Cohen I. R. and Weiner H. L. (2012). Antigen microarrays identify CNS-produced autoantibodies in RRMS. *Neurology* **78**,532-9.

Racke M. K., Lovett-Racke A. E. and Karandikar N. J. (2010). The mechanism of action of glatiramer acetate treatment in multiple sclerosis. *Neurology* **74 Suppl 1**,S25-30.

Ramagopalan S. V., Byrnes J. K., Orton S. M., Dyment D. A., Guimond C., Yee I. M., Ebers G. C. and Sadovnick A. D. (2010). Sex ratio of multiple sclerosis and clinical phenotype. *Eur J Neurol* **17**,634-7.

Rand K. H., Houck H., Denslow N. D. and Heilman K. M. (1998). Molecular approach to find target(s) for oligoclonal bands in multiple sclerosis. *J Neurol Neurosurg Psychiatry* **65**,48-55.

Rassenti L. Z., Kohsaka H. and Kipps T. J. (1995). Analysis of immunoglobulin VH gene repertoire by an anchored PCR-ELISA. *Ann N Y Acad Sci* **764**,463-73.

Ravetch J. V., Siebenlist U., Korsmeyer S., Waldmann T. and Leder P. (1981). Structure of the human immunoglobulin mu locus: characterization of embryonic and rearranged J and D genes. *Cell* **27**,583-91.

Reiber H., Ungefehr S. and Jacobi C. (1998). The intrathecal, polyspecific and oligoclonal immune response in multiple sclerosis. *Mult Scler* **4**,111-7.

Retter I., Althaus H. H., Munch R. and Muller W. (2005). VBASE2, an integrative V gene database. *Nucleic Acids Res* **33**,D671-4.

Rhyner C., Weichel M., Hubner P., Achatz G., Blaser K. and Crameri R. (2003). Phage display of human antibodies from a patient suffering from coeliac disease and selection of isotype-specific scFv against gliadin. *Immunology* **110**,269-74.

Richl P., Stern U., Lipsky P. E. and Girschick H. J. (2008). The lambda gene immunoglobulin repertoire of human neonatal B cells. *Mol Immunol* **45**,320-7.

Riechmann L. and Holliger P. (1997). The C-terminal domain of TolA is the coreceptor for filamentous phage infection of E. coli. *Cell* **90**,351-60.

Rioux J. D., Goyette P., Vyse T. J., Hammarstrom L., Fernando M. M., Green T., De Jager P. L., Foisy S., Wang J., de Bakker P. I. et al. (2009). Mapping of multiple susceptibility variants within the MHC region for 7 immune-mediated diseases. *Proc Natl Acad Sci U S A* **106**,18680-5.

Rodriguez M., Karnes W. E., Bartleson J. D. and Pineda A. A. (1993). Plasmapheresis in acute episodes of fulminant CNS inflammatory demyelination. *Neurology* **43**,1100-4.

Rogozin I. B., Pavlov Y. I., Bebenek K., Matsuda T. and Kunkel T. A. (2001). Somatic mutation hotspots correlate with DNA polymerase eta error spectrum. *Nat Immunol* **2**,530-6.

Rosati G. (2001). The prevalence of multiple sclerosis in the world: an update. *Neurol Sci* **22**,117-39.

Rothwell P. M. and Charlton D. (1998). High incidence and prevalence of multiple sclerosis in south east Scotland: evidence of a genetic predisposition. *J Neurol Neurosurg Psychiatry* **64**,730-5.

Roxanis I., Micklem K., McConville J., Newsom-Davis J. and Willcox N. (2002). Thymic myoid cells and germinal center formation in myasthenia gravis; possible roles in pathogenesis. *J Neuroimmunol* **125**,185-97.

Rudick R., Polman C., Clifford D., Miller D. and Steinman L. (2012). Natalizumab: Bench to Bedside and Beyond. *Arch Neurol*,1-11.

Ruiz M., Giudicelli V., Ginestoux C., Stoehr P., Robinson J., Bodmer J., Marsh S. G., Bontrop R., Lemaitre M., Lefranc G. et al. (2000). IMGT, the international ImMunoGeneTics database. *Nucleic Acids Res* **28**,219-21.

Ruiz M., Pallares N., Contet V., Barbi V. and Lefranc M. P. (1999). The human immunoglobulin heavy diversity (IGHD) and joining (IGHJ) segments. *Exp Clin Immunogenet* **16**,173-84.

Sambrook Joseph and Russell David William. (2001). *Molecular Cloning: A Laboratory Manual*. Cold Spring Harbor Laboratory Press.

Sanna M. G., Liao J., Jo E., Alfonso C., Ahn M. Y., Peterson M. S., Webb B., Lefebvre S., Chun J., Gray N. et al. (2004). Sphingosine 1-phosphate (S1P) receptor subtypes S1P1 and S1P3, respectively, regulate lymphocyte recirculation and heart rate. *J Biol Chem* **279**,13839-48.

Sawcer S., Hellenthal G., Pirinen M., Spencer C. C., Patsopoulos N. A., Moutsianas L., Dilthey A., Su Z., Freeman C., Hunt S. E. et al. (2011). Genetic risk and a primary role for cell-mediated immune mechanisms in multiple sclerosis. *Nature* **476**,214-9.

Schroeder A., Mueller O., Stocker S., Salowsky R., Leiber M., Gassmann M., Lightfoot S., Menzel W., Granzow M. and Ragg T. (2006). The RIN: an RNA integrity number for assigning integrity values to RNA measurements. *BMC Mol Biol* **7**,3.

Segal B. M., Constantinescu C. S., Raychaudhuri A., Kim L., Fidelus-Gort R. and Kasper L. H. (2008). Repeated subcutaneous injections of IL12/23 p40 neutralising antibody, ustekinumab, in patients with relapsing-remitting multiple sclerosis: a phase II, double-blind, placebo-controlled, randomised, dose-ranging study. *Lancet Neurol* **7**,796-804.

Sellebjerg F., Christiansen M. and Garred P. (1998). MBP, anti-MBP and anti-PLP antibodies, and intrathecal complement activation in multiple sclerosis. *Mult Scler* **4**,127-31.

Serafini B., Rosicarelli B., Magliozzi R., Stigliano E. and Aloisi F. (2004). Detection of ectopic B-cell follicles with germinal centers in the meninges of patients with secondary progressive multiple sclerosis. *Brain Pathol* **14**,164-74.

Sidhu S. S. (2001). Engineering M13 for phage display. *Biomol Eng* **18**,57-63.

Silber E., Semra Y. K., Gregson N. A. and Sharief M. K. (2002). Patients with progressive multiple sclerosis have elevated antibodies to neurofilament subunit. *Neurology* **58**,1372-81.

Silver N., Best S., Jiang J. and Thein S. L. (2006). Selection of housekeeping genes for gene expression studies in human reticulocytes using real-time PCR. *BMC Mol Biol* **7**,33.

Silverton E. W., Navia M. A. and Davies D. R. (1977). Three-dimensional structure of an intact human immunoglobulin. *Proc Natl Acad Sci U S A* **74**,5140-4.

Simon K. C., Munger K. L. and Ascherio A. (2012). Vitamin D and multiple sclerosis: epidemiology, immunology, and genetics. *Curr Opin Neurol* **25**,246-51.

Sindic C. J., Delacroix D. L., Vaerman J. P., Laterre E. C. and Masson P. L. (1984). Study of IgA in the cerebrospinal fluid of neurological patients with special reference to size, subclass and local production. *J Neuroimmunol* **7**,65-75.

Smith-Jensen T., Burgoon M. P., Anthony J., Kraus H., Gilden D. H. and Owens G. P. (2000). Comparison of immunoglobulin G heavy-chain sequences in MS and SSPE brains reveals an antigen-driven response. *Neurology* **54**,1227-32.

Söderström N. and Biörklund A. (1974). Organization of the invading lymphoid tissue in human lymphoid thyroiditis. *Scand J Immunol* **3**,295-301.

Stan A. D., Ghose S., Gao X. M., Roberts R. C., Lewis-Amezcua K., Hatanpaa K. J. and Tamminga C. A. (2006). Human postmortem tissue: what quality markers matter? *Brain Res* **1123**,1-11.

Stendahl-Brodin L. and Link H. (1980). Relation between benign course of multiple sclerosis and low-grade humoral immune response in cerebrospinal fluid. *J Neurol Neurosurg Psychiatry* **43**,102-5.

Sun J. B., Olsson T., Wang W. Z., Xiao B. G., Kostulas V., Fredrikson S., Ekre H. P. and Link H. (1991). Autoreactive T and B cells responding to myelin proteolipid protein in multiple sclerosis and controls. *Eur J Immunol* **21**,1461-8.

Swanton J. K., Fernando K., Dalton C. M., Miszkiel K. A., Thompson A. J., Plant G. T. and Miller D. H. (2006). Modification of MRI criteria for multiple sclerosis in patients with clinically isolated syndromes. *J Neurol Neurosurg Psychiatry* **77**,830-3.

Swanton J. K., Rovira A., Tintore M., Altmann D. R., Barkhof F., Filippi M., Huerga E., Miszkiel K. A., Plant G. T., Polman C. et al. (2007). MRI criteria for multiple sclerosis in patients presenting with clinically isolated syndromes: a multicentre retrospective study. *Lancet Neurol* **6**,677-86.

Swingler R. J. and Compston D. A. (1992). The morbidity of multiple sclerosis. *Q J Med* **83**,325-37.

Thacker E. L., Mirzaei F. and Ascherio A. (2006). Infectious mononucleosis and risk for multiple sclerosis: a meta-analysis. *Ann Neurol* **59**,499-503.

Thio M., Blokhuis B. R., Nijkamp F. P. and Redegeld F. A. (2008). Free immunoglobulin light chains: a novel target in the therapy of inflammatory diseases. *Trends Pharmacol Sci* **29**,170-4.

Tibbling G., Link H. and Ohman S. (1977). Principles of albumin and IgG analyses in neurological disorders. I. Establishment of reference values. *Scand J Clin Lab Invest* **37**,385-90.

Tomita H., Vawter M. P., Walsh D. M., Evans S. J., Choudary P. V., Li J., Overman K. M., Atz M. E., Myers R. M., Jones E. G. et al. (2004). Effect of agonal and postmortem factors on gene expression profile: quality control in microarray analyses of postmortem human brain. *Biol Psychiatry* **55**,346-52.

Tomlinson I. M., Cook G. P., Carter N. P., Elaswarapu R., Smith S., Walter G., Buluwela L., Rabbitts T. H. and Winter G. (1994). Human immunoglobulin VH and D segments on chromosomes 15q11.2 and 16p11.2. *Hum Mol Genet* **3**,853-60.

Torrey E. F., Webster M., Knable M., Johnston N. and Yolken R. H. (2000). The stanley foundation brain collection and neuropathology consortium. *Schizophr Res* **44**,151-5.

Tranquill L. R., Cao L., Ling N. C., Kalbacher H., Martin R. M. and Whitaker J. N. (2000). Enhanced T cell responsiveness to citrulline-containing myelin basic protein in multiple sclerosis patients. *Mult Scler* **6**,220-5.

Trapp B. D., Peterson J., Ransohoff R. M., Rudick R., Mork S. and Bo L. (1998). Axonal transection in the lesions of multiple sclerosis. *N Engl J Med* **338**,278-85.

Tremlett H., Paty D. and Devonshire V. (2005). The natural history of primary progressive MS in British Columbia, Canada. *Neurology* **65**,1919-23.

Tremlett H., Paty D. and Devonshire V. (2006). Disability progression in multiple sclerosis is slower than previously reported. *Neurology* **66**,172-7.

Tselis A. (2012). Epstein-Barr virus cause of multiple sclerosis. *Curr Opin Rheumatol* **24**,424-8.

Tullman M. J., Oshinsky R. J., Lublin F. D. and Cutter G. R. (2004). Clinical characteristics of progressive relapsing multiple sclerosis. *Mult Scler* **10**,451-4.

Tuohy V. K., Lu Z., Sobel R. A., Laursen R. A. and Lees M. B. (1989). Identification of an encephalitogenic determinant of myelin proteolipid protein for SJL mice. *J Immunol* **142**,1523-7.

Tzartos J. S., Friese M. A., Craner M. J., Palace J., Newcombe J., Esiri M. M. and Fugger L. (2008). Interleukin-17 production in central nervous system-infiltrating T cells and glial cells is associated with active disease in multiple sclerosis. *Am J Pathol* **172**,146-55.

van der Heijden M., Kraneveld A. and Redegeld F. (2006). Free immunoglobulin light chains as target in the treatment of chronic inflammatory diseases. *Eur J Pharmacol* **533**,319-26.

van Noort J. M., Bsibsi M., Gerritsen W. H., van der Valk P., Bajramovic J. J., Steinman L. and Amor S. (2010). Alphab-crystallin is a target for adaptive immune responses and a trigger of innate responses in preactive multiple sclerosis lesions. *J Neuropathol Exp Neurol* **69**,694-703.

van Sechel A. C., Bajramovic J. J., van Stipdonk M. J., Persoon-Deen C., Geutskens S. B. and van Noort J. M. (1999). EBV-induced expression and HLA-DR-restricted presentation by human B cells of alpha B-crystallin, a candidate autoantigen in multiple sclerosis. *J Immunol* **162**,129-35.

Vandesompele J., De Preter K., Pattyn F., Poppe B., Van Roy N., De Paepe A. and Speleman F. (2002). Accurate normalization of real-time quantitative RT-PCR data by geometric averaging of multiple internal control genes. *Genome Biol* **3**,RESEARCH0034.

Venken K., Hellings N., Liblau R. and Stinissen P. (2010). Disturbed regulatory T cell homeostasis in multiple sclerosis. *Trends Mol Med* **16**,58-68.

Vercellino M., Plano F., Votta B., Mutani R., Giordana M. T. and Cavalla P. (2005). Grey matter pathology in multiple sclerosis. *J Neuropathol Exp Neurol* **64**,1101-7.

Victora G. D. and Nussenzweig M. C. (2012). Germinal centers. *Annu Rev Immunol* **30**,429-57.

Viglietta V., Baecher-Allan C., Weiner H. L. and Hafler D. A. (2004). Loss of functional suppression by CD4+CD25+ regulatory T cells in patients with multiple sclerosis. *J Exp Med* **199**,971-9.

Villar L. M., Gonzalez-Porque P., Masjuan J., Alvarez-Cermeno J. C., Bootello A. and Keir G. (2001). A sensitive and reproducible method for the detection of oligoclonal IgM bands. *J Immunol Methods* **258**,151-5.

Villar L. M., Masjuan J., Gonzalez-Porque P., Plaza J., Sadaba M. C., Roldan E., Bootello A. and Alvarez-Cermeno J. C. (2002). Intrathecal IgM synthesis in neurologic diseases: relationship with disability in MS. *Neurology* **58**,824-6.

von Andrian U. H. and Mempel T. R. (2003). Homing and cellular traffic in lymph nodes. *Nat Rev Immunol* **3**,867-78.

von Budingen H. C., Gulati M., Kuenzle S., Fischer K., Rupprecht T. A. and Goebels N. (2010). Clonally expanded plasma cells in the cerebrospinal fluid of patients with central nervous system autoimmune demyelination produce "oligoclonal bands". *J Neuroimmunol* **218**,134-9.

von Budingen H. C., Harrer M. D., Kuenzle S., Meier M. and Goebels N. (2008). Clonally expanded plasma cells in the cerebrospinal fluid of MS patients produce myelin-specific antibodies. *Eur J Immunol* **38**,2014-23.

Wang X. and Stollar B. D. (1999). Immunoglobulin VH gene expression in human aging. *Clin Immunol* **93**,132-42.

Wardemann H., Yurasov S., Schaefer A., Young J. W., Meffre E. and Nussenzweig M. C. (2003). Predominant autoantibody production by early human B cell precursors. *Science* **301**,1374-7.

Warren K. G. and Catz I. (1994). Relative frequency of autoantibodies to myelin basic protein and proteolipid protein in optic neuritis and multiple sclerosis cerebrospinal fluid. *J Neurol Sci* **121**,66-73.

Warren K. G., Catz I. and Steinman L. (1995). Fine specificity of the antibody response to myelin basic protein in the central nervous system in multiple sclerosis: the minimal B-cell epitope and a model of its features. *Proc Natl Acad Sci U S A* **92**,11061-5.

Warrington J. A., Nair A., Mahadevappa M. and Tsyganskaya M. (2000). Comparison of human adult and fetal expression and identification of 535 housekeeping/maintenance genes. *Physiol Genomics* **2**,143-7.

Weber M. S., Hemmer B. and Cepok S. (2011). The role of antibodies in multiple sclerosis. *Biochim Biophys Acta* **1812**,239-45.

Wegner C., Esiri M. M., Chance S. A., Palace J. and Matthews P. M. (2006). Neocortical neuronal, synaptic, and glial loss in multiple sclerosis. *Neurology* **67**,960-7.

Weigert M., Perry R., Kelley D., Hunkapiller T., Schilling J. and Hood L. (1980). The joining of V and J gene segments creates antibody diversity. *Nature* **283**,497-9.

Weinshenker B. G., Bass B., Rice G. P., Noseworthy J., Carriere W., Baskerville J. and Ebers G. C. (1989). The natural history of multiple sclerosis: a geographically based study. I. Clinical course and disability. *Brain* **112 (Pt 1)**,133-46.

Williams S. C., Frippiat J. P., Tomlinson I. M., Ignatovich O., Lefranc M. P. and Winter G. (1996). Sequence and evolution of the human germline V lambda repertoire. *J Mol Biol* **264**,220-32.

Willis S. N., Mallozzi S. S., Rodig S. J., Cronk K. M., McArdel S. L., Caron T., Pinkus G. S., Lovato L., Shampain K. L., Anderson D. E. et al. (2009). The microenvironment of germ cell tumors harbors a prominent antigen-driven humoral response. *J Immunol* **182**,3310-7.

Wingerchuk D. M., Lucchinetti C. F. and Noseworthy J. H. (2001). Multiple sclerosis: current pathophysiological concepts. *Lab Invest* **81**,263-81.

Winter G., Griffiths A. D., Hawkins R. E. and Hoogenboom H. R. (1994). Making antibodies by phage display technology. *Annu Rev Immunol* **12**,433-55.

Yamada M., Wasserman R., Reichard B. A., Shane S., Caton A. J. and Rovera G. (1991). Preferential utilization of specific immunoglobulin heavy chain diversity and joining segments in adult human peripheral blood B lymphocytes. *J Exp Med* **173**,395-407.

Ye J., Coulouris G., Zaretskaya I., Cutcutache I., Rozen S. and Madden T. L. (2012). Primer-BLAST: A tool to design target-specific primers for polymerase chain reaction. *BMC Bioinformatics* **13**,134.

Yu X., Gilden D., Schambers L., Barmina O., Burgoon M., Bennett J. and Owens G. (2011). Peptide reactivity between multiple sclerosis (MS) CSF IgG and recombinant antibodies generated from clonally expanded plasma cells in MS CSF. *J Neuroimmunol* **233**,192-203.

Yurasov S., Wardemann H., Hammersen J., Tsuiji M., Meffre E., Pascual V. and Nussenzweig M. C. (2005). Defective B cell tolerance checkpoints in systemic lupus erythematosus. *J Exp Med* **201**,703-11.

Zaadstra B. M., Chorus A. M., van Buuren S., Kalsbeek H. and van Noort J. M. (2008). Selective association of multiple sclerosis with infectious mononucleosis. *Mult Scler* **14**,307-13.

Zampieri S., Mahler M., Bluthner M., Qiu Z., Malmegrim K., Ghirardello A., Doria A., van Venrooij W. J. and Raats J. M. (2003). Recombinant anti-P protein autoantibodies isolated from a human autoimmune library: reactivity, specificity and epitope recognition. *Cell Mol Life Sci* **60**,588-98.

Zeman A. Z., Kidd D., McLean B. N., Kelly M. A., Francis D. A., Miller D. H., Kendall B. E., Rudge P., Thompson E. J. and McDonald W. I. (1996). A study of oligoclonal band negative multiple sclerosis. *J Neurol Neurosurg Psychiatry* **60**,27-30.

Zhang J., Markovic-Plese S., Lacet B., Raus J., Weiner H. L. and Hafler D. A. (1994). Increased frequency of interleukin 2-responsive T cells specific for myelin basic protein and proteolipid protein in peripheral blood and cerebrospinal fluid of patients with multiple sclerosis. *J Exp Med* **179**,973-84.

Zhang Y., Da R. R., Hilgenberg L. G., Tourtellotte W. W., Sobel R. A., Smith M. A., Olek M., Nagra R., Sudhir G., van den Noort S. et al. (2005). Clonal expansion of IgA-positive plasma cells and axon-reactive antibodies in MS lesions. *J Neuroimmunol* **167**,120-30.

Zipper H., Brunner H., Bernhagen J. and Vitzthum F. (2004). Investigations on DNA intercalation and surface binding by SYBR Green I, its structure determination and methodological implications. *Nucleic Acids Res* **32**,e103.

Zivadinov R., Weinstock-Guttman B., Hashmi K., Abdelrahman N., Stosic M., Dwyer M., Hussein S., Durfee J. and Ramanathan M. (2009). Smoking is associated with increased lesion volumes and brain atrophy in multiple sclerosis. *Neurology* **73**,504-10.

Zouali M. and Theze J. (1991). Probing VH gene-family utilization in human peripheral B cells by in situ hybridization. *J Immunol* **146**,2855-64.

Zuckerman N. S., Hazanov H., Barak M., Edelman H., Hess S., Shcolnik H., Dunn-Walters D. and Mehr R. (2010). Somatic hypermutation and antigen-driven selection of B cells are altered in autoimmune diseases. *J Autoimmun* **35**,325-35.